Dynamics of human decision-making under uncertainty in health and disease

Fitzroy Wickham

University of Oxford

St. John's College

D.Phil. in Clinical Neurosciences

My grandmother was a fire and brimstone preacher
My mother is a genius
My father commanded respect
When my father and grandmother died, they left no instructions
Just a legacy to protect

I | Abstract

This thesis investigated how humans reduce uncertainty in decision-making and how this capacity is disrupted by brain pathology, with a focus on white matter (WM) damage in cerebral small vessel disease (SVD) and lesions in the medial frontal lobe (MFL). Multi-modal neuroimaging and variants of a relatively novel decision-making behavioural paradigm were employed to characterize the neural and cognitive mechanisms underlying decision-making under uncertainty.

Chapter 2 established the structural context for subsequent behavioural analyses by examining WM integrity in SVD using structural MRI and diffusion-weighted imaging (DWI) with diffusion tensor imaging (DTI) and neurite orientation dispersion and density imaging (NODDI). Compared to age-matched healthy controls (HC), SVD patients exhibited widespread WM macro- and microstructural disruption, including reduced fractional anisotropy (FA) and neurite density index (NDI), increased mean diffusivity (MD) and isotropic volume fraction (ISOVF), and variable orientation dispersion (ODI). WM damage correlated with cognitive performance, education, and affective measures in controls, whereas in SVD patients, impairments were strongly driven by pathology.

Chapter 3 examined behavioural performance on the core Circle Quest (CQ) task. SVD participants sampled less information, were less sensitive to sampling cost, reward, and uncertainty, and tolerated higher uncertainty compared to HCs. Reduced WM integrity predicted lower sampling efficiency, reduced reward sensitivity, and poorer precision in localizing target locations, linking structural disruption to functional deficits.

Chapter 4 extended this investigation using an effort-based variant of the CQ task. Introducing physical effort increased offer acceptance and partially restored sensitivity to reward and uncertainty in SVD patients, aligning their behaviour more closely with controls.

These findings suggest that motivational engagement can modulate impairments in decision-making under uncertainty.

Chapter 5 applied the CQ paradigm to patients with MFL lesions. MFL patients showed reduced evidence accumulation in the active task, increased risk-taking in the passive task, and diminished sensitivity to cost and reward compared to HCs and lesion controls. This highlights the selective contribution of the MFL to value-based decision-making.

Overall, this thesis demonstrates that WM disruption in SVD and focal MFL lesions produce consistent impairments in decision-making under uncertainty. Behavioural deficits manifest as reduced information sampling, increased uncertainty tolerance, and riskier choices, with task context and motivational variables modulating performance. These findings advance our understanding of the neural substrates of adaptive decision-making and suggest potential avenues for interventions targeting cognitive and motivational processes.

II | Acknowledgments

"Likkle but Tallawah"

Many things in life seem insignificant on initial glance, but upon closer investigation, their hidden potential is revealed. That is the idea that shaped this thesis—from the brain's white matter to small vessel disease to decision-making. But, in championing concepts that have often been overlooked in neuroscience, I found that I had, at times, lost sight of my own potential. Consequently, I want to thank those who constantly advocated on my behalf and reminded me of my own potential; this work exists because of your unwavering support.

It is only fitting that I begin this list with the brilliant mind, Professor Masud Husain, who took a chance on me. Thank you, Masud, for being my primary supervisor and for keeping your promise to transform me into a PhD student. Your acumen, empathy and patience kept me motivated every step of the way. I would also like to thank my secondary supervisor, Professor Sanjay Manohar. I am deeply humbled to have been one chief beneficiary of wisdom from such a razor-sharp thinker. Thank you for your willingness to help me troubleshoot the many problems I faced during this process and for always challenging me to see beyond my limited perspective.

I would also like to express my gratitude to the following parties for being a part of my DPhil journey:

To the research participants, for devoting hours of your lives to scientific research with the only expectation that I complete my studies and send you my findings. To my fellow lab members, for inspiring me with your own work and helping me navigate the treacherous waters of academia. To Bahaa, for being a reliable port of call whenever I needed training,

clarification and guidance. To Pierre, for designing such an incredible behavioural task. To Imran, for assisting with participant recruitment and overall encouragement. To John and Alberto, for sharing your expertise in neuroimaging analyses.

To the countless friends I made over these past few years. To my Oxford postgraduate Caribbean community, for being my home away from home. To my New College friends, for the gift of amity. To Christina, Mark and their family, for keeping me grounded.

To the Rhodes Trust for funding my postgraduate journey. To Mary Eaton, especially, for being a pillar of strength and a beacon of light throughout this entire process.

To my mentors from Jamaica and my undergraduate institution, Wesleyan University, for your relentless support that carried me to this moment and continues to sustain me.

To my mother, Florence Wickham, my first and greatest teacher, thank you for gifting me your love of knowledge. Your passion lights my way every single day. I am your proud son. To my sister, Kimberly, thank you for helping to lay the strong scientific foundation upon which all my academic success is built. To my late father, Ronald Wickham, and my late grandmother, Lillian Brown, your sacrifices shaped me, your love steadied me, and even in your absence you continue to remind me of my purpose.

Finally, I give thanks to the Almighty, who placed these cherished souls in my path and endowed me with the gifts needed to finish this chapter of my life. All praise and glory be unto You.

Table of Contents

1| General Introduction

Both uncertainty and decision-making are pervasive features of the human experience. Their intersection—how individuals seek information to reduce uncertainty before acting—is central to adaptive behaviour (Attaallah et al., 2025). Although many experimental paradigms investigate decision-making, they typically place participants under fixed exposure to information (e.g., Clark et al., 2006; Furl & Averbeck, 2011; Hertwig et al., 2004; Kahneman & Tversky, 1979; Pytlik et al., 2020; Steingroever, 2013; Villar et al., 2015), thereby limiting control over what or how long to sample before coming to a decision. Few tasks allow participants to regulate the amount and quality of information they sample based on the current level of uncertainty (Juni et al., 2016; Petitet et al., 2021), which might better reflect real-world decision contexts.

The primary aim of this thesis is to examine how humans reduce uncertainty in decision-making, and how this capacity is affected by structural brain pathology. I examine the behaviour of healthy individuals and compare them to that of patients with cerebrovascular small vessel disease (SVD). This is a condition associated with WM pathology and known to impair executive function, processing speed, and several other aspects of cognition (Hamilton et al., 2021; Østergaard et al., 2016; Zanon Zotin et al., 2021), yet in which decision-making behaviour remains relatively underexplored. I also assess performance on the same decision-making task in individuals with medial frontal lobe (MFL) lesions, leveraging a group of patients that has historically been highly informative in studying decision-making (Bechara & Van Der Linden, 2005; Manes et al., 2002). This approach allows for a comparative analysis of decision-making deficits arising from subcortical WM versus MFL damage, helping to improve understanding of the neural substrates of uncertainty-driven decision behaviour.

To begin, I consider how some aspects of decision-making have been investigated in prior research. In presenting this work I will first discuss some of their major findings in healthy participants, before considering published research using the Circle Quest task (Petitet et al., 2021). This is a relatively new paradigm which examines decision-making under uncertainty and is central to the studies I have performed in this thesis. Subsequently in this introductory chapter, I will discuss current knowledge regarding the impact of SVD and MFL lesions on decision-making.

OVERVIEW OF DECISION-MAKING PARADIGMS

Decision-making in humans has been extensively studied over the last century and has been defined as the selection of an option from among alternatives after careful examination according to an individual's personal values and preferences (Fülöp, 2005). It is estimated that the average adult human makes around 35,000 decisions per day (Sahakian et al., 2013). That is over 100 decisions each hour or just about three decisions every minute of a person's life. These decisions can range from very mundane tasks like deciding what font to use for typing a document to something more remarkable like deciding which journal to submit an article to.

Researchers have developed ingenious ways to investigate decision-making, using a range of behavioral paradigms that attempt to replicate real-life situations, with varying degrees of success. Here, I review some of the most well-known paradigms along with some lesser-known ones, attempting to categorize them according to how they explore human decision-making. Decision-making has been investigated in a multitude of ways, for example using descriptive probabilistic tasks, temporal discounting paradigms, and effort-based decision-making (EBDM) tasks (M. F. Green et al., 2015; Kahneman & Tversky, 1979; Watts et al., 2018). These paradigms typically involve known probabilities, rewards, or

outcomes. In contrast, when individuals must make decisions without full information about outcomes or probabilities, they are engaging in decision-making under uncertainty. This form of decision-making has been examined using paradigms such as exploration–exploitation trade-off tasks (EETs), foraging or patch-leaving frameworks, and information sampling tasks (ISTs) (Averbeck, 2015).

This review is not exhaustive but is an attempt to summarize some of the work that has been conducted on human decision-making that is relevant to the research presented in this thesis which focuses on decision-making under uncertainty and EBDM. I will not consider some of the earliest decision-making tasks, including the Matching Familiar Figures Test, Haptic-Visual Matching Test, and Picture Completion Reasoning Test developed by Kagan in 1964, which were designed to classify children's behavior as either impulsive or reflective (Kagan, 1964). Similarly, I exclude tasks such as the Trust Game, designed specifically to examine the social dimensions of decision-making (Brülhart & Usunier, 2004; Burks et al., 2003). Finally, behavioural paradigms with a primary focus on response inhibition, such as the Traffic Lights, Go/No Go and Stop Signal tasks (Adam et al., 2013; DeVito et al., 2009; Gillespie et al., 2022), will also not be considered here.

1.1 DESCRIPTIVE PROBABILISTIC TASKS

Many decision-making paradigms require the evaluation of options followed by choice selection based on expected rewards, loss, potential punishment, effort, perceived risk, uncertainty, or other tradeoffs (Ernst & Paulus, 2005; Klein-Flügge et al., 2016; Mata et al., 2011; Vaidya & Fellows, 2017). Bernoulli's exploration of the St. Petersburg Paradox (a famous coin-toss problem that reveals a discrepancy between expected value and how people actually make decisions under uncertainty) in the early 18th century led to the development of Expected Utility Theory (EUT), which showed that people value outcomes based on utility,

not solely on raw monetary value (Bernoulli, 1738). However, it took another 200 years before Von Neumann and Morgenstern would formalize EUT into a normative model using mathematical axioms to explain rational decision-making under risk (Binmore, 2012). Their contributions to Game Theory sparked a revolution in the decision-making literature and during the 20th Century concepts such as Subjective Expected Utility Theory (SEU), Bounded Rationality and Prospect Theory were introduced to the field of economics (Kahneman & Tversky, 1979; Neumann, 1944; Simon, 1955; Tversky & Kahneman, 1974).

To test their decision-making theories, economists often posed simple thought experiments such as the St. Petersburg Paradox, but it was Kahneman and Tversky who popularized the use of Descriptive Probabilistic Decision-Making Tasks to explain human behaviour. These tasks assessed risky choices, where outcomes had variable, but explicit, probabilities and magnitudes, attempting to replicate real life gambling problems.

In their 1979 study, Kahneman and Tversky presented 14 decision problems to multiple participant groups, with sample sizes ranging from 64 to 95 individuals (Kahneman & Tversky, 1979). Their findings challenged the prevailing normative theories of the time and led to the development of Prospect Theory, which introduced an S-shaped value function—characterized by asymmetry around a reference point and a steeper slope for losses than for gains—in contrast to the smooth, concave utility curve posited by EUT. This observable phenomenon is termed loss aversion. Additionally, it has been found that humans tend to overweight the occurrence of rare events in such experiments. Gigerenzer and Goldstein (1996) introduced the "Take The Best" heuristic (TTB) as an ecologically rational alternative to models like Prospect Theory, emphasizing simplicity and adaptive fit to real-world environments (Gigerenzer & Goldstein, 1996). While their initial support for TTB was grounded in computational modeling, subsequent work included empirical investigations;

however, behavioral validation remains relatively limited compared to other decision-making theories (Gigerenzer et al., 2008).

Classical Probabilistic Decision-Making Tasks have often been simplified to binary choices in the literature, which may limit the ability to generalize findings from such experiments to real-life decisions, where individuals typically face a wider range of options. The decision problems presented have also often been descriptive in nature, requiring respondents to express a preference with minimal engagement, thereby offering only a narrow understanding of the cognitive processes underlying their decisions. More recent findings support the hypothesis that increased engagement with available choices might alter participants' behaviour (Hertwig et al., 2004; Morwitz & Fitzsimons, 2004).

1.2 TEMPORAL TASKS

Certain decision-making paradigms specifically isolate and manipulate temporal parameters to examine their influence on human behaviour; these are typically classified as Temporal Decision-Making Tasks (Bailey et al., 2021). They provide insight into how individuals choose between options that vary temporally, such as immediate versus delayed rewards. A real-life example of a temporal dilemma is the decision to spend or invest one's income. Upon receiving a paycheck, an individual may feel inclined to allocate remaining funds toward immediate pleasures, thereby obtaining instant gratification. Alternatively, they might consider investing the money with the expectation of receiving greater returns in the near future. However, delaying gratification involves considerable risk: market volatility may erode the investment's value, the cost of desired goods could increase significantly, or the individual may not live long enough to enjoy the eventual payoff. These outcomes, while unfavorable, are generally quantifiable and have estimable probabilities, which classifies them as risks rather than true uncertainties. While delayed rewards may offer greater utility in

theory, the inherent risks associated with future outcomes complicate the decision-making process.

In the well-known **Marshmallow Test** study, Shoda, Mischel, and Peake (1990) attempted to predict developmental outcomes in children from the psychological conditions underlying their delay of gratification behaviour (Kable & Glimcher, 2007b, 2007a; Shoda et al., 1970). The researchers tested 185 preschoolers and tracked their progress for over a decade. The test involved placing a child in a quiet room where a bell and a selection of reward items (e.g., marshmallows, pretzels, colored poker chips) — chosen based on individual preferences identified during pretesting — were presented. The child was asked to indicate a preference between receiving one or two of the items. The experimenter then explained that they would leave the room temporarily: if the child waited until the experimenter's return, they would receive their preferred (larger) reward; if the child could not wait, they could ring the bell to summon the experimenter but would then only receive the less preferred (smaller) reward. In most cases the experimenter would leave for at least 15 minutes or whenever the child rang the bell. Researchers found that children who had longer delay times went on to report better coping behaviour, higher SAT scores and fewer behavioural problems in their adolescences.

Delayed Discounting Tasks (DDT) have been fundamental paradigms used to help understand intertemporal choice by assessing the human tendency to devalue rewards as the delay to their receipt increases. In DDT, participants are asked to choose between a smaller, immediate reward and a larger, delayed reward (Guo et al., 2022; Mitchell et al., 2005). Mok et al. (2021) investigated delay and probability discounting in 30 healthy controls and found that, while the two forms of discounting were related, they reflected distinct cognitive processes and contributed uniquely to individual differences in impulsivity (Mok et al., 2021). Similarly, Fu et al. (2022) examined 30 healthy participants and reported typical delay

discounting behavior (Fu et al., 2022). Across both studies, healthy individuals consistently exhibited standard discounting patterns whereby subjective value of rewards declined as delays increased. Participants generally preferred larger, delayed rewards over smaller, immediate ones; however, as the delay to the larger reward lengthened, they increasingly favored the smaller, immediate reward.

In the **Delayed Occlusion Task** (DOT), participants made a choice between viewing a novel, desirable occluded image immediately or viewing the nonoccluded image after a delay (Patt et al., 2021). This task was administered to 16 healthy controls, who demonstrated typical temporal discounting behavior. Specifically, they tended to choose viewing the occluded image sooner when delays were long, and preferred the nonoccluded image when delays were short (Patt et al., 2023). Their choices reflected a systematic devaluation of the nonoccluded image as the delay to view it increased. Another study combined elements of the DOT with effort-based decision-making in a group of 18 healthy male participants (Prévost et al., 2010). Participants had to either wait or squeeze a hand grip to view nonoccluded erotic images as opposed to seeing the blurred image immediately. Their behavior was also consistent with typical temporal discounting behavior, which was shown to be cognitively distinct from effort discounting behavior.

Empirical research consistently shows that healthy individuals tend to prefer immediate over delayed rewards, even when the delayed rewards are objectively larger, illustrating the well-established phenomenon of temporal discounting (L. Green & Myerson, 2004; McClure et al., 2004). A noteworthy limitation of temporal discounting tasks is that the isolation of delay often results in repetitive and abstract contexts, potentially encouraging participants to adopt decision-making strategies that may not generalize to real-world behavior. Furthermore, the use of hypothetical rewards and relatively short time horizons may fail to elicit emotional responses comparable to those involved in real-life decisions.

1.3 EFFORT-BASED DECISION-MAKING (EBDM) TASKS

Effort-Based Decision-Making (EBDM) tasks assess how the subjective value of a reward declines as the required effort increases (Docx et al., 2015) – how reward is discounted by effort. Put differently, they aim to quantify the trade-off between effort and reward in experimental settings by measuring the extent to which individuals are willing to exert effort to obtain a reward (Renz et al., 2023).

EBDM tasks are typically categorized into two main types: physical and cognitive (M. F. Green et al., 2015). In the lab, participants must make a choice between a difficult and an easy option to perform a physically or cognitively demanding task. Successful completion of either option yields a reward; however, the more challenging option is associated with a higher reward value.

Physical EBDM tasks can be broadly categorized into motoric tasks, which involve executing specific movements (e.g., button pressing or cycling), and strength-based tasks, which require participants to exert force beyond a predetermined threshold to obtain a reward (Colón-Semenza et al., 2021; Erfanian Abdoust et al., 2024; M. F. Green et al., 2015; Kim et al., 2022; Le Heron, Manohar, et al., 2018). The **Effort Expenditure for Rewards Task** (EEfRT) is a computerized button pressing paradigm that was developed to investigate anhedonia in humans (Treadway et al., 2009). Modifications have been made to EEfRT over the years (Barch et al., 2014; Fervaha et al., 2013; Treadway et al., 2012), but essentially it remains a task that requires varying amounts of speeded manual button pressing on a keyboard for either a high effort option associated with high reward or a low effort option associated with a low reward. The probability of receiving the associated reward is varied across trials irrespective of the chosen option. The discrete fine motor version of the EEfRT, which typically involves keyboard-based responses, has also been adapted to incorporate full-body physical exertion, such as stationary cycling (Colón-Semenza et al., 2021). The

underlying principle remains the same, but effort is modified by varying the resistance of the revolutions and the duration for cycling.

The **Balloon Effort Task** (BET) is another computerized paradigm that requires participants to press the left and right buttons on a game controller alternately to inflate one of two balloons. The 'easy' balloon requires fewer presses and yields a smaller reward, whereas the 'hard' balloon requires significantly more presses but provides a higher reward upon explosion (Gold et al., 2013).

Strength-based EBDM tasks are commonly referred to as hand grip effort tasks, as they typically require participants to use a handheld dynamometer to exert force exceeding a predefined threshold in order to obtain a reward (Docx et al., 2015; M. F. Green et al., 2015; Hartmann et al., 2015). One version of this task is known as the **Apple Gathering Task** developed by Bonnelle et. al 2015 (Figure 1).

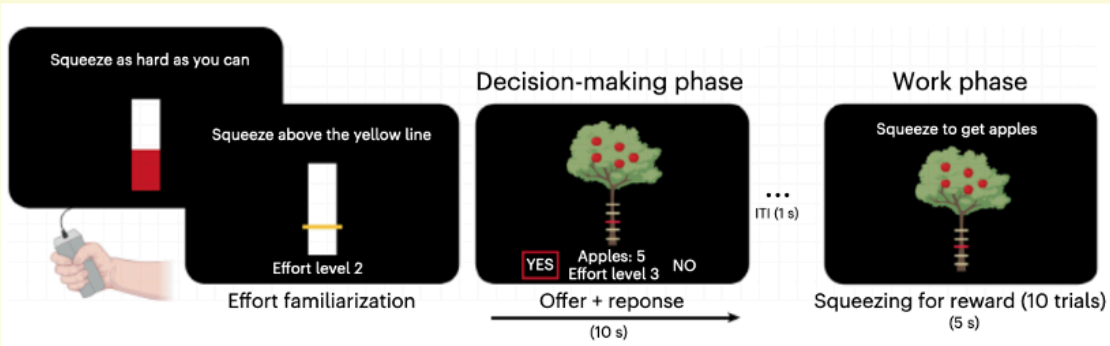

Figure 1. Apple Gathering effort-based decision-making task. After calibrating the hand-held dynamometer to each participant's MVC, participants practiced producing different effort levels indicated by a yellow line; a higher line denoted increased effort. In the main task, they decided whether the offered reward (apples) was worth the required effort. Trials were randomly selected at the end to be physically executed for apples. Reproduced from Attaallah et al., 2024, Nature Human Behaviour, 8, under a Creative Commons Attribution 4.0 International License.

At the start of this behavioral paradigm, participants are asked to grasp a handheld dynamometer in their dominant hand and squeeze it to have it calibrated to their individual maximal voluntary contraction (MVC). Once the device has been calibrated and the

participant is familiar with the extent of exerted force on a graduated scale from 1-5 (5 being the greatest exertion) they are presented with the onscreen task. An apple tree is displayed in the center of the screen with apples (reward) and on the tree trunk the amount of effort required to harvest the apples is shown. The reward and effort vary between trials. On each trial, participants are asked if they would be willing to exert the specified force for the specified reward. If they do not deem the reward worth the required effort, they can select 'No' and move on to another trial but if they select 'Yes' they must then squeeze the handheld with their dominant hand to harvest the apples (Bonnelle et al., 2015; Chong et al., 2017a). Le Heron et. al 2018 conducted a study involving 19 healthy controls using the Apples Gathering Task. These participants exhibited intact, graded effort aversion, demonstrating a willingness to exert greater physical effort as reward value increased (Le Heron, Manohar, et al., 2018).

Cognitive effort tasks have also been deployed to study how humans make decisions which require mental effort. Originally developed to study motivation in non-human animals, the **Progressive Ratio Task (PRT)** has been adapted for human research to assess motivational 'breakpoints'—the point at which an individual ceases to exert effort for a reward (Bland et al., 2016; Heath et al., 2019). Further modifications have transformed the PRT into a cognitive EBDM task (Wolf et al., 2014). In this version of the PRT, participants were presented with pairs of numbers on a screen and asked to identify the larger number. The task consisted of three monetary rewards, each with seven trial blocks. The number of correct responses required to obtain the reward increased with each successive trial block within a reward level, thereby manipulating the level of cognitive effort demanded. Participants were allowed to skip blocks. Wolf et al., 2014 conducted a study with 41 schizophrenic patients and 37 controls. Their findings showed that reduced function in the

ventral striatum was associated with motivation impairments on the PRT in schizophrenic patients.

Demand Selection Tasks (DST) are another example of cognitive EBDM paradigms, that allow for the evaluation of participants' natural preferences or aversions to effort (Gold et al., 2015). Kool et al. (2011) employed a battery of DST variants across six separate experiments in healthy participants, with sample sizes ranging from 16 to 84 per group. Each experiment adhered to the core principle of offering participants a choice between a low-demand and a high-demand option, with the latter involving greater cognitive control requirements such as increased task or strategy switching, frequent context shifts, elevated working memory load, and/or more complex arithmetic processing. Participants were informed that they could freely choose either option across the numerous trials. Results supported the "law of least mental effort," with participants demonstrating a consistent preference for the less cognitively demanding alternatives (Kool et al., 2010).

There is a well-established consensus in the literature that, irrespective of effort type, humans tend to prefer options that are less physically or cognitively demanding (Chong et al., 2017a; Kool et al., 2010; Prévost et al., 2010). While effort aversion can be attenuated by significantly increasing reward value, individuals with intact effort discrimination still tend to prefer easier tasks (Treadway et al., 2012; Westbrook et al., 2013). A recurring theme in EBDM tasks is the inability to completely isolate temporal effects on human behaviour since more effortful tasks often take a longer time to complete compared to simpler options. While there is a wealth of research to elucidate the neural mechanisms underpinning EBDM in animals, studies exploring these processes in humans remain relatively limited (Löffler, 2015; Salamone & Correa, 2024). In this thesis, I will introduce a new version of Circle Quest decision-making task (see below) that requires EBDM.

1.4 EXPLORATION-EXPLOITATION TRADE-OFF (EET) TASKS AND DECISION-MAKING UNDER UNCERTAINTY

As noted earlier, humans routinely face decision-making scenarios involving multiple, non-binary options in everyday life. In an ideal context, it would therefore be optimal to evaluate each available option thoroughly to accurately assess its potential value. However, individuals and organizations typically operate under constraints of limited time and resources, which restrict their ability to thoroughly explore all available options. Additionally, uncertainty arises because information regarding each variable is often incomplete, requiring decisions to be made based solely on the decision-maker's subjective estimation of each option's utility. Experiments involving EET tasks such as Bandit Tasks and the Iowa Gambling Task (IGT) offer some insight into how humans approach this choice dilemma under time and resource constraints.

In **Multi-arm Bandit tasks**, players engage with two or more rewarding options, incurring a cost from an allocated money pot each time they make a selection (Scott, 2010; Slivkins, 2024). Each available option returns various rewards at different unknown probabilities, and the participant is tasked with maximizing their rewards by allocating the majority (or all) of their money to the most rewarding option. Multi-arm bandit tasks give rise to the exploration versus exploitation dilemma that often befalls humans in everyday life (Averbeck, 2015a; Blanco & Sloutsky, 2024; Laureiro-Martínez et al., 2015; Wyatt et al., 2024). Exploration refers to the idea of assessing all presented options repeatedly to determine the best one before committing to it, while exploitation refers to the idea of committing to an option early-on and reaping its benefits with little or no regard to the alternatives.

Though they are entirely different approaches to the same problem, both exploration and exploitation compete for the same scarce resource, i.e. money allocated (Gupta et al.,

2006). Participants who use too much of their limited resource to learn something about the reward probability of each available option risk having fewer resources for exploitation once they have settled on the most rewarding option. However, those who settle for a rewarding option quickly rather than exploring other options run the risk of missing out on a much more rewarding option. Multi-arm bandit tasks take into consideration the fact that humans are not only limited by time, but resources as well. Furthermore, these paradigms allow for participants to return to a previously exploited option—though they must still do so sequentially— and they are not penalized with time delays when switching between the various options.

There are many variations of the multi-arm bandit task. In the stationary version, participants select between two possible actions (bandits) that each has a different stationary payout where each reward and the probability of winning that reward remain fixed throughout the experiment (Averbeck, 2015a). In three-armed novelty version, participants choose from three instead of two arms where the probability for each is different, but the reward is the same for every option (Averbeck, 2015a). For each trial, however, there is a chance that one of the available options will be replaced by a new option, but while an option is available (remains unchanged) its probability is stationary. In non-stationary bandit tasks, participants have two possible arms to choose from, but their rewards change over time, with the expected reward following a decaying random walk (Averbeck, 2015a).

Infinite bandit tasks present participants with an infinite number of arms to choose from to maximize reward (Berry et al., 1997) while in contextual bandit tasks, reward and probability varies from individual to individual depending on their performance (L. Li et al., 2010). The adversarial bandit introduces the element of an adversary: instead of rewards being determined by a stochastic system, an adversary controls the payout of each arm (Auer

et al., 2002; Cesa-Bianchi & Lugosi, 2012); whereas in dueling versions**,** the reward is not absolute, but rather relative (Yue et al., 2012).

An important development in this field was the introduction of the continuous bandit task, in which exploration and exploitation phases of the experiment are separated. The participant is allowed to explore each arm a finite number of times and then reports which arm they think is the best from the available options. They are then free to exploit their chosen arm. A key new metric from this design is that of 'simple regret' – the difference between the average payout of the recommended arm and the average payout of the participant's chosen arm (Bubeck et al., 2011). Finally, in the strategic arm bandit each arm effectively acts as its own strategic agent. One participant (the principal) will pull an arm to receive some reward, but the chosen arm will keep some unknown portion of that reward for itself and give the remainder to the principal. The other arms will receive no reward unless they are selected. Each strategic arm tries to maximize its own utility over the course of the experiment (Braverman et al., 2019).

Though many forms of the bandit task exist, the vast majority of these paradigms have only been studied and modelled for healthy individuals (Averbeck, 2015a; Berry et al., 1997b; Bouneffouf et al., 2017; Kveton et al., 2019; Villar et al., 2015). Results from healthy participants show that they balance the exploration–exploitation dilemma in an adaptive and dynamic manner (Navarro et al., 2016), demonstrating a tendency to increase exploration in response to novelty (Wittmann et al., 2008).

The **Iowa Gambling Task (IGT)** can be conceptualized as a four-arm bandit task. Players are given (loaned) a certain amount of resource (money) and presented with four decks (A, B, C and D) of cards. They are then instructed to select one card at a time from any of the decks (with order totally dependent on the participant) and their aim is to maximize their profit on the loaned money as each card has a certain predetermined value. Turning a

card reveals how much money the participant wins but the card also has a penalty associated with it that the participant must pay (the reward and penalty varies with each deck). The task ends after a series of 100 card selections. Unbeknownst to the player, decks A and B yield higher immediate rewards with greater future penalty that usually incur a net loss, whereas the less rewarding decks C and D yield a greater future net gain (Bechara et al., 1994).
In a study involving 44 healthy controls, Bechara and colleagues found these participants made more selections from the "good" decks (C and D) and avoided the "bad" decks (A and B) (Bechara, 1994). They sampled all decks initially and only returned to the bad decks occasionally after having committed to the good decks. A subset of 5 participants from the control group showed improved performance in repeat testing over a period of 6 months. The healthy controls were able to select the good decks despite a proven inability to keep track of the magnitudes and frequencies of punishment from each deck.

Bechara showed that although healthy human volunteers were usually unable to calculate figures of net losses or gains in exploration-exploitation tasks, they could correctly identify the better options, decks C and D, based on their estimations from experience (Bechara et al., 1994) and this is reflected in their performance on the IGT. However, Steingroever challenged these assumptions citing several studies that show evidence for healthy controls (1) having more variability in their performance than was previously shown, (2) preferring decks B and D which have infrequent losses, and (3) not showing a definitive behavioural switch from exploration to exploitation (Steingroever, 2013). Nevertheless, others have been able to replicate Bechara's findings, commenting that deviations from the procedural details in other studies might have accounted for inter-study variability (Bull et al., 2015).

Mathematical modelling has attempted to explain people's ability to estimate losses and gains, showing how confirmatory biases overestimate the value of more valuable options

and underestimate the value of less valuable options (Lefebvre et al., 2022). There is evidence to suggest that humans may not necessarily be choosing the objectively best choice but instead arrive at conclusions early on, and any new evidence that contradicts their belief is discarded (Palminteri et al., 2017). While this does not result in them making the best decision in every trial, the robustness of the technique as predicted by a Bayesian ideal observer model yields an overall benefit and maximization of reward. Additionally, as humans age, they exhibit more avoidance to net loss by refraining from disadvantageous options (Cauffman et al., 2010).

Although EET tasks such as bandit paradigms and the IGT have provided valuable insights into decision-making, participants are often left unaware of what the ideal outcome should be if the best deck/arm was exploited to the full extent (Deshmukh et al., 2020). However, many real-life scenarios pose a similar challenge in that it may be impossible to attain perfection and regret is inevitable. Nevertheless, EET tasks cannot provide much insight on situations where perfection is attainable. These tasks also heavily rely on participants' memories as they must keep mental logs of previous outcomes for each individual deck/arm. Thus, poor memory would be an important confound to performance, on either bandit tasks or the IGT.

1.5 FORAGING TASKS AND DECISION-MAKING UNDER UNCERTAINTY

Foraging tasks are experimental designs that require subjects to explore a physical or virtual environment in search of a diminishing reward. Generally, subjects are not limited to how long they can remain in the same environment, and they may choose to stay for as long as they see fit before deciding to move to a novel environment in hopes that this "fresh" location will yield a much greater reward than their previous one. Such tasks were developed upon the evolutionary principle that the survival of animals from across species depended on their

ability to acquire energy from their environment in an efficient manner by hunting and gathering their food from areas with ample resources until they became so depleted that it necessitated relocation to a new one (Seidenbecher et al., 2020). Departing to a novel location often requires greater time or effort and carries the risk of lower reward than the previous foraging site, thereby introducing uncertainty.

Over the years, behavioral paradigms that incorporate the foraging or patch leaving model have provided insight about various topics of interest, from visual attention to reinforcement learning and value-based decision-making(Kristjánsson et al., 2020; Seidenbecher et al., 2020). For researchers interested in studying decision-making, the rate at which the reward diminishes in a particular location and the cost of leaving for a new location are some key factors manipulated in the paradigm (Kilpatrick et al., 2021; Mobbs et al., 2018). These manipulations serve to influence the amount of time subjects spend in the same location and how often subjects switch to a new location.

Due to the uncertainty of the reward in the new location, participants risk making poor economic choices, which is more reflective of real-life and makes foraging tasks particularly useful for evaluating how humans go about making decisions. Take for example a person applying to university. They might have applied to several universities and been offered a place to study their desired major in each, but it isn't possible for them to attend all these universities at once. Therefore, they will have to forego accepting all the enrollment offers except for one. If they find that their selection is not as rewarding as they might have hoped, they may have to put in the effort to reapply to and interview for other opportunities or simply remain in their secured program with its current benefits. An example of a foraging task in the scientific literature is the Patch Leaving Task.

The **Patch Leaving Task** involves human research participants harvesting from a virtual location (patch) that provides a reward that is gradually reduced as time goes on

(Averbeck, 2015a). Participants are free to leave the patch whenever they choose and move to a new patch. When presented with this "fresh" patch, they may choose to harvest there or continue to another patch without first harvesting. The choice to move on will incur a time delay. The total time for the experiment is usually fixed so the number of patches visited is dependent on the participant. Constantino and Daw (2015) found that the decisions of 47 healthy participants in a foraging-style task were guided more by the overall reward environment than by trial-by-trial learning. This suggests that people may use broader contextual information to regulate their behavior, rather than relying solely on immediate feedback (S. M. Constantino & Daw, 2015; Sutton, 1988).

The foraging task literature has consistently shown that humans tend to remain longer than is necessary in a harvesting environment which adversely affects their likelihood of maximizing reward (Harhen & Bornstein, 2023; Lenow et al., 2017; Marzecová et al., 2021). According to optimal choice as given by the marginal value theorem (MVT) which was originally developed for animal foraging studies (S. M. Constantino & Daw, 2015; Hutchinson et al., 2008) a participant should leave a current patch when the reward from that patch falls below the average reward from the previous patches. Despite this suboptimal harvesting performance in foraging tasks, humans are able to adapt to changing environments and respond appropriately to the richness of a particular space relative to other environments as predicted by optimal choice (Simonelli et al., 2025). Humans were found to be most sensitive to time whether that was the current interval gone without harvesting, the interval preceding the last capture and time spent in the current environment. While humans do show signs of being responsive to effort costs and rewards (Chong et al., 2017) they are not as sensitive to these factors (despite them being displayed on screen) as they are to the temporal factors (Hutchinson et al., 2008).

Some limitations of foraging tasks are that they operate under the assumption that a participant cannot return to a previous option after abandoning it and that they are only constrained by time. The sequential manner in which participants are required to approach the task only allows them to move in one direction. If they move to a new location only to find it less rewarding than their previous one—even in its depleted state—they cannot return, and must either remain or move on again, facing uncertainty about whether the next location will offer a better payoff, all while incurring additional costs such as time delays. While participants are not limited to how long they can spend in one location, there is a time limit for the overall experiment in which they must try to maximize their rewards. This is one important limitation in foraging tasks which makes them unlike real-life situations where humans are also limited by energy and resources.

1.6 INFORMATION SAMPLING TASKS AND DECISION MAKING UNDER UNCERTAINTY

Decision-making tasks in which participants gather useful cues before reaching a final decision with the aim to minimize risks and maximize rewards, are known as information sampling tasks (Averbeck, 2015a). Unlike the previously discussed exploration-exploitation tasks, information sampling tasks typically feature: (1) potential penalties for gathering more information; (2) rewards contingent only on the final decision; and (3) clearly defined optimal outcomes. Here, the reward depends not on a probabilistic structure but on the participant's accuracy i.e. how closely their final choice aligns with the optimal behavior. In these paradigms, participants must implement a stopping policy: a strategy for determining when they have gathered enough information to make the best decision (Baumann et al., 2020). A real-world example is a person deciding whether to purchase a car: they may gather information from various sources including online reviews, friends, or dealerships, and

prioritize certain attributes (e.g., brand, mileage, cost) over others (e.g., color). Several experimental paradigms have been developed to model this process in the lab.

The **Card-Sampling Paradigm** was introduced by Hertwig and colleagues, building on earlier work (Barron & Erev, 2003; Kahneman & Tversky, 1979). Participants are presented with three decks of cards, each with different payout distributions. They may sample as many cards as desired from each deck before choosing one deck for a final card pick with a real monetary payoff. Hertwig et al. (2004) compared a description group, who received explicit probability information, with an experience group, who learned through repeated sampling. While both groups faced structurally identical problems, description participants overweighted rare events, whereas experience participants underweighted them (Hertwig et al., 2004). This effect consistent with prior findings from Barron & Erev (2003) and Kahneman & Tversky (1979) that showed description–experience gaps.

The **Cambridge Gamble Task (CGT)**, originally named the Information Sampling Task, was developed by Clark et al. (2006, 2009). In this touchscreen task, participants open grey boxes in a 5x5 matrix to reveal either blue or yellow colors, aiming to identify the majority color. In the Fixed Win (FW) condition, there is no cost for opening boxes whereas in the Decreasing Win/Reward Conflict (DW/RC) condition, each additional box incurs a cost, reducing the final reward. Across multiple studies, healthy controls demonstrated a cautious and reflective decision-making style, gathering more evidence and exhibiting lower uncertainty tolerance than clinical populations (Clark et al., 2006, 2008, 2009).

The Beads Task (Furl & Averbeck, 2011) presents participants with two urns: one mostly blue, the other mostly green. After being told the bead proportion (e.g., 60/40 or 80/20), participants draw beads one at a time, incurring a small penalty per draw, and guess the urn at any point. Compared to a Bayesian ideal observer model, participants significantly undersampled, treating information gathering as costly. Though both model and participants

increased sampling with more ambiguous sequences (60/40), the model showed a much greater increase. **The Fish Task** is structurally similar to the Beads Task but involves a more intuitive narrative: a fisherman draws either blue or orange fish from two ponds with inverse ratios (e.g., 80:20 vs. 20:80). Participants observe fish drawn in succession and decide which pond is the source of the samples. Pytlik et al. (2020) found that fewer than half of healthy controls exhibited a jumping-to-conclusions (JTC) bias, as indicated by lower draw-to-decision scores, suggesting some individuals made decisions with minimal evidence (Pytlik et al., 2020).

The Perceptual-Motor Estimation Task (or **Dart Task)** (Juni et al., 2016) involves estimating the location of a hidden circle by touching the screen. Participants may request cues (dart throws) with varying sampling costs across conditions. The task reveals that participants adaptively adjust their sampling based on cost and cue dispersion but still deviate from ideal observer models, sometimes oversampling in high-stakes conditions.

This review of research into decision-making highlights key trends. While early studies (e.g. Tversky & Edwards, 1966) found oversampling, later paradigms like the Card-sampling and Beads tasks revealed undersampling, likely due to implicit costs. When explicit sampling costs are introduced, as in the Dart Task or CGT, participants demonstrate cost-sensitive behavior, adjusting their strategies accordingly. However, a persistent limitation of laboratory-based sampling tasks is that even when sampling costs are defined, they may fail to reflect the complexities of real-world decisions.

CIRCLE QUEST (CQ) DECISION-MAKING TASK

Circle Quest (CQ) is a more recent information sampling paradigm introduced by Petitet et al. (2021). In the **active version** of this touchscreen task, participants search for the location

of a hidden purple circle but can determine both the number and placement of samples themselves. Unlike in the Dart Task (Juni et al., 2016), they have agency. They tap the screen to obtain information about the location of the hidden circle. Each sample they obtain is either a white dot (miss: this location is not over the hidden circle) or a purple dot (hit) which gives an indication of where the circle is hidden (Petitet et al., 2021).

Participants decide when they have sufficient samples to make an informed decision about where the hidden purple circle is located. They then have to drag a blue circle to indicate the presumed location and receive feedback based on spatial accuracy (**Figure 2**). Sampling incurs a cost, reducing the final reward. CQ also includes a **passive version** of the task, where participants evaluate the informativeness of completed searches and accept or reject associated reward offers (**Figure 3**). In this version, there is no direct agency over sampling locations or number. By contrast, in the active version of the CQ task, participants sample and thereby reduce uncertainty about the location of the hidden circle before committing to a decision (**Figure 4**).

Using CQ, Petitet et al. (2021) found a speed–efficiency trade-off: people sampled with greater efficiency (reduced uncertainty about the location of the hidden circle more effectively) when they took longer to deliberate about where they sampled on the screen (**Figure 5A**). In one condition, where participants had to explicitly report their estimate of uncertainty, they proved to be very good at being able to do so. Further, in other conditions, it was found that they adjusted sampling behavior based on manipulated parameters such as reward magnitude, error cost, and time pressure (**Figure 5B**). Importantly, under severe time constraints, participants overcame the trade-off by sampling both faster and more efficiently.

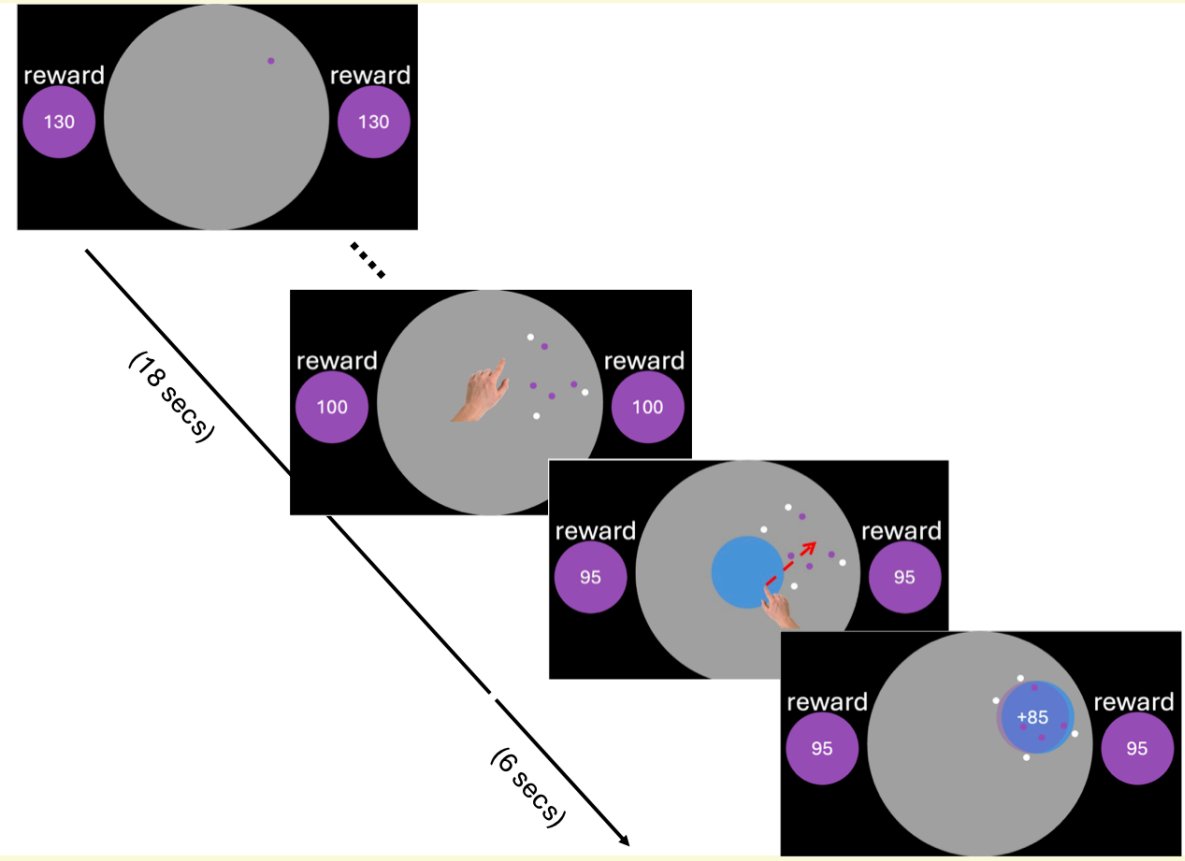

Figure 2. Circle Quest (CQ) active sampling task. Active sampling version of the CQ task where participants tap the screen to locate a hidden purple circle, then drag a blue disk to its presumed location. Participants lose credits each time they tap the screen and place a dot, and their final reward is determined by the accuracy of their placement.

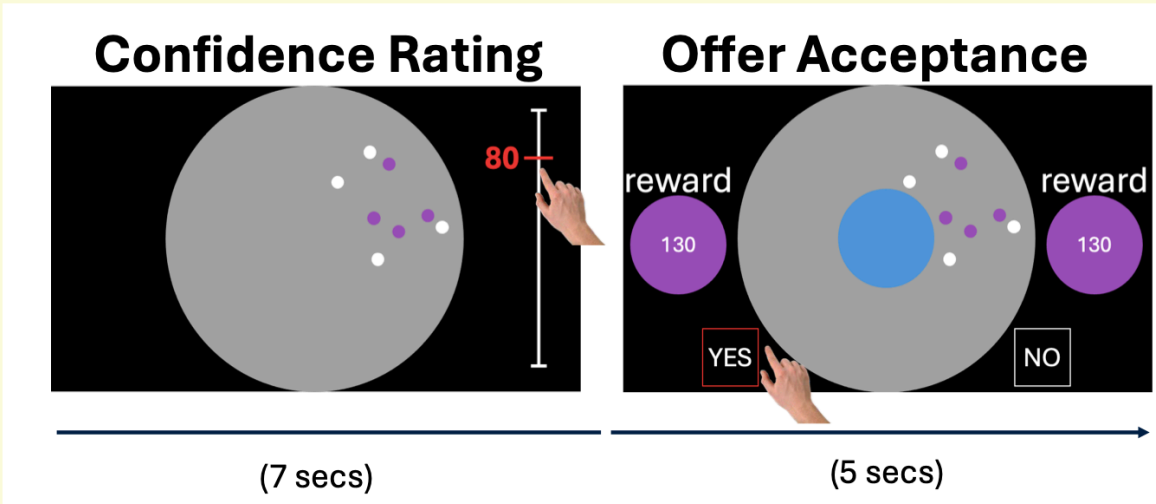

Figure 3. Circle Quest (CQ) passive choice task. Passive choice version of CQ task where participants evaluate the informativeness of completed searches before accepting or rejecting the trials based on the associated reward offers.

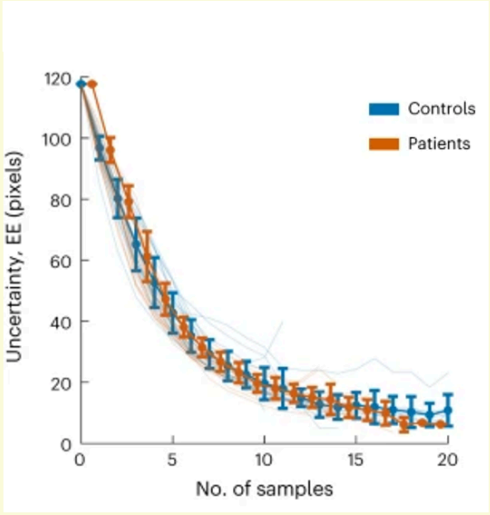

Figure 4. Uncertainty reduction through information gathering in the CQ Active Sampling task.
In this task, participants actively decided both how many samples to collect and where to place each one, granting them full control over the informativeness of their sampling strategy. As expected, uncertainty about the hidden circle's location—quantified as expected error (EE)—tended to decrease as sampling progressed. Data shown are from a cohort of 19 autoimmune limbic encephalitis (ALE) patients and 19 age-matched healthy controls.
Adapted with permission from Attaalah et al. (2024). The role of the human hippocampus in decision-making under uncertainty. Nature Human Behaviour. https://doi.org/10.1038/s41562-024-01855-2

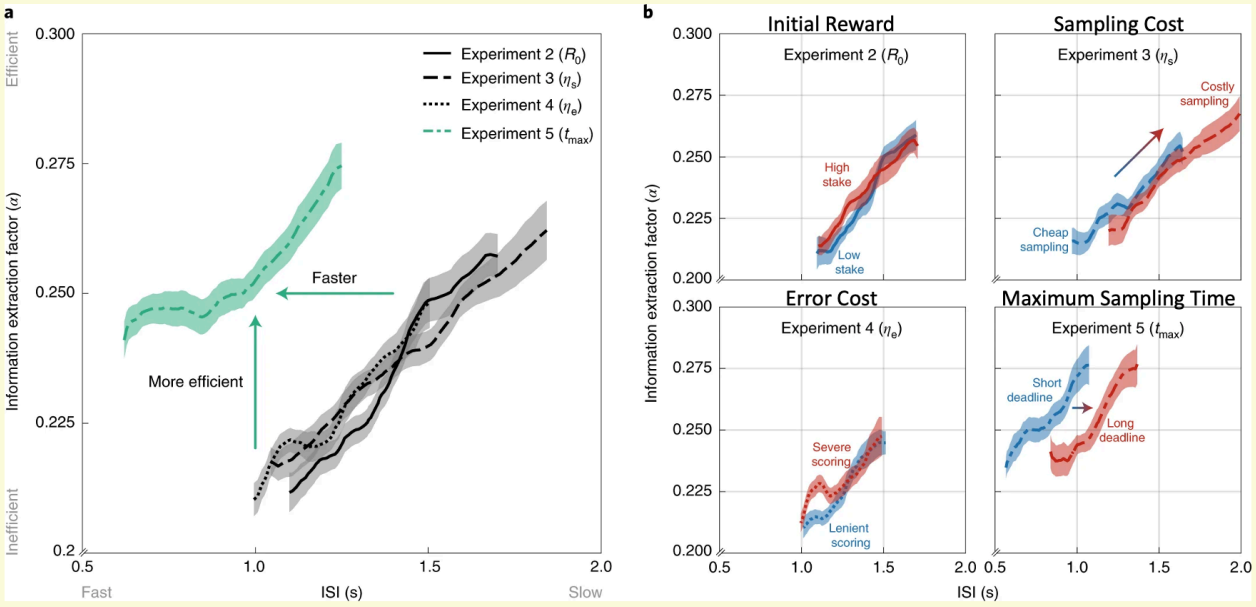

Figure 5. Sampling efficiency for the four CQ experimental conditions. (**A**) Four task parameters (initial reward (R_0), sampling cost (η_s), error cost (η_e), and maximum sampling time (t_{max})) were manipulated to create different versions of the active sampling CQ task. Participants demonstrated the highest sampling efficiency under significant time pressure. The information extraction factor (α) refers to the rate at which participants reduced uncertainty (expected error) by accumulating more dots during the active sampling task and ISI is the intersampling interval, time between successive samples. (**B**) Comparing economic constraints (experiments 2–4) with time pressure (experiment 5) revealed distinct patterns: under economic constraints, participants showed a trade-off between speed and efficiency (slower sampling led to greater information gain), whereas under time pressure, participants were able to break this trade-off by sampling both quickly and efficiently.
Adapted with permission from Petitet et al. (2021), The computational cost of active information sampling before decision-making under uncertainty, Nature Human Behaviour, Springer Nature.

The studies presented in this thesis utilize CQ as the behavioral paradigm to investigate decision-making under uncertainty in humans. Elderly healthy controls (HC), SVD patients and MFL patients were tested using the active and passive versions of the CQ task introduced by Petitet et al., 2021. However, my focus was not on exploring the speed-

efficiency trade-off within these groups, but rather to investigate whether structural brain changes (in SVD and MFL patients) affect sensitivity to sampling cost, reward and uncertainty. Additionally, I tested a modified version of the CQ paradigm in HC and SVD patients to examine how the presence of physical effort might alter the participants' observed behaviour on the CQ task. This version, designed to investigate effort-based decision-making (EBDM) under uncertainty, was similar to the passive version of CQ (Attaallah et al., 2024a). However, participants had to make a decision (accept or reject trials) after considering three attributes (reward, uncertainty *and effort*) instead of only two (reward and uncertainty).

The CQ paradigm offers several key advantages over traditional decision-making tasks. Unlike descriptive probabilistic tasks that rely on binary choices, CQ promotes greater engagement through its continuous, interactive nature. Unlike temporal tasks with hypothetical delayed rewards, CQ provides real, immediate incentives, enhancing ecological validity. In the new variant I introduced, it also introduces an effort component, addressing an underexplored factor in human decision-making. Compared to bandit tasks, CQ reduces memory demands while still allowing for optimal strategies. Unlike foraging tasks, CQ limits resources and energy expenditure, encouraging more strategic behavior. Additionally, CQ features explicit sampling costs—unlike most information sampling paradigms—making information gathering both costly and meaningful. While the Dart Task (Juni et al., 2016) also includes explicit sampling costs, CQ uniquely gives participants agency to choose where to sample next, allowing some samples to be more informative than others. Together, these features make CQ a dynamic and realistic paradigm well-suited for studying complex decision-making.

1.7 SUMMARY ON DECISION-MAKING TASKS

Decision-making research encompasses a range of behavioural paradigms, with many aiming to maximize rewards while minimizing time, effort, and cost. This body of research reveals key aspects of decision-making behaviour in healthy humans, shedding light on how they balance rewards, costs, uncertainty, and effort in complex and dynamic environments. Descriptive Probabilistic Tasks reveal that people tend to overweight rare events and exhibit loss aversion, meaning they dislike losses more than they value equivalent gains (Kahneman & Tversky, 1979). Temporal discounting tasks show people's preference for immediate rewards over larger delayed ones, illustrating the human bias toward instant gratification. Effort-based decision-making paradigms replicate real-life scenarios where physical or cognitive effort is required, and research consistently finds that people generally avoid higher effort regardless of its nature. Exploration-exploitation tasks highlight humans' capacity to select better options among alternatives, even though choices are often influenced by personal biases; notably, this discriminatory ability tends to improve with age (Cauffman, 2010). Foraging tasks simulate environments of diminishing returns, demonstrating that individuals are particularly sensitive to time, costs, and rewards and adjust their behaviour appropriately when rewards fall below ideal thresholds (S. M. Constantino & Daw, 2015). Finally, information sampling paradigms require participants to actively gather information to make accurate decisions, showing that people prefer to tolerate low levels of uncertainty and are sensitive to sampling costs (Clark et al., 2009; Juni et al., 2016). They also tend to sample more efficiently when deliberating longer and can even overcome the typical speed-efficiency trade-off under significant time pressure (Petitet et al., 2021).

In conclusion, research on decision-making reveals that humans tend to exhibit strong aversions to loss, effort, and delay. While they often rely on heuristics and occasionally adopt suboptimal strategies, cognitively intact individuals are generally capable of identifying and

selecting more rewarding options from among alternatives. Each decision-making paradigm offers valuable insight into different facets of human behaviour; however, many carry inherent limitations in ecological validity. The rationale for selecting CQ as the paradigm for the studies in this thesis lies in its ability to address several of these limitations. By integrating interactive sampling, explicit costs, and real-time reward feedback, CQ provides a dynamic and realistic framework for investigating how structural brain changes and physical effort demands shape human decision-making under uncertainty. The following section will examine how structural brain changes such as vascular pathology and brain lesions impact decision-making, highlighting the effects of structural disruption on cognitive control and valuation mechanisms.

THE ROLE OF WHITE MATTER (WM) DYSFUNCTION IN DECISION-MAKING

In the previous section, I discussed findings from the human decision-making literature in healthy individuals. Here, I examine how a neurological disorder with vascular pathology can influence decision-making behaviour, assess its validity as a research model, and propose a suitable task for investigating its impact on decision processes. SVD is a neurodegenerative condition that selectively affects the white matter (WM) in the brain (Pantoni, 2010; Wardlaw et al., 2019). It offers an important opportunity to examine the role of WM dysfunction – or functional disconnection – on decision-making.

1.8 Cerebrovascular Small Vessel Disease (SVD)

SVD refers to a group of diseases that damage the small blood vessels of the brain and is the most common cause of vascular dementia (Q. Li et al., 2018; Pinter, 2015; Teng et al., 2017). Magnetic resonance imaging (MRI) is the primary modality for *in vivo* detection of SVD-related changes due to its superior sensitivity to soft tissue contrast and microstructural

abnormalities (Berger, 2002). MRI operates on the principle of nuclear magnetic resonance, leveraging the abundant hydrogen protons in water and fat molecules within biological tissues (**Figure 6A**). Under normal physiological conditions, these protons spin with random orientations but remain susceptible to magnetic induction due to their intrinsic angular momentum (spin) and associated magnetic moments. (**Figure 6B**). In a strong static magnetic field (B_0), these protons align either parallel or anti-parallel to the field, generating a net longitudinal magnetization vector (**Figure 6C**). When a radiofrequency (RF) pulse tuned to the Larmor frequency is applied, it transfers energy to the system, causing hydrogen protons to shift from a low- to a high-energy state. This process tips the net magnetization vector from its alignment along the longitudinal axis into the transverse plane, generating a coherent signal that can be detected as it decays over time. Upon cessation of the RF pulse, the protons return to equilibrium via two relaxation processes: longitudinal (T1) and transverse (T2) relaxation.

Crucially, the relaxation times of hydrogen protons vary across tissue types due to differences in molecular environments; for example, water-rich cerebrospinal fluid (CSF) has longer T1 and T2 relaxation times than both grey matter (GM) and myelin-dense WM (WM), with WM exhibiting the shortest relaxation times due to its tightly packed, lipid-rich microstructure. These differences are exploited by tailored pulse sequences (e.g., T1-weighted, T2-weighted, and FLAIR) to generate tissue-specific contrast. In the context of SVD, these sequences enable the visualization of characteristic lesions including white matter hyperintensities (WMHs) on T2 and FLAIR, lacunes and microinfarcts as hypointense cavities, cerebral microbleeds via susceptibility-weighted imaging (SWI), enlarged perivascular spaces, and regional or global atrophy (**Figure 7**). This high-resolution structural imaging allows for mapping of lesion burden and distribution, making SVD an important

model for investigating the correlation between neuroimaging markers, clinical severity, and cognitive or behavioral outcomes.

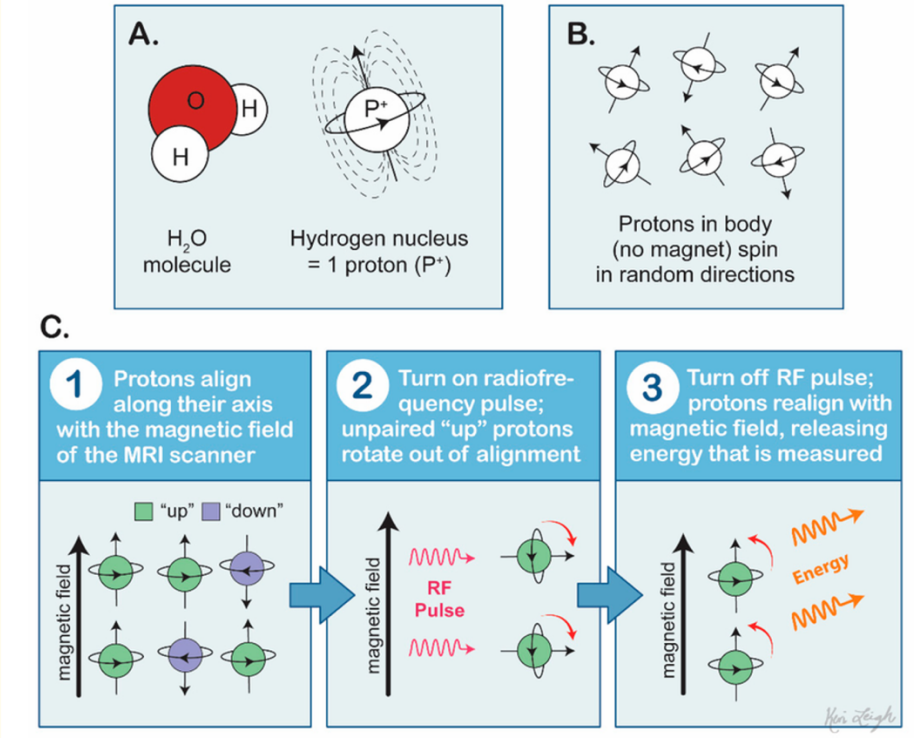

Figure 6. The Physics of MRI. (**A**) Hydrogen atoms, abundant in brain tissue due to their presence in water molecules, possess intrinsic spin. (**B**) In the absence of an external magnetic field, the spins of hydrogen atoms are randomly oriented. (**C**) In the presence of a strong magnetic field, protons align parallel to the field. A radiofrequency (RF) pulse temporarily disrupts this alignment; as the protons realign with the field, they emit energy, which is captured to generate high-resolution images of brain tissue.
Adapted from Fordham et al. (2021), "Differentiating Glioblastomas from Solitary Brain Metastases," Cancers, 13(12), 2960. https://doi.org/10.3390/cancers13122960. Licensed under CC BY 4.0 (https://creativecommons.org/licenses/by/4.0/).

Compared to age-matched healthy individuals, SVD patients typically show and quantifiable abnormalities in WM and GM microstructure. Advanced MRI analysis techniques such as Brain Intensity AbNormality Classification Algorithm (BIANCA), Diffusion Tensor Imaging (DTI), Tract-Based Spatial Statistics (TBSS), and Neurite Orientation Dispersion and Density Imaging (NODDI) can help to assess microstructural

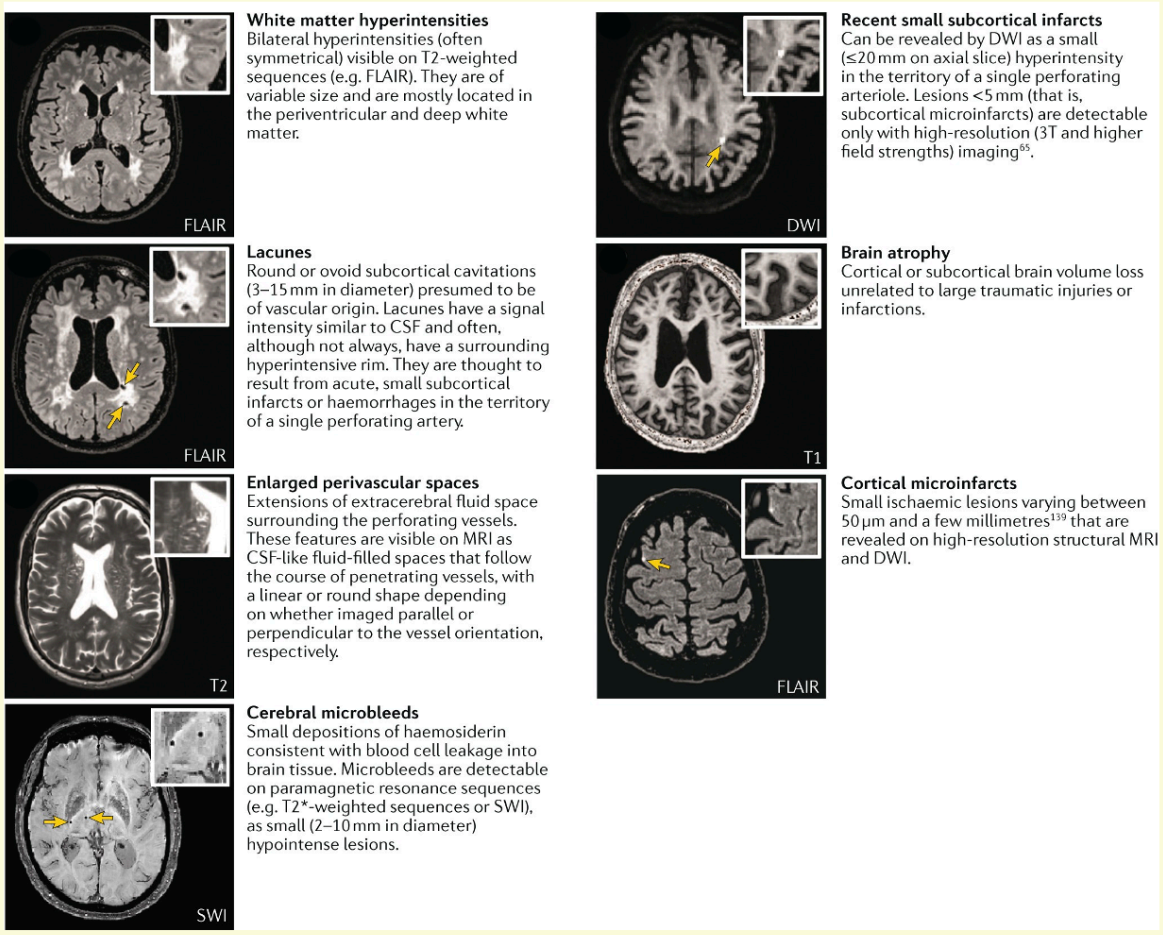

Figure 7. Features of cerebrovascular SVD on MRI. This schematic illustrates key MRI markers of cerebral SVD, including white matter hyperintensities, lacunes, cerebral microbleeds, and enlarged perivascular spaces, as observed on conventional imaging sequences. Figure adapted from ter Telgte et al., 2018. Permission requested.

changes in the brain associated with SVD (Griffanti et al., 2016a; O'Donnell & Westin, 2011; Smith et al., 2006; H. Zhang et al., 2012).

BIANCA, a supervised machine learning algorithm applied to FLAIR and T1-weighted images, automatically segments WMHs by classifying voxels based on intensity and spatial features, providing objective measures of WMH volume and distribution (Griffanti et al., 2016a). WMH are common radiological features of normal ageing, however, their progression is typically more extensive and accelerated in individuals with SVD (Jochems et al., 2022).

DTI characterizes the directional movement of water molecules, producing metrics such as fractional anisotropy (FA), mean diffusivity (MD), radial diffusivity (RD), and axial

diffusivity (AD). Reduced FA and elevated MD are observed in SVD patients, indicating demyelination, axonal degeneration, and increased extracellular water (Duering et al., 2018). TBSS, a voxel-wise statistical analysis of DTI data, enhances the anatomical alignment of WM tracts across individuals and reveals focal microstructural damage along the major fiber bundles. SVD patients show decreased WM integrity, predominantly in the forceps minor, forceps major, corticospinal tracts, inferior fronto-occipital fasciculus, superior and inferior longitudinal fasciculi, and anterior thalamic radiation (Hu et al., 2022).

NODDI, an advanced multi-shell diffusion imaging model, distinguishes between intra-neurite and extra-neurite water compartments and provides indices such as neurite density index (NDI) and orientation dispersion index (ODI) (H. Zhang et al., 2012). In SVD, reduced NDI and altered ODI are indicative of disrupted neurite integrity and altered microstructural organization (Dobrynina et al., 2024; Hong et al., 2021). However, NODDI metrics have been reported to be less reproducible (Konieczny et al., 2021). Collectively, these advanced MRI techniques allow for the characterization of tissue damage beyond conventional imaging markers.

Additionally, studies have provided strong evidence of SVD markers' association with stroke, dementia and even depression (Rensma et al., 2018; Stewart et al., 2021). SVD has also been associated with impairments in executive function, information processing speed, and overall cognition (Croall et al., 2017; Huijts et al., 2013), discussed further below. Moreover, cognitive symptoms in SVD may progress gradually in some individuals, although the rate of decline is highly variable (Aarsland et al., 2004; Ide et al., 2024; Lawrence et al., 2015; Wilkosz et al., 2010). This relative preservation of function in the earlier stages can be advantageous for clinical research, as individuals are more likely to retain the cognitive capacity to engage in complex behavioural tasks. SVD stands to offer important insights into WM dysfunction, particularly in the frontal lobes, which are commonly and

disproportionately affected by deep WMHs (Sachdev et al., 2007; Wen & Sachdev, 2004). This predilection is attributed to the vulnerability of frontal perforating arteries to ischemia and age-related vascular risk (Gootjes et al., 2004). Frontal WMH burden is consistently among the highest observed inageing and SVD cohorts, and is significantly associated with cognitive performance in domains such as executive function and processing speed (Vergoossen et al., 2021).

1.9 Role of WM in Cognition and Decision-Making in SVD

Previous research studies involving SVD patients have found that WMH burden contributes to impaired performance on tests of executive function, attention, memory and psychomotor speed as well as on global cognitive test scores (Alves et al., 2008; Jochems et al., 2025; Jokinen et al., 2009; van der Flier et al., 2005; Verdelho et al., 2007; S. Wang et al., 2022). For example, Jochems et al. (2025) demonstrated that WMH progression showed poorer performance on executive tasks such as the Trail Making Test (TMT). Similarly, Wang and colleagues (2022) found that increased WMHs correlated with slowed psychomotor speed on the TMT. Moreover, specific WM tracts, including the anterior thalamic radiation and superior longitudinal fasciculus, have been linked to these cognitive deficits, suggesting that disruption of fronto-subcortical circuits plays a key role in the observed impairments (Crockett et al., 2021; Huang et al., 2020; X. Li et al., 2024). However, there has been a relative lack of work on how SVD might impact human decision-making.

One group of investigators reported that poorer decision-making abilities on the IGT in older adults is associated with cortical WM integrity throughout the human brain (Timpe et al., 2011). In a different study which examined EBDM using the Apple Gathering Task in 82 patients with SVD significant differences were found between the way some patients performed compared to age-matched controls (Saleh et al., 2021a). Specifically, SVD

patients with clinical apathy (loss of motivation to execute goal-directed behaviour) were less likely to accept offers when either the reward was low, or the effort required was high. Similarly, in an investigation of patients with a genetic form of SVD, Cerebral Autosomal Dominant Arteriopathy with Subcortical Infarcts and Leukoencephalopathy (CADASIL), using the same task, apathy was associated with diminished reward sensitivity, but with relatively preserved effort discrimination (Le Heron, Manohar, et al., 2018). These findings imply that reduced goal-directed behaviour in SVD may stem more from both blunted reward sensitivity and increased effort aversion. However, both studies reported weak associations between behavioural outcomes and WM structural measures, highlighting the need for further research into the neurobiological mechanisms underlying these effects.

In this thesis, I use the CQ task to examine decision-making under uncertainty in SVD. To the best of my knowledge this form of decision-making has not been investigated previously in SVD. The nature of WM disruption in SVD provides an important system in which to examine whether – and how – such changes in WM tracts affects performance when people make decisions under uncertainty.

DECISION-MAKING IN PATIENTS WITH MEDIAL FRONTAL LESIONS

In the previous section we discussed how SVD, a vascular pathology affecting the brain's WM matter, can influence decision-making. In this thesis, I also attempted to examine a second group of patients with specific damage to the medial frontal lobe (MFL).

1.10 HUMAN DECISION-MAKING AND THE FRONTAL LOBE

Human decision-making is often an underdiscussed component of executive functioning. Other components of executive function such as working memory have often taken priority when evaluating the behavioral implications of frontal lobe damage (Baddeley, 1992). Nevertheless, some cognitive assessments of patients with frontal lobe damage have focused

on working memory and problem-solving abilities, with problem-solving representing a cognitive domain that is more closely related to decision-making (Burgess, 2010; Koechlin, 2016; Roca et al., 2010; Stuss, 2011; Stuss & Alexander, 2000).

Other investigators have employed some of the decision-making tasks I discussed in earlier sections of this chapter. For example, a study by Cardoso and colleagues (2014) reported evidence of patients with frontal lobe damage having impaired performance on the IGT when compared to controls (Cardoso et al., 2014). As discussed earlier, however, the IGT is heavily reliant on intact memory and does not adequately account for the cost of sampling additional information. A task such as the CQ paradigm, which allows for active sampling while isolating components such as cost and reward while minimizing memory confounds, may offer better insights into these unresolved issues. Although many studies have investigated patients with frontal pathology, here I focus on patients with lesions to the medial frontal lobe (MFL), a region critically involved in reward-based decision-making and performance monitoring (Kennerley & Walton, 2011a; Silvetti et al., 2014).

1.11 MEDIAL FRONTAL LOBE

The MFL is a critical region of the human brain (Figure 8) which consists of a dorsal region that includes the anterior cingulate cortex (ACC) and the prefrontal cortex (PFC) (Vega et al., 2016). The PFC is also subdivided into several regions, including the dorsomedial prefrontal cortex (dmPFC), the ventromedial prefrontal cortex (vmPFC) and the medial orbitofrontal cortex (mOFC).

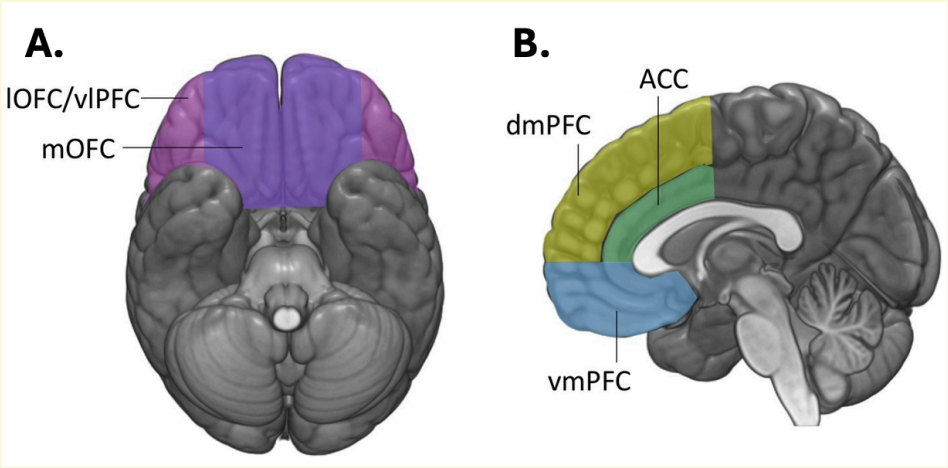

Figure 8. Subregions of the MFL. (**A**) Ventral view illustrating the medial orbitofrontal cortex (mOFC) flanked on both sides by the lateral orbitofrontal cortex (lOFC) and ventrolateral prefrontal cortex (vlPFC) . (**B**) Sagittal view illustrating the dorsomedial prefrontal cortex (dmPFC), ventromedial prefrontal cortex (vmPFC), and anterior cingulate cortex (ACC). These regions are critical for decision-making, social cognition, and emotion regulation. Adapted from: Messimeris D, Levy R, Le Bouc R. (2023). Economic and social values in the brain: evidence from lesions to the human ventromedial prefrontal cortex. Front Neurol. Sec. https://doi.org/10.3389/fneur.2023.1198262. Licensed under CC BY 4.0 (https://creativecommons.org/licenses/by/4.0/).

1.12 HUMAN DECISION-MAKING IN MFL LESIONED PATIENTS

Damage to the MFL has been associated with a variety of cognitive and affective deficits, including impairments in executive functions, attentional control, self-referential processing, emotion regulation, social cognition, and decision-making (Yuan & Raz, 2014). However, the effects of MFL lesions on human decision-making remain contentious in the literature, possibly because of the functional and structural heterogeneity of this area of the brain (Brand et al., 2006; Yu et al., 2020). Human decision-making can be categorized into various types of cognitive process, each of which may recruit different parts of the frontal lobe. Additionally, the discourse may be further complicated because of the brain's remarkable ability to compensate for damage, especially in cases where a structure is bilateral (Voytek et al., 2010).

At the turn of the century, Bechara provided evidence for six patients with bilateral damage to the vmPFC who made poor decisions when presented with the IGT (Bechara,

1994; Bechara et al., 2000). The vmPFC lesioned patients' apparent 'myopic' view of future consequences made them more inclined to choose the disadvantageous card decks over the advantageous options. Manes and his colleagues (2002) found similar results a few years later when they reported impaired performance of 18 patients with single focal lesions to the dorsomedial prefrontal cortex (dmPFC) on the IGT (Manes et al., 2002). This same study, however, found no significant impairments when patients performed the Gamble Task and the Risk Task (Rogers, Everitt, et al., 1999; Rogers, Owen, et al., 1999), both designed to assess different aspects of decision-making under uncertainty. In the Gamble Task, participants choose between red and blue boxes with varying probabilities of reward, followed by a separate betting phase where they wager based on confidence—allowing probabilistic reasoning and risk preference to be independently assessed. In contrast, the Risk Task embeds the gamble within the decision itself by varying both reward magnitude and probability across options, thereby capturing the trade-off between likely but low-reward choices and unlikely but high-reward alternatives. The preserved performance on these tasks suggests that medial frontal lobe damage, regardless of lateralization, may not disrupt externally guided probabilistic or risk-based decisions, but may instead impair decisions requiring prospective, internally generated evaluation.

Another investigation conducted by Fellows and Farrah in 2005 also reported that damage to either the vmPFC or dorsolateral prefrontal cortex (dlPFC) resulted in impaired performance on the IGT in 20 lesioned patients (Fellows & Farah, 2005). However, when a version of the task was administered with "shuffled" decks (the order of cards within each deck was randomized on every trial) only patients with dlPFC lesions remained impaired. This contrasts with the original version of the task, in which fixed card sequences within each deck allow participants to gradually learn from consistent reward and punishment patterns. By removing these predictable sequences, the shuffled version minimized reliance on

habitual learning and instead emphasized abstract value representation and prospective reasoning. The findings suggest that damage to the vmPFC may disrupt future-oriented planning and the ability to assign long-term value to choices, rather than impair general learning of reward contingencies.

Beyond tasks involving ambiguity, such as the IGT, the vmPFC has also been consistently implicated in decision-making under risk, where outcome probabilities are explicitly known. Clark et al. (2004 and 2008) showed that patients with lesions to the vmPFC exhibited increasing betting behavior when asked to complete the CGT compared to controls (Clark et al., 2008; Clark & Manes, 2004). They accomplished this first in a group of 46 patients with unilateral lesions of the frontal lobe and later in a group of 20 patients with focal lesions to the vmPFC. Similar findings were reported by Weller et. al, 2007 when riskier decision-making was observed in seven patients with bilateral vmPFC lesions who completed a computerized version of the cup task, a similar paradigm to the CGT without the wagering, which has sure gain and sure loss trials with the additional option to choose an alternative that was 50/50 no gain/loss or greater gain/greater loss (Weller et al., 2007). Lesioned individuals performed sub-optimally when considering both greater gains and losses.

The Roulette Betting Task (RBT), which resembles the CGT but includes both positive and negative odds, was used by Studer et al. (2015) to replicate Clark's earlier findings of increased betting behaviour in 13 patients with vmPFC lesions. (Studer et al., 2015). Similarly, Levens and colleagues used a gambling task in a separate cohort of 13 patients with frontal lobe lesions and reported comparable results, further supporting Clark's conclusions regarding the role of frontal regions in decision-making under risk (Levens et al., 2014). Somewhat contrary to these findings, however, there is a report in the literature that

although patients with bilateral damage to the vmPFC are indeed risky decision-makers, this might occur only in cases of sure loss (Pujara et al., 2015).

Risky decision-making unlike those under uncertainty show no evidence of being affected by damage to the dmPFC. Rogers, Everitt et al. 1999 had participants complete a version of the CGT and found that 20 patients with either dorsolateral or dorsomedial lesions were unimpaired compared to controls (Rogers, 1999).

Despite the overwhelming evidence that damage to the vmPFC might result in sub-optimal performance in decision-making tasks, there is a case to be made that lesions to this brain region might have positive effects on human decision-making. As was highlighted earlier, the evaluation stage of decision-making is susceptible to individual biases. Manohar et. al, 2021 provided evidence for an ameliorating effect (better performance) of vmPFC lesions using a reversal learning and gambling task that included probabilistic learning and a post-decision wager (S. Manohar et al., 2021). Consistent with previous betting tasks, 16 patients with unilateral lesions of the vmPFC placed higher bets than healthy controls. These patients, unlike their healthy counterparts, also showed weaker biases in their responses to the outcome of previous trials and the unchosen option. One lone patient with bilateral lesions of the vmPFC included in the experiment proved to be an anomaly. Though he was also less biased along with the other lesioned patients, he had the best overall performance among all participants, exhibiting a more rational betting strategy than even healthy controls.

While the ACC is widely implicated in decision-making, particularly in evaluating outcomes and guiding adaptive behavior, the effects of focal ACC lesions in humans remain underexplored (Baird, 2006). Much of our understanding stems from animal electrophysiology and human neuroimaging studies (Gangopadhyay et al., 2021; Monosov et al., 2020; S. Wang et al., 2017) , which have linked the ACC to functions such as conflict monitoring, error detection, and value-based adjustment. Although some lesion studies, such

as those examining frontal lobe damage (e.g., (Bechara, 1994, 2004; Bechara et al., 2000; Fellows & Farah, 2005, 2007), involve portions of the ACC, these lesions typically span multiple medial structures, making it difficult to isolate the functional contribution of the ACC itself. A similar issue arises in lesion cases reported by Manohar et al., where parts of the ACC is involved but the damage is not exclusive. This underscores a key methodological challenge in human lesion research, where damage restricted solely to a part of the brain is exceedingly rare. Moreover, recruiting patients with well-characterized, anatomically selective lesions remains inherently difficult (Rorden & Karnath, 2004). As a result, while converging evidence supports the ACC's role in decision-making, definitive lesion-based dissociation studies in humans remain limited, reinforcing the continued importance of multimodal approaches that integrate lesion studies with neuroimaging and behavioral analysis.

CONCLUSION

Effective decision-making relies on the coordinated activity of several key brain regions, each contributing to different stages of the process (Broche-Pérez et al., 2016; Opris & Bruce, 2005). Notably, these regions are not always anatomically adjacent, underscoring the distributed and integrative nature of the neural networks involved, as well as the critical role of WM pathways that support their interconnectivity. SVD is a neurodegenerative disorder that disrupts network connectivity within the brain, and research has shown impairment, at least in effort-based decision-making in this patient group (Le Heron, Manohar, et al., 2018; Saleh et al., 2021a). While this behavioural dysfunction has been linked to apathy, the underlying structural and functional mechanisms remain unclear, warranting further investigation using more nuanced paradigms such as the CQ paradigm.

The MFL also plays a crucial role in human decision-making and damage to this brain area can alter behavior significantly. Given the anatomical and clinical rarity of lesions confined solely to the anterior cingulate cortex (ACC), isolating its causal contribution to human decision-making remains a key gap in the lesion literature. In contrast, lesions of the dmPFC and vmPFC in humans has been studied quite extensively but with varying results, as discussed above. Damage to these areas of the prefrontal cortex have largely been shown to have deleterious effects on human decision-making but in rare cases such injuries can result in advantageous behavior (S. Manohar et al., 2021). Possible reasons for the heterogeneity in the data surrounding the effect of dmPFC and vmPFC lesions could be due to the inconsistencies in extent of the lesions, lateralization of the injury and the compensatory responses. Notwithstanding, there is much evidence to suggest the dmPFC's importance in decision-making under uncertainty and the vmPFC's significance in both decision-making under uncertainty and with risk. Damage to the vmPFC leads to an impaired ability to foresee future consequences, learn from experience to influence future decisions, and produces riskier behavior in humans (Bechara et al., 2000; Clark et al., 2008). vmPFC damage may also reduce subjective bias in a way that leads to more rationale decision-making.

One aim of this thesis is to evaluate decision-making in a representative group of MFL patients by examining the roles of the dmPFC, vmPFC and ACC, in conjunction with the WM tracts that project to and from these regions, using the CQ task paradigm. The chapters that follow are structured as outlined below, each addressing a specific aspect of the research topic:

In **Chapter 2**, I will present an analysis of neuroimaging data from SVD patients comparing them to age-matched healthy controls (HCs), establishing the structural context for subsequent behavioral findings.

In **Chapter 3**, I will focus on behavioural findings from the core CQ task paradigm administered to SVD participants and HCs and evaluate these in relation to clinical characteristics and neuroimaging markers.

In **Chapter 4**, I will extend this investigation to a new effort-based variant of the CQ task within the same groups (SVD and HCs), integrating behavioral outcomes with clinical and structural imaging data to assess the influence of physical effort.

In **Chapter 5**, I will consider the performance of MFL patients compared to HCs on the CQ task. Behavioral patterns are interpreted alongside neuroimaging and clinical profiles to elucidate the role of MFL in decision-making.

In **Chapter 6**, I will synthesize the insights from all preceding chapters, drawing together behavioral, clinical, and neuroimaging evidence to address the central research question of how uncertainty in decision-making is managed, and how this is disrupted by structural brain pathology.

2| Impact of SVD on the human brain

2.1 Abstract

SVD is conventionally diagnosed based on characteristic neuroimaging abnormalities visible on structural MRI scans. WMH, lacunes, perivascular spaces, and microbleeds are commonly reported features. The analyses presented in this chapter compared neuroimaging measures in patients with SVD and age-matched healthy controls (HC), with the aim of establishing the structural context for the behavioural findings reported in subsequent chapters.

WMH burden was quantified using the FSL BIANCA algorithm, which revealed the expected increase in WMH volume in the SVD group relative to HC. Diffusion MRI analyses, conducted with both diffusion tensor imaging (DTI) and neurite orientation dispersion and density imaging (NODDI), demonstrated widespread reductions in WM microstructural integrity in patients with SVD. Tract-based spatial statistics (TBSS) confirmed the diffuse nature of these alterations across major WM tracts. Together, these findings align with prior reports of SVD-related disruption to global WM architecture.

In summary, the results of this chapter establish that the SVD group recruited for this study differed significantly from the age-matched HC group across several neuroimaging measures. These analyses demonstrate that the SVD sample is representative of the disease population and provide the necessary structural context for interpreting the neuroimaging–behavioural relationships examined in subsequent chapters.

2.2 Introduction

SVD is a chronic, progressive condition commonly seen in ageing populations and associated with a range of structural abnormalities in the brain (Pantoni, 2010). Although its underlying pathology evolves over many years, the diagnosis is typically based on characteristic

neuroimaging findings (Duering et al., 2012; Huijts et al., 2013; Konieczny et al., 2021). Conventional MRI markers of SVD include white matter hyperintensities (WMH), lacunes, enlarged perivascular spaces, cerebral microbleeds, and cortical atrophy (Wardlaw et al., 2019). These features, standardised in criteria such as STRIVE-1 (Wardlaw et al., 2013) and STRIVE-2 (Duering et al., 2023), form the basis of most clinical and research definitions of the disease. However, many of these imaging markers are not exclusive to SVD and may also be present, to a lesser degree, in healthy ageing (O'Sullivan et al., 2001). This complicates the diagnostic process and necessitates a nuanced interpretation of structural imaging findings.

A further limitation of conventional structural MRI lies in its inability to directly visualise the small perforating arterioles affected in SVD (Blair et al., 2017). Most clinical protocols rely on 1.5T or 3T MRI, which are insufficiently sensitive to detect damage at the level of microvasculature. Consequently, assessments of disease burden often depend on the volume or distribution of secondary features such as WMH or microbleeds.

Visual rating scales are commonly used to assess WMH, but they are inherently limited by subjectivity and inter-rater variability. Examples of these scales include the Fazekas (Fazekas et al., 1987), the Scheltens (Scheltens et al., 1993) and the Age-Related White Matter Changes (ARWMC) (Wahlund et al., 2001). The Fazekas scale (**Figure 2-1**) is the simplest of the three instruments and remains the most widely used, providing separate 0–3 scores for periventricular and deep WMH (Gouw et al., 2006). This anatomical distinction (as determined by their proximity to the lateral ventricles) is clinically relevant, since WMH in these regions may arise from different pathological mechanisms and might have distinct associations with cognitive and functional outcomes (Cai et al., 2022). Emerging evidence suggests that the distribution of WMH could serve as a proxy for differing underlying pathophysiological mechanisms; however, further research is needed to clarify the extent and consistency of these associations.

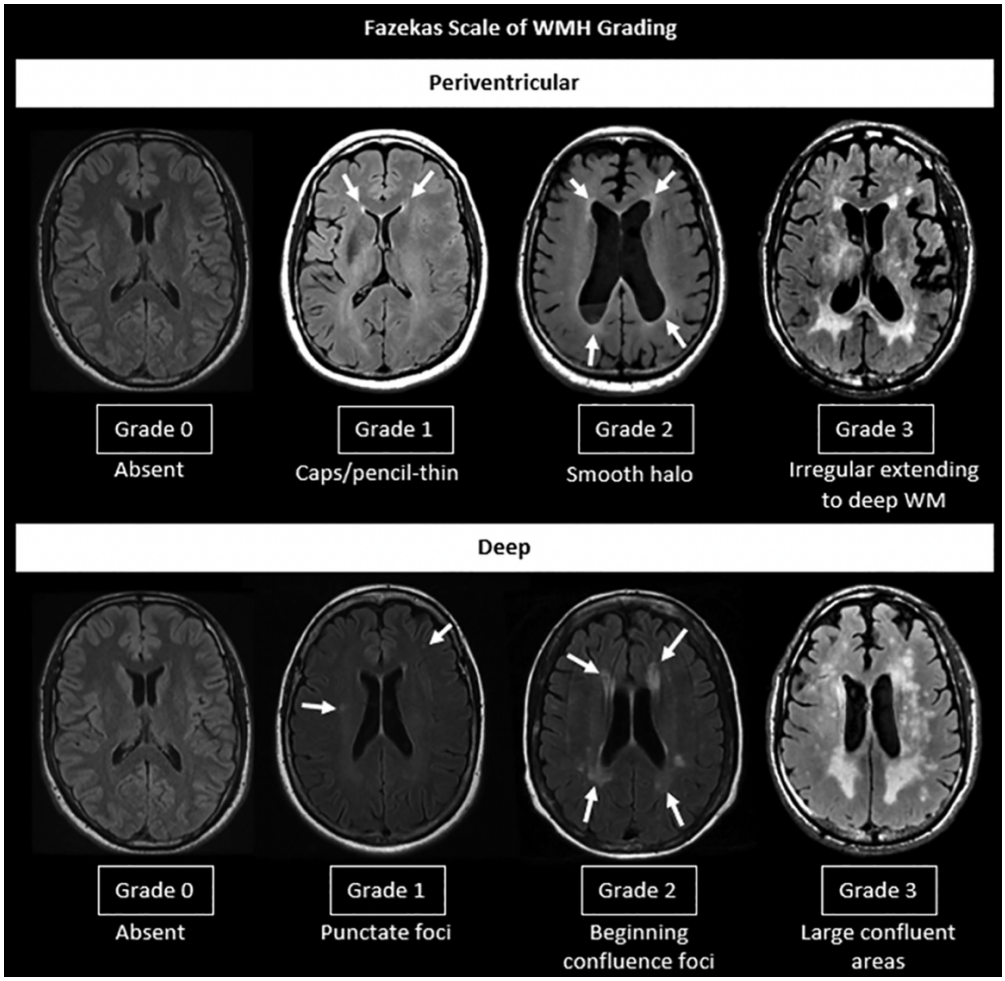

Figure 2-1. Fazekas scale for grading WMH on MRI. Visual classification of WMH severity in periventricular and deep white matter regions, ranging from absent (Grade 0) to severe (Grade 3). This widely used qualitative tool aids in the standardised assessment of WMH burden in both clinical and research settings. Reproduced from Mahammedi et al. (2021) with permission.

Periventricular WMH are often associated with chronic interstitial fluid accumulation, venous collagenosis, or age-related disruption of ependymal lining (Cai et al., 2022; Lahna et al., 2022), whereas deep WMH are more typically linked to underlying small-vessel ischemic injury or microinfarcts (Shim et al., 2015). These regional differences in WMH distribution may have implications for clinical outcomes, although findings across studies are not entirely consistent. Some research suggests that deep WMH are more frequently associated with impairments in executive function, attention, and motor performance, whereas periventricular WMH have been linked to global cognitive decline and slower processing speed (Delano-Wood et al., 2009; Soriano-Raya et al., 2012; D. M. J. van den Heuvel et al., 2006). However, other

studies, such as Sanderson-Cimino et al. (2022), have reported associations between periventricular WMH and deficits in executive function, working memory, and episodic memory, highlighting the need for further investigation into region-specific cognitive correlates (Sanderson-Cimino et al., 2021).

Given their distinct pathological and clinical implications, it is useful to separately quantify periventricular and deep WMH in research settings. To improve objectivity and reproducibility in this process, automated tools based on structural MRI have been developed and are increasingly used to assess WMH burden with greater precision than traditional visual rating scales.

2.2.1 Structural MRI and WMH

Volumetric approaches using automated segmentation algorithms, such as BIANCA (Brain Intensity AbNormality Classification Algorithm) (Griffanti et al., 2016b), The Wisconsin White Matter Hyperintensities Segmentation Toolbox (W2MHS) (Ithapu et al., 2014) and the Lesion Growth Algorithm (LGA) (Schmidt et al., 2012), offer a more reproducible and objective alternative to traditional visual rating scales and are increasingly used in clinical research. These tools allow for more precise quantification of WMH burden and reduce the inter-rater variability inherent in subjective scales like Fazekas. BIANCA was used for WMH segmentation and quantification in this chapter and the rest of this thesis. However, it is important to note that WMH visible on structural MRI represent only the most overt manifestations of WM damage and may underestimate the true extent of microstructural disruption (Promjunyakul et al., 2018). In many cases, injury extends beyond these hyperintense lesions into normal-appearing white matter (NAWM), which is not captured by volumetric segmentation alone (Mayer et al., 2022; Tuladhar et al., 2015). To address this limitation, diffusion MRI offers a more sensitive method for assessing the integrity of WM

architecture at the microstructural level and is increasingly employed in SVD research (Y. Wang et al., 2024).

2.2.2 Diffusion MRI and WM microstructure

Diffusion MRI enables the evaluation of microstructural WM integrity beyond what is visible on conventional structural scans (Brandhofe et al., 2021; Budisavljevic et al., 2025). Traditional diffusion tensor imaging (DTI) quantifies the directional movement of water molecules within brain tissue, providing metrics such as fractional anisotropy (FA) and mean diffusivity (MD). In patients with SVD, numerous studies have demonstrated reduced FA and increased MD in both WMH and NAWM (Duering et al., 2018; Hu et al., 2022; Mayer et al., 2022; Tuladhar et al., 2015). These findings indicate widespread microstructural damage that extends beyond the WMH lesions captured on structural MRI, reflecting processes such as demyelination, axonal loss, and gliosis (Barker et al., 2013; McAleese et al., 2017; Silbert et al., 2021). This sensitivity to microstructural disruption has made DTI an important tool in elucidating the relationship between WM integrity and cognitive as well as motor deficits in SVD (Mascalchi et al., 2019; Nitkunan et al., 2008; Pasi et al., 2016).

More recently, advanced diffusion models such as neurite orientation dispersion and density imaging (NODDI) have been developed to overcome some of the limitations inherent in the simpler DTI framework (H. Zhang et al., 2012). Unlike DTI, which provides composite measures that can be influenced by multiple underlying factors, NODDI decomposes the diffusion signal into biologically meaningful compartments, including intra-cellular (neurite density), extra-cellular, and free water fractions. This allows for more precise characterisation of microstructural alterations, potentially distinguishing between changes in neurite density versus alterations in the surrounding environment such as inflammation or edema. Applying these sophisticated techniques in SVD research holds promise for detecting early or subtle

disease-related changes, refining our understanding of disease progression, and improving the sensitivity of imaging biomarkers for clinical trials and therapeutic monitoring.

2.2.3 Connectomics and WM

In recent years, connectomics has emerged as a powerful framework for investigating the impact of SVD on large-scale brain network organisation (Aykan et al., 2025; Lawrence et al., 2014; C. Liu et al., 2025; Ogut, 2025; Pasi et al., 2016; Yang et al., 2024). While conventional diffusion MRI analyses provide region- or tract-specific markers of WM microstructural integrity, structural connectomics (Sporns et al., 2005) allows for a more comprehensive characterisation of how SVD-related WM damage disrupts inter-regional communication across the brain. This approach models the brain as a network, or graph, where regions of interest serve as nodes and WM pathways as edges, enabling the quantification of connectivity patterns at both global and local scales. Such methods are particularly relevant for SVD, a condition known to affect distributed subcortical and periventricular WM pathways that support cognitive, motor, and affective functions (Sanderson-Cimino et al., 2021).

Despite the growing utility of structural connectomics in clinical neuroscience, several methodological considerations should be acknowledged when applying these techniques to SVD (Yang et al., 2024). First, WMH and tissue damage can introduce artefacts or reduce the reliability of fibre tracking, particularly in regions where signal-to-noise ratio is already compromised (Y. Liu et al., 2021; Taghvaei et al., 2023). Although anatomically constrained tractography and advanced diffusion models help mitigate some of these issues, the presence of lesions still poses challenges for accurate streamline reconstruction. Furthermore, connectome metrics are inherently dependent on the chosen parcellation scheme and tractography parameters, which can affect reproducibility across studies (Bonilha et al., 2015; Borrelli et al., 2022; Gajwani et al., 2023; Radwan et al., 2022). Nonetheless, the integration

of microstructural (e.g., FA) and macrostructural (e.g., fibre bundle capacity) measures into a unified network model offers a unique way to capture the distributed nature of SVD-related pathology (Y. Feng et al., 2025). In this study, structural connectomics provides a framework for exploring how alterations in WM pathways may mediate the relationship between lesion burden and behavioural outcomes, which will be examined in subsequent chapters.

The current chapter presents imaging analyses conducted on patients with SVD and age-matched healthy controls (HC), with the primary aim of characterising group differences in structural and diffusion-based imaging markers. These analyses were intended to determine whether the current sample exhibits a pattern of neuroimaging findings consistent with previous literature. WMH burden was quantified using BIANCA, while DTI and NODDI metrics were assessed across major WM tracts using tract-based spatial statistics (TBSS). In doing so, this chapter establishes the structural context necessary for interpreting the neuroimaging–behavioural associations explored in subsequent chapters.

2.3 Methods

2.3.1 Participants, demographics, and consent

Fifty SVD participants aged between 50–90 years were initially recruited through the Cognitive Disorders Clinic at the John Radcliffe Hospital in Oxford. Patients had been referred to the clinic for complaints about their cognition. Patients with significantly greater WMH load than expected for their age, as determined from clinical (structural) scans, and without features to suggest an alternative diagnosis (such as Alzheimer's disease) were diagnosed with SVD and invited to participate in our research studies. Patients with other neurological comorbidities such as previous major stroke, Parkinson's disease or epilepsy were excluded from participation. Of the 50 SVD cases, one participant did not provide consent for MRI due to

claustrophobia, and five were deemed to have contraindications to MRI by radiographers. The remaining 44 participants (25 males, 19 females) underwent research MRI scanning.

Fifty-eight age-matched healthy controls were recruited through a volunteer database of people who expressed interest in being contacted for research participation. The sex ratio of the healthy volunteers did not differ significantly from the patient group. Cognitive function screening was carried out using the Addenbrooke's Cognitive Examination-III (ACE-III) (Hsieh et al., 2013).

Permission to conduct this study was obtained from the local ethics committee. All subjects provided written consent in accordance with the Declaration of Helsinki and the study was approved by the Local NHS research ethics committee

2.3.2 MRI acquisition

MRI data were acquired using 3T Siemens scanners at two locations: a Magnetom Prisma at the Oxford Centre for Human Brain Activity (OHBA), and a Magnetom Verio at the John Radcliffe Hospital, Oxford. Scanner protocols were closely matched across sites. Minor differences (e.g., a 20 ms difference in T1 inversion time) were accounted for during preprocessing and statistical modelling. Structural, diffusion, and resting-state functional scans were collected using the following parameters:

- **Structural imaging** included a T1-weighted MPRAGE sequence (TR = 2000 ms, TE = 2.01 ms, TI = 880 ms, flip angle = 8°, voxel size = 1.0 mm isotropic), and a T2-weighted fluid-attenuated inversion recovery (T2-FLAIR) sequence (TR = 5000 ms, TE = 397 ms, TI = 1800 ms, variable flip angle mode, voxel size = 1.0 × 1.0 × 1.05 mm).
- **Diffusion-weighted images** were acquired using echo planar imaging (EPI) with multiband acceleration (factor 3), TR = 3600 ms, TE = 92 ms, and voxel size = 2.0 ×

2.0 × 2.0 mm. Two phase-encoding directions were used: anterior–posterior (AP) and posterior–anterior (PA). The AP scan included 104 diffusion directions: 8 volumes with b = 0 s/mm², 50 with b = 1000 s/mm², and 50 with b = 2000 s/mm². The PA scan included 6 directions (4 b = 0 s/mm² and 2 with b = 1000 s/mm²), to support distortion correction.

2.3.3 MRI pre-processing and analysis

2.3.3.1 Structural

Segmentation and quantification of WMH

WMH segmentation and quantification were used as an initial step to verify whether the two groups differed in terms of cerebrovascular disease burden. WMH were segmented using BIANCA (Griffanti et al., 2016b), as described in Chapter 1. BIANCA was applied to brain-extracted T2-FLAIR images, with additional structural information from each participant's T1-weighted image to improve classification accuracy. The algorithm requires a training dataset with manually labelled WMH and non-WMH voxels; these labels were obtained from the UK Biobank Brain Imaging Processing Pipeline (Alfaro-Almagro et al., 2018). BIANCA outputs a probabilistic map representing the likelihood of each voxel being classified as WMH. These probability maps were thresholded at 0.8, resulting in binary WMH masks (1 = WMH, 0 = non-WMH). For each participant, total WMH volume was computed using fslstats, and an independent two-sample t-test was conducted to assess group differences in WMH burden between participants with SVD and healthy controls.

2.3.3.2 Diffusion

Diffusion MRI preprocessing and analysis for DTI and NODDI

Diffusion-weighted images were first corrected for susceptibility-induced distortions using TOPUP in FSL (Andersson et al., 2003). The output from TOPUP was then passed to EDDY, which corrects for eddy currents and participant motion (Andersson & Sotiropoulos, 2016).

Two models were used to analyze the corrected diffusion data: Diffusion Tensor Imaging (DTI) and Neurite Orientation Dispersion and Density Imaging (NODDI) (Croall et al., 2017; H. Zhang et al., 2012). The DTI model was fit using FSL's dtifit tool, while the NODDI model was estimated using the Accelerated Microstructure Imaging via Convex Optimization (AMICO) framework (Daducci et al., 2015). AMICO provides an efficient method for fitting biophysical models such as NODDI, maintaining accuracy while substantially reducing computation time.

Voxel-wise statistical analysis of diffusion metrics was conducted using Tract Based Spatial Statistics (TBSS) (Smith et al., 2006). FA images from all participants were slightly eroded, and end slices were removed to eliminate potential outliers. Each FA image was then non-linearly aligned to the FMRIB58_FA standard-space template (1 mm isotropic resolution) using FNIRT. The aligned FA images were merged into a 4D file, skeletonised, and thresholded at FA > 0.2 to generate a WM skeleton representing common tracts across participants. Skeletonised images were created using tbss_non_FA for the additional diffusion metrics: MD from DTI; and NDI, ODI, and isotropic volume fraction (ISOVF) from NODDI.

Group comparisons were performed using FSL's randomise with 5000 permutations, employing the same GLM used in the VBM analysis, with age, sex, and years of education included as covariates. Results were corrected for multiple comparisons using TFCE, and significance was defined as $\alpha = 0.05$.

Diffusion MRI preprocessing and analysis for atlas-level connectomics

To characterise the likely anatomical loci of significant WM effects, the thresholded statistical output from each TBSS GLM (i.e., the TFCE-corrected significant clusters) was converted into binary masks. These masks represented the set of voxels on the TBSS skeleton that showed significant associations for each diffusion metric. As this approach does not reconstruct individual streamlines, the resulting maps are intended solely for visualisation of probable tract involvement rather than for quantitative tractography.

Each binary significance mask was projected onto the JHU ICBM-DTI-81 WM atlas (Mori et al., 2008)in MNI 1 mm space to identify the major tracts most likely to contain the significant voxels. This procedure was implemented in R. For each tract in the atlas, the number of significant voxels intersecting that tract was quantified and expressed as a proportion of the total tract volume, thereby providing an estimate of the percentage of each tract affected in the corresponding TBSS contrast.

To estimate the potential cortical endpoints of the affected tracts, the Harvard–Oxford cortical atlas (1 mm MNI) (Harvard - Oxford Cortical Structural Atlas (RRID:SCR_001476) http://fsl.fmrib.ox.ac.uk/fsl/fslwiki/Atlases) was loaded and a k-nearest neighbours (k-NN) search was performed from each significant voxel to the nearest cortical label. This allowed us to approximate which grey-matter regions the disrupted WM pathways may connect. Labels from both the JHU and Harvard–Oxford atlases were then combined to generate anatomically interpretable tract–endpoint pairs.

Finally, a connectogram was constructed to visualise the pattern of putative disconnections across the cortex (**Figure 2-2**) . Using a custom R script inspired by the circlize framework (Gu et al., 2014), a circular connectome was generated with all 48 cortical regions from the Harvard–Oxford atlas represented as nodes along the circumference. Weighted arcs were drawn between node pairs according to the percentage of the corresponding tract affected:

wider arcs indicate a greater proportion of tract involvement. Colour mapping was used to distinguish between positive and negative associations across diffusion metrics, with cool (blue) hues indicating greater WM integrity associated with the behavioural or clinical variable, and warm (yellow–red) hues indicating reduced integrity. This approach provides a coherent visual summary of the most likely WM pathways and cortico-cortical connections contributing to each clinical or behavioural association examined in the subsequent chapters.

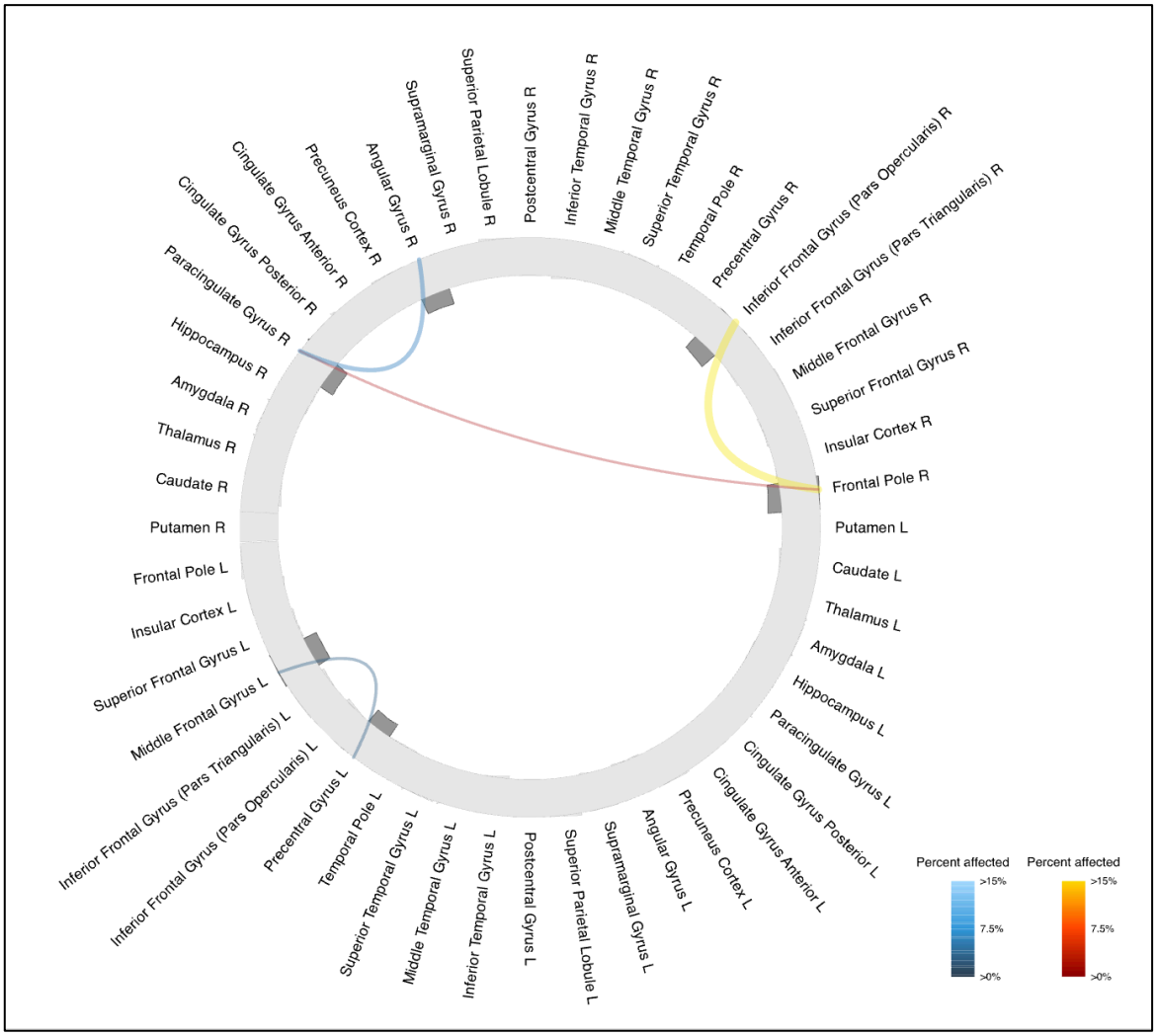

Figure 2-2. Example of Connectogram Circular connectome generated using R script showing all 48 cortical regions from the Harvard-Oxford atlas. The connections shown above are purely for visualisation purposes.

The atlas-based interpretation of TBSS results used in this thesis was inspired by recent developments in tract-level diffusion MRI analysis. Tractography-informed approaches such

as tractography atlas-based spatial statistics (TABSS) (D. Wang et al., 2016), and automated multi-atlas tract-extraction pipelines for tract-specific statistical analysis (Jin et al., 2016) illustrate the value of summarising WM abnormalities at the level of anatomically defined pathways rather than isolated skeleton voxels. Similarly, work on skeletonized atlas-based segmentation (S. Zhang & Arfanakis, 2014) demonstrates that overlaying a WM atlas onto a TBSS skeleton can improve anatomical interpretability by reducing partial-volume and misregistration errors. Although the present implementation does not reproduce these methods directly, it was informed by their shared principles: mapping voxel wise diffusion abnormalities onto tract-level anatomical units to aid visualisation and interpretation. Nevertheless, because this approach does not reconstruct subject-specific streamlines, any inferred tract involvement remains necessarily coarse and probabilistic, indicating likely rather than definitive disconnection.

2.4 Results

2.4.1 Demographics and WMH volume

Participants with SVD did not differ significantly from healthy controls in terms of age or sex ratio but had spent fewer years in full time education (**Table 2-1**). In terms of their cognitive status, although the mean Addenbrookes Cognitive Examination-III (ACE-III) score for participants with SVD was statistically smaller than that for healthy controls, both these scores were still within normal limits for non-demented elderly populations (Beishon et al., 2019; Elamin et al., 2016; Hsieh et al., 2013; McCarthy et al., 2024).

Number of Participants	Diagnosis		p-value[2]
	HC N = 58[1]	SVD N = 44[1]	
Age (years)	68.7 ± 8.4	70.3 ± 8.9	0.4
Gender			0.13
Male	23 (40%)	25 (57%)	
Female	35 (60%)	19 (43%)	
YOE	22.8 ± 10.4	18.2 ± 3.1	0.003
Total ACE-III	97.3 ± 2.4	90.5 ± 7.5	<0.001
Total AMI	1.1 ± 0.4	1.6 ± 0.6	<0.001
Total BDI-II	6.0 ± 4.8	14.2 ± 10.6	<0.001
Total BIS-II	69.4 ± 12.9	80.0 ± 7.9	<0.001
HADS Depression	5.0 ± 3.5	8.7 ± 1.8	<0.001
HADS Anxiety	8.1 ± 4.5	11.2 ± 3.0	<0.001

[1] Mean ± SD; n (%)

[2] Welch Two Sample t-test; Pearson's Chi-squared test

Table 2-1: Demographic and cognitive measures. HC = Healthy Controls, SVD = Cerebrovascular Small Vessel Disease, YOE = Years of Education, ACE-III = Addenbrooke's Cognitive Examination III, AMI = Apathy Motivation Index, BDI-II=Beck Depression Inventory II, BIS-II = Barrat Impulsiveness Scale II, HADS =Hospital Anxiety and Depression Scale.

As expected, WMH volume as computed by BIANCA was significantly greater in the SVD group compared to the healthy control group (**Figure 2-3a**). WMH were present in participants in both groups, albeit to a lesser extent in healthy controls. This increased WMH burden in the SVD group remained significant even after adjusting for head size (**Figure 2-3b**). Further analysis revealed that the SVD group exhibited significantly greater periventricular and deep WMH load relative to controls (**Figures 2-3c & 2-3d**). Group-level overlays of the BIANCA-derived WMH masks showed a substantially larger number of affected voxels in the SVD group, with lesion distribution extending more extensively beyond the lateral ventricles (**Figures 2-4a & 2-4b**).

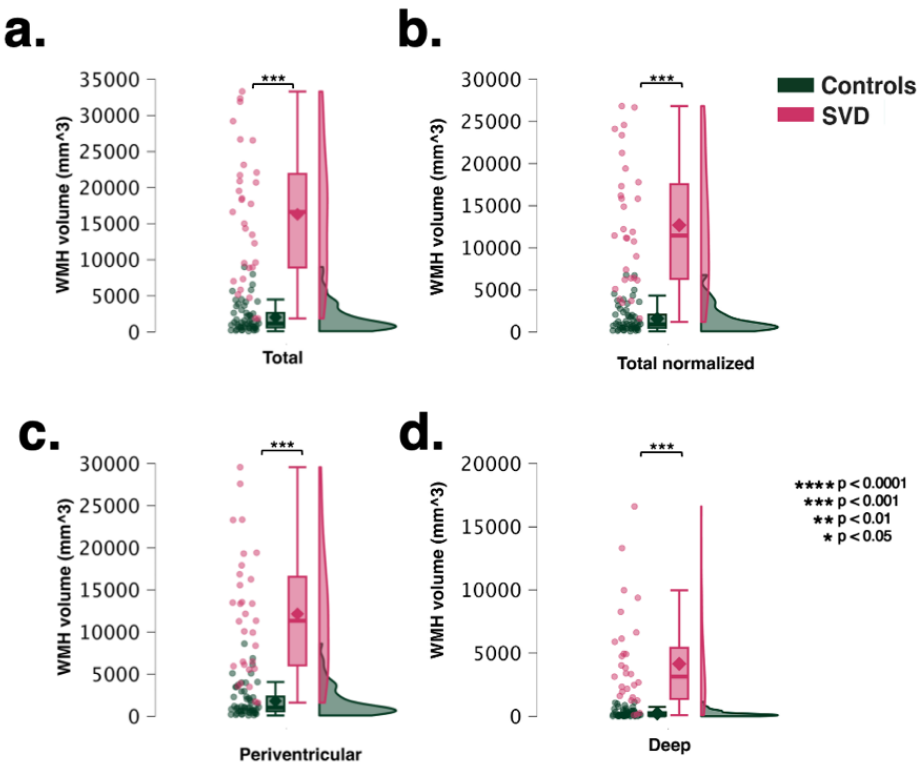

Figure 2-3. WMH volume in healthy controls and SVD (a) SVD patients had significantly greater total WMH lesions than controls. **(b)** The elevated total WMH burden in SVD participants remained significant when head size was controlled for in the analyses. (c) Patients had significantly greater periventricular WMH burden and (d) significantly greater deep WMH burden than controls.

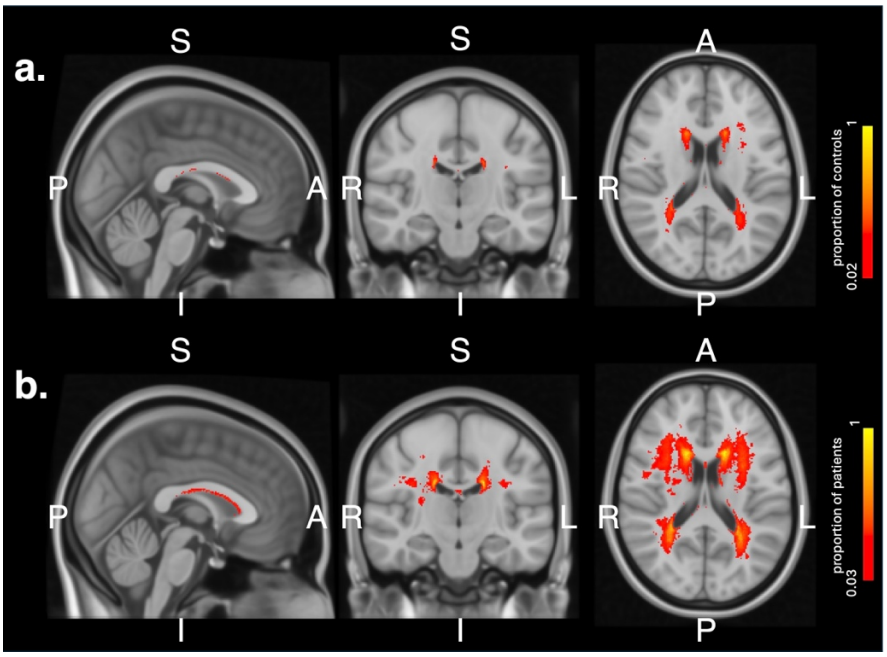

Figure 2-4. BIANCA masks showing WMH burden by group (a) Controls had WMH lesions consistent with healthy ageing. **(b)** SVD patients had significantly greater WMH burden surrounding the ventricles and extending into the deep WM.

2.4.2 Clinical Predictors of WMH Volume

Linear regression analyses were conducted to examine the relationship between total WMH volume (log-transformed) and a range of demographic and clinical predictors, including age, gender, years of education (YOE), Addenbrooke's Cognitive Examination (ACE-III) scores, Apathy and Motivation Index (AMI), Beck Depression Inventory (BDI-II), Barratt Impulsiveness Scale (BIS-II), and Hospital Anxiety and Depression Scale (HADS) scores. In the full sample, the overall model was significant ($F(9, 66) = 13.60$, $p < .001$), explaining approximately 65% of the variance in log-transformed WMH volume (adjusted $R^2 = 0.60$). Significant positive associations were found between WMH volume and age ($\beta = 0.021$, $p < .001$; **Figure 2-5a**), AMI ($\beta = 0.254$, $p = .032$; **Figure 2-5d**), and HADS depression scores ($\beta = 0.094$, $p < .001$; **Figure 2-5e**), while ACE scores were negatively associated with WMH volume ($\beta = –0.040$, $p = .002$; **Figure 2-5c**).

When the analysis was conducted separately by group, the pattern of associations differed. In the healthy control group, the model was also significant ($F(9, 36) = 5.67$, $p < .001$), accounting for 59% of the variance in WMH volume (adjusted $R^2 = 0.48$). Within this group, WMH volume was positively associated with age ($\beta = 0.031$, $p < .001$; **Figure 2-5b**), HADS depression ($\beta = 0.082$, $p = .005$; **Figure 2-5f**), and negatively associated with BIS scores ($\beta = –0.018$, $p = .027$; **Figures 2-5g & 2-5h**). No other predictors reached significance. In contrast, the model in the SVD group was not statistically significant ($F(9, 20) = 1.67$, $p = .164$), explaining only 17% of the variance in WMH volume (adjusted $R^2 = 0.17$). Although HADS depression showed a trend-level association with WMH volume in the patient group ($\beta = 0.103$, $p = .056$; **Figure 2-5f**), no predictors were statistically significant.

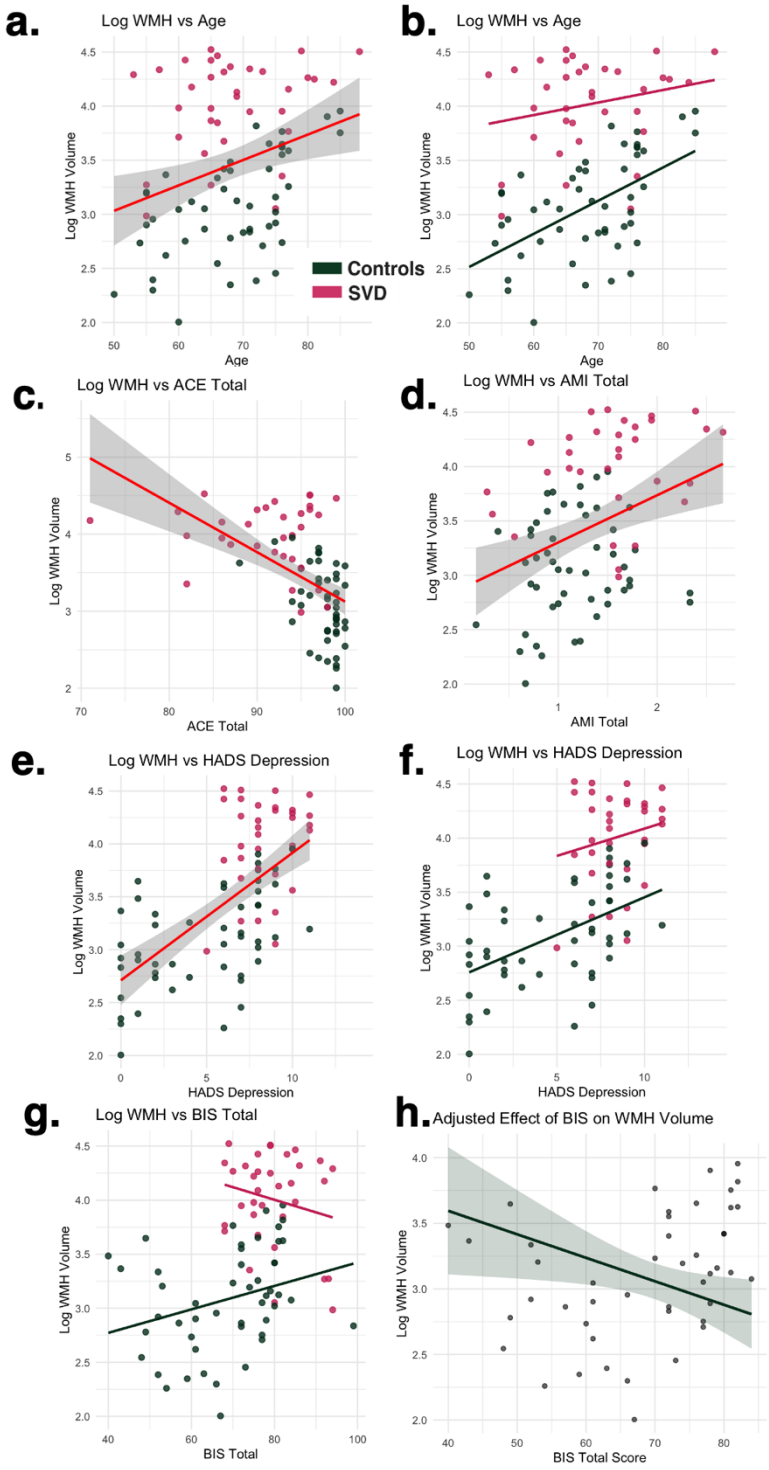

Figure 2-5. log-transformed total WMH volume vs demographic and clinical measures (a) WMH burden increased significantly with age across both groups which may have been driven by **(b)** Significant correlation of WMH volume with increasing age in controls. **(c)** Overall, there was a significantly negative correlation between total WMH volume and ACE scores. **(d)** WMH burden in participants showed a significantly positive correlation with AMI scores. **(e)** Total WMH volume increased significantly with increased HADS depression scores across both groups which may have been driven by **(f)** Significant correlation of WMH volume with increasing HADS depression in controls. The relationship between WMH volume and HADS depression approaches significance in SVD. **(g)** WMH burden was significantly correlated with BIS scores in controls and appears to be positive but **(h)** Adjusting the effect of BIS on log WMH volume from a multiple linear regression model controlling for clinical variables showed that the association is negative and statistically significant.

2.4.3 Widespread reduction in white matter tract integrity with DTI and NODDI

To investigate the impact of SVD on the microstructural integrity of WM tracts in the brain, TBSS was applied to diffusion MRI data processed using two modelling approaches: DTI and NODDI (see Ch 1 for details on TBSS and the individual models).

To quantify the extent of diffusion MRI-detected alterations, these changes were expressed as percentages of the WM skeleton. A total of 136,000 non-zero voxels constituted the WM skeleton. As shown in **Table 2-2**, FA values differed significantly between the two cohorts in 69,694 voxels (51.25%), while MD was altered in 81,912 voxels (60.23%). For NODDI metrics, significant changes were observed in 83,083 voxels (61.09%) for NDI, and 39,810 voxels (29.27%) for ISOVF. ODI was lower in SVD in 351 voxels (0.26%) and higher in 7,410 voxels (5.45%) compared to controls.

DTI		
Diffusion Metric	No. of affected voxels (out of 136,000)	Percentage of TBSS skeleton (%)
FA	69,694	51.25
MD	81,912	60.23
NODDI		
Diffusion Metric	No. of affected voxels (out of 136,000)	Percentage of TBSS skeleton (%)
NDI	83,083	61.09
ISOVF	39,810	29.27
ODI (Control > SVD)	351	0.26
ODI (SVD > Control)	7,410	5.45

Table 2-2: Extent of White Matter Microstructural Alterations in SVD Compared to Controls (a) This table shows the percentage of WM skeleton voxels that showed significant differences between the SVD cohort and controls across various diffusion MRI metrics, based on TBSS results.

Further visualisation analyses revealed that SVD was associated with widespread microstructural abnormalities across much of the entire WM skeleton, with alterations

detected in all major tract classes (**Figures 2-6 & 2-7**). Among the association fibres, which facilitate intrahemispheric connectivity, prominent changes were observed in several long-range pathways including the superior longitudinal fasciculus, inferior longitudinal fasciculus, inferior fronto-occipital fasciculus, arcuate fasciculus, cingulum, and middle longitudinal fasciculus. In the commissural system, which supports interhemispheric communication, both the forceps major and forceps minor demonstrated significant microstructural disruption. Additionally, changes were evident in key projection fibres, particularly the anterior thalamic radiation, corticospinal tract, and acoustic radiation, reflecting compromised connectivity between cortical and subcortical regions. Taken together, these findings highlight the diffuse impact of SVD on WM architecture, extending across tracts subserving a wide range of cognitive, sensory, and motor functions.

Directionality of change across diffusion parameters was biologically consistent. With DTI, individuals with SVD exhibited lower FA and higher MD relative to controls (**Figures 2-6a & 2-6b**). NODDI metrics similarly showed reduced NDI and increased ISOVF in the SVD group (**Figures 2-7a & 2-7b**). ODI demonstrated regionally specific alterations. Specifically, ODI was reduced in SVD participants in the left forceps minor, left anterior thalamic radiation, and left corticospinal tract (**Figure 2-7c**), whereas increased ODI was observed in the forceps major, inferior longitudinal fasciculus, inferior fronto-occipital fasciculus, and superior longitudinal fasciculus (**Figure 2-7d**).

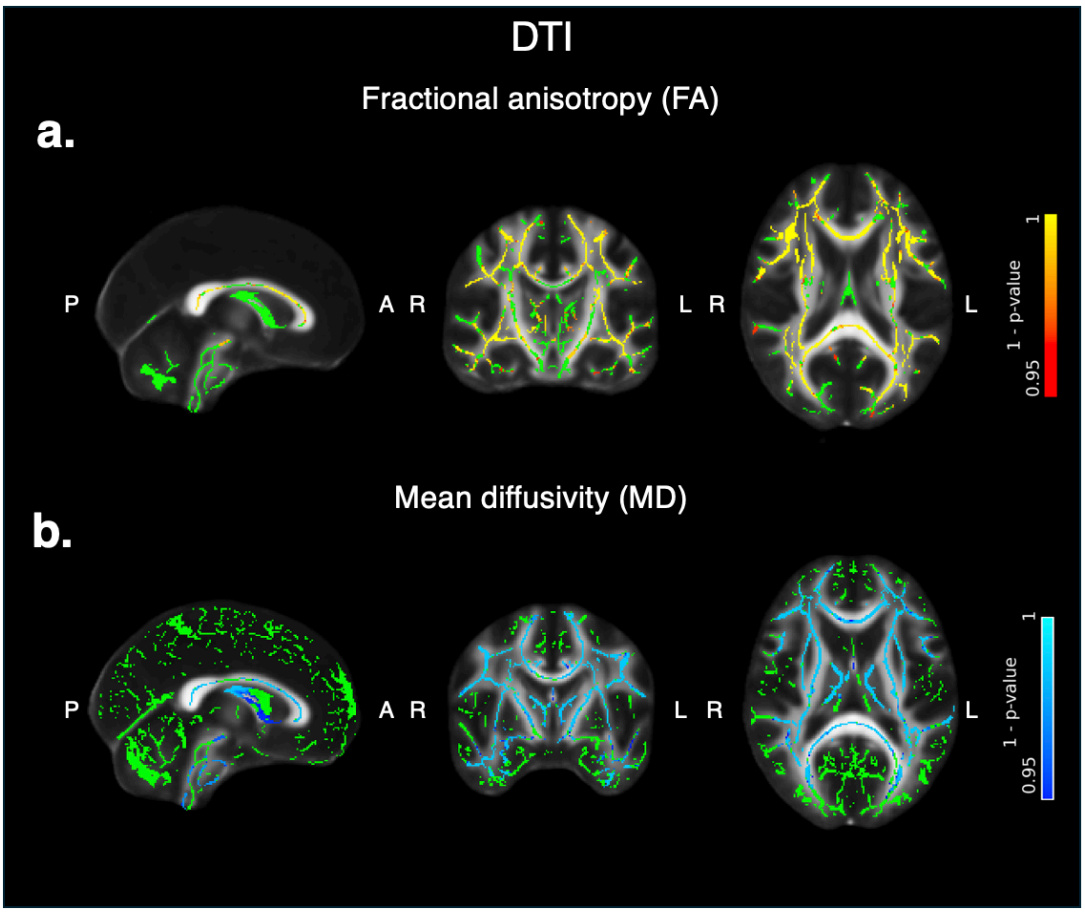

Figure 2-6. TBSS analysis of white matter microstructural integrity using the DTI model (a) SVD participants had lower FA (shown in red-yellow) in several white matter tracts compared to healthy elderly controls. **(b)** Many of the same tracts also demonstrated higher MD in SVD participants (shown in blue-light blue). The white matter skeleton is shown in green. Positive and negative correlations are shown in warm and cool colors respectively for imaging analyses.

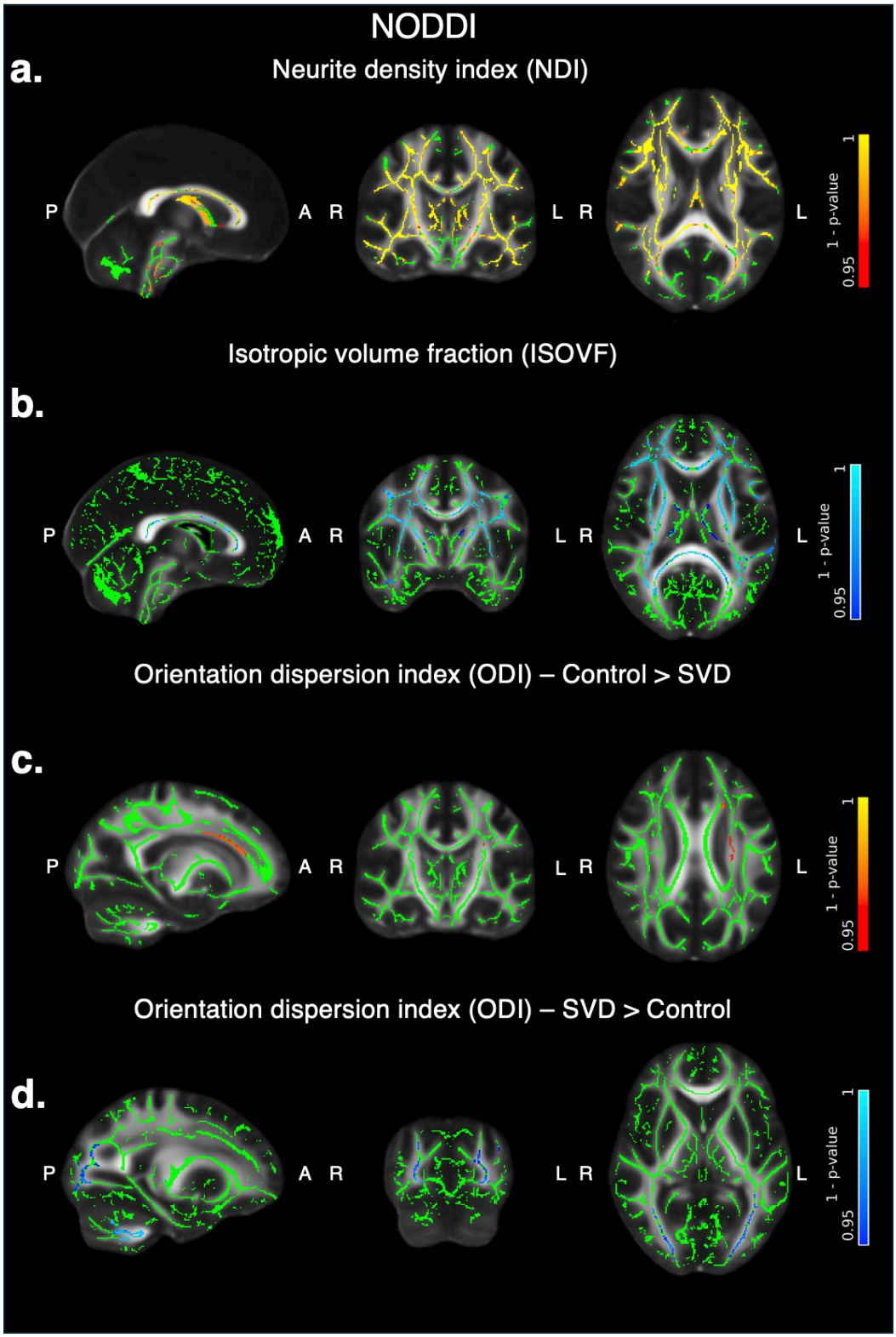

Figure 2-7. Impact of SVD on white matter microstructural integrity as detected with NODDI (a) SVD participants had lower NDI and **(b)** and higher ISOVF compared to healthy elderly controls. **(c)** Lower ODI in SVD was seen in the forceps minor, anterior thalamic radiation and corticospinal tract, all in the left hemisphere. **(d)** Higher ODI in SVD was observed in the forceps major, inferior longitudinal fasciculus, inferior fronto-occipital fasciculus and superior longitudinal fasciculus. The white matter skeleton is shown in green. Positive and negative correlations are shown in warm and cool colors respectively for imaging analyses.

2.4.4 Correlations of patient demographics and clinical measures with WM integrity

TBSS analysis, with $\alpha = 0.05$ and TFCE correction for multiple comparisons, was conducted using the DTI model on the whole cohort. These analyses demonstrated that lower FA and higher MD were associated with increasing age and with higher scores on the AMI, BDI-II, BIS-II, and HADS questionnaires (**Figures 2-8 & 2-9**). WM changes related to the direction of water diffusion were generally more widespread for apathy and depression, but more posterior and left-lateralized for impulsivity. In contrast, WM changes related to the rate of water diffusion were more widespread for impulsivity and depression but tended to be more posterior and left-lateralized for apathy. Years of education showed a negative correlation with MD.

Similar TBSS analyses were performed using the NODDI model, again with $\alpha = 0.05$ and TFCE correction. These revealed that lower NDI and higher ISOVF were associated with increasing age and with higher scores on the AMI and HADS measures (**Figures 2-10 & 2-11**). Reductions in neuronal density were more widespread for depression than for apathy, affecting more anterior WM tracts, whereas the presence of free water was predominantly left-lateralized for both measures. Lower NDI was also negatively correlated with scores on the BDI-II and BIS-II, and positively correlated with ACE-III scores and years of education (**Figure 2-10**). The spatial pattern of reduced neuronal density associated with BDI-II scores differed slightly from the pattern observed with HADS, though the effects remained similarly widespread. Impulsivity effects for NDI were right-lateralized.

ODI showed a bidirectional relationship with age: a superior portion of the right corticospinal tract exhibited increased dispersion, whereas a more medial segment of the same tract and the left anterior thalamic radiation showed reduced neuronal dispersion (**Figure 2-12**). ODI also demonstrated a positive correlation with ACE-III scores, with increased dispersion observed in the left anterior thalamic radiation and the forceps minor.

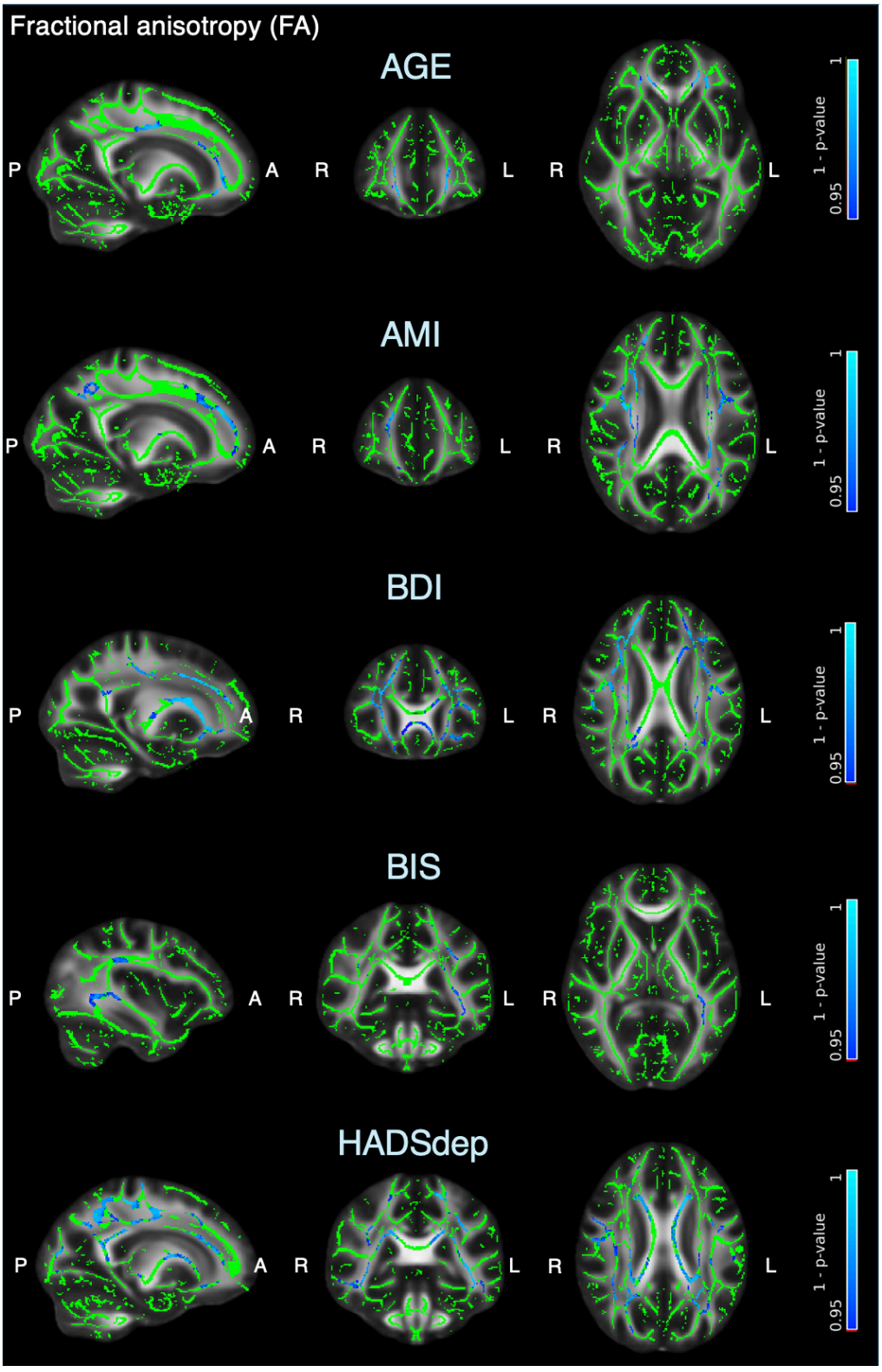

Figure 2-8. Correlation of DTI-FA with participant clinical data Unidirectional water movement along WM tracts was reduced in association with increasing age and with higher levels of apathy (AMI), depression (BDI-II; HADS), and impulsivity (BIS-II). The WM skeleton is shown in green and significant voxels are shown in blue-light blue for negative correlations.

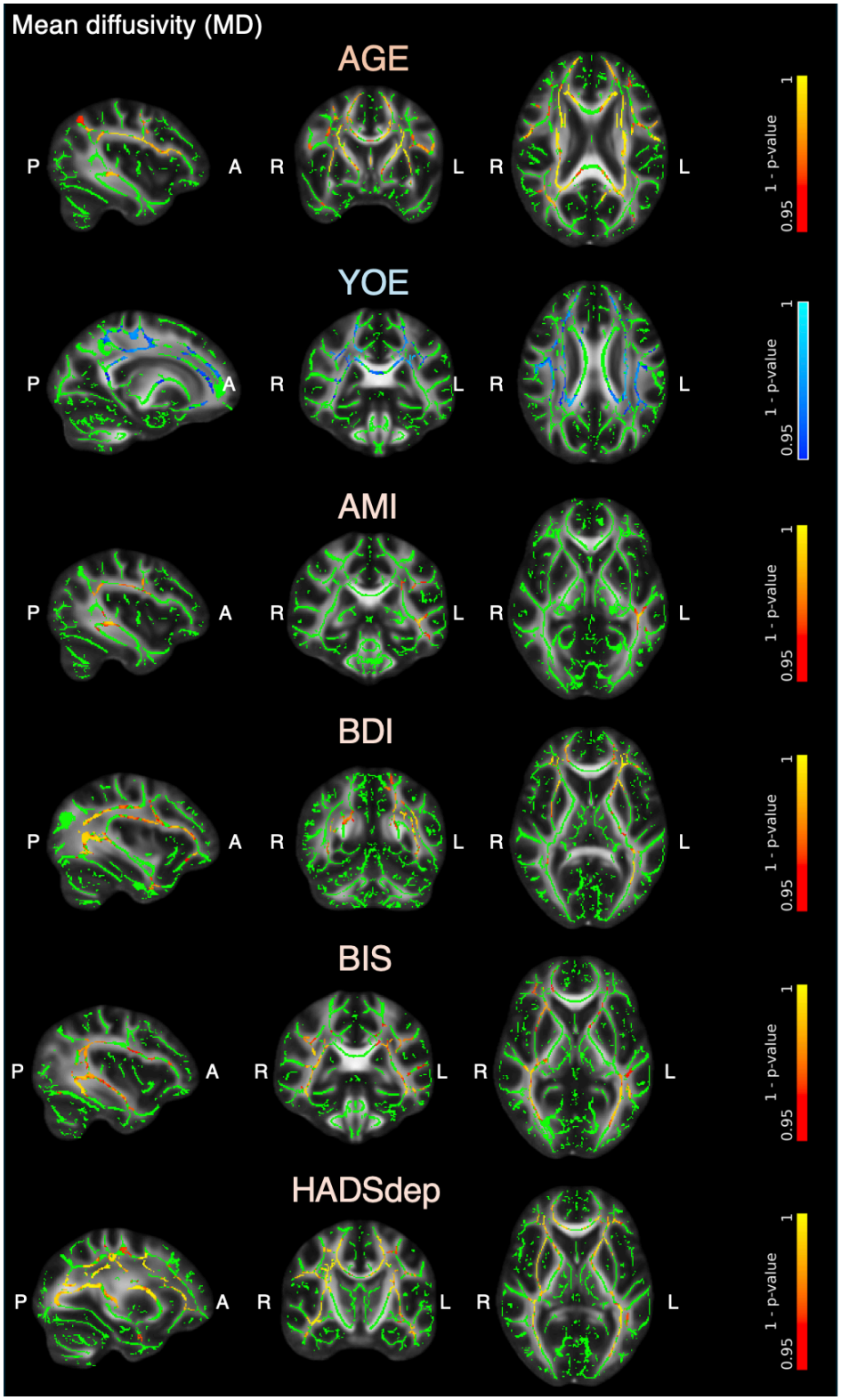

Figure 2-9. Correlation of DTI-MD with participant clinical data The rate of water diffusion along WM tracts increased in association with increasing age and with higher levels of apathy (AMI), depression (BDI-II; HADS), and impulsivity (BIS-II). However, there was a negative correlation with years of education. The WM skeleton is shown in green and significant voxels are shown in red-yellow for positive correlations and blue-light blue for negative correlations.

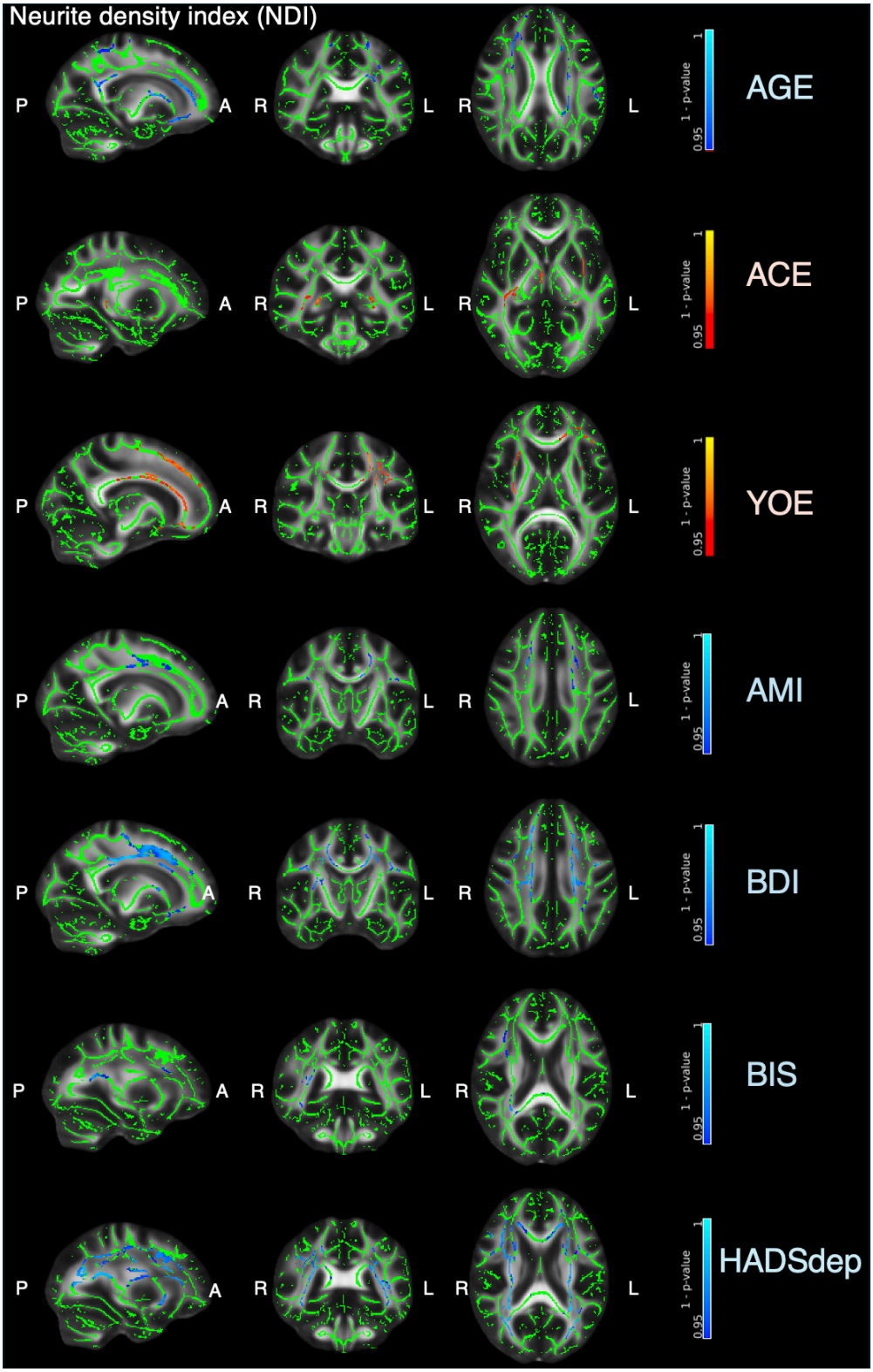

Figure 2-10. Correlation of NDI with participant clinical data as detected using NODDI Neuron density decreased in association with increasing age and with higher levels of apathy (AMI), depression (BDI-II; HADS), and impulsivity (BIS-II). However, positive correlations were observed in relation to cognition (ACE-III) and years of education. The WM skeleton is shown in green and significant voxels are shown in red-yellow for positive correlations and blue-light blue for negative correlations.

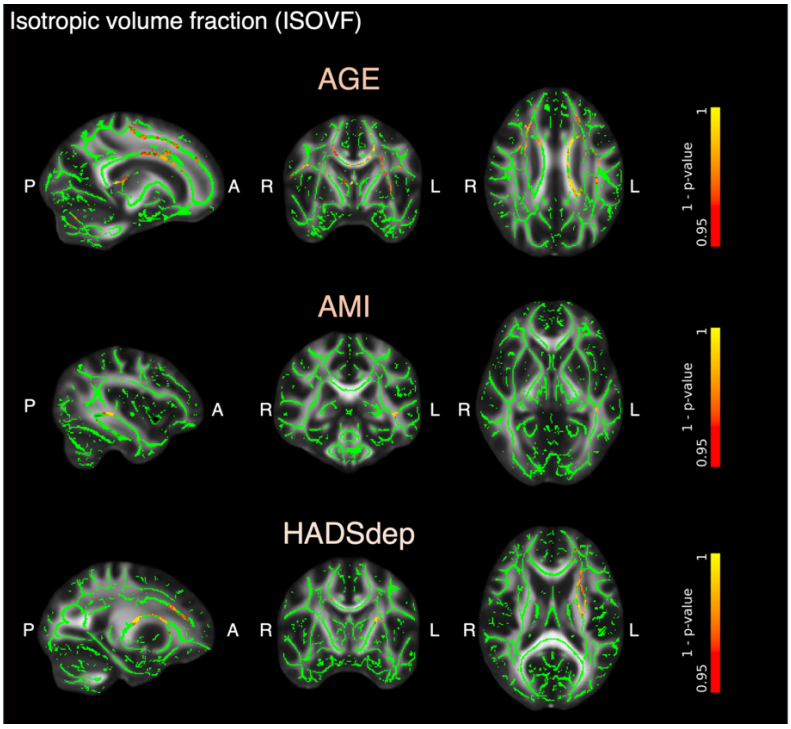

Figure 2-11. Correlation of ISOVF with participant clinical data as detected using NODDI The measure of free water in brain tissue increased in association with increasing age and with higher levels of apathy (AMI) and depression (HADS). The WM skeleton is shown in green and significant voxels are shown in red-yellow for positive correlations.

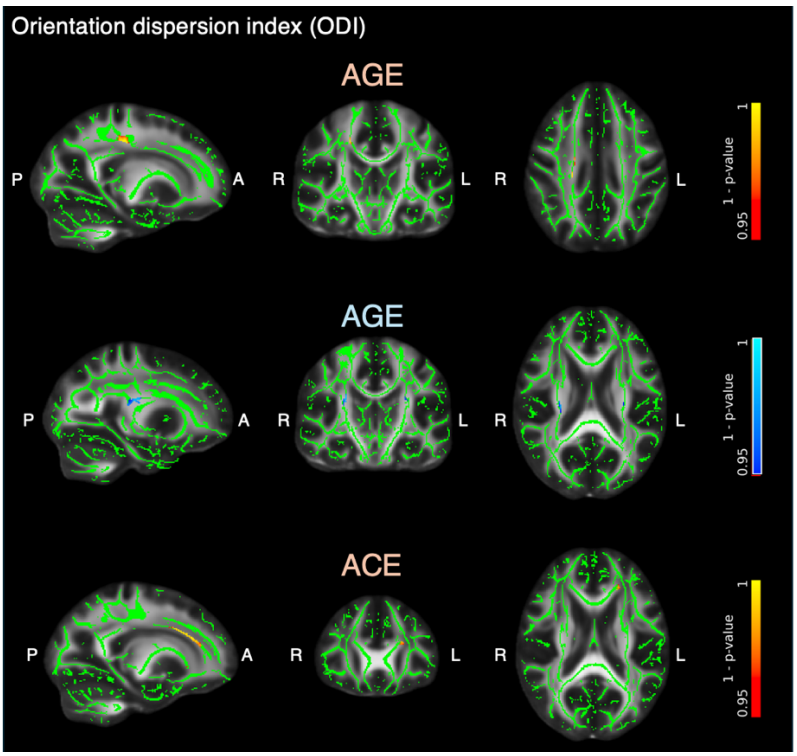

Figure 2-12. Correlation of ODI with participant clinical data as detected using NODDI Greater neuronal dispersion was associated with better cognitive performance (ACE-III). A bidirectional relationship with age was also observed. The WM skeleton is shown in green and significant voxels are shown in red-yellow for positive correlations and blue-light blue for negative correlations.

2.4.5 Higher cognition and more years of education predict increased connectivity

Significant TBSS clusters were registered to the JHU WM atlas (Mori et al., 2008) to delineate the implicated tracts and estimate the proportion of supra-threshold voxels per tract. The anterior–posterior or superior–inferior endpoints of each tract were linked to the nearest cortical labels in the Harvard–Oxford atlas (Harvard - Oxford Cortical Structural Atlas (RRID:SCR_001476) http://fsl.fmrib.ox.ac.uk/fsl/fslwiki/Atlases), generating a tract-to-cortex correspondence. This information was subsequently aggregated to produce a connectome/disconnectome, with edge weights representing the percentage of affected voxels in each tract. Cognition was associated with increased WM integrity, reflected by higher neuronal density (**Figure 2-13**) and dispersion (**Figure 2-14**) across several tracts, including

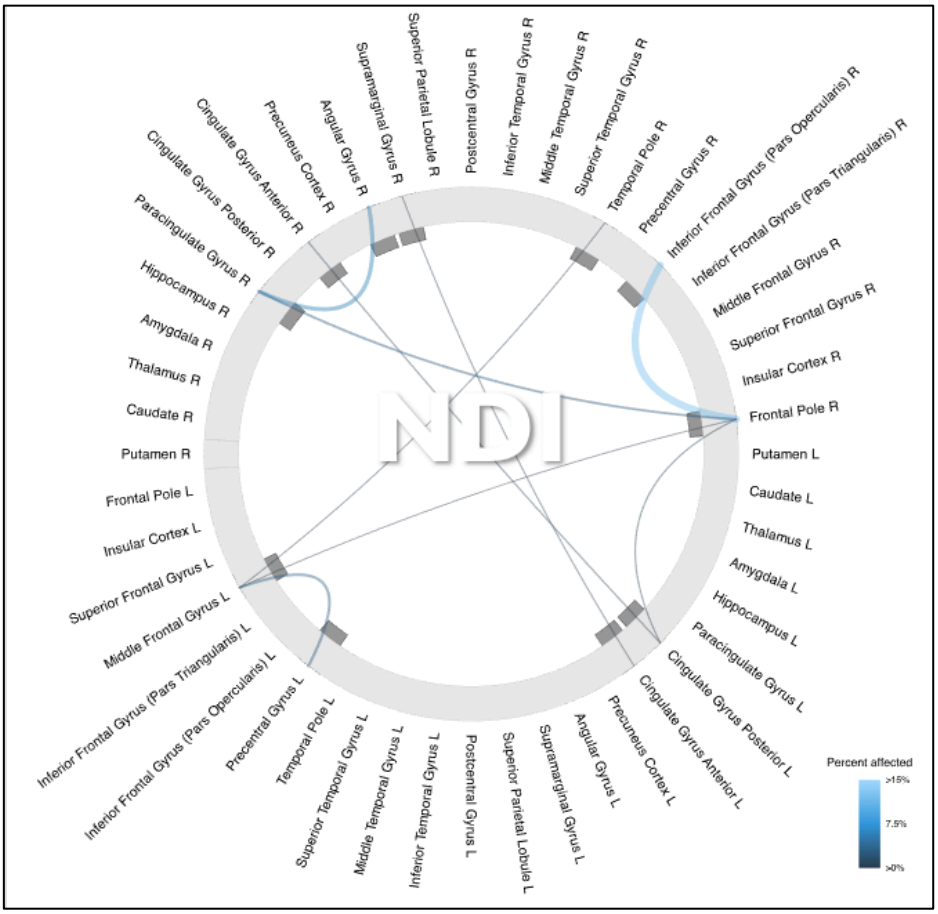

Figure 2-13. Connectome for NODDI NDI with ACE Cognition (ACE-III) was linked to greater neuronal density mainly in right lateralized frontal regions

those linking the frontal pole and middle frontal gyrus. These same pathways—along with connections involving the anterior cingulate gyrus, supramarginal gyrus, and precuneus—also demonstrated greater integrity with higher years of education, as indicated by reduced water-diffusion rates (**Figure 2-15**) and increased neuronal density (**Figure 2-16**).

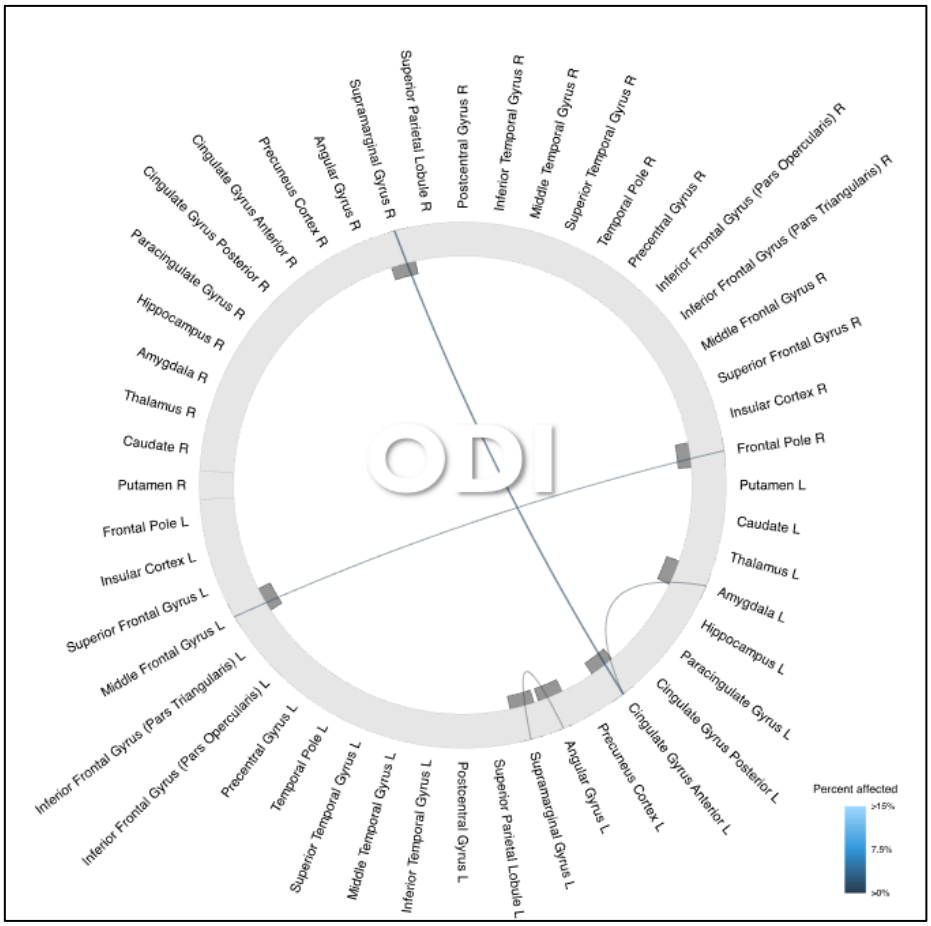

Figure 2-14. Connectome for NODDI ODI with ACE Cognition (ACE-III) was linked to higher neuronal dispersion in bilateral areas of both the frontal and parietal lobes.

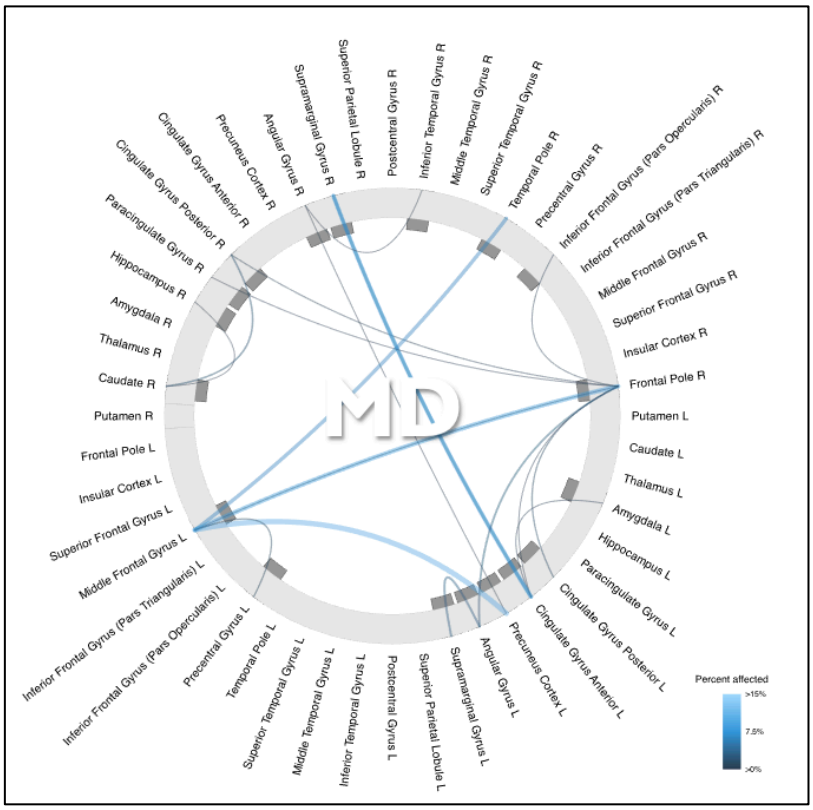

Figure 2-15. Connectome for DTI MD and YOE More years of education was associated with reduced water dispersion along WM tracts between frontal, temporal, parietal and subcortical brain regions.

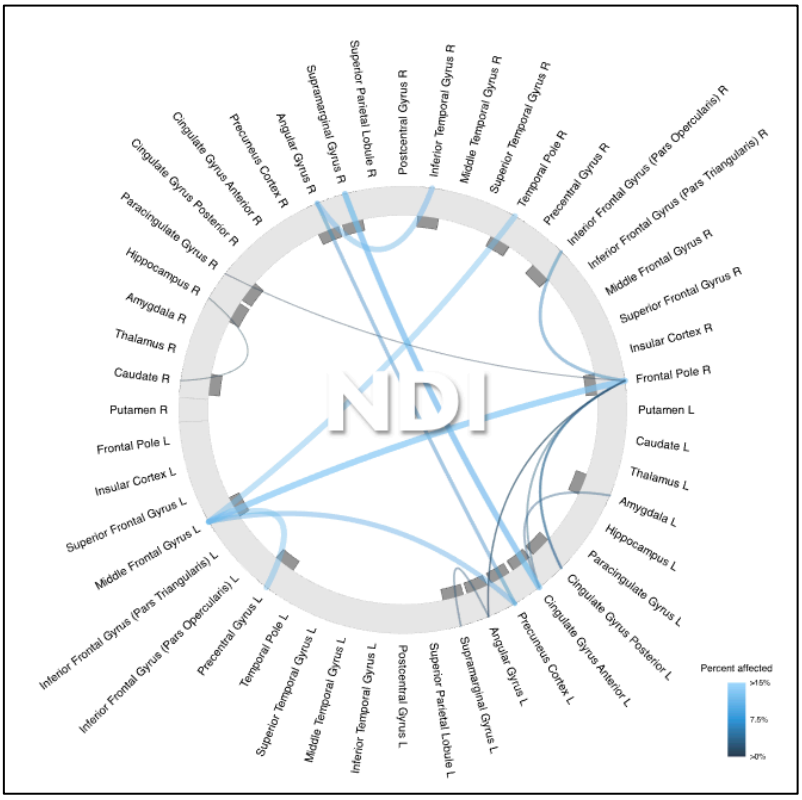

Figure 2-16. Connectome for NODDI NDI with YOE More years of education was associated with greater neuronal density in WM tracts between frontal, temporal, parietal and subcortical brain regions.

2.4.6 Increased age, apathy, depression and impulsivity predict reduced connectivity

Ageing was associated with decreased WM integrity, reflected by increased directions and rate of water diffusion (**Figures 2-17a & 2-17b**), reduced neuronal density (**Figure 2-18a**) and more free water surrounding tracts (**Figure 2-18b**). Affected tracts included those projecting to the frontal pole, middle frontal, anterior cingulate and supramarginal gyri. Ageing seemingly had a more complicated relationship with orientation dispersion of neurons (**Figures 2-19a & 2-19b**). Tracts projecting to the frontal pole, middle frontal gyrus and precuneus showed signs or both increased and decreased organization. Notably, there were other tracts connecting frontal, temporal, parietal and subcortical regions that showed decreased organization of neurons throughout the brain.

Apathy, as measured using AMI, consistently showed negative correlations with WM integrity, reflected by increased directions and rate of water diffusion (**Figures 2-20a & 2-20b**), reduced neuronal density (**Figure 2-21a**) and more free water surrounding tracts (**Figure 2-21b**). Tracts projecting to the right frontal pole were consistently implicated across all measures. Weakened connectivity was observed in tracts leading to the left middle frontal gyrus as determined by FA, MD and NDI. The caudate, paracingulate and precentral gyri also had noticeably weakened connections.

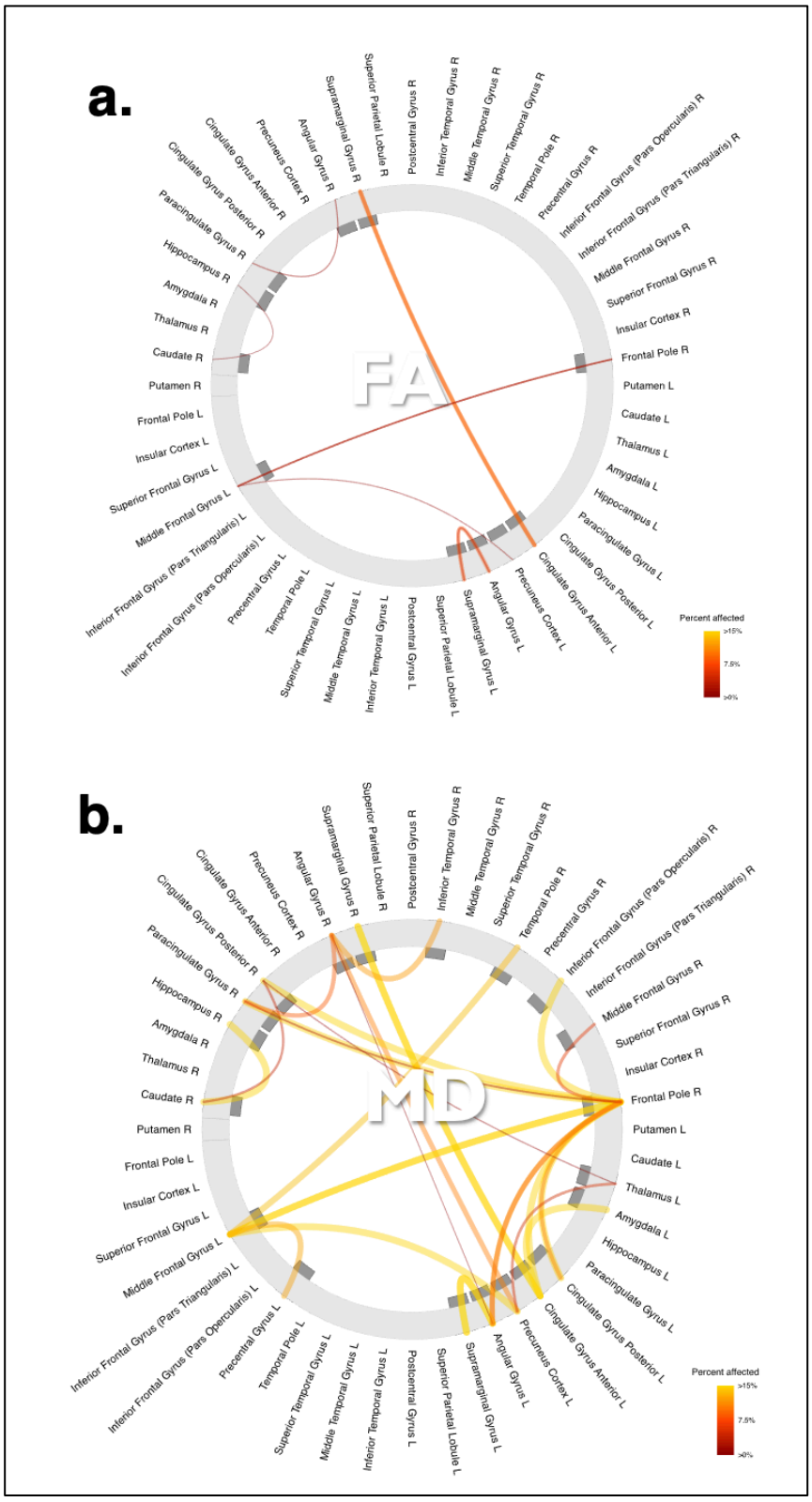

Figure 2-17. Disconnectome for DTI with Age Increasing age was linked to **(a)** reduced unidirectional movement of water in frontal, parietal and subcortical brain areas. There was also **(b)** increased water diffusion from between frontal, temporal, parietal and subcortical brain regions.

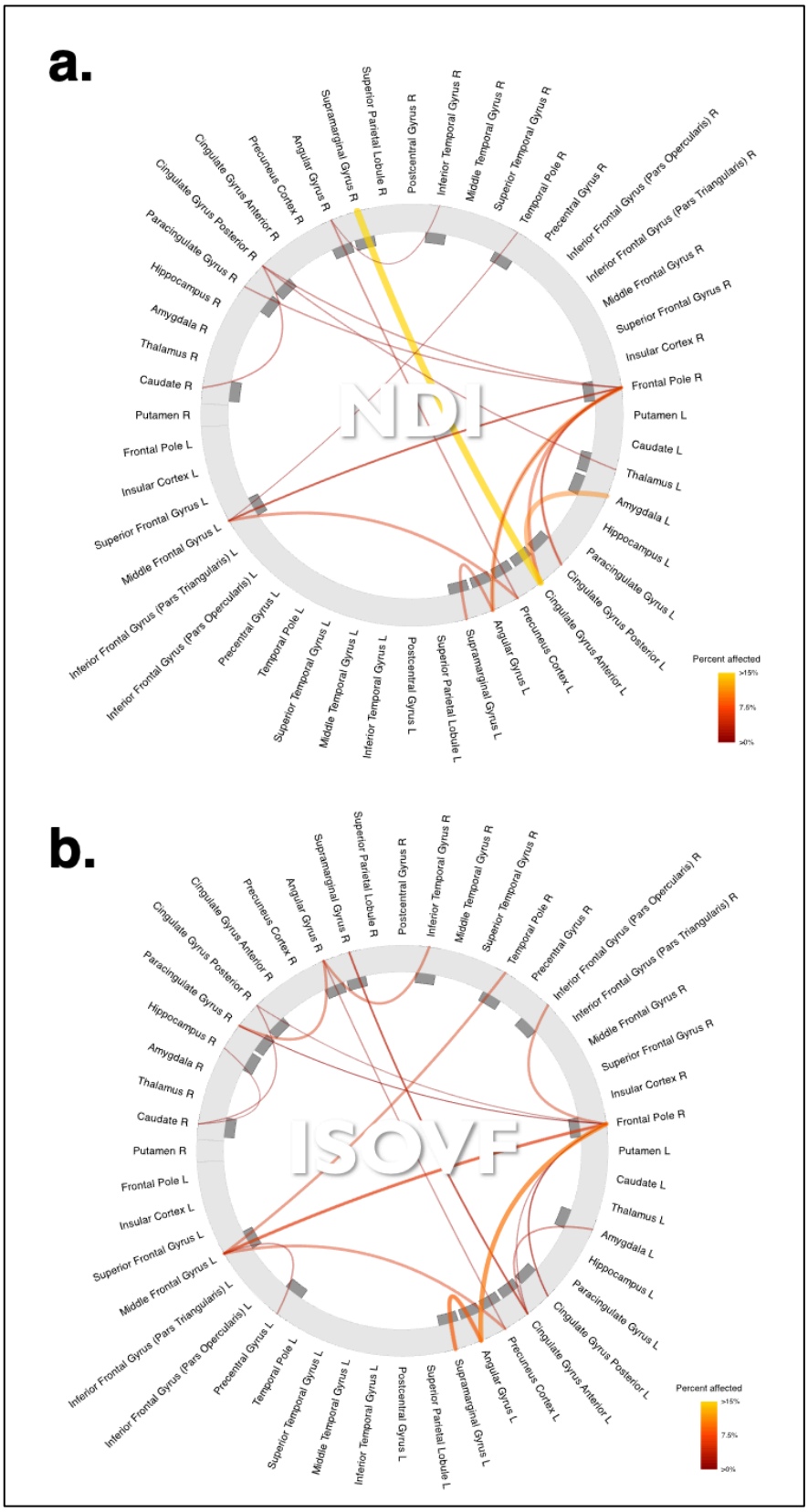

Figure 2-18. Disconnectome for NODDI's NDI and ISOVF with Age Increasing age was linked to **(a)** reduced neuronal density **(b)** and more free water surrounding tracts between frontal, temporal, parietal and subcortical brain regions.

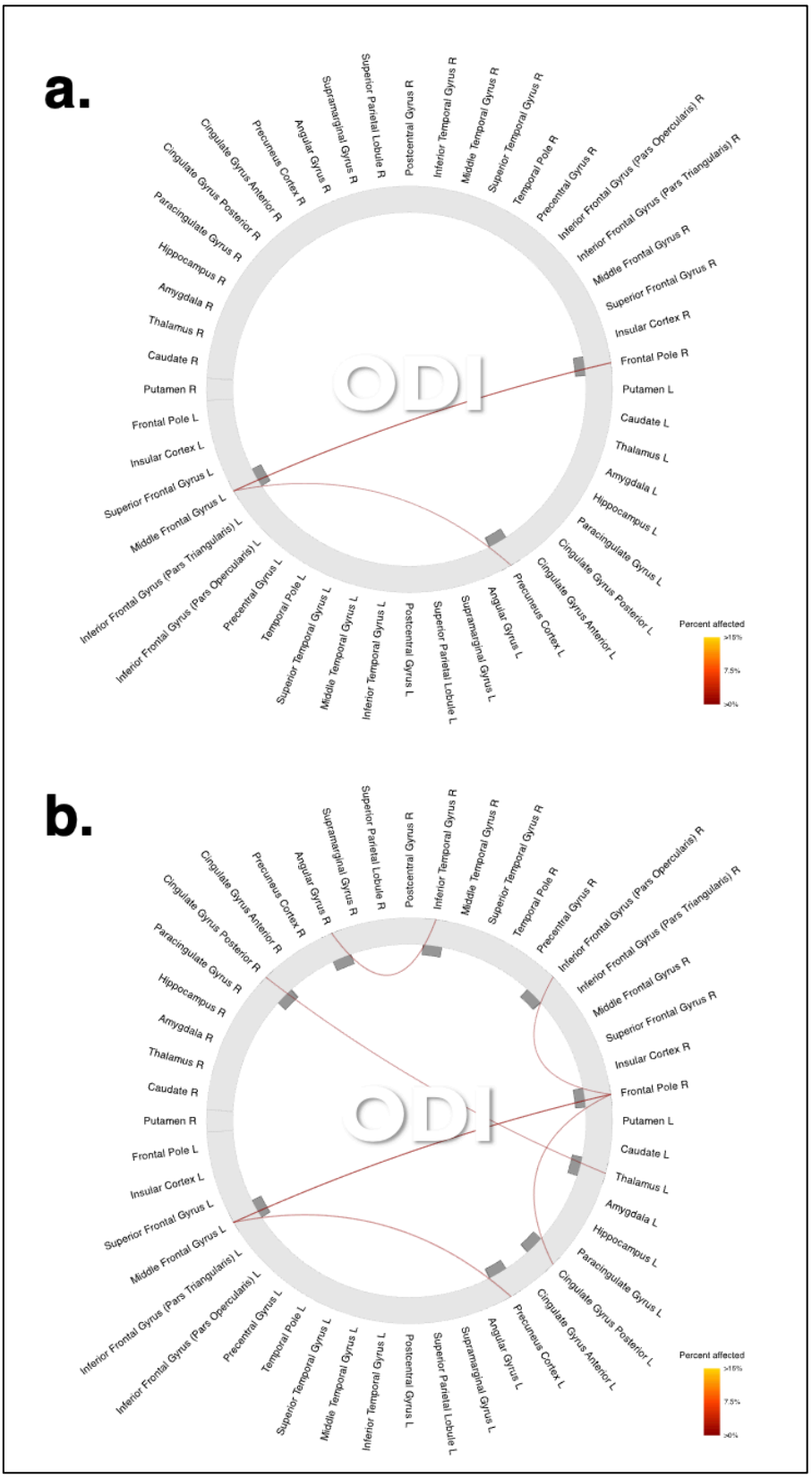

Figure 2-19. Disconnectome for NODDI's ODI with Age A bidirectional relationship was observed with **(a)** higher neuronal dispersion in select frontal and parietal regions **(b)** and reduced neuronal dispersion in frontal, temporal, parietal and subcortical regions.

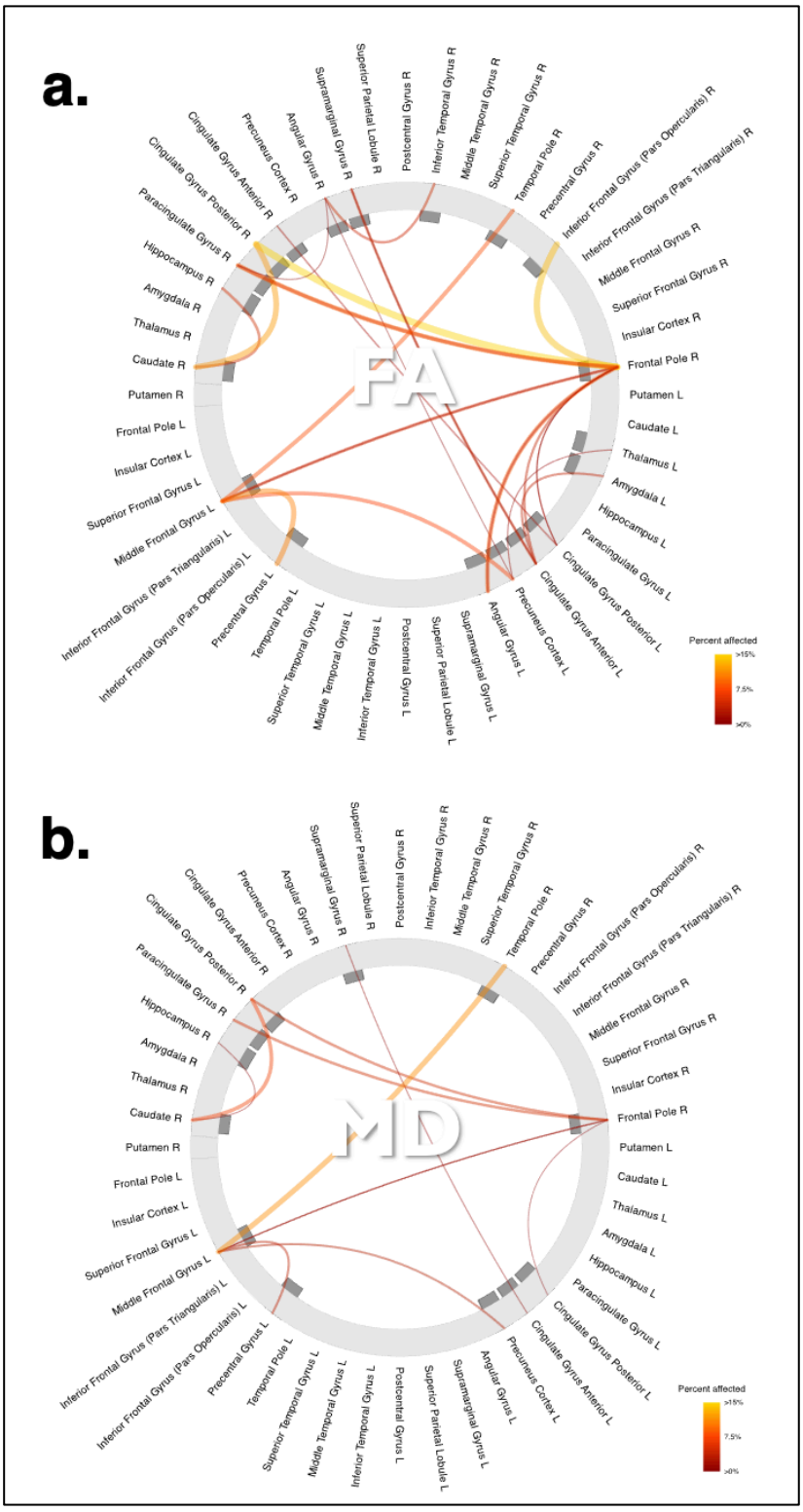

Figure 2-20. Disconnectome for DTI with AMI Increased apathy was linked to **(a)** reduced unidirectional movement of water **(b)** and increased water dispersion in frontal, temporal, parietal and subcortical brain areas.

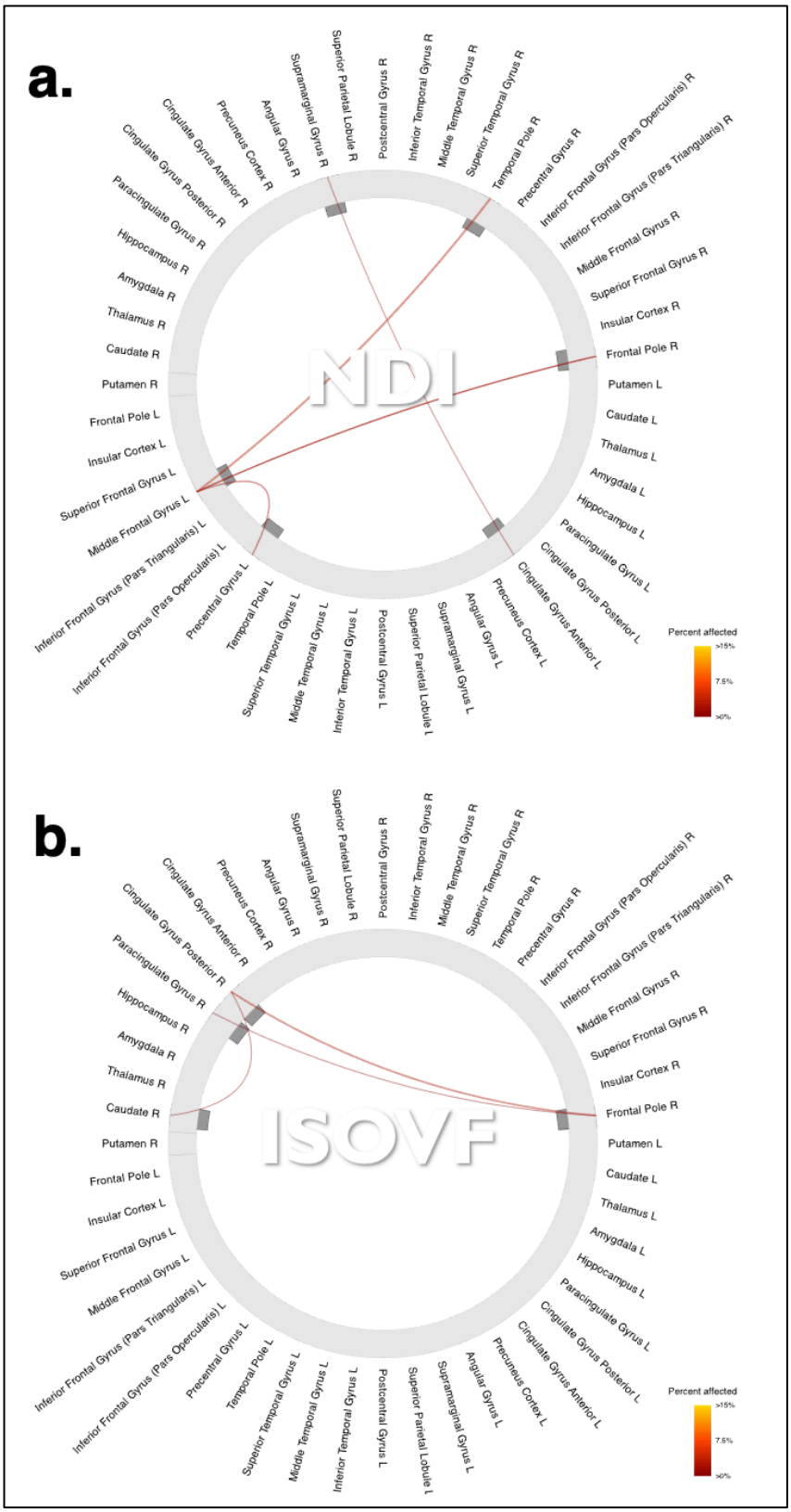

Figure 2-21. Disconnectome for NODDI with AMI Increased apathy was linked to **(a)** reduced neuronal density in frontal, temporal, parietal regions **(b)** and more free water surrounding tracts between frontal, parietal and subcortical brain regions.

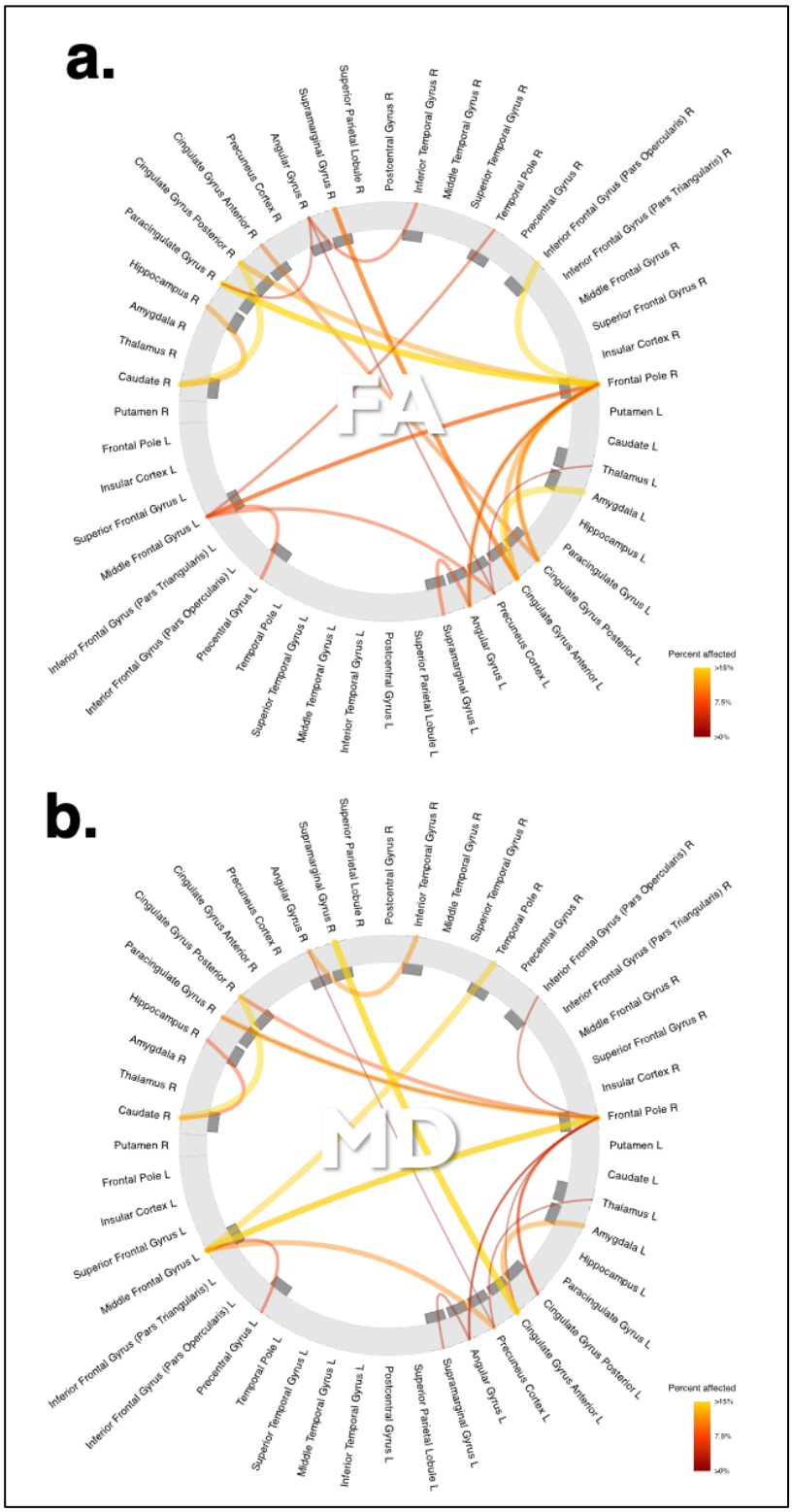

Figure 2-22. Disconnectome for DTI with BDI Increased depression as measured by BDI-II was linked to **(a)** reduced unidirectional movement of water and **(b)** increased water dispersion in several frontal, temporal, parietal and subcortical brain areas.

Depression, as measured by both BDI-II and HADS-depression, consistently showed negative correlations with WM integrity, reflected by increased directions and rate of water diffusion (**Figures 2-22a & 2-22b & 2-24a & 2-24b**) and reduced neuronal density (**Figures 2-23 & 2-25a**). Across both depression measures, almost identical connections between the right frontal pole and left middle frontal gyrus; left middle frontal and left precentral gyri; right frontal pole and right paracingulate gyrus; left anterior cingulate gyrus with the left amygdala and right supramarginal gyrus; and the right caudate with the right hippocampus and right posterior cingulate gyrus showed significant reduction in WM integrity as determined by FA, MD and NDI.

Depression, as measured by HADS-depression, showed that there was significantly more free water surrounding WM tracts as determined by ISOVF (**Figure 2-25b**). Weakened connectivity was observed in tracts between the left anterior cingulate gyrus and left amygdala; the right frontal pole and bilateral posterior cingulate gyri; and the right frontal pole and left angular gyrus.

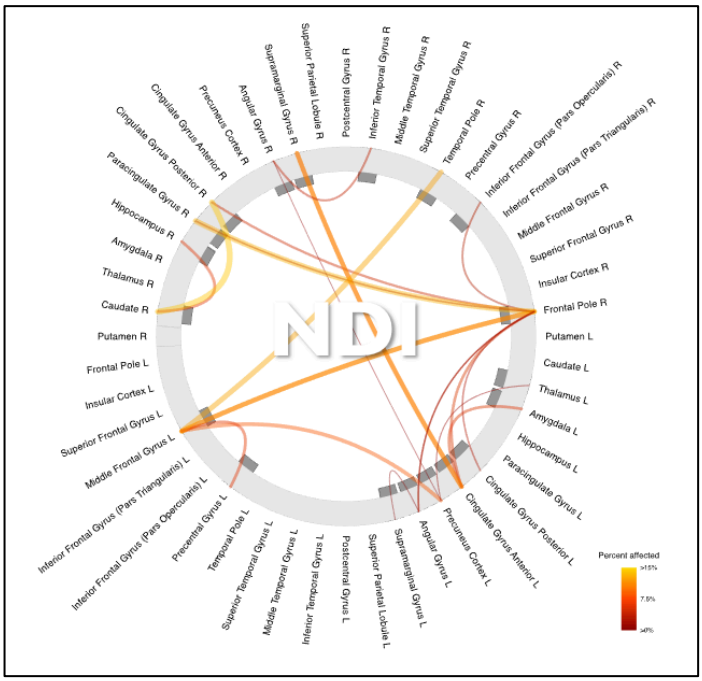

Figure 2-23. Disconnectome for NODDI with BDI Increased depression as measured by BDI-II was linked to **(a)** reduced neuronal density in several frontal, temporal, parietal and subcortical brain areas.

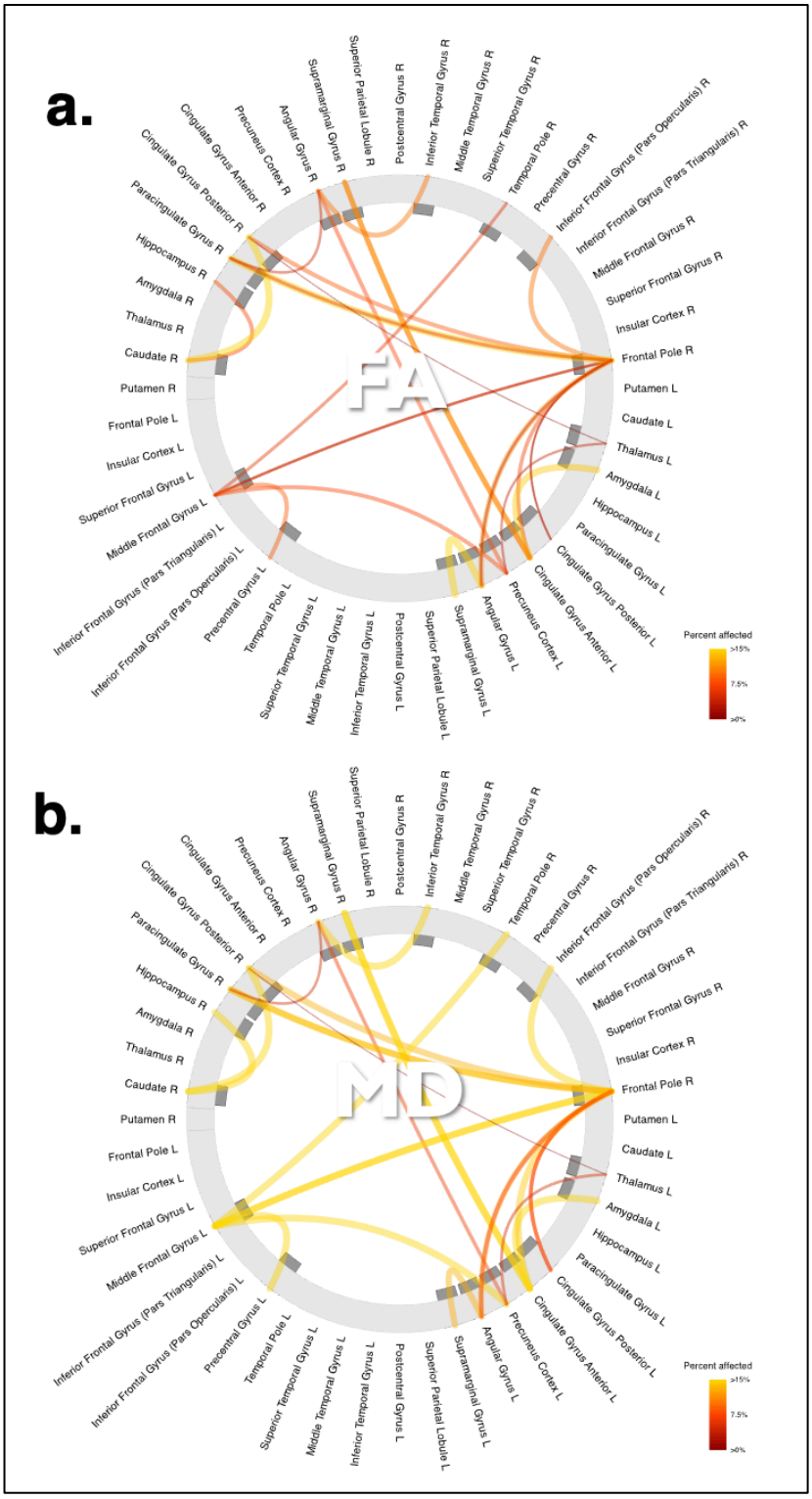

Figure 2-24. Disconnectome for DTI with HADS-depression Increased depression as measured by HADS was linked to **(a)** reduced unidirectional movement of water, **(b)** increased water dispersion **(c)** and reduced neuronal density in almost identical connections between the frontal, temporal, parietal and subcortical areas of the brain. **(d)** There was also more free water surrounding tracts between frontal, parietal and subcortical brain regions.

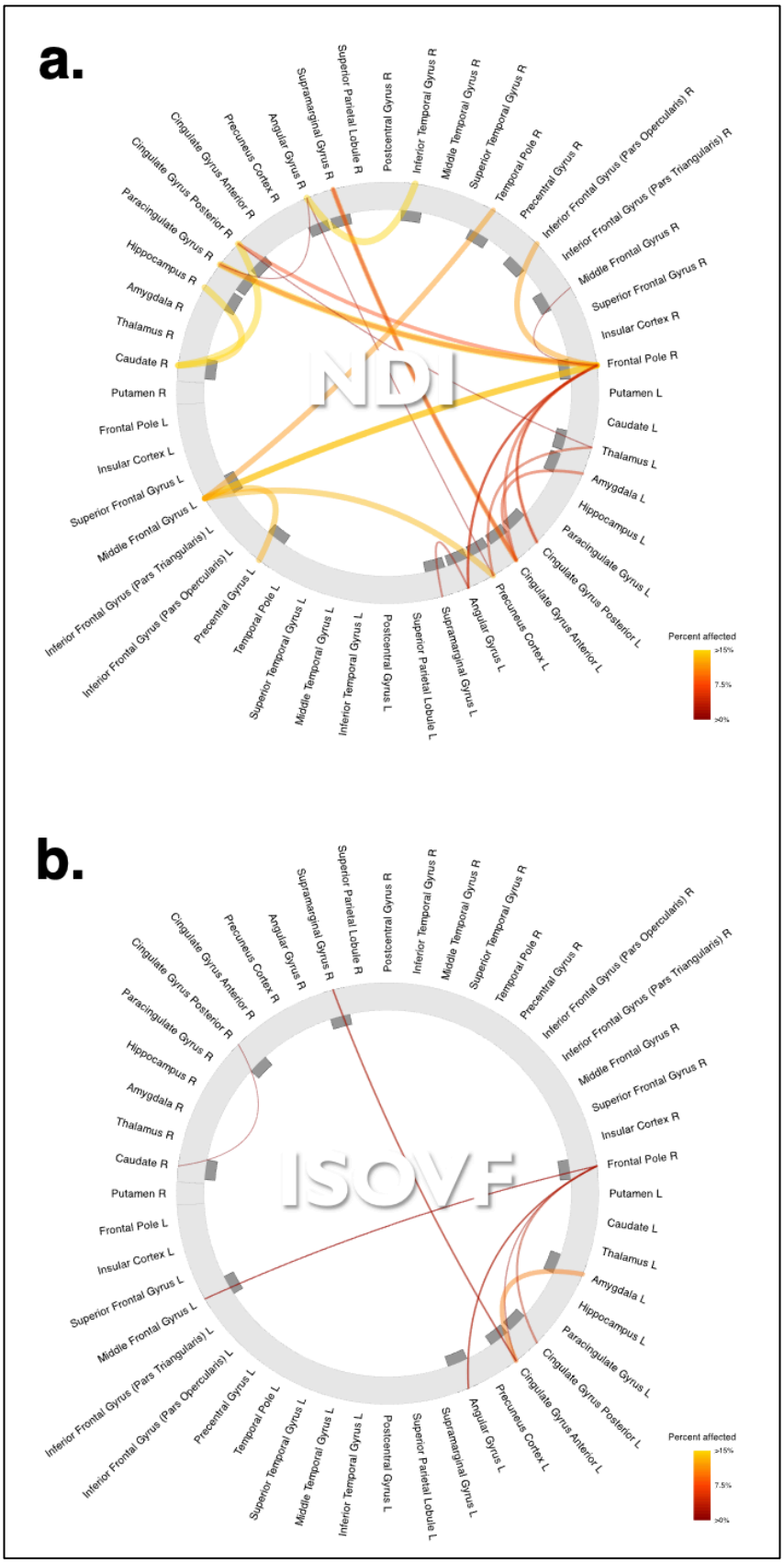

Figure 2-25. Disconnectome for NODDI with HADS-depression Increased depression as measured by HADS was linked to **(a)** reduced neuronal density in almost identical connections between the frontal, temporal, parietal and subcortical areas of the brain. **(b)** There was also more free water surrounding tracts between frontal, parietal and subcortical brain regions.

Increased impulsivity, as measured by the BIS-II, showed associations with a reduction in overall WM integrity. This was reflected in increased directions and rate of water diffusion (**Figures 2-26a & 2-26b**), reduced neuronal density (**Figures 2-27a**) and more free water surrounding WM tracts (**Figure 2-27b**). Similar disconnections to the previously reported depression measures (**Figures 2-22b & 2-24b**)were observed for impulsivity but only as modelled by MD (**Figure 2-26b**). These include links between the right frontal pole and left middle frontal gyrus; left middle frontal and left precentral gyri; right frontal pole and right paracingulate gyrus; left anterior cingulate gyrus with the left amygdala and right supramarginal gyrus; and the right caudate with the right hippocampus and right posterior cingulate gyrus. The impulsivity disconnectome as modelled by FA showed a similar pattern with the exception of projections from the left anterior cingulate gyrus to the left amygdala and right supramarginal gyrus (**Figure 2-26a**). The connection between the left anterior cingulate gyrus and left amygdala was yet again shown to be weakened by the ISOVF disconnectome (**Figure 2-27b**) along with projections to the right frontal pole, left posterior cingulate gyrus, and left middle frontal and precentral gyri. The NDI disconnectome (**Figure 2-27a**) showed similar weakened connectivity to the MD model (**Figure 2-26b**) between the right frontal pole and left middle frontal gyrus; left middle frontal and left precentral gyri; right frontal pole and right paracingulate gyrus; left anterior cingulate gyrus and right supramarginal gyrus; and the right caudate with the right hippocampus. The NDI model also highlighted a disconnection between the left thalamus and left precuneus cortex that was less salient in previous models.

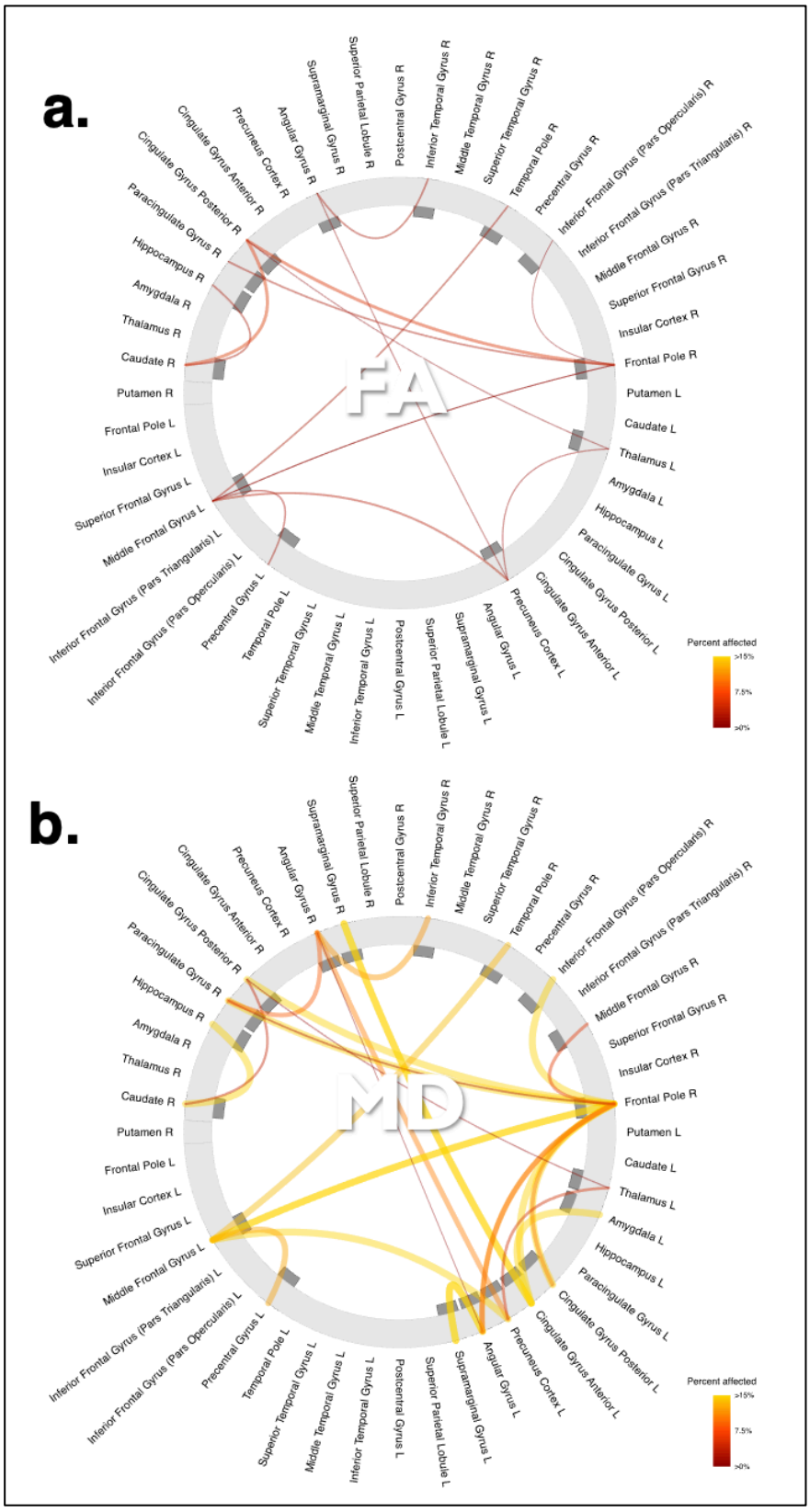

Figure 2-26. Disconnectome for DTI with BIS Increased impulsivity as measured by BIS-II was linked to **(a)** reduced unidirectional movement of water and **(b)** increased water dispersion in frontal, temporal, parietal and subcortical brain areas.

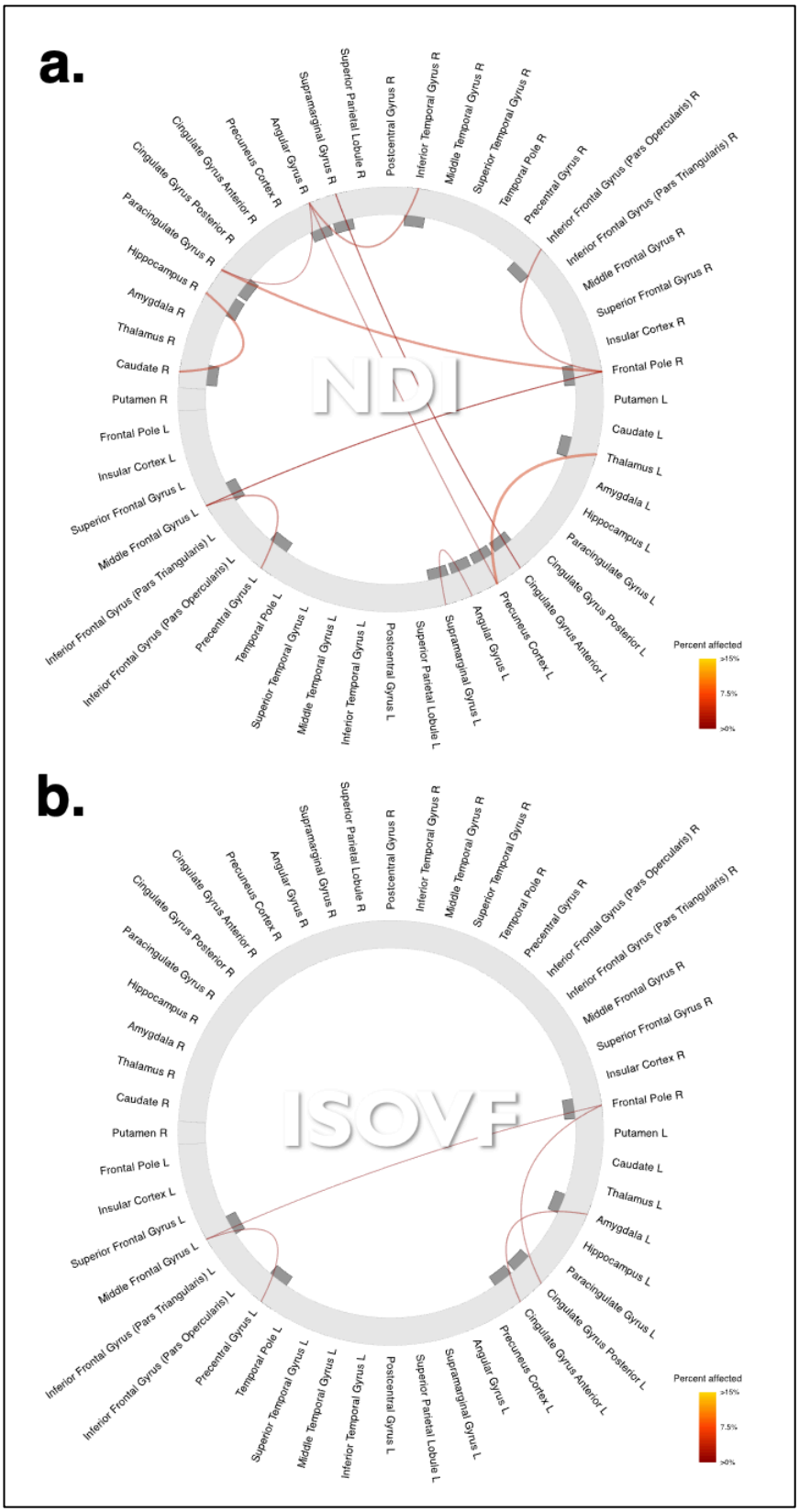

Figure 2-27. Disconnectome for NODDI with BIS Increased impulsivity as measured by BIS-II was linked to **(a)** reduced neuronal density in frontal, temporal, parietal and subcortical brain areas. **(b)** There was also more free water surrounding tracts between frontal, parietal and subcortical brain regions.

2.5 Discussion

The primary aim of this chapter was to characterise structural and diffusion-derived neuroimaging markers in individuals with SVD relative to age-matched HC. This was done in an effort to establish the structural context needed to interpret the neuroimaging–behavioural associations that will be examined in subsequent chapters. Overall, the pattern of findings was highly consistent with established literature on SVD (Duering et al., 2018; Mayer et al., 2022; Tuladhar et al., 2015), indicating that the current sample demonstrates the expected macrostructural and microstructural signatures of the neurodegenerative disorder. By combining quantitative WMH estimation with diffusion MRI modelling using both DTI and NODDI within a TBSS framework, this chapter provides a comprehensive overview of WM alterations that are both widespread and biologically interpretable.

As expected, participants with SVD exhibited substantially greater WMH burden than those in the HC group, both in terms of total lesion volume and regional distribution (**Figures 2-3 & 2-4**). Although some degree of WMH was observed in the healthy ageing group, lesions in SVD were considerably more extensive and involved both periventricular and deep WM regions. Group-level lesion probability maps further indicated that the SVD group showed WMH extending considerably beyond periventricular boundaries, supporting the presence of a generalised small vessel pathology. Importantly, the two groups were matched on age and sex, and although the SVD group had spent fewer years in formal education and showed slightly lower cognitive scores (**Table 2-1**), both groups performed within normal limits for their age group on the ACE-III (Beishon et al., 2019; McCarthy et al., 2024). Thus, group differences in WMH and subsequent diffusion abnormalities likely reflect disease-specific processes rather than demographic or cognitive confounds.

The analysis of clinical predictors of WMH burden revealed a nuanced pattern. When examined across the full cohort, WMH volume was strongly positively correlated with age,

apathy and depression (**Figure 2-5**), but negatively correlated with ACE-III scores (**Figure 2-5c**). However, these associations were mainly driven by the HC group. Among HC, being older and having higher HADS-depression scores were good predictors of increased WMH burden, and impulsivity showed an additional negative association. In contrast, no predictors reached significance within the SVD group, where the model explained minimal variance. This divergence might suggest that once vascular injury becomes established, inter-individual variability in demographic or clinical characteristics contributes relatively little to explaining further lesion accumulation. Alternatively, it is possible that selection bias within the patient group limited the detection of such associations.

The TBSS analyses provided a more detailed account of microstructural WM changes and demonstrated widespread alterations across all major tract categories. More than half of the WM skeleton showed significant differences between groups in FA, MD, NDI, or ISOVF, and regionally specific changes were observed in ODI (**Table 2-2**). The directionality of these findings aligned with established pathophysiological interpretations (Duering et al., 2018; Hu et al., 2022; Mayer et al., 2022; Tuladhar et al., 2015). Lower FA and higher MD in SVD reflect disruptions to fibre coherence and increased diffusivity (**Figure 2-6**); reduced NDI and increased ISOVF indicate diminished axonal density and altered extracellular composition(**Figure 2-7**); and bidirectional ODI changes suggest region-specific differences in fibre dispersion potentially linked to both degenerative and compensatory processes (**Figure 2-7**). These alterations encompassed extensive association fibres (e.g., superior longitudinal, inferior longitudinal, and inferior fronto-occipital fasciculi), commissural fibres including the forceps major and minor, and projection pathways such as the anterior thalamic radiation and corticospinal tract. The breadth of these disruptions highlights the diffuse nature of SVD-related microstructural injury.

When clinical and demographic variables were examined in relation to WM integrity across the whole cohort, a coherent set of associations emerged. Increasing age, higher levels of apathy, depression, and impulsivity were each linked to reduced WM integrity, though with distinct spatial patterns across DTI (**Figures 2-8 & 2-9**) and NODDI metrics (**Figures 2-10 & 2-11 & 2-12**). Tract changes associated with apathy and depression were relatively widespread, whereas impulsivity effects were more posterior or lateralised depending on the model. Reductions in neuronal density and increases in extracellular free water were common features associated with negative affective and motivational states. Having more years of education and better cognitive performance showed the opposite pattern, being associated with reduced rates of water diffusion and higher neuronal density across fronto-parietal and fronto-cingulate pathways. These findings are broadly consistent with concepts of cognitive reserve (Arenaza-Urquijo et al., 2011; Bozzali et al., 2015; Brickman et al., 2011), suggesting that education and preserved cognitive functioning may confer resilience at the level of microstructural connectivity.

Connectome-based analyses further underscored these associations by demonstrating that cognition and education were linked to increased structural connectivity in tracts connecting frontal, parietal, cingulate, and limbic regions (**Figures 2-12 & 2-13 & 2-14 & 2-15**). In contrast, ageing and higher levels of apathy, depression, and impulsivity predicted reduced connectivity across many of the same networks (**Figures 2-16 & 2-17 & 2-18 & 2-19 & 2-20 & 2-21 & 2-22 & 2-23 & 2-24 & 2-25 & 2-26 & 2-27**). Particularly noteworthy was the convergence of disconnection patterns across multiple behavioural measures, with consistent involvement of pathways linking the frontal pole, middle frontal gyrus, anterior cingulate cortex, amygdala, paracingulate gyrus, and supramarginal gyrus. These results indicate that vulnerability within fronto-cingulo-limbic circuits may represent a shared structural substrate underlying variation in mood, motivation, and impulse control, with SVD

exacerbating disruptions within these systems. Further research is needed to see if similar neurocircuitry underlie behavioural deficits.

This study had several limitations. Despite careful case–control matching, the SVD sample may have been influenced by selection bias, resulting in a relatively homogeneous patient group that could have obscured relationships between clinical measures and imaging markers. Secondly, although the combination of DTI and NODDI provided a rich characterisation of WM architecture, these models have inherent constraints, including sensitivity to partial volume contamination and limited specificity in regions with severe lesion burden. Finally, even though the study was sufficiently powered for voxel-wise analyses, the sample size may still have been inadequate to detect more subtle effects, especially for predictors with restricted variance.

2.6 Conclusion

Taken together, the findings presented in this chapter confirm that the current sample of patients exhibit the hallmark structural and microstructural characteristics of SVD. This establishes a detailed anatomical context for interpreting the behavioural and cognitive associations explored in later chapters of this thesis. The demonstration of extensive WMH burden, widespread diffusion abnormalities, and systematic relationships between WM integrity and clinical measures highlights the multifaceted impact of SVD on brain structure. Moreover, the identification of tracts whose integrity varies systematically with cognition, education, age, and psychopathology provides a principled foundation for understanding how vascular injury shapes behaviour.

3| Impact of SVD on DM under uncertainty

3.1 Abstract

WMH burden in SVD is well established as a major contributor to overall cognitive impairment. However, most studies of SVD have focused on executive and psychomotor functions, with relatively little attention to decision-making processes. This chapter addresses that gap by using behavioural data from the CQ task paradigm (described in Chapter 1) to examine sampling behaviour under uncertainty in humans. On the *active version* of the CQ paradigm, SVD patients earned lower rewards, demonstrated higher tolerance for uncertainty and poorer placement accuracy compared to healthy controls. On the CQ *passive version*, they exhibited riskier decision-making, accepting more offers overall, and showed diminished sensitivity to both uncertainty and reward relative to controls. To investigate the neural correlates of these behavioural patterns, BIANCA, TBSS and NODDI analyses were applied to assess WMH volume and WM microstructural integrity. WMH volume was significantly associated with reward earned in CQ, uncertainty tolerance and placement precision. Additionally, disruptions in the WM microstructural integrity of several tracts including the forceps major, inferior fronto-occipital fasciculus, inferior longitudinal fasciculus, superior longitidunial fasciculus and posterior thalamic radiation demonstrated significant negative correlations with reward earnings and placement precision. Offer acceptance showed strong positive correlations with disruptions in the corpus callosum and superior corona radiata. Widespread disconnection between frontal, parietal, temporal and subcortical regions predicted abberant decision-making behaviour. These findings provide novel insights into the brain networks underlying decision-making impairments in SVD, highlighting the role of WMH burden and tract-specific microstructural integrity in shaping behaviour under uncertainty.

3.2 Introduction

Active information sampling is fundamentally a process of reducing uncertainty before committing to a course of action (Attaallah et al., 2025; Keller et al., 2020; Petitet et al., 2021). Decades of behavioural and computational research have highlighted how individuals actively gather information, weigh potential costs, and balance the trade-off between exploration and exploitation to improve choice accuracy in decision-making (Gupta et al., 2006; Juni et al., 2016; Klein-Flügge et al., 2016; Mata et al., 2011). Models such as sequential sampling frameworks and evidence accumulation models (e.g., drift-diffusion) emphasize that choices unfold over time, guided by the integration of noisy evidence until a threshold is reached (Forstmann et al., 2016). Together, these literatures establish uncertainty reduction as a central organizing principle of decision-making research. Paradigms such as Bandit tasks and Foraging tasks have provided insights into how humans manage limited resources when faced with uncertainty (Averbeck, 2015b; S. Constantino & Daw, 2015; Scott, 2010). Other paradigms, like the Beads Task, probe the problem of optimal stopping, requiring participants to weigh the costs and benefits of additional evidence against the risk of making premature or delayed choices (Furl & Averbeck, 2011). However, these decision-making paradigms stop short of allowing participants to fully manipulate uncertainty.

The CQ task offers key advantages over traditional decision-making paradigms. As described in Chapter 1, CQ requires participants to actively sample information before making a choice, with complete agency to determine both how many samples to collect and where to place them. This flexibility means that information gathering can be adapted strategically, embedding uncertainty reduction directly into the task structure (Attaallah et al., 2021, 2024b). Unlike paradigms where information is passively provided, CQ mirrors real-world decision contexts where individuals ideally recognize that additional sampling may not always reduce uncertainty in a meaningful way, and must weigh the potential usefulness of new information

against the costs of time, effort, or resources (Petitet et al., 2021). In doing so, it creates an ecologically valid setting in which uncertainty reduction is not abstract but behaviourally consequential. Within the decision-making landscape, the CQ task represents a methodological advance for studying how people resolve uncertainty in dynamic environments.

A growing body of neuroscience research shows that reducing uncertainty relies on distributed interactions among cortical and subcortical regions, including the prefrontal cortex, parietal cortex, striatum, and the amygdala (Critchley et al., 2001; Huettel et al., 2005a; Mushtaq et al., 2011; Oswald et al., 2015; Stern et al., 2010; Volz et al., 2003). Functional neuroimaging studies reveal that these regions flexibly coordinate through large-scale networks, each potentially contributing to distinct aspects of decision-making (Xue et al., 2010). The frontoparietal control network, encompassing dorsolateral prefrontal and posterior parietal cortices, is considered to support adaptive evidence evaluation, enabling flexible integration of incoming information to guide choices (Marek & Dosenbach, 2018). The cingulo-opercular network, including the anterior cingulate cortex and anterior insula, is proposed to maintain task set stability and sustained engagement, ensuring consistent performance over time (Schimmelpfennig et al., 2023). Complementing these, the salience network appears to be important in detecting behaviourally relevant or unexpected stimuli, facilitating rapid allocation of cognitive resources, while the default mode network contributes to internal simulation and the evaluation of potential outcomes (Chand & Dhamala, 2016; Lamichhane & Dhamala, 2015). Finally, reward and valuation circuits, including the ventromedial prefrontal cortex, orbitofrontal cortex, and striatum, have been implicated in encoding subjective value and prediction errors that inform choice under uncertainty (Gendolla et al., 2014). Dynamic interactions among these networks may be crucial for integrating task information, monitoring performance, and flexibly adjusting behaviour, supporting the complex process of uncertainty reduction during decision-making.

WM tracts provide the structural connectivity that enables coordination across distributed decision-making networks (M. Li et al., 2024). In particular, the superior longitudinal fasciculus and cingulum bundle have been shown to support communication between prefrontal, parietal, and cingulate regions that underlie evidence accumulation and cognitive control (Heilbronner & Haber, 2014; Heilbronner & Hayden, 2016; Pisner et al., 2019). Efficient uncertainty reduction prior to committing to a decision might not depend only on regional brain activity but also on the integrity of WM pathways linking decision-related networks (Penke et al., 2010). WM pathology, such as WMH, represents a potentially significant source of disruption to these integrative processes and remains a characteristic feature of SVD (Pantoni, 2010; Wardlaw et al., 2019). WMH reflect microvascular injury that compromises axonal and myelin integrity, thereby degrading signal transmission between distributed brain networks (Gootjes et al., 2004; Sachdev et al., 2007; Wen & Sachdev, 2004). Although WMH burden in SVD is well established as a major contributor to overall cognitive impairment, most prior work has emphasized deficits in executive and psychomotor domains (Jochems et al., 2025; S. Wang et al., 2022). Despite their established role in other cognitive domains, the influence of WMH on decision-making, and on processes of uncertainty reduction, remain poorly understood. This chapter addresses that gap by applying behavioural data from the CQ task paradigm to investigate how WMH burden may alter sampling behaviour in decision-making under uncertainty in humans.

3.3 Methods

3.3.1 Participants, demographics, and consent

Forty-seven SVD participants aged between 50-90 years (27 males, 20 females) were recruited through the Cognitive Disorders Clinic at the John Radcliffe Hospital in Oxford. The majority of these volunteers were also those who had undergone MRI scanning as described in Chapter 2. Patients had been referred to the clinic for complaints about their cognition. Patients with significantly greater WMH load than expected for their age, as determined from clinical (structural) scans, and without features to suggest an alternative diagnosis (such as Alzheimer's disease) were diagnosed with SVD and invited to participate in our research studies. Patients with other neurological comorbidities such as previous major stroke, Parkinson's disease or epilepsy were excluded from participation. Their performance in this study was compared to that of sixty-five age-matched healthy controls who were also part of the cohort in the previous chapter. Demographics are presented in **Table 3-1**.

The two groups did not differ significantly in terms of age or sex ratio. However, healthy controls had significantly more years of full-time education compared to SVD patients. Cognitive screening using ACE-III (Addenbrookes Cognitive Examination-III) revealed significantly higher scores in healthy controls, although both groups had scores that were within normal limits for the general population (Hsieh et al., 2013; Mathuranath et al., 2000). Patients scored significantly higher on the Apathy Motivation Index (AMI), Beck Depression Inventory-II (BDI-II) and Barratt Impulsiveness Scale (BIS-II) (Ang et al., 2016; Beck et al., 1961a; Patton et al., 1995) than control participants. Additionally, the SVD cohort had significantly higher scores on both subscales of the Hospital Anxiety and Depression Scale (HADS) (Zigmond & Snaith, 1983).

Number of Participants	Diagnosis		p-value[2]
	HC N = 65[1]	SVD N = 47[1]	
Age (years)	69.4 ± 8.6	70.2 ± 9.6	0.6
Gender			0.3
Male	29 (45%)	27 (57%)	
Female	36 (55%)	20 (43%)	
YOE	22.4 ± 8.8	18.3 ± 3.2	0.001
Total ACE-III	97.5 ± 2.3	89.9 ± 9.0	<0.001
Total AMI	1.2 ± 0.5	1.6 ± 0.6	<0.001
Total BDI-II	6.3 ± 5.1	15.0 ± 10.5	<0.001
Total BIS-II	69.8 ± 13.1	79.8 ± 7.7	<0.001
HADS Depression	5.1 ± 3.3	8.7 ± 1.9	<0.001
HADS Anxiety	8.6 ± 4.6	10.9 ± 3.1	0.003

[1] Mean ± SD; n (%)

[2] Welch Two Sample t-test; Pearson's Chi-squared test

Table 3-1: Demographic and questionnaire measures. HC = Healthy Controls, SVD = Cerebrovascular Small Vessel Disease, YOE = Years of Education, ACE-III = Addenbrooke's Cognitive Examination III, AMI = Apathy Motivation Index, BDI-II=Beck Depression Inventory II, BIS-II = Barrat Impulsiveness Scale II, HADS =Hospital Anxiety and Depression Scale.

Permission for this study was obtained from the local ethics committee. All subjects provided written consent in accordance with the Declaration of Helsinki and the study was approved by the University of Oxford ethics committee.

3.3.2 Experimental setup

"Circle Quest" paradigm

Circle Quest is a decision-making behavioural paradigm comprised of two separate conditions:

1. Active information-sampling task and
2. Passive choice task

The tasks were not counterbalanced: all participants performed the active information-sampling task before the passive choice task.

Stimuli

Stimuli were presented on a 17-inch touchscreen PC using MATLAB version 2018a (MathWorks; https://uk.mathworks.com) and Psychtoolbox version 3. Participants performed the tasks in a quiet testing room sitting within reaching distance of the screen (~50 cm). An experimenter was present in the room at all times during the behavioural testing which took about 90 mins on average to complete (Petitet et al., 2021).

Circle Quest Active information-sampling task

The objective in this version was to earn as many credits as possible. To accomplish this, participants had to localize a hidden purple circle as accurately as they could using cues (samples) they generated themselves (**Figure 3-1**). A circular grey mask (search space) was shown on the visual display and individuals were told that a purple circle (radius = 130 pixels; area = 5.80% of the search space) was hidden within this search space. Participants were instructed to tap anywhere within the search space to gather information about where the purple circle was hidden. A small dot (radius = 4 pixels) appeared wherever they touched the grey space. If the dot was purple, it signified that this location was within the area of the hidden purple circle. However, if the dot was white instead, this meant the participant had touched outside the area of the hidden purple circle. These dots remained on the screen for the duration of the information-sampling phase and until the end of the trial to reduce memory load for participants.

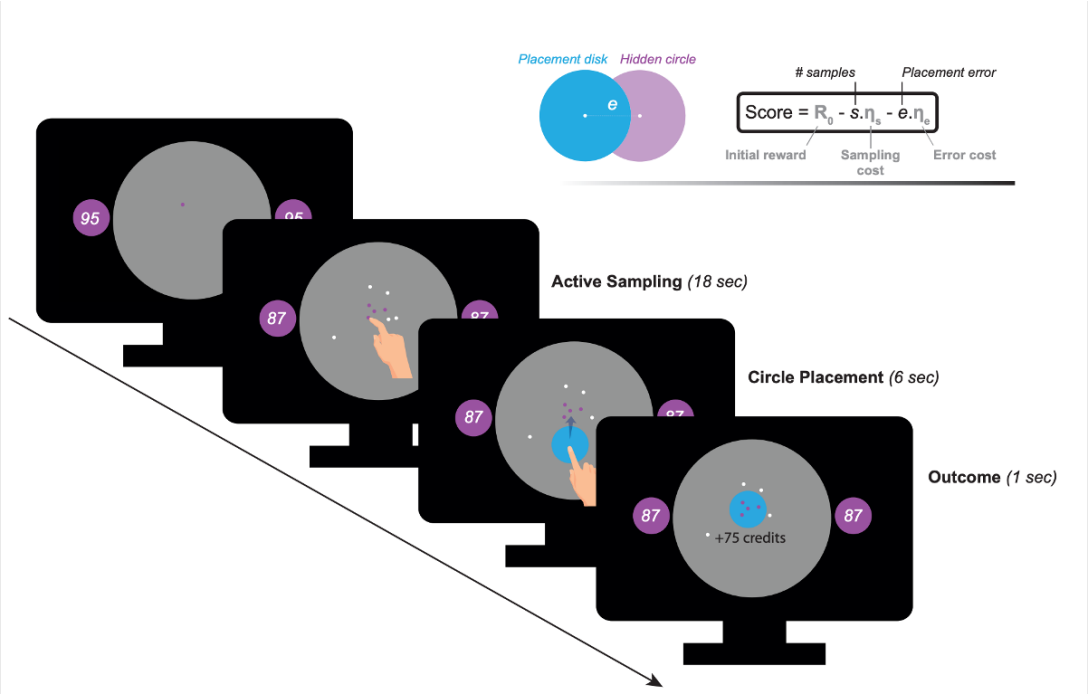

Figure 3-1. Active version of the CQ task. Participants searched for a hidden purple circle by sampling touchscreen locations that produced purple (inside) or white (outside) dots. Two reference circles displayed the initial credit reserve (R_0 = 95 or 130 credits). During an 18 secs sampling period, each touch reduced credits according to the sampling cost (η_s = –1 or –5 credits/sample). Afterward, participants positioned a blue circle to indicate the hidden circle's location, and the resulting score was shown as feedback. *Source: Attaallah et al., eLife (2022), https://elifesciences.org/articles/75834.*

Only one purple circle was hidden within the grey search space during a given trial. Participants were provided with one purple dot at the start of each trial as an initial clue to the circle's likely location to reduce the search time. The location of this first purple dot was drawn randomly from inside the hidden circle and was always at least 260 pixels away (the diameter of the hidden circle) from the edge of the search space, to ensure it always carried the same amount of information (expected error at the start of the search = 86.7 pixels). For each trial, a purple circle was shown on both sides of the grey search space to remind subjects of the size of the hidden circle they were searching for.

The maximum number of credits a participant could win (reward/reward) per trial was displayed within these perpetual purple circles on either side of the grey search space. The number of credits decreased each time the screen was touched to obtain a sample (sample cost), regardless of whether the dot generated was purple or white. The active information-sampling

task was divided into four separate blocks of 25 trials each. Two of these blocks had initial rewards/stakes of 130 credits and the remaining two had initial rewards/stakes of 95 credits. The sampling cost or number of credits decreased by either 1 or 5 credits resulting in 4 different conditions i.e. four separate blocks. These blocks were counterbalanced within participant groups.

For each trial, participants had a maximum of 18 seconds to gather as many samples as they desired. They could stop information gathering at any point before the time ended, however, no extra credits were gained by finishing early. After the 18 seconds, a blue disk—the same size as the hidden purple circle (radius = 130 pixels) — appeared in the middle of the screen. An additional 6 seconds was then provided so this blue circle could be dragged on the touchscreen to where participants thought the purple circle was hidden based on the configuration of white and purple dots they had generated. Their final score was then displayed onscreen.

This score was calculated using the formula for reward

$$(R_f) = R_0 - (s \times \eta_s) - (e \times \eta_e) \qquad \textit{Equation 1}$$

where R_f is the final reward, R_0 is initial reward/stake, s is the sampling cost, η_s is the number of samples, e is the penalty per pixel and η_e is the distance (in pixels) of the blue disks centre from that of the hidden purple circle. Essentially, participants won all the remaining credits post sampling ($R_0 - (s \times \eta_s)$) after a penalty reflecting how far they placed the blue disk from the actual hidden circle ($e \times \eta_e$) was deducted. This meant there were two ways to lose credits: (1) by sampling more information and (2) by greater mis-localization of the true location of the hidden circle. To maximize reward, they had to sample efficiently, using the least number of samples that contained sufficient information to best localize the hidden purple circle. Participants were told that overall credit earnings would later be converted to British pounds and 400 credits was the equivalent of £1.

Circle Quest Passive choice task

This version of Circle Quest (**Figure 3-2**) did not involve any active sampling, so participants had no agency over the choice or number of samples. Instead, they were shown a 'snapshot' of someone's search and asked to make judgments on how much confidence they had in where the purple circle was located and whether they would accept or reject the offer to place the blue circle on the basis of the information they had and the credits on offer. The experiment involved manipulation of the expected error (uncertainty) in localization and the number of credits on offer (initial reward/stake) in each trial to assess how sensitive individuals were to each variable.

Uncertainty, EE (expected error), was calculated as the mean difference between all potential solutions given the current search using a recursive exponential decay model:

$$EE_s = (1-\alpha)(EE_{s-1} - EE_\infty) + EE_\infty \qquad \textit{Equation 2}$$

where EE_s is the expected error after the s^{th} sample, α is the information extraction rate that quantifies the sampling efficiency, EE_{s-1} is the expected error after the previous ($s-1^{th}$) sample and EE_∞ is asymptotic expected error i.e. the lowest error achievable after infinite samples.

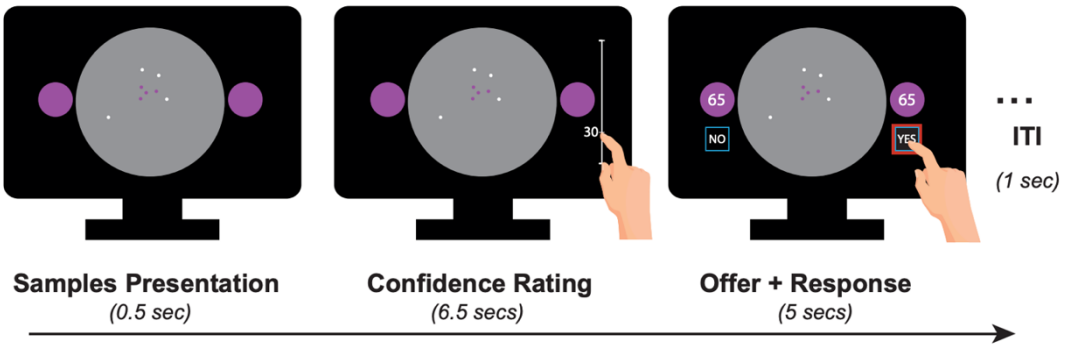

Figure 3-2. Passive version of the CQ task. Participants viewed completed searches and provided confidence ratings (later z-scored and sign-flipped to yield subjective uncertainty estimates) reflecting their perceived ability to locate the hidden circle. Ratings were made by tapping along a vertical scale ranging from 0 (bottom) to 100 (top). After submitting their ratings, participants received a reward offer (R_0 = 40, 65, 90, or 115 credits) and indicated their willingness to place the blue circle by tapping "yes" to accept or "no" to reject the trial.
Source: Attaallah et al., eLife (2022), https://elifesciences.org/articles/75834.

The passive choice task was divided into two phases: an uncertainty rating phase followed by an offer acceptance phase. No feedback was provided in either phase since there were no "correct answers", only subjective responses.

Uncertainty Rating

At the start of each trial participants were shown a 'snapshot' of a completed search with dots on the screen in various configurations. Each trial had eight sample dots in total, half of which were positive samples (purple) and the other half which were negative samples (white). The uncertainty, EE, was manipulated by varying the spatial configuration of the displayed samples. The expected error ranged from 10–70 pixels. This meant the further the positive samples were from each other, the lower the expected error would be. Each participant viewed the exact same trials (total N=100), but the order in which trials was presented was randomized. Participants were asked to make a rating of how confident they were about the location of the hidden purple circle based on the completed search. This rating acted as a proxy for their assessment of uncertainty and was performed using a scale from 1-100 displayed on the side of the screen corresponding to the handedness of the participant. Each completed search appeared on the screen for 0.5 seconds after which the rating scale appeared alongside for an additional 6.5 seconds. During this time participants were expected to make their rating. If they failed to do so in time, the task would move on to the subsequent trial. However, the missed trial would later reappear so all participants would complete all 100 trials.

Offer Acceptance

Once a participant made a rating of the completed search, the trial would progress to the next phase of the task: offer acceptance or rejection. The rating scale would disappear at this point and on each side of the completed search, two purple circles containing the number of credits

on offer were presented instead. There were four credit options (40, 65, 90 or 115). Below the search space on either side was displayed a 'YES' and a 'NO' option which participants could select to accept or reject an offer respectively for the chance to place the blue disk where the hidden purple circle was located. The 'YES' and 'NO' options switched sides randomly during the task to avoid any bias to choose the same option. Participants only accepted or rejected reward offers but did not actually place the blue disk. To incentivize the context, they were told they would later receive ten of the trials from those they accepted to then place the blue circle and collect more credits.

Protocol

Cognitive examination and questionnaires

All study participants were received cognitive examination using the ACE-III which took about 15 mins to complete. Version A of the ACE was administered to the healthy elderly controls while versions B and C were administered to SVD patients since they were more likely to have already been exposed to version A in clinical visits. In addition to the cognitive testing, participants completed established self-report questionnaire measures of apathy (Apathy and Memory Index, AMI), impulsivity (Barratt Impulsiveness Scale, BIS), depression (Beck Depression Inventory, BDI) and anxiety (Hospital and Anxiety Depression Scale, HADS) (Ang, 2017; Beck et al., 1961b; Patton et al., 1995; Zigmond & Snaith, 1983). Two of the questionnaires, AMI and BIS, were completed prior to start of Circle Quest while the other two, BDI and HADS, in between the active information-sampling task and the passive choice task of Circle Quest.

Fatigue ratings during the task

Throughout Circle Quest, participants rated their level of subjective fatigue on a scale from 0 to 100 at the start of each experimental block in both the active and passive sampling conditions. Their prompt to report this rating came in the form of a vertical visual analogue scale that appeared in the middle of the screen underneath the text, 'How tired do you feel?' The top of the scale was labelled 'Extremely' and the bottom was labelled 'Not at all' to indicate the highest and lowest extremes of fatigue.

Experimental design

The active-information sampling variant of Circle Quest was preceded by an exposure session during which participants were introduced to the task, given instructions, and allowed to practice sampling and placing the blue disk. First, they had three practice trials that required them to touch the screen and gather cues to the location of the hidden purple circle. They could acquire as many dots as they desired and when they were content with their search, they would hit the spacebar key to make the blue disk appear. Then they would drag this disk to where they thought the hidden purple circle was located. They received feedback in the form of a faded purple circle showing them the actual location of the hidden circle.

The next part of the exposure session had five blocks of 20 exposure trials (100 trials in total). This time participants were shown completed searches with eight samples (four positive dots and four negative dots) in different configurations to vary the level of uncertainty and the blue disk in the middle of the screen. Each trial also had an associated reward offer and these were either 40, 65, 90 or 115 credits. This part of the exposure session introduced individuals to the credit and scoring function of the task. Participants were required to move the blue disk to where they thought the hidden purple circle was located and then they received feedback in the form of the faded purple circle showing them the actual location of the hidden

circle and the number of credits they won. Note that it was possible to receive negative credit scores.

After completing the exposure session, participants engaged in the active information-sampling version followed by the passive choice version.

3.4 Results

3.4.1 SVD patients earned fewer credits and spent less time on sampling than controls

The effects of group, initial reward, and sampling cost on task performance were investigated using a linear mixed-effects model. This revealed strong main effects of both initial reward and sampling cost on total reward earnings. Overall, participants earned significantly more when the initial reward was high (Main effect of initial reward: $\beta = +35.75$, 95% CI = [34.66, 36.84], $t_{6630} = 32.87$, $p < 0.0001$), and significantly less when the sampling cost was high (Main effect of cost: $\beta = –36.40$, 95% CI = [–37.85, –34.95], $t_{6630} = –25.07$, $p < 0.0001$; **Figure 3-3a**). SVD patients earned significantly less overall than healthy controls (Main effect of group: $\beta = –7.08$, 95% CI = [–8.84, –5.32], $t_{6630} = –4.01$, $p < 0.001$), indicating a consistent reduction in reward performance. This group difference was most pronounced in the high-reward condition, as evidenced by a significant group × reward interaction ($\beta = –4.77$, 95% CI = [–6.17, –3.37], $t_{6630} = –3.40$, $p < 0.001$), suggesting that SVD patients benefitted less from high-reward opportunities. Post hoc comparisons, Bonferroni-corrected for multiple testing, confirmed that SVD patients earned significantly less in all task conditions (all $p_{((corr))} < 0.001$), reinforcing the conclusion that reward maximization was systematically impaired in SVD patients across the board.

A separate linear mixed-effects model revealed a significant main effect of group on sampling time. SVD participants sampled for significantly shorter time than healthy controls overall (Main effect of group: $\beta = –1.86$, 95% CI = [–2.5, –1.22], $t_{6630} = –2.91$, $p < 0.01$; **Figure 3-3b**). There was also a main effect of sampling cost, with participants taking less time to sample under high-cost conditions ($\beta = –0.89$, 95% CI = [–1.06, –0.72], $t_{6630} = –5.27$, $p < 0.001$), reflecting cost-sensitive adjustments in behaviour. However, neither the main effect of reward ($\beta = –0.22$, $p = 0.42$) nor any interaction terms reached significance (ps > 0.34), suggesting that both groups modulated their time spent sampling similarly in response to cost and reward level.

Bonferroni-corrected post hoc comparisons showed that SVD patients spent significantly less time sampling in all four task conditions (low cost/low reward: $p_{((corr))} = 0.0036$; low cost/high reward: $p_{((corr))} = 0.016$; high cost/low reward: $p_{((corr))} = 0.013$; and high cost/high reward condition ($p_{((corr))} = 0.044$). These results show that SVD participants spent less time on information sampling overall, despite making similar adjustments to sampling cost and reward as controls which suggests that they generally understood what was required of them in the task.

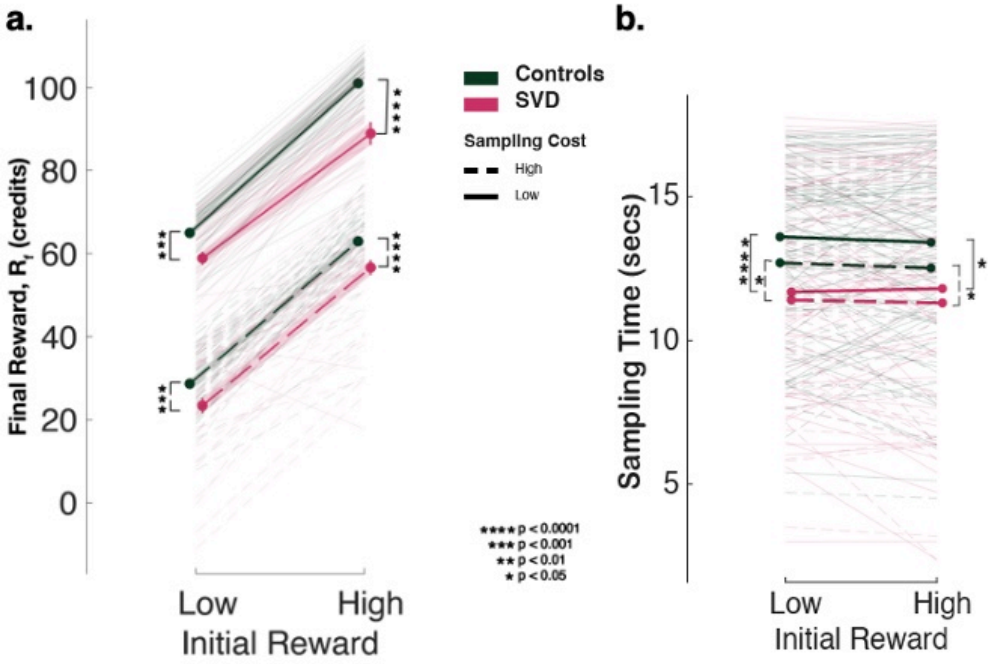

Figure 3-3. SVD patients accrued less reward than healthy controls due to reduced time on task. (a) Across different conditions of the active version, SVD patients consistently won significantly less reward (credits) than the healthy controls. **(b)** SVD patients generally spent significantly less time than healthy controls gathering samples before placing the blue circle.

3.4.2 SVD patients were less sensitive to sampling cost and tolerated more uncertainty

A linear mixed-effects model revealed that participants collected significantly fewer samples under high-cost conditions (Main effect of sampling cost: $\beta = -2.16$, 95% CI = [–2.89, –1.43], $t_{6630} = -5.71$, $p < 0.0001$; **Figure 3-4a**). There was also a significant interaction between group and sampling cost ($\beta = 0.98$, 95% CI = [0.07, 1.89], $t_{6630} = 2.11$, $p < 0.05$), indicating that

the effect of cost on sampling differed between SVD patients and controls. Specifically, controls showed a larger cost-related increase in sampling compared to SVD patients when information became cheaper. There were no significant effects of group ($\beta = -0.90$, $p = 0.23$), initial reward ($p = 0.68$), or any other interactions (ps > 0.54). These findings indicate that while sampling quantity was cost sensitive for both groups, SVD patients were significantly less sensitive than controls.

A linear mixed-effects model examining deviation from Bayes-optimal sampling revealed a significant main effect of sampling cost ($\beta = +4.12$, 95% CI = [3.75, 4.49], $t_{6630} = 11.21$, $p < 0.0001$; **Figure 3-4b**). When compared to the Bayesian ideal observer model (Equation 1), participants under-sampled in low-cost conditions (mean deviation = -2.21 ± 0.079) and over-sampled in high-cost conditions (mean deviation = $+2.44 \pm 0.065$), reflecting a consistent directional bias in their sampling behaviour. There was also a significant interaction between group and sampling cost ($\beta = 1.01$, 95% CI = [0.54, 1.48], $t_{6630} = 2.13$, $p < 0.05$), indicating that the effect of cost on deviation from optimal differed between SVD patients and controls. Specifically, SVD patients showed a significantly greater deviation from optimal sampling (undersampled more) compared to controls when sampling was cheap. There were no other significant main effects of group ($\beta = -1.00$, $p = 0.13$) or initial reward ($\beta = 0.16$, $p = 0.52$), and no other significant interactions (all ps > 0.41). These findings indicate that while deviation from the Bayesian ideal observer was broadly cost-sensitive, the sensitivity to cost differed by group with SVD patients being less sensitive.

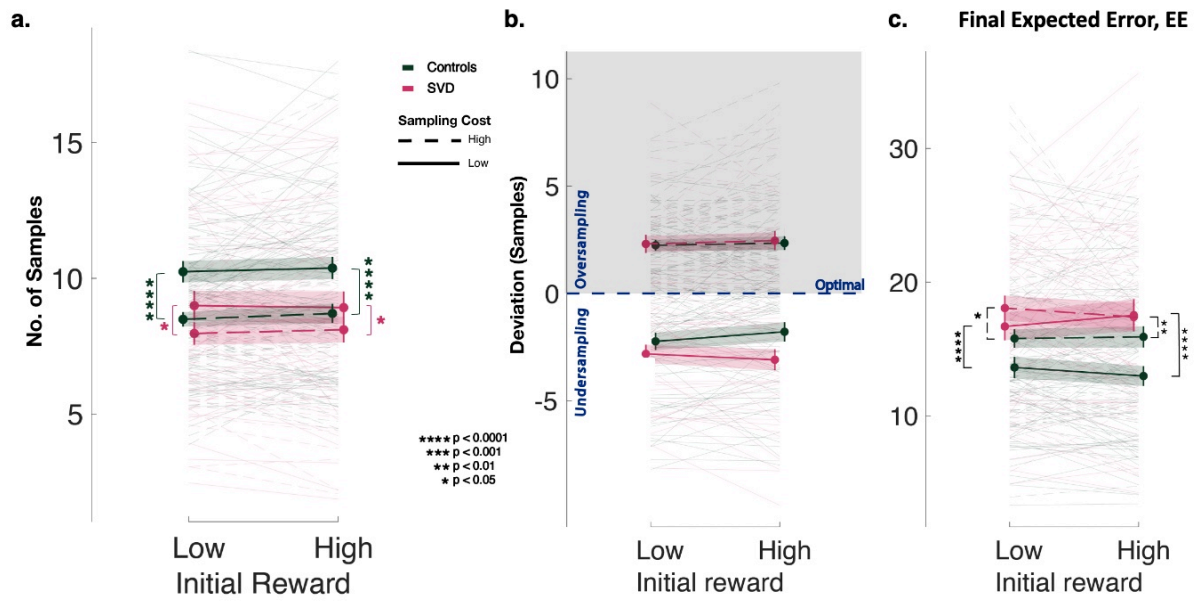

Figure 3-4. Sampling behaviour of participants. (a) Controls increased the number of samples they collected significantly more than SVD patients when sampling cost decreased. **(b)** Both groups of participants oversampled in the high sampling cost condition and undersampled in the low sampling cost condition when compared to the Bayes-optimal sampler. **(c)** SVD patients reduced uncertainty (the expected error) significantly less than controls before placing the blue circle.

A linear mixed-effects model revealed that SVD participants tolerated significantly more uncertainty after sampling compared to controls (β = +4.35, 95% CI = [2.93, 5.77], t_{6630} = 3.06, $p < 0.01$; **Figure 3-4c**). This main effect was consistent across all task conditions, and there was a significant interaction between group and sampling cost (β = -1.31, 95% CI = [0.69, 1.93], t_{6630} = -2.12, $p < 0.05$) and group and initial reward (β = 1.69, 95% CI = [0.93, 2.45], t_{6630} = 2.22, $p < 0.05$). Specifically, at the end of sampling controls had significantly reduced uncertainty compared to SVD patients when sampling cost became cheaper and there was more reward to be won. Participants also showed significantly greater residual uncertainty in high-cost trials compared to low-cost (β = +2.17, 95% CI = [0.89, 3.45], t_{6630} = 3.32, $p = 0.0009$), indicating that sampling cost had an impact on how people sampled (Petitet et al., 2021). Bonferroni-corrected post hoc comparisons confirmed that SVD participants had significantly higher final uncertainty in all four conditions (all corrected $ps < 0.05$). There was no effect of initial reward ($p = 0.34$). These results suggest that while both groups were sensitive to

sampling cost, SVD patients consistently failed to reduce uncertainty to the same extent as controls before committing to a decision. This might be indicative of an impairment in efficient information seeking, greater uncertainty tolerance, or both.

3.4.3 SVD patients had lower accuracy and precision compared to healthy controls

Task accuracy was defined as the placement of the blue disk relative to the actual hidden circle, reflecting how close their final choice was to the true target. A linear mixed-effects model showed that SVD participants placed the blue disk significantly further from the target location compared to controls, i.e. they demonstrated worse localization accuracy ($\beta = +6.85$, 95% CI = [3.98, 9.72], $t_{6630} = 4.75$, $p = 2.04 \times 10^{-6}$; **Figure 3-5a**). Importantly, as might be expected, both groups' localization errors increased with greater final expected uncertainty (expected error, EE; see Equation 2) after sampling. The significant group differences were most pronounced at lower levels of uncertainty, where final mean uncertainties for controls and SVD participants were 14.56 ± 0.132 and 17.78 ± 0.231, respectively.

To determine whether the reduced localization accuracy in SVD participants was specific to the CQ active version or reflected a broader impairment, performance in the training session under low and high uncertainty conditions was also examined. On a Wilcoxon rank-sum test, SVD participants were significantly less accurate than controls in the low uncertainty condition (Bin 1; median uncertainty, EE = 11.09; $p = 0.005$; **Figure 3-5b**). In contrast, no significant group difference was found under high uncertainty (Bin 2; median uncertainty, EE = 27.12; $p = 0.879$). The impairment under low, but not high, uncertainty suggests that the reduced localization accuracy in SVD participants is unlikely to stem simply from a generalized sensorimotor dysfunction.

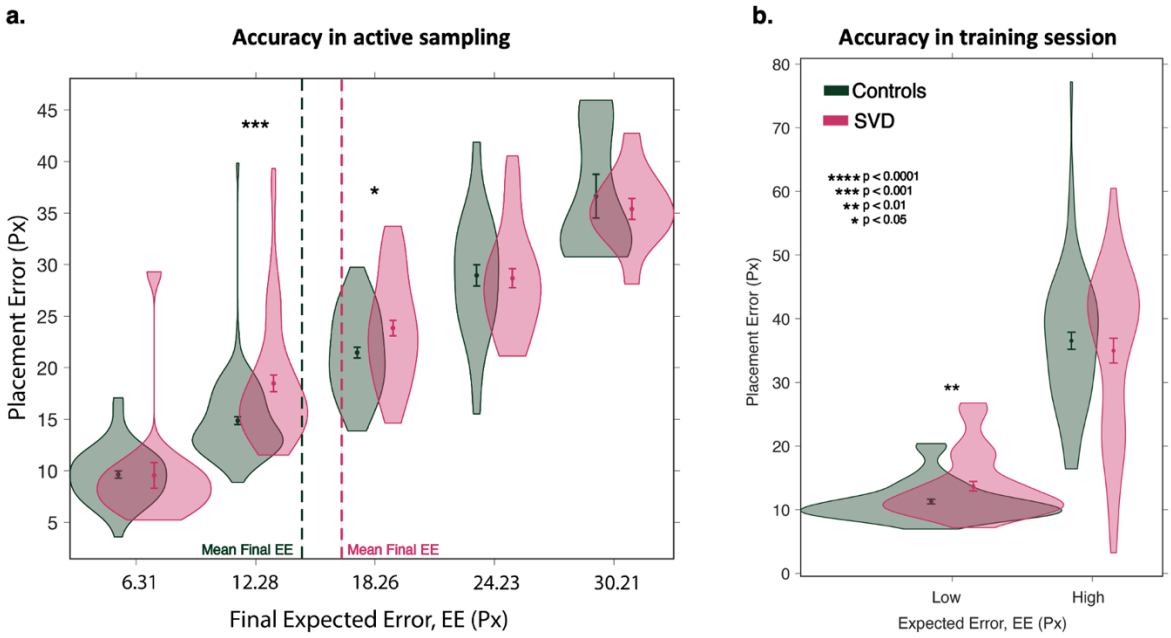

Figure 3-5. Accuracy as a function of expected error. (a) SVD patients placed the blue circle significantly farther from the hidden circle than controls in the active version at lower levels of uncertainty. **(b)** Similarly, in the training session, patients were less accurate at placing the blue circle at lower levels of uncertainty.

Task precision was defined as the placement of the blue disk relative to the participants' own search locations (dots on the screen), reflecting how consistently they used the information they had just gathered. In relation to accuracy, precision was quantified as the absolute difference between participants' observed accuracy and their final expected error, computed from their search using a centroid method of hits, excluding misses:

$$D_P = |D_A - EE_f| \qquad \textit{Equation 3}$$

where D_P is precision, representing the distance in pixels of the placed blue disk from the participant-derived optimal location based on their completed search; D_A is accuracy, the distance in pixels of the placed blue disk from the hidden circle (target); and EE_f is the final expected error, also measured in pixels, representing the remaining uncertainty after the search. Lower D_P values indicate that participants' performance was closer to the expected error derived from their sampling, reflecting more effective use of previously sampled information,

whereas higher D_P values indicate greater deviation from the expected error. On average, precision and accuracy were closely aligned in both groups, with final placement errors (accuracy) of 19.38 ± 0.36 and 23.24 ± 0.39 pixels from the hidden circle for controls and patients, respectively. These average deviations occurred when the final uncertainty was significantly different between both groups (**Figure 3-6a**).

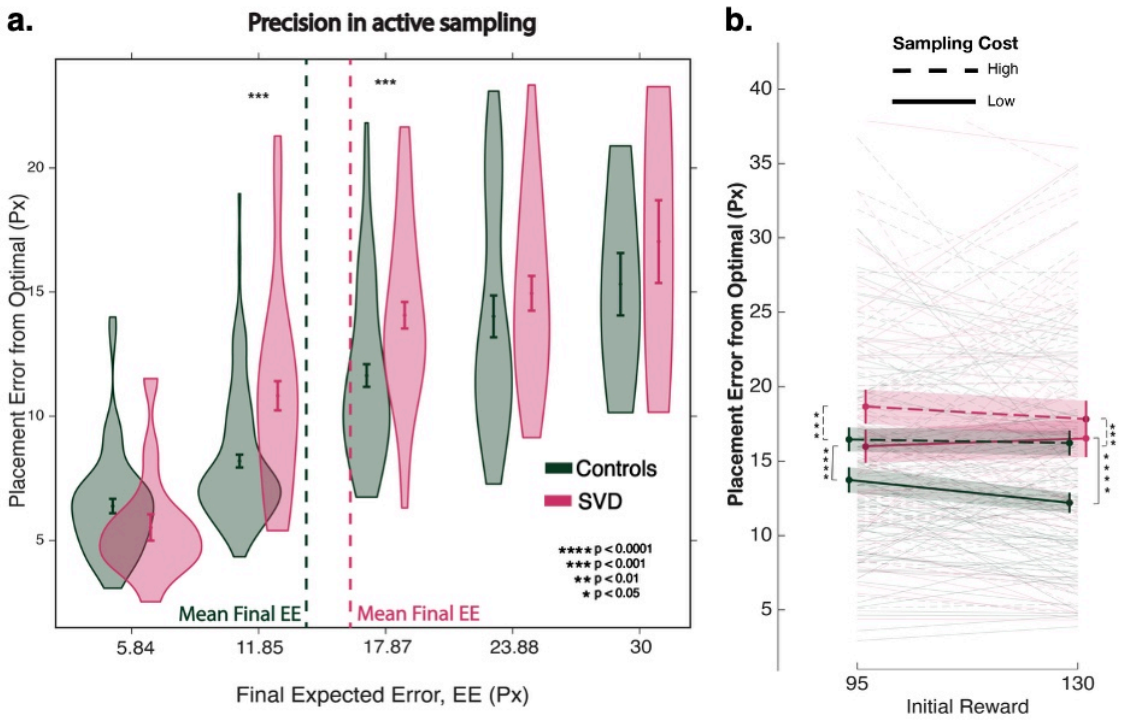

Figure 3-6. Participants' precision of placement (a) SVD patients placed the blue circle at a significantly greater distance from the optimal location defined by their own completed search. **(b)** SVD patients were significantly less precise than controls in all four conditions.

A linear mixed-effects model showed that placement precision was significantly influenced by sampling cost and group. Higher sampling costs were associated with decreased placement precision ($\beta = +2.98$, SE = 0.75, $t_{6626} = 3.96$, $p = 7.54 \times 10^{-5}$; **Figure 3-6b**), and SVD patients exhibited greater imprecision than controls ($\beta = +3.92$, SE = 1.03, $t_{6626} = 3.79$, $p = 1.52 \times 10^{-4}$). Additionally, the interaction between initial reward and group was significant ($\beta = +2.24$, SE = 1.11, $t_{6626} = 2.01$, $p = 0.044$), indicating that the effect of reward on placement

precision varied between groups. Specifically, controls showed significantly greater precision when the initial reward increased. There were no other significant main effects or interactions, including initial reward alone and its interaction with sampling cost or group, were not significant (all $p > 0.05$). Post-hoc comparisons across conditions revealed that placement imprecision was significantly higher for SVD patients in all four conditions (low cost/low reward: $t = 3.92$, Bonferroni-corrected $p = 0.00036$); low cost/high reward: $t = 4.50$, Bonferroni-corrected $p = 2.77 \times 10^{-5}$); high cost/low reward: $t = 4.21$, Bonferroni-corrected $p = 0.0001$); and high cost/high reward: $t = 4.40$, Bonferroni-corrected $p = 4.32 \times 10^{-5}$).

3.4.4 Information extraction rate of participants

Information extraction rate did not differ significantly by group, sampling cost, or initial reward (all $p > 0.25$; **Figure 3-7**), indicating consistent efficiency in information acquisition across conditions. Patients tended to sample faster than controls, as reflected by generally shorter inter-sampling intervals (ISI) in SVD participants. ISI increased significantly with higher sampling costs ($\beta = +0.17$, 95% CI $\approx [0.11, 0.23]$, $t_{6630} = 6.01$, $p < 0.0001$; **Figure 3-7**). There was a significant interaction between group and sampling cost on ISI ($\beta = -0.09$, 95% CI $\approx [-0.134, 0.46]$, $t_{6630} = -2.06$, $p < 0.05$; **Figure 3-8b**) suggesting that patients' sampling speed was less sensitive to cost manipulations than controls. Post-hoc comparisons revealed that controls slowed down significantly at higher sampling costs (low cost vs. high cost at low reward: $t = 0.17$, Bonferroni-corrected $p < 0.0001$); and low cost vs. high reward at high reward: ($t = 0.18$, Bonferroni-corrected $p < 0.0001$). SVD patients did not slow down significantly (all $ps > 0.068$). The stable information extraction rates across groups and conditions imply a speed-efficiency trade-off in sampling behaviour for both controls and SVD patients.

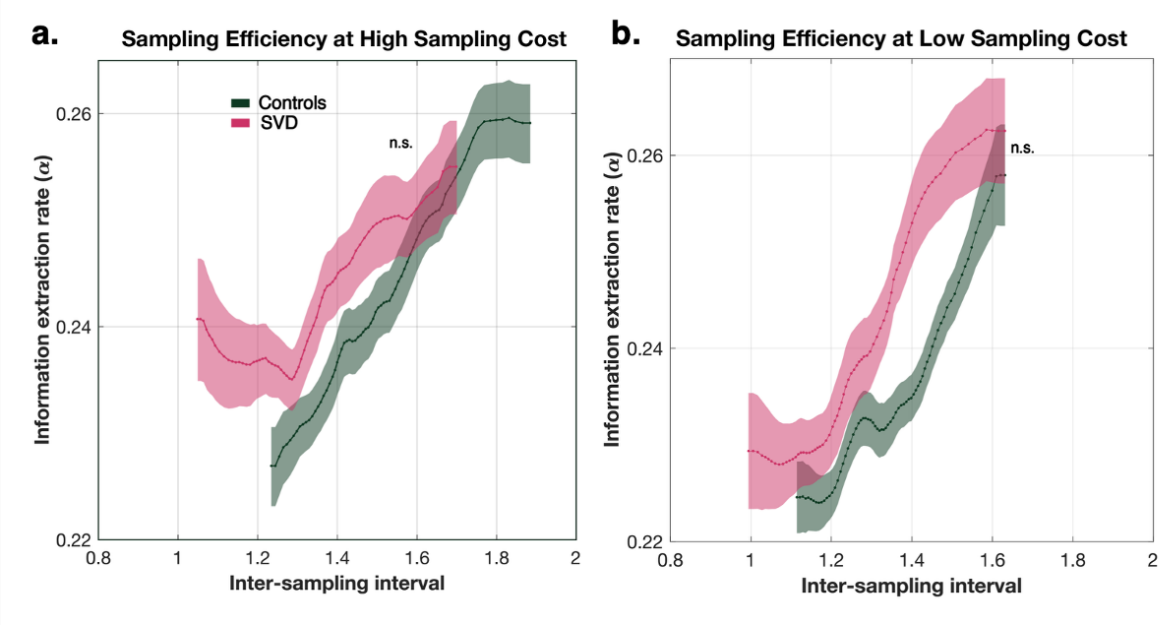

Figure 3-7. Relationship between information extraction and inter-sampling interval (a) SVD patients gathered samples faster than controls in the high sampling cost condition but were less efficient, i.e. they did not extract as much information per sample. **(b)** In contrast, patients gathered samples faster than controls in the low sampling cost condition and were more efficient in their sampling behaviour.

3.4.5 Temporal aspects of sampling and placement behaviour

A linear mixed-effects model showed that pre-sampling time was significantly influenced by sampling cost (β = +0.30, 95% CI ≈ [0.23, 0.37], t_{6630} = 4.45, $p < 0.0001$; **Figure 3-8a**) and group (β = -0.32, 95% CI ≈ [0.19, 0.45], t_{6630} = -2.39, $p = 0.017$). Patients initiated sampling significantly sooner than controls, as demonstrated by shorter pre-sampling times under high sampling cost conditions (high cost/low reward: $t = –2.95$, $p = 0.0032$, Bonferroni-corrected $p = 0.013$; high cost/high reward: $t = –3.03$, $p = 0.0024$, Bonferroni-corrected $p = 0.097$). While pre-sampling times were also shorter for patients under low sampling cost conditions, these differences did not survive correction for multiple comparisons (all Bonferroni-corrected ps > 0.068). This indicates that patients began collecting information significantly earlier than controls in trials where sampling cost was high. Patients also showed a trend toward faster sampling rates, as shown by the significant interaction between group and sampling cost for ISI (see above section). Contrastingly, patients took longer to place the blue disk marking their final choice, though this effect was not significant (group effect: t_{6630} = 1.22, $p = 0.22$; **Figure**

3-8c). These findings suggest that although patients start sampling earlier and sample more quickly in some conditions, they may require additional time for final decision placement.

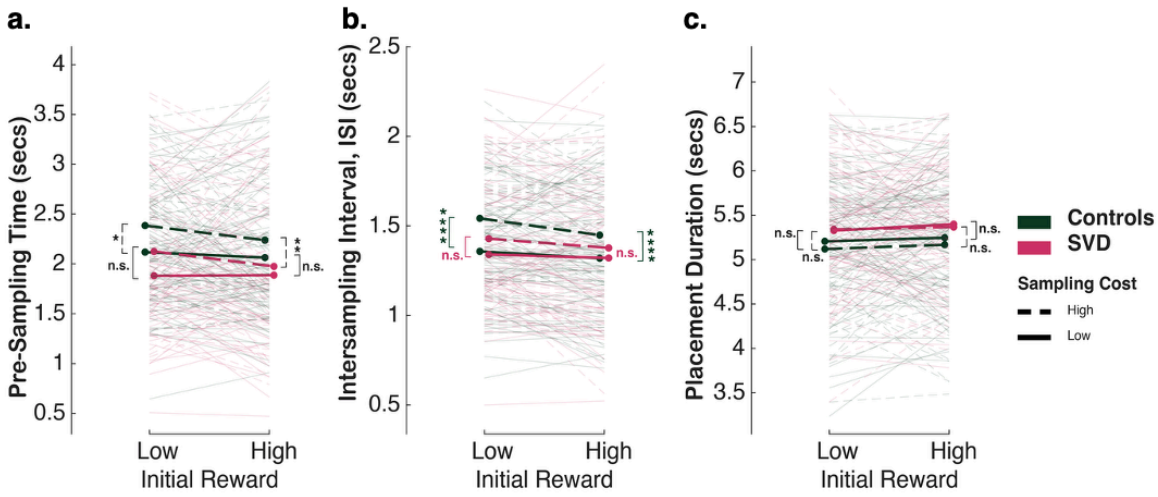

Figure 3-8. Timing-related measures of sampling and response in SVD and control participants (a) SVD patients began sampling significantly quicker than controls in the active version. **(b)** Patients sampled faster than controls, spending less time between gathering each sample, though the difference was not significant. **(c)** Patients were slower at placing the blue circle than controls, but not significantly.

3.4.6 SVD patients' cognition predicts their performance on the CQ task active version

Correlations were performed between the behavioural measures from the active version of the CQ task and participant clinical scores (ACE-II, AMI, BDI-II, BIS-II and HADS). In patients, ACE scores were significantly associated with both task final reward earnings and placement precision. Patients with higher ACE scores earned significantly greater rewards on the task (R^2 = 0.36, p = 3.48 × 10^{-5}, FDR-adjusted p = 0.0029; **Figure 3-9a**). ACE scores were also associated with reduced placement error, such that patients with stronger cognitive scores positioned the blue disk closer to the optimal location based on their search (R^2 = 0.28, p = 2.83 × 10^{-4}, FDR-adjusted p = 0.0119; **Figure 3-9b**). No other significant relationships were observed between behavioural and clinical measures, nor were any behavioural–clinical relationships observed in the control group following correction for multiple comparisons. These findings indicate that within patients, cognitive ability, as assessed by the ACE, but not

self-reported mood, impulsivity, or anxiety symptoms, is selectively linked to maximizing reward and to more precise placement.

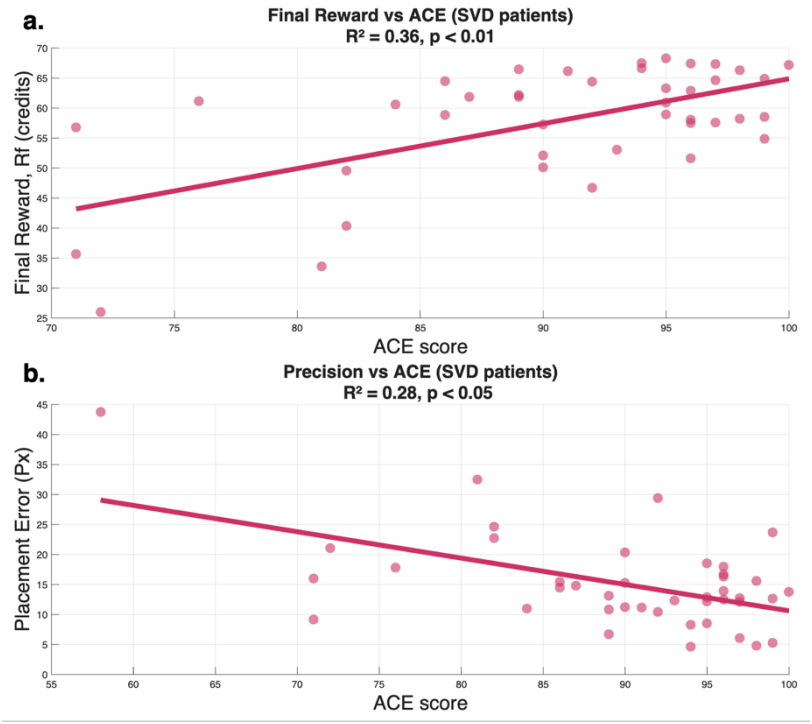

Figure 3-9. SVD patients' ACE scores predicts their performance on the active version (a) SVD patients with higher cognition (ACE) scores earned more reward than patients with lower cognition scores. **(b)** SVD patients with higher cognition (ACE) scores were more precise in placing the blue circle, i.e. they were better able to use the sensory information they had gathered during the information sampling phase of the active version.

Similar correlations were conducted for the behavioural measures from the passive version of the CQ task and the participants' clinical variables. In this case, no significant associations survived correction for multiple comparisons (all FDR-adjusted ps > 0.05;).

3.4.7 SVD patients were less sensitive to uncertainty and reward than healthy controls

On the passive version of the CQ task, participants' subjective uncertainty ratings increased significantly with objective uncertainty, EE, across both groups, indicating that they were aware of different levels of uncertainty in the task ($\beta = 1.16$, SE = 0.10, 95% CI [0.96, 1.36], $t_{556} = 11.37$, $p < 0.0001$; **Figure 3-10a**). However, SVD patients showed attenuated sensitivity to uncertainty, reflected in a significant group × uncertainty interaction ($\beta = -0.38$, SE = 0.068,

95% CI [–0.51, –0.25], t_{556} = –5.62, p < 0.0001). Additionally, SVD participants gave lower overall uncertainty ratings than controls (β = –0.08, SE = 0.022, 95% CI [–0.13, –0.04], t_{556} = –3.73, p = 0.0002). These results indicate that while both groups scaled their uncertainty ratings appropriately, patients consistently perceived less uncertainty overall and were less responsive to changes in actual uncertainty levels. Group-wise linear fits further supported this dissociation: subjective ratings closely tracked objective uncertainty in controls (R^2 = 0.556), but the relationship was notably weaker in SVD patients (R^2 = 0.161). The overall model explained a substantial proportion of the variance in subjective ratings (marginal R^2 ≈ 0.57; conditional R^2 ≈ 0.75).

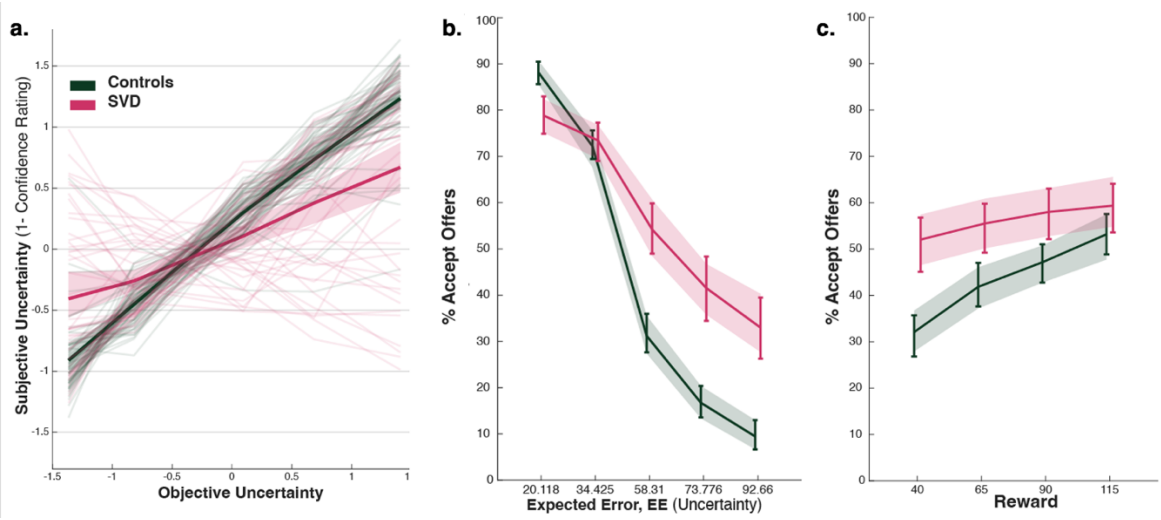

Figure 3-10. SVD patients had reduced sensitivity to uncertainty and reward than healthy controls (a) SVD patients demonstrated impaired ability to perceive uncertainty compared to healthy controls in the passive version. **(b)** Patients accepted significantly more offers at higher levels of uncertainty (expected error) than controls. **(c)** Patients did not alter their offer acceptance in the same way as healthy controls, who accepted more offers as reward increased.

Participants' likelihood of accepting offers decreased significantly as uncertainty increased (β = –0.016, SE = 0.00045, 95% CI [–0.0171, –0.0153], t_{10921} = –35.65, p < 0.0001; **Figure 3-10b**), reflecting greater caution under more uncertain conditions. However, this effect differed by group, with patients showing a reduced negative impact of uncertainty on acceptance (group × uncertainty interaction: β = 0.0046, SE = 0.00030, 95% CI [0.0040,

0.0052], t_{10921} = 15.07, p < 0.0001), indicating relatively less sensitivity to uncertainty compared to controls.

Additionally, SVD patients were generally more likely to accept offers overall (β = 0.24, SE = 0.041, 95% CI [0.15, 0.32], t_{10921} = 5.69, p < 0.0001). Reward positively influenced acceptance rates across groups (β = 0.0040, SE = 0.00048, 95% CI [0.0031, 0.0050], t_{10921} = 8.30, p < 0.0001; **Figure 3-10c**), but this effect was attenuated in patients (group × reward interaction: β = –0.0018, SE = 0.00032, 95% CI [–0.0024, –0.0012], t_{10921} = –5.53, p < 0.0001). This interaction reflects a markedly flatter slope for patients, who exhibited a substantially reduced sensitivity to changes in reward magnitude compared to controls. Consequently, while controls' acceptance rates increased notably with higher rewards, patients' acceptance behaviour remained relatively stable across reward levels. These findings suggest that while patients show a generally increased acceptance tendency, their choices are less modulated by both uncertainty and reward magnitude compared to controls.

3.4.8 Total WMH volume was significantly correlated with final reward, final uncertainty and precision on the active version of the CQ task

Linear models were conducted to examine whether log-transformed total WMH volume was associated with behavioural performance on the active and passive versions of the CQ task. For the active version, models included the following dependent variables: final reward, number of samples, time, intersampling interval, uncertainty (final expected error), precision (placement error from optimal), sampling efficiency, and pre-sampling time. For the passive version, models were conducted on the number of accepted offers and uncertainty ratings. All models controlled for age and gender. Of these variables, only three showed significant associations with WMH volume: higher WMH was associated with lower final reward (p < 0.001; **Figure 3-11a**), greater uncertainty (p = 0.001; **Figure 3-11b**), and poorer precision (p <

0.001; **Figure 3-11c**). The model for uncertainty explained the most variance (R^2 = 0.22), followed by the models for final reward (R^2 = 0.17) and precision (R^2 = 0.17).These findings suggest a specific link between WMH burden and impairments in reward outcomes, active sampling and decision-making variability in the active version of the task.

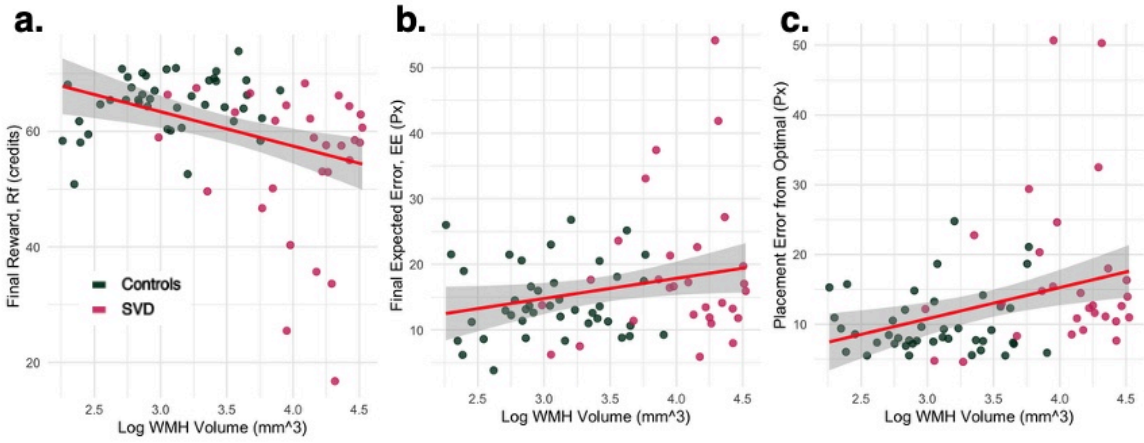

Figure 3-11. WMH total volume as correlated with CQ behavioural metrics (a) Final reward earned in the active version of the CQ task decreased as the total WMH volume in participants increased . **(b)** There was a positive correlation between the final expected error after sampling and the total WMH volume across partipants. **(c)** Placement error of the blue circle in relation to the existing search was positively correlated with total WMH volume across participants.

3.4.9 Final reward and placement precision from active task related to FA in specific WM tracts

TBSS analysis, with α= 0.05 and correcting for multiple comparisons with TFCE, using the DTI model on the whole cohort (across both groups) demonstrated that higher FA values were associated with increased reward earnings across large parts of the WM skeleton (**Figure 3-12a**). These changes were most prominent in the bilateral sagittal stratum (including the inferior fronto-occipital fasciculus and inferior longitudinal fasciculus), bilateral superior longitudinal fasciculus, the bilateral posterior corona radiata, the right retrolenticular part of the internal capsule, the right posterior thalamic radiation (including optic radiation), the right uncinate fasciculus, the tapetum and forceps major. Across the whole cohort, higher FA values in the right posterior thalamic radiation was also associated with increased placement precision (**Figure 3-12b**).

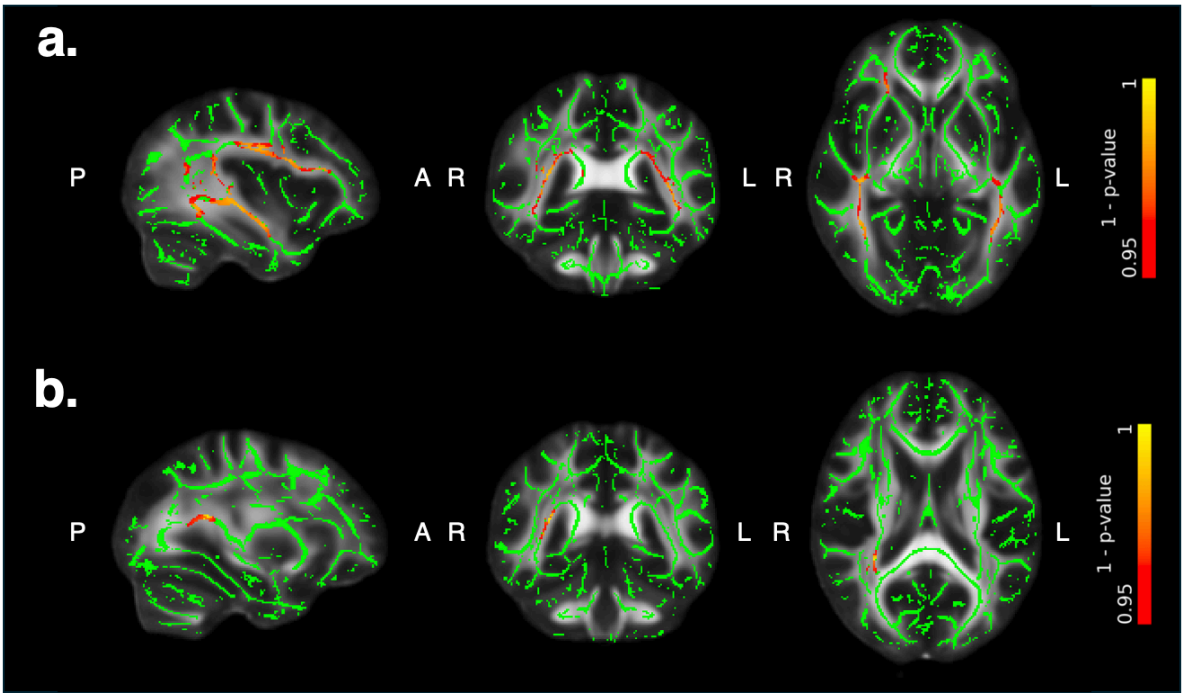

Figure 3-12. TBSS analysis of CQ active version using the DTI model (a) Higher reward earnings was associated with increased FA across many areas of the WM skeleton. **(b)** Increased placement precision of the blue circle was associated with increased FA in WM tracts in the right hemisphere of the brain.

3.4.10 Final uncertainty after sampling predicts higher FA in specific WM tracts

TBSS analysis ($\alpha = 0.05$), corrected for multiple comparisons using TFCE and based on the DTI model across the entire cohort, did not reveal any significant associations with final uncertainty. However, when uncertainty was decomposed into its individual components (number of samples and sampling efficiency or information extraction rate) and each was examined while controlling for the other, higher FA values were found to be associated with an increase in both quantity and efficiency of sampling across several WM tracts (**Figure 3-13a**). In the case of sampling quantity, these changes were most prominent in the bilateral anterior corona radiata bilaterally. Across the whole cohort, higher FA values in the right superior corona radiata, the genu of the corpus callosum (including the forceps minor), the cingulum, and the bilateral anterior corona radiata were also associated with increased sampling efficiency (**Figure 3-13b**).

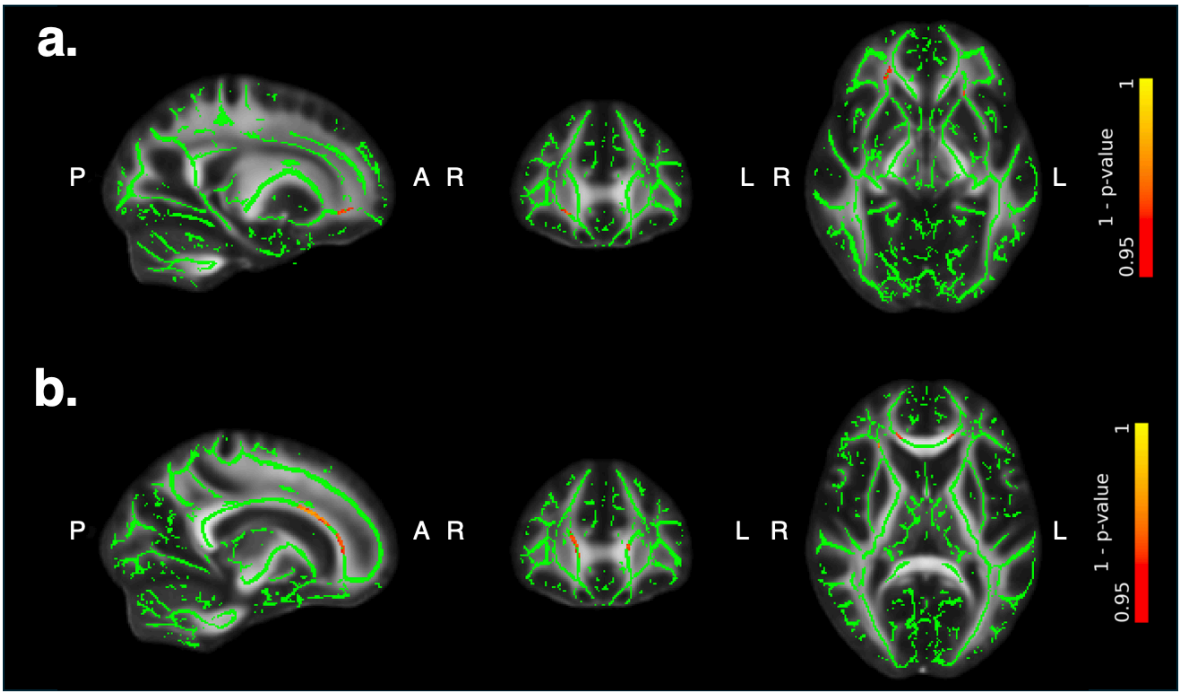

Figure 3-13. TBSS analysis of CQ active version using the DTI model (a) Increased number of samples was associated with increased FA across many areas of the WM skeleton. **(b)** Higher sampling efficiency was associated with increased FA in several WM tracts.

3.4.11 Uncertainty rating and proportion of accepted offers on passive tasks predict FA in WM tracts

TBSS analysis, with $\alpha = 0.05$ and correcting for multiple comparisons with TFCE, using the DTI model on the whole cohort demonstrated that higher FA values were associated with a positive slope for uncertainty rating (**Figure 3-14a**). These changes were most prominent in the left external capsule, left uncinate fasciculus, left anterior corona radiata, right anterior thalamic radiation and the genu of the corpus callosum (including the forceps minor). Further analyses showed that lower FA values were associated with increased offer acceptance in the passive version of the CQ task (**Figure 3-14b**). These changes were most prominent in the left frontal aslant tract, left superior thalamic radiation, left superior corona radiata and left superior longitudinal fasciculus.

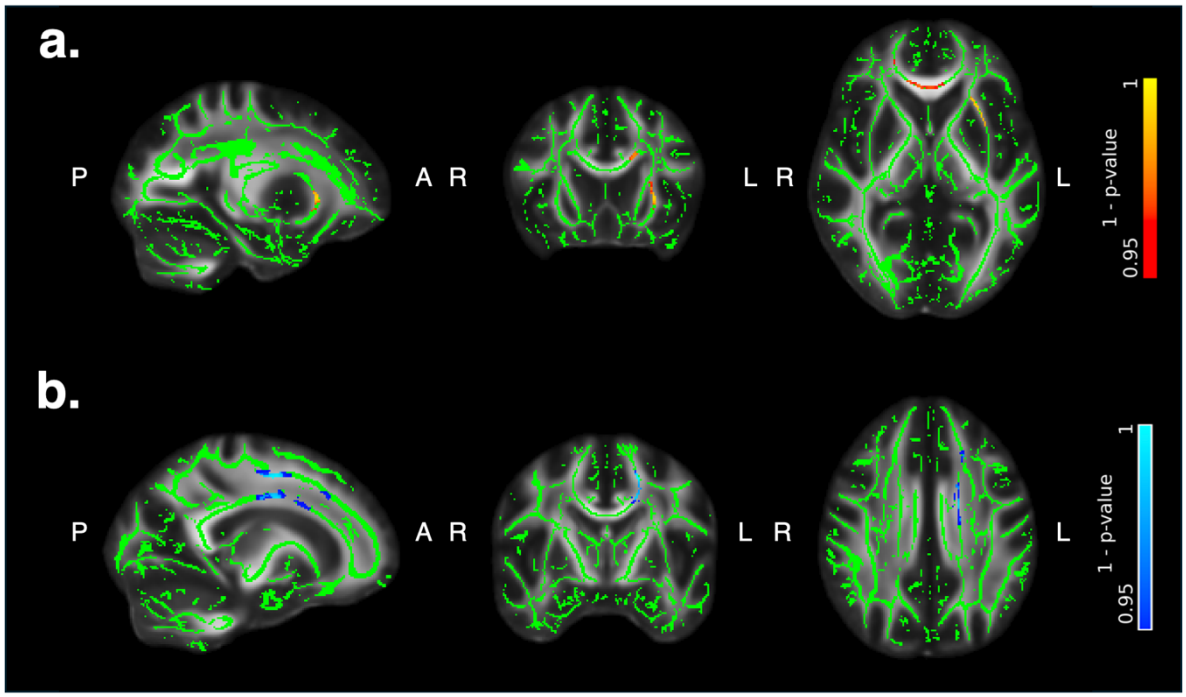

Figure 3-14. TBSS analysis of CQ passive version using the DTI model (a) A positive slope for uncertainty rating was associated with increased FA across many areas of the WM skeleton. **(b)** Increased offer acceptance was associated with reduced FA in WM tracts in the left hemisphere of the brain.

Additional TBSS analyses using the DTI model for behavioural metrics from both task versions did not reveal any significant effects. Similarly, TBSS analyses using the NODDI model showed no significant associations with behaviour.

3.4.12 Disconnectome associated with behavioural deficits in decision-making under uncertainty

Significant TBSS clusters were mapped onto the JHU white-matter atlas to identify affected WM tracts and quantify the proportion of each tract showing supra-threshold effects. The anterior and posterior (or superior/inferior) voxel coordinates of each tract were then assigned to the nearest cortical regions in the Harvard–Oxford atlas, producing a tract-to-cortex mapping for all tracts implicated by TBSS. These data were combined to generate a disconnectome, in which edges reflect the percentage of affected voxels within each tract. In the active version of the CQ task, disconnection associated with reduced winnings was widespread in WM tracts

throughout the brain (**Figure 3-15**) while those associated with reduced sampling (**Figures 3-16&17**) and precision (**Figure 3-18**) were mostly confined to the frontal lobes. Similarly, in the passive version of the CQ task, WM disconnections associated with impaired uncertainty ratings and increased offer acceptance (**Figures 3-19&20**) were mostly confined to the frontal lobes. WM tracts projecting to the angular gyrus, anterior cingulate gyrus, frontal pole, middle frontal gyrus and supramarginal gyrus were consistently implicated across behavioural metrics.

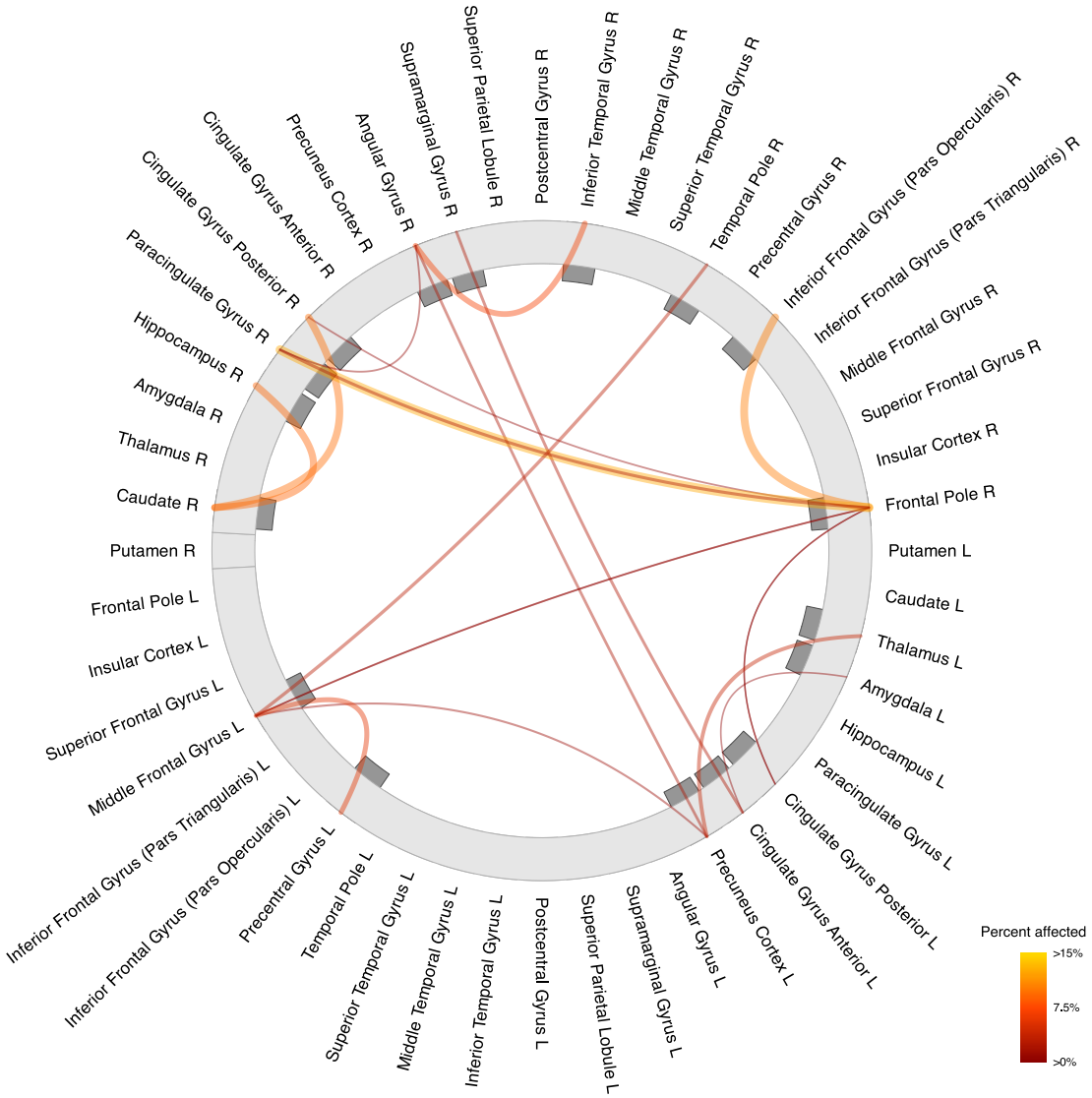

Figure 3-15. Disconnectome associated with reduced reward earnings. Widespread disruption was observed in WM tracts connecting frontal, temporal, parietal, and subcortical regions.

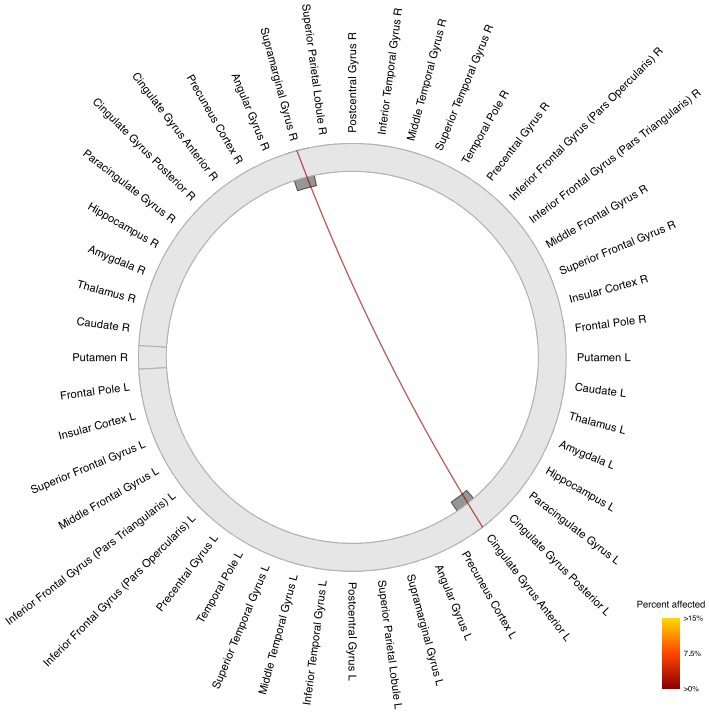

Figure 3-16. Disconnectome associated with reduced number of samples. Disruption was observed in WM connections within the right frontal pole and between the right supramarginal gyrus and left anteriour cingulate gyrus.

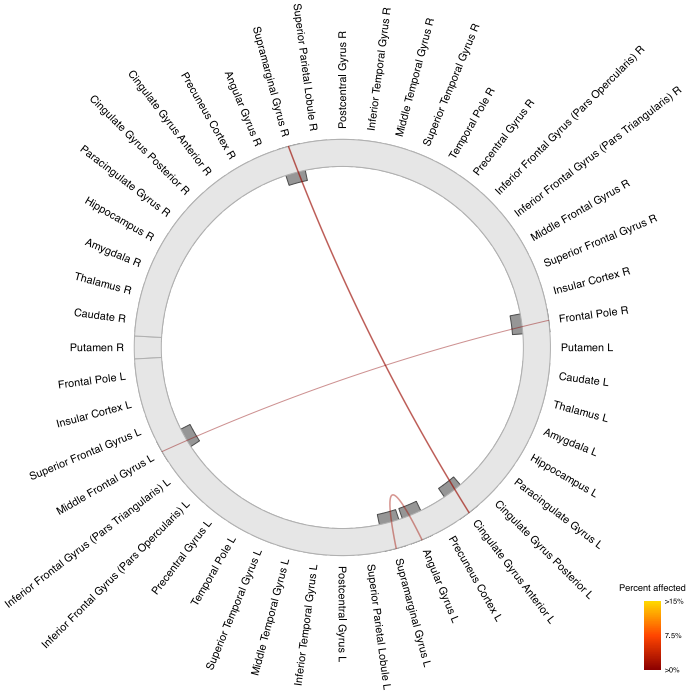

Figure 3-17. Disconnectome associated with reduced sampling efficiency. Disruption was observed in WM connections within the left angular gyrus and between the left supramarginal gyrus and left angular gyrus; right frontal pole and left middle frontal gyrus; and left anterior cingulate gyrus and right supramarginal gyrus.

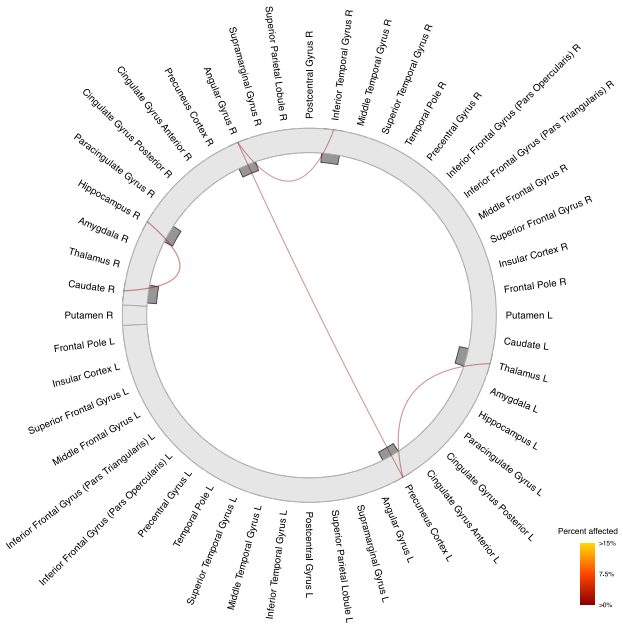

Figure 3-18. Disconnectome associated with reduced precision. Major disruptions were observed in WM connections between the right caudate and right hippocampus; left thalamus and left precuneus cortex; and right angular gyrus and right inferior temporal gyrus.

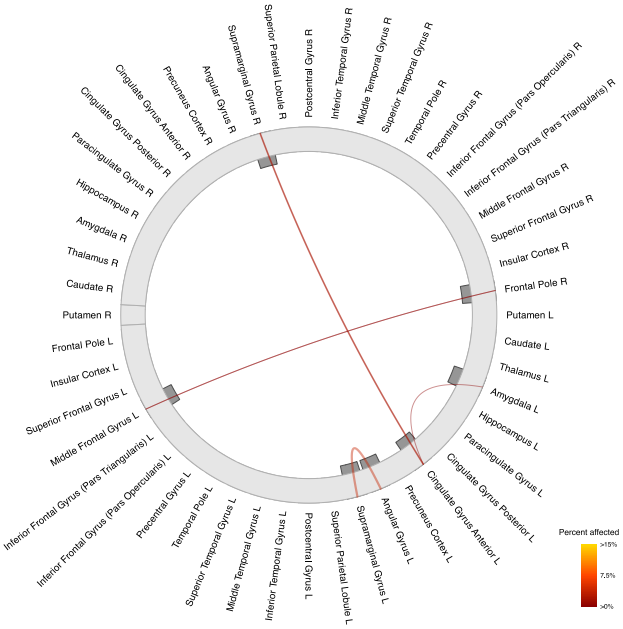

Figure 3-19. Disconnectome associated with the slope of uncertainty ratings Disruption was observed in WM connections between left anterior cingulate gyrus and right supramarginal gyrus; left supramarginal gyrus and left angular gyrus; the right frontal pole and left middle frontal gyrus; left anterior cingulate gyrus and left amygdala; and within the right frontal pole and left angular gyrus.

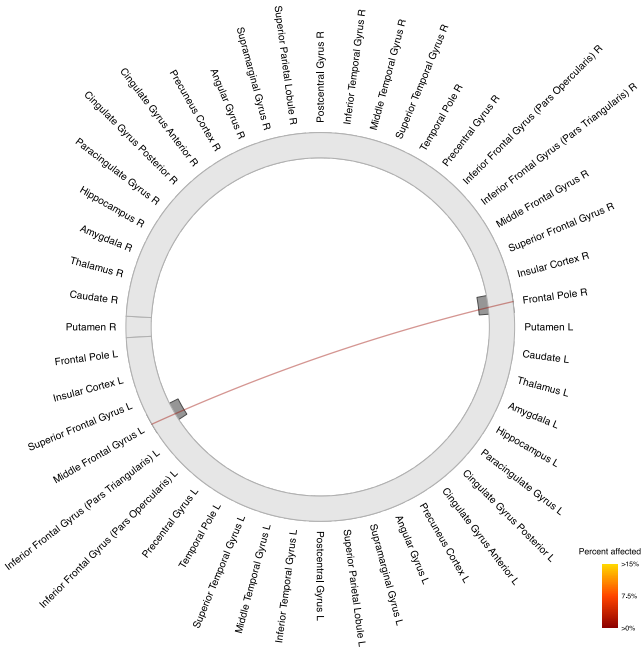

Figure 3-20. Disconnectome associated with increased offer acceptance. Disruption was observed in WM connections within the right frontal pole and left angular gyrus; and between the right frontal pole and left middle frontal gyrus.

3.5 Discussion

In this chapter the behaviour of SVD patients when making decisions under uncertainty on both active and passive versions of the CQ task was examined and compared to healthy controls. Performance on the tasks was related to microstructural disruption of WM. WMH burden is a well-established contributor to executive and psychomotor deficits (Jochems et al., 2025; S. Wang et al., 2022), but its impact on decision-making processes, particularly those involving the evaluation of cost, uncertainty, and reward, remains underexplored. The CQ task was used to investigate whether the integrity of WM pathways affects how individuals adjust their information sampling in response to changing task demands (Petitet et al., 2021).

The findings demonstrated that SVD patients exhibit reduced sensitivity to key decision variables: they were less responsive to sampling cost in the active condition (**Figure 3-4a**), less influenced by reward in the passive condition (**Figure 3-10c**), and showed attenuated

sensitivity to uncertainty across both task versions (**Figures 3-4c & 3-10a**). These behavioural deficits were mirrored in the neuroimaging results, which revealed that reduced fractional anisotropy (FA) in a network of WM tracts – including the inferior fronto-occipital fasciculus (IFOF), inferior longitudinal fasciculus (ILF), superior longitudinal fasciculus (SLF), genu and splenium of corpus callosum, and the anterior and superior corona radiata – was associated with poorer reward acquisition, diminished placement accuracy, and reduced sensitivity to reward and uncertainty (**Figures 3-12 & 3-13 & 3-14**). Identifying the projections of these WM tracts showed disruption of networks involving key frontal, parietal, temporal and subcortical brain regions (**Figures 3-15 & 3-16 & 3-17 & 3-18 & 3-19 & 3-20**). These results support the hypothesis that microvascular damage to WM tracts may impair the integration of value-relevant information during decision-making, and how this may disrupt adaptive behaviour in uncertain environments in people with SVD.

In the active version of the CQ task, SVD participants earned significantly less overall, and this was most pronounced in high-reward contexts (**Figure 3-3a**). This suggests that patients with SVD are less able to capitalise on favourable reward contingencies, potentially due to impaired reward learning or reduced motivation. It has been hypothesized that in SVD, WM integrity disruption has deleterious effects on the brain's reward networks (Lisiecka-Ford et al., 2018). This reduction in reward efficiency in turn leads to apathy, but although the SVD patients were more apathetic than the controls participants, their AMI scores were not found to be associated with final reward outcome on the task. However, significant correlations were made with microstructural damage in WM tracts implicated in integrating visual information with executive planning and value estimation. Crucially, reduced earnings were associated with lower FA in bilateral IFOF, ILF, right forceps major, and bilateral SLF (Conner et al., 2018; Goldstein et al., 2025; Herbet et al., 2018; Janelle et al., 2022). Total WMH volume also had a significant negative correlation to the final total earnings on the task (**Figure 3-11**).

Additionally, SVD participants with higher ACE scores tended to earn more (**Figure 3-9a**), highlighting a behavioural link between global cognitive function and task performance. These results suggest that cognitive impairment may hinder the ability to sufficiently integrate information, thereby limiting the capacity to benefit from high-reward conditions, whereas symptoms of apathy or reduced motivation appear unlikely to be the primary explanation.

Although SVD participants adjusted their sampling behaviour to cost and reward manipulations similarly to controls, they spent less time sampling overall and initiated sampling sooner (**Figures 3-3b & 3-8a**). This indicates a general reduction in deliberation time, potentially reflecting either an impulsivity-related mechanism or a compensatory strategy in the face of cognitive fatigue. It should be noted that SVD patients were significantly more impulsive as measured by the BIS questionnaire, though their impulsivity scores did not correlate to their time spent sampling. Their reduced sensitivity to sampling cost, especially under low-cost conditions, resulted in greater deviation from optimal sampling when compared to the Bayesian ideal observer model (**Figure 3-4b**), with patients undersampling more than controls. These behaviours suggest a blunted ability to flexibly adapt effortful information gathering when it is most beneficial. The fact that both groups showed similar directional patterns (e.g., increased sampling when cost decreased) implies that SVD participants retained a basic understanding of task contingencies but were less able to implement these optimally.

Oversampling and undersampling are both decision-making behaviours that have been reported in healthy controls. In the Dart Task, participants demonstrated cost adjusted sampling and similar to our participants in the CQ active version, they oversampled when sampling became more expensive (Juni et al., 2016). However, these researchers did not report any undersampling which was previously observed in other decision-making paradigms, such as the Card Sampling and Beads Tasks, where sampling cost was implicit (Furl & Averbeck, 2011; Hertwig et al., 2004). Oversampling has also been reported in a decision-making task with

implicit sampling cost (Tversky & Edwards, 1966). Key distinctions in the Tversky & Edwards' task, however, are that 1) participants had very limited control over their sampling and were not allowed to employ a stopping policy as every trial had to be completed and 2) each trial was both a sample and decision that could yield feedback and reward. One could conclude that when humans are allowed more agency over sampling, they tend to show cost adjusted behaviour when gathering information but oversample in expensive environments and undersample when cost is either too cheap or implicit.

Another key finding was that SVD participants tolerated significantly more uncertainty after sampling before they committed to a decision (**Figure 3-4c**), particularly under conditions that would normally incentivize further exploration (e.g., low cost, high reward). While some previous investigations have reported dysfunctional decision-making in SVD, to our knowledge this is the first study to explicitly show any relationship between SVD and uncertainty (Le Heron, Manohar, et al., 2018; Saleh et al., 2021a). Crucially, there was a significant positive correlation between final uncertainty and total WMH volume (**Figure 3-11b**) suggesting that those with more advance SVD were less able to reduce uncertainty. Inefficient decision-making was also evident in the SVD patients' reduced localization accuracy (**Figure 3-5a**) and higher placement imprecision (**Figure 3-6**), indicating that even when they gathered information, they were less able to integrate it effectively into goal-directed action. Although motor deficits have been associated with SVD (Su et al., 2017), impairments in manual dexterity are also common in healthy ageing populations and have been positively correlated with greater WMH burden (Nyquist et al., 2015). As SVD patients exhibited reduced accuracy and precision in the active CQ task only under low-uncertainty conditions, but prior to the point where the location of the hidden circle was easily inferable, it is unlikely that these deficits were primarily due to motor impairment. Precision impairments were associated with reduced FA in right-lateralized tracts of the posterior thalamic radiation (including the optic

radiation), consistent with previous work linking these pathways to visuo-spatial integration and attentional updating (de Schotten et al., 2011). Additionally, lower ACE scores and higher total WMH volume were both negatively correlated with placement precision (**Figures 3-9b & 3-11c**). Taken together, these findings would be consistent with the view that structural disconnection might disrupt both the quality and the utility of evidence accumulated during active sampling.

Performance in the passive version of the CQ task revealed further dissociations in decision-making between the participant groups. While both groups scaled their uncertainty ratings in line with the objective expected error (**Figure 3-10a**), SVD patients consistently reported less uncertainty overall and were also less responsive to actual uncertainty changes. This may reflect impaired introspective access to uncertainty or reduced confidence calibration, both of which are crucial for appropriately modulating decision thresholds (Elosegi et al., 2024; Jackson et al., 2016; B. Li et al., 2024). In terms of behaviour, patients showed an increased general tendency to accept offers, but their choices were less modulated by both reward magnitude and uncertainty level. Imaging analyses from this study revealed that increased offer acceptance was associated with reduced FA in the superior corona radiata, the right external capsule, and the left-dominant body of the corpus callosum. These tracts have been associated with cognitive control, action selection and probabilistic outcome evaluation. For example, reduced FA in the corpus callosum predicted impaired performance on the IGT (Lane et al., 2010), and lower integrity of corona radiata and corpus callosum fibres has been linked to impulsivity and executive decline (M. Feng et al., 2024; Goldwaser et al., 2022).The superior corona radiata, in particular, projects to prefrontal brain regions implicated in inhibitory control and it has been shown in adolescence studies that reduced integrity in this tract can lead to that riskier behaviour (Goldenberg et al., 2017; Jacobus et al., 2013). These findings suggest that reduced structural integrity in key fronto-striatal and thalamocortical pathways may contribute

to a shift toward more impulsive or risk-tolerant decision-making in SVD, characterized by diminished sensitivity to both reward value and uncertainty.

SVD patients' pattern of blunted sensitivity to external decision variables (e.g., cost, uncertainty, and reward; **Figures 3-4a & 3-10b & 3-10c**) and internal variables (e.g., perceived uncertainty, placement accuracy; **Figures 3-10a & 3-5a**) converges across both task versions, pointing to a general deficit in adaptive value-guided behaviour. The distributed WM abnormalities associated with these impairments support the notion that SVD affects large-scale brain networks required for integrating sensory evidence with motivational and contextual information. This is consistent with recent models of cognitive impairment in SVD, which emphasise disrupted communication between prefrontal, parietal, and subcortical regions (Lawrence et al., 2013). The disconnectome analyses in this chapter further reinforce this interpretation. Reduced reward earnings were associated with widespread disconnection across frontal, temporal, parietal, and subcortical regions, including the angular gyrus, anterior cingulate, frontal pole, middle frontal gyrus, supramarginal gyrus, paracingulate gyrus, hippocampus, amygdala, caudate, precentral gyrus, and inferior temporal gyrus (**Figure 3-15**). Measures of information sampling behaviour showed a similar pattern. Reduced sampling quantity was linked to disconnection within the frontal pole and between the supramarginal gyrus and anterior cingulate gyrus (**Figure 3-16**) whereas reduced sampling efficiency was associated with disruptions within the angular gyrus, between the angular and supramarginal gyri, and in fronto-cingulo-parietal pathways (**Figure 3-17**). Reduced placement precision was associated with disconnection between subcortical–limbic and thalamo-parietal regions, including pathways linking the right caudate to the right hippocampus, the left thalamus to the precuneus cortex, and the right angular gyrus to the inferior temporal gyrus (**Figure 3-18**). Aberrant uncertainty ratings were linked to broader fronto-parietal and limbic disconnection, including pathways between the anterior cingulate gyrus, supramarginal gyrus, angular gyrus,

and amygdala, as well as recurrent disruptions in the tract connecting the right frontal pole and left middle frontal gyrus (**Figure 3-19**). Finally, increased offer acceptance was associated with disruptions in WM pathways linking the right frontal pole with the left angular gyrus, and within the frontal pole itself—connections that normally contribute to the evaluation of prospective outcomes and behavioural inhibition (**Figure 3-20**). Together, these patterns suggest that value-guided behaviour in SVD is compromised not by isolated lesions but by distributed disruptions within a set of fronto-parietal, limbic, and subcortical pathways that reliably recruit the angular gyrus, anterior cingulate gyrus, frontal pole, middle frontal gyrus and supramarginal gyrus which may collectively support uncertainty monitoring, evidence accumulation, reward evaluation, and action selection.

This study had some limitations. First, participants in the SVD group were predominantly in the early stages of the disease and largely non-demented. As a result, the findings may not be generalisable to the broader SVD population, particularly individuals with more advanced disease progression or greater cognitive impairment. The relationship between task performance and cognitive impairment suggests more profound deficits might be observable in a cohort with more severe disease that might be more representative of people with vascular dementia. A second limitation is that patients were selected from a Cognitive Disorders clinic rather than recruited through broader population screening, which may introduce selection bias. A third limitation is that the imaging analyses relied on standard brain atlases to define WM tracts and cortical regions; as such, the localization of disconnectome effects represents probabilistic estimates rather than definitive anatomical boundaries, and individual variability in WM anatomy may lead to some misassignment of tracts or nodes.

3.6 Conclusion

On a relatively new test of decision-making, SVD patients exhibited reduced sensitivity to cost, reward, and uncertainty, alongside a diminished ability to utilise self-generated spatial cues, resulting in decreased accuracy and precision. Their behaviour also reflected increased risk-taking, as evidenced by premature and faster sampling strategies, higher uncertainty retention and a higher rate of offer acceptance. Higher WMH burden predicts lower reward earnings, greater uncertainty tolerance and reduced placement precision in the active version of the CQ task. The findings also demonstrate that WM integrity, particularly in fronto-parietal, fronto-subcortical, and select temporal pathways, plays a critical role in supporting decision-making under uncertainty. Disruption to these connections may lead to widespread damage in the brain's decision-making network. By linking specific behavioural impairments to underlying structural connectivity, this work offers a new data on how cerebrovascular pathology impacts decision-making processes and underscores the value of integrating behavioural and imaging approaches in SVD research.

4| Impact of SVD on EBDM under uncertainty

4.1 Abstract

EBDM is increasingly recognised as a critical domain of cognitive-motivational functioning, yet it has received limited attention in the context of SVD. In this chapter, a novel effort-based variant of the passive CQ paradigm was administered to some of the participants from Ch 3 and the results from SVD patients and age-matched HC were compared. On this task, participants evaluated trials based on varying levels of reward, uncertainty, and crucially also physical effort required to accept an offer. Strikingly, the introduction of effort altered the behavioural profile of the SVD group. Whereas they had previously shown riskier and less reward-sensitive choices on the standard passive version of the CQ paradigm, here (where the third variable of effort also had to be evaluated) their offer acceptance rates, as well as their sensitivity to both reward and uncertainty, more closely aligned with the patterns observed in the HC group.

Behavioural outcomes were examined in relation to various clinical measures as well as structural imaging indices. Tract-specific preserved axonal coherence and myelination in fronto-striatal and cingulo-opercular WM pathways (identified with TBSS and NODDI) correlated with increased offer acceptance and overall task engagement. Improved network connectivity along fronto-parietal and fronto-temporal pathways was also linked to greater offer acceptance. However, no significant correlations were found with WMH volume and clinical measures in this group. Together, these findings indicate that introducing physical effort can modulate decision-making in SVD. The presence of this third variable when participants made decisions reduced previously observed group differences between SVD patients and the HC group.

4.2 Introduction

There is growing theoretical and empirical support for the view that EBDM underlies the allocation of cognitive and physical resources in the service of motivated action(Gómez Escobar & Mitchell, 2025; Kurniawan et al., 2011). EBDM refers to the processes by which individuals evaluate whether potential rewards are worth the physical or cognitive effort required to obtain them (Docx et al., 2015; Renz et al., 2023). This domain of cognitive function is fundamental to everyday goal-directed behaviour, yet it remains underexplored in clinical populations with known motivational and cognitive impairments. In recent years, EBDM paradigms have provided insight into disorders such as depression, Parkinson's disease, and schizophrenia (Ang et al., 2022; Chen et al., 2020; Chong et al., 2015; Colón-Semenza et al., 2021; Culbreth et al., 2018; Saperia et al., 2023), but their application to SVD has been minimal (Le Heron, Manohar, et al., 2018; Saleh et al., 2021b). Given that SVD is a leading cause of vascular cognitive impairment and is associated with apathy and other motivational symptoms, understanding how effort influences decision-making in this population is both timely and important.

In this chapter, I extend the investigation from Ch 3 by introducing a novel, effort-based variant of the CQ task. Whereas the standard passive CQ task involved choices based on reward and uncertainty, this modified version required participants also to consider the physical exertion that would be required in each trial. This additional component aims to better capture the motivational challenges faced by individuals with SVD, and to assess whether introducing effort alters their behavioural profile in meaningful ways. By comparing performance on this task between SVD participants and age-matched controls, this chapter first aims to evaluate how physical effort modulates decision-making in a patient group already characterised by subtle cognitive and motivational changes (Le Heron, Manohar, et al., 2018; Saleh et al., 2021b).

A key question that this chapter seeks to answer is whether adding an effort component affects the decision-making tendencies previously observed in SVD. In Ch 3, participants with SVD demonstrated increased risk-taking and reduced reward sensitivity compared to controls, suggesting altered valuation processes. Emerging evidence suggests that incorporating physical effort into decision-making tasks can alter how individuals evaluate rewards and make choices under uncertainty (Summerside & Ahmed, 2021; van As et al., 2021). For example, studies in healthy individuals have found that effort demands can amplify the subjective value of rewards, a phenomenon sometimes interpreted through the lens of effort justification or increased salience of high-effort outcomes (Clay et al., 2022; Pan et al., 2023; Wu & Zheng, 2023; Zentall, 2010). However, other studies report reward discounting with increasing effort, whereby individuals devalue outcomes that require more effort to obtain (Nishiyama, 2016).

This apparent discrepancy likely reflects the context-dependent nature of effort valuation, including whether effort is experienced prospectively or retrospectively, the degree of perceived control, and the motivational relevance of the task. Supporting this view, recent work by Marcowski et al. (2025) demonstrates that effort can exert positive, negative, or even nonmonotonic effects on outcome value, depending on how the effort–reward relationship is framed. These findings underscore that the integration of effort costs in decision-making is not fixed but dynamically shaped by contextual and cognitive factors. In clinical contexts, particularly those involving motivational deficits, effort has been proposed as a means of re-engaging disrupted valuation circuits and promoting more goal-directed behaviour (Berwian et al., 2020; Chong et al., 2015). However, it remains unclear whether such effects are also observed in populations with cerebrovascular pathology, such as SVD, where both apathy and reduced reward sensitivity are common.

Research on healthy and clinical populations suggests that EBDM might be supported by a distributed network of brain regions, including the anterior cingulate cortex (ACC), ventral

striatum, insula, dorsomedial and dorsolateral prefrontal cortex (Arulpragasam et al., 2018; Chong et al., 2017a; Lopez-Gamundi et al., 2021). These areas are thought to encode the subjective value of effortful actions, integrating information about anticipated rewards, task demands, and internal states such as fatigue or motivation (Barakat et al., 2025; Hogan et al., 2019). The ACC, in particular, has been implicated in evaluating effort costs and guiding action selection accordingly (P. Croxson et al., 2009). While structural and functional integrity of these networks is often compromised in disorders like Parkinson's disease and depression (Bore et al., 2023; Le Heron, Plant, et al., 2018), less is known about their involvement in SVD, where microvascular pathology may lead to subtle but widespread disruptions in WM connectivity (Le Heron, Manohar, et al., 2018; Saleh et al., 2021b). In addition to behavioural analyses, this chapter will incorporate neuroimaging data, including WMH quantification using BIANCA, WM microstructure assessed through TBSS applied to DTI and NODDI, and structural connectomics, to investigate the integrity of brain networks implicated in motivated behaviour.

This chapter explores whether the introduction of physical effort modifies patients' sensitivity to reward and uncertainty in decision-making. In so doing, it is important to consider that any observed group-level similarities in task performance may mask individual differences in motivational capacity. To explore this, behavioural findings will be examined alongside clinical measures of apathy, depression, impulsivity, and cognition, as well as neuroimaging indices of vascular burden and WM microstructure. These multimodal analyses will help determine whether comparable task behaviour reflects a genuine preservation of motivational function in SVD, or whether it may instead signal a compensatory shift in strategy or engagement. Understanding these dynamics has important implications for how apathy and related symptoms are conceptualised in the context of cerebrovascular disease, and how they might respond to interventions that recruit effortful action.

4.3 Methods

4.3.1 Participants, demographics, and consent

Thirty-four SVD participants aged between 50-80 years (20 males, 14 females) were recruited through the Cognitive Disorders Clinic at the John Radcliffe Hospital in Oxford. This group was a subset of the individuals who underwent testing as described in Ch 3. Their performance in this study was compared to that of forty-five age-matched healthy controls who were also part of the cohort in the previous chapter. Demographics are presented in **Table 4-1**.

	Diagnosis		
Number of Participants	**HC** N = 45[1]	**SVD** N = 34[1]	**p-value**[2]
Age (years)	72.2 ± 7.3	70.4 ± 8.8	0.3
Gender			0.4
Male	21 (47%)	20 (59%)	
Female	24 (53%)	14 (41%)	
YOE	23.8 ± 11.5	18.3 ± 3.2	0.004
Total ACE-III	97.1 ± 2.6	91.7 ± 7.2	<0.001
Total AMI	1.2 ± 0.5	1.6 ± 0.5	0.006
Total BDI-II	7.7 ± 5.8	14.6 ± 10.9	0.002
Total BIS-II	74.7 ± 10.9	80.3 ± 7.4	0.010
HADS Depression	6.8 ± 2.7	8.8 ± 1.7	<0.001
HADS Anxiety	10.2 ± 3.6	10.5 ± 3.1	0.6

[1] Mean ± SD; n (%)

[2] Welch Two Sample t-test; Pearson's Chi-squared test

Table 4-1: Demographic and questionnaire measures. HC = Healthy Controls, SVD = Cerebrovascular Small Vessel Disease, YOE = Years of Education, ACE-III = Addenbrooke's Cognitive Examination III, AMI = Apathy Motivation Index, BDI-II=Beck Depression Inventory II, BIS-II = Barrat Impulsiveness Scale II, HADS =Hospital Anxiety and Depression Scale.

The two groups did not differ significantly in terms of age or sex ratio. However, healthy controls had more years of full-time education compared to SVD patients. Cognitive screening using ACE-III revealed significantly higher scores in healthy controls, although both

groups had scores that were within normal limits for the general population (Hsieh et al., 2013; Mathuranath et al., 2000). There were significantly more people with apathy and depression in the SVD cohort, as measured using the Apathy Motivation Index (AMI) and Beck Depression Inventory-II (BDI-II) respectively (Ang et al., 2016; Beck et al., 1961a). Additionally, patients scored higher on the Barratt's Impulsivity Scale (BIS) than control participants (Patton et al., 1995).

All participants provided written consent in accordance with the Declaration of Helsinki and the study was approved by the NHS ethics committee.

4.3.2 Experimental setup

"CQ with effort" paradigm

The CQ with effort task is an EBDM behavioural paradigm **(Figure 4-1)** developed from the passive choice task of the original CQ task described in Ch 3. Here, participants have to evaluate three variables – uncertainty, reward and effort – when deciding whether to accept offers on a passive version of the CQ task. The effort in this case was physical effort normalized to each participant's maximum voluntary contraction (MVC).

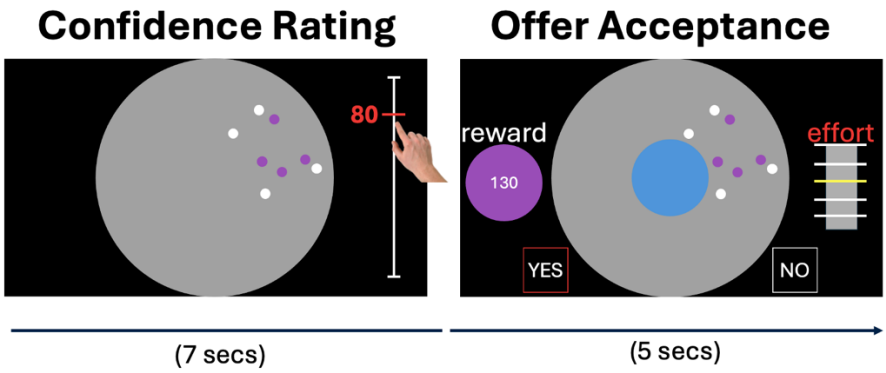

Figure 4-1. Passive version of the CQ task with effort. Participants viewed completed searches and provided confidence ratings reflecting their perceived ability to locate the hidden circle. Ratings were made by tapping along a vertical scale ranging from 0 (bottom) to 100 (top). After submitting their ratings, participants received a reward offer (R_0 = 40, 65, 90, or 115 credits) and effort requirement (1 to 5). They indicated their willingness to place the blue circle by tapping "yes" to accept or "no" to reject the trial.

Stimuli

This task was presented on a 17-inch touchscreen PC using MATLAB version 2018a (MathWorks; https://uk.mathworks.com) and Psychtoolbox version 3. Participants performed the tasks in a quiet testing room sitting within reaching distance of the screen (~50 cm). An experimenter was present in the room at all times during the behavioural testing which took about 90 mins on average to complete (Petitet et al., 2021).

As previously described in Ch 3, a circular grey mask (search space) was shown on the visual display, and individuals were told that a singular purple circle (radius = 130 pixels; area = 5.80% of the search space) was hidden within this search space in any given trial. Eight dots (radius = 4 pixels) coloured purple or white were shown within the grey search space. A small purple dot indicated a location within the area of the hidden purple circle. A small white dot, however, indicated a location which was outside the area of the hidden purple circle.

Physical Effort Calibration

A hand-held dynamometer was used to measure effort in the task. For calibration, prior to the main experiment, participants were asked to squeeze the handle as hard as they could with their preferred hand in order to establish their maximal voluntary contraction (MVC). To establish the physical demands for the 5 different effort levels participants were asked to squeeze the dynamometer while receiving feedback in the form of a red bar drawn on a vertical bar. As soon as the desired effort level was reached, this bar turned yellow, and participants were allowed to relax their grip. The 5 effort levels corresponded to 16, 32, 48, 64, and 80% of MVC, with each effort level experienced twice.

Passive choice task with effort

This variation of CQ involved the manipulation of the expected error or uncertainty and the number of credits on offer (initial reward/stake) as previously. Crucially, in addition, the physical effort level required for each trial was a new variable in this version of the passive task. Performance on the task can reveal how sensitive individuals were to each of these three variables. Uncertainty, EE, was calculated as the mean difference between all potential solutions given the current search i.e.

$$EE_s = (1-\alpha)(EE_{s-1} - EE_\infty) + EE_\infty \qquad \textit{Equation 1}$$

where EE_s is the expected error after the s^{th} sample, α is the information extraction rate that quantifies the sampling efficiency, EE_{s-1} is the expected error after the previous ($s-1^{th}$) sample and EE_∞ is asymptotic expected error i.e. the lowest error achievable after infinite samples.

The task was divided into two phases: an uncertainty rating phase and an offer acceptance phase. No feedback was provided in either phase since there were no "correct answers", only subjective responses.

Uncertainty Rating

As previously in the passive version of the CQ task described in Ch 3, at the start of each trial participants were shown a complete search with the eight dots on the screen in various configurations. Each trial had eight sample dots in total, half of which were positive samples (purple) and the other half which were negative samples (white). The uncertainty, EE, was manipulated by varying the spatial configuration of the displayed samples. The expected error ranged from 10–70 pixels. This meant the further the positive samples were from each other, the lower the expected error would be. Each participant saw the same exact trials that were in total 100, but the order in which they saw them was randomized. They were asked to make a

rating of how confident they were about the location of the hidden purple circle based on the completed search. This rating was performed on a scale from 1-100 displayed on the side of the screen corresponding to the handedness of the participant. Each completed search appeared onscreen alone for 0.5 seconds after which the rating scale appeared alongside for an additional 6.5 seconds. During this time participants were expected to make their rating. If they failed to do so in time the task would move on to the subsequent trial. However, the missed trial would later reappear so all participants would complete all 100 trials.

Offer Acceptance

Once a participant made a successful rating of the completed search, the trial would progress to the next phase of the task, the offer acceptance. The rating scale would disappear at this point and on the left side of the completed search, a purple circle containing the number of credits on offer was presented. This purple circle also reminded participants of the size of the hidden circle they were searching for. There were four credit options offered throughout the entirety of the task (40, 65, 90 or 115). Thus, the reward on offer was presented in this way.

In this version of the task, each trial also was associated with a physical effort (squeeze of the dynamometer) required to accept the offer. The amount of effort required on a trial was indicated on a vertical bar segmented into five equal parts, displayed on the right side of the screen with lines running across horizontally at each graduation. Each graduation represented a different effort level with the topmost line representing the highest effort level (5) and the line closest to the bottom representing the lowest effort level (1). One line would be coloured yellow to indicate the required effort level while the other lines remained grey. One of five possible effort levels was offered on any given trial (effort level 1, 2, 3, 4 or 5, corresponding to 16, 32, 48, 64, and 80% of MVC for each participant).

Below the search space on either side was displayed a 'YES' and a 'NO' option which participants could select to accept or reject an offer respectively for the chance to place the blue disk where the hidden purple circle was located. The 'YES' and 'NO' options switched sides randomly during the task to avoid any bias to choose the same option. Note participants only accepted or rejected reward offers but did not actually place the blue disk. To incentivize the context, they were informed that, at the end of the experiment, 20 trials would be randomly selected from the set they had accepted. For each of these selected trials, they would be required to place the blue circle at the indicated location and earn credits, but only if they successfully met the required effort level by squeezing the dynamometer. This meant that actual rewards depended on their ability to exert the required effort on those trials, thereby reinforcing the importance of their decisions during the task.

Protocol

Cognitive examination and questionnaires

All study participants were received cognitive assessment using the ACE-III which took about 15 mins to complete. Version A of the ACE was administered to the healthy elderly controls while versions B and C were administered to SVD patients since they were more likely to have already been exposed to version A in a prior study or clinical visits.

In addition to the cognitive testing, participants completed established self-report questionnaire measures of apathy (Apathy and Memory Index, AMI), impulsivity (Barratt Impulsiveness Scale, BIS), depression (Beck Depression Inventory, BDI) and anxiety (Hospital and Anxiety Depression Scale, HADS) (Ang, 2017; Beck et al., 1961b; Patton et al., 1995; Zigmond & Snaith, 1983). Individuals completed all four questionnaires on the day of the behavioural testing. Two of the questionnaires, the AMI and BIS, were completed prior to the

start of CQ, while the final two, the BDI and HADS, were administered at the end of the session.

Fatigue ratings during the task

Throughout CQ, participants rated their level of subjective fatigue on a scale from 0 to 100 at the start of each experimental block. Their prompt to report this rating came in the form of a vertical visual analogue scale that appeared in the middle of the screen underneath the text, 'How tired do you feel?' The top of the scale was labelled 'Extremely' and the bottom was labelled 'Not at all' to indicate the highest and lowest extremes of fatigue.

Experimental design

The passive choice task with effort variant of CQ was preceded by an exposure session during which participants were introduced to the task, given instructions, and allowed to practice sampling and placing the blue disc. First, they had three practice trials that required them to touch the screen and gather samples to help them localize the hidden purple circle. They could acquire as many samples (dots) as they desired and when they were satisfied with their search, they would hit the spacebar key to make the blue disc appear. Then they would drag this disc to where they thought the hidden purple circle was located. They received feedback in the form of a faded purple circle showing them the actual location of the hidden circle.

The next part of the exposure session had five blocks of 20 exposure trials (100 trials in total). This time participants were shown completed searches with eight samples (four positive dots and four negative dots) in different configurations to vary the level of uncertainty and the blue disk in the middle of the screen. Each trial also had an associated reward offer and these were either 40, 65, 90 or 115 credits. This part of the exposure session introduced individuals to the credit and scoring function of the task. Participants were required to move the blue disk to

where they thought the hidden purple circle was located and then they received feedback in the form of the faded purple circle showing them the actual location of the hidden circle and the number of credits they won. Note that it was possible to receive negative credit scores.

4.4 Results

4.4.1 Participants' offer acceptance modulated by uncertainty, reward and effort

On the CQ task with effort, participants' subjective uncertainty ratings increased significantly with objective uncertainty, EE, across both groups ($\beta = 1.32$, SE = 0.22, 95% CI [0.88, 1.76], $t_{390} = 5.90$, $p < 0.0001$; **Figure 4-2a**). However, patients showed attenuated sensitivity to uncertainty, reflected in a significant group × uncertainty interaction ($\beta = –0.37$, SE = 0.15, 95% CI [–0.66, –0.08], $t_{390} = –2.50$, $p = 0.013$), indicating shallower slopes in their subjective ratings across uncertainty compared to controls. The overall group difference in uncertainty ratings was small and not statistically significant ($\beta = 0.078$, SE = 0.042, 95% CI [–0.004, 0.16], $t_{390} = 1.86$, $p = 0.064$). These results indicate that while both groups scaled their uncertainty ratings appropriately, patients were less responsive to changes in actual uncertainty levels but did not differ substantially in their overall perceived uncertainty.

Participants' likelihood of accepting an offer decreased as uncertainty increased ($\beta = 0.00101$, SE = 0.00078, 95% CI [–0.00052, 0.00254], $t_{16273} = 1.29$, $p = 0.195$; **Figure 4-2b**), but this change was not statistically significant. This is likely due to large variability across participants in both groups. Although the group × uncertainty interaction was significant ($\beta = –0.00234$, SE = 0.00052, 95% CI [–0.00335, –0.00132], $t_{16273} = –4.51$, $p < 0.00001$), the effect size was extremely small, and raw data suggest both groups responded similarly to uncertainty, with overlapping confidence intervals and some uncertainty levels appearing steeper for patients.

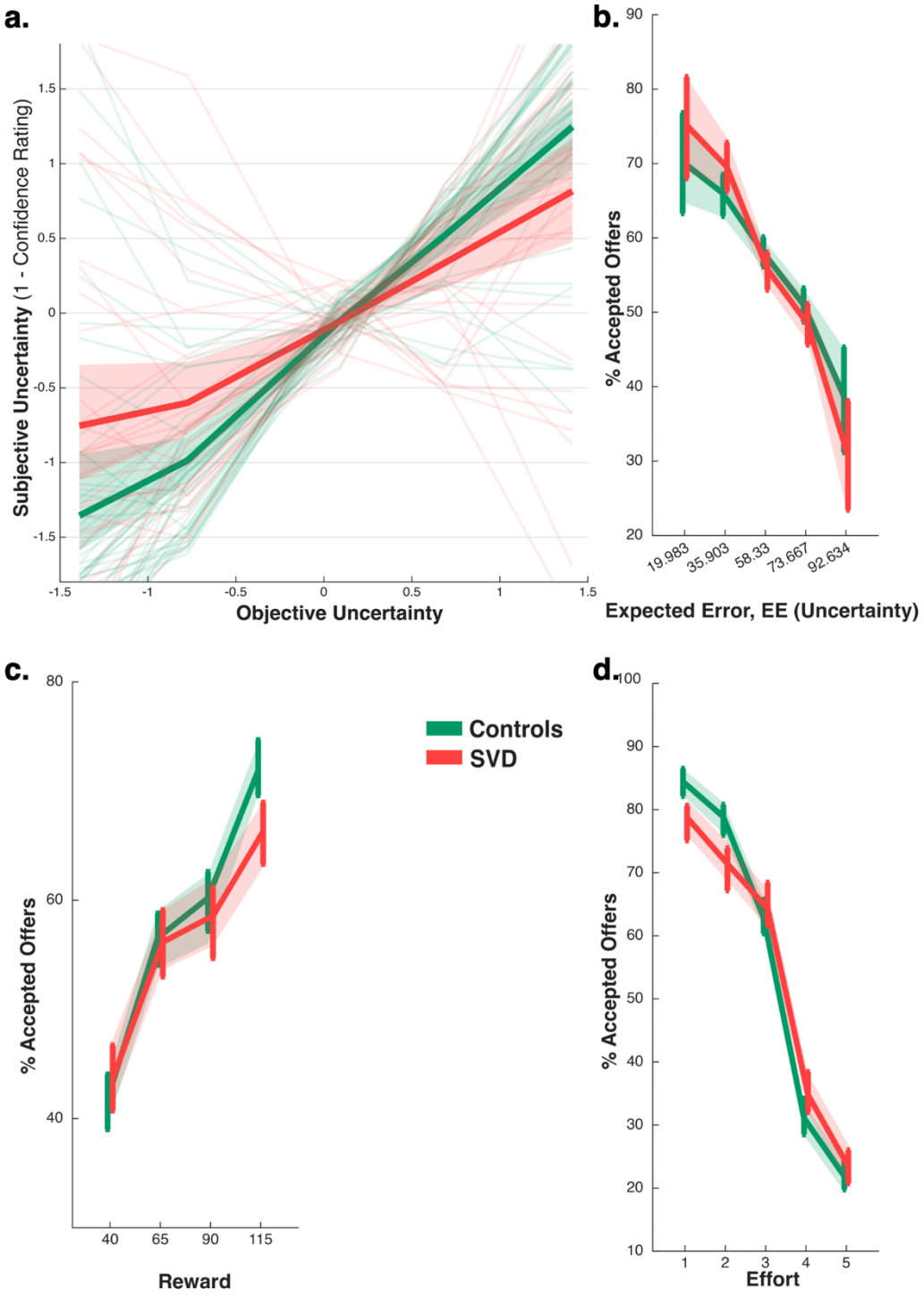

Figure 4-2. Participants' performance on the passive version of the CQ task with effort. (a) SVD patients showed impaired perception of uncertainty compared to controls during the confidence rating phase. **(b)** Both groups accepted fewer trials as uncertainty increased. **(c)** Both groups accepted more trials as reward increased. **(d)** Both groups accepted fewer trials as effort increased.

Participants' offer acceptance increased significantly as reward increased ($\beta = 0.00551$, SE = 0.00039, 95% CI [0.00474, 0.00628], $t_{16273} = 13.98$, $p < 0.0001$; **Figure 4-2c**). However,

this effect differed by group, with patients showing a reduced positive impact of reward on choice (group × reward interaction: $\beta = -0.00111$, SE = 0.00026, 95% CI [–0.00162, –0.00059], $t_{16273} = -4.21$, $p < 0.0001$), indicating relatively less sensitivity to reward magnitude compared to controls. The overall group difference was not statistically significant ($\beta = 0.0698$, SE = 0.0398, 95% CI [–0.0082, 0.148], $t_{16273} = 1.75$, $p = 0.079$).

Participants' likelihood of accepting offers decreased significantly as effort increased ($\beta = -1.27$, SE = 0.044, 95% CI [–1.36, –1.19], $t_{16273} = -29.23$, $p < 0.0001$; **Figure 4-2d**), reflecting reduced willingness to exert higher effort. However, this effect differed by group, with SVD patients having a slightly shallower slope (group × effort interaction: $\beta = 0.173$, SE = 0.029, 95% CI [0.116, 0.230], $t_{16273} = 5.96$, $p < 0.00001$), indicating relatively less sensitivity to effort compared to controls. However, patients were less likely to accept offers at low effort levels ($\beta = -0.099$, SE = 0.037, 95% CI [–0.171, –0.027], $t_{16273} = -2.69$, $p = 0.007$) than controls.

4.4.2 The inclusion of physical effort altered participants' behaviour on the passive version of the CQ task

Further analyses were conducted to determine whether participant behaviour on the passive version of the CQ task changed when physical effort was introduced. To achieved this, data form those participants who had performed the experiments in this and the previous chapter were analysed. Linear mixed-effects models were conducted to examine whether decision time differed between patients and controls during the CQ task with effort. Models included decision time as the dependent variable, with group entered as a fixed factor and participant as a random effect. The analysis revealed no significant group differences in decision time ($p = 0.158$), suggesting comparable response speeds between both groups. To further explore the influence of effort demands, additional analyses were conducted in a subset of participants who completed both the effort and no-effort conditions of the CQ task passive version. In this subset,

group differences in decision time were again nonsignificant when models were fitted separately for each condition (no-effort: $p = 0.284$; effort–PC: $p = 0.136$; **Figure 4-3**). However, when data from both experiments were combined in a single model including condition and group as fixed factors, there was a strong main effect of condition ($p < 0.001$) and a significant group × condition interaction ($p < 0.001$). Nonparametric tests confirmed these effects, with all task versions showing significant group differences ($p \leq 0.0016$). These findings suggest that while decision time did not differ robustly between groups within individual task contexts, performance was nonetheless modulated by the presence of effort demands, with evidence for differential group sensitivity to experimental condition.

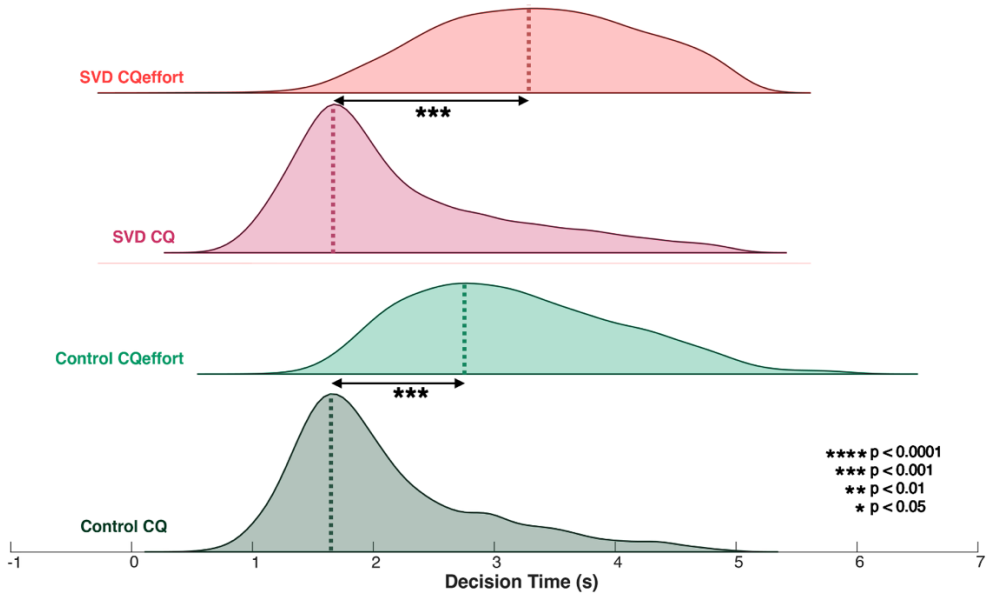

Figure 4-3. Decision time on the CQ task passive version with and without effort. Both groups took significantly longer to make a decision when physical effort was included as a third variable.

Generalised linear mixed-effects models were conducted to examine whether the percentage of accepted offers varied as a function of reward and uncertainty across experimental conditions (effort vs. no-effort). The model included group, condition, and their interaction as fixed factors, with random intercepts for participants. Across all participants, acceptance rates increased significantly with reward level (F (1,13 581) = 540.6, $p < 0.001$;

Figures 4-4a & 4-4c) and decreased with increasing uncertainty (F (1,13 581) = 1778.6, p < 0.001; **Figures 4-4b & 4-4d**). A strong main effect of condition was observed (F (1,13 581) = 98.97, p < 0.001), qualified by a significant group × condition interaction (F (1,13 581) = 7.43, p = 0.006).

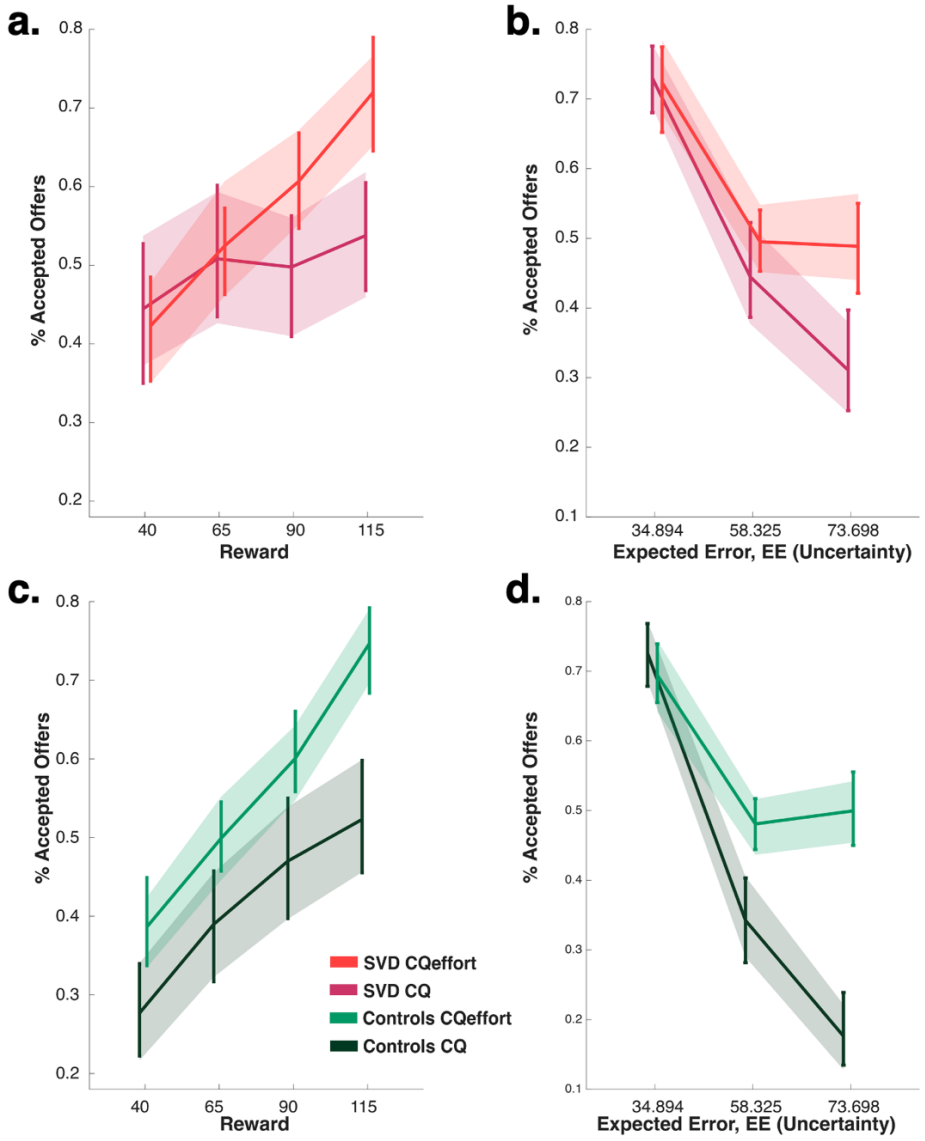

Figure 4-4. Participants' behaviour on the CQ task passive version with and without effort.
(a) SVD patients became more sensitive to reward in the effort condition **(b)** and accepted more offers at higher levels of uncertainty. **(c)** Healthy controls accepted more offers in the effort condition at all reward levels **(d)** and at higher levels of uncertainty.

Within-group analyses revealed that controls were highly sensitive to both reward and uncertainty in both conditions (no-effort: reward F(1,7746) = 429.5, p < 0.001; uncertainty

$F(1,7746) = 1138.9$, $p < 0.001$; effort: reward $F(1,7746) = 429.5$, $p < 0.001$; uncertainty $F(1,7746) = 1138.9$, $p < 0.001$). They also showed a robust effect of effort ($F(1,7746) = 111.9$, $p < 0.001$), with higher acceptance overall when effort was required. In contrast, patients displayed markedly weaker modulation by reward and uncertainty in the no-effort condition (reward: $F(1,5833) = 134.0$, $p < 0.001$; uncertainty: $F(1,5833) = 642.5$, $p < 0.001$). However, under effort, sensitivity increased considerably (reward: $F(1,5833) = 16.96$, $p < 0.001$; uncertainty: $F(1,5833) = 17.0$, $p < 0.001$), resulting in choice patterns statistically indistinguishable from controls (effort: group $F(1,5833) = 1.2$, $p = 0.273$). The group × condition interaction from the combined model ($F(1,13\ 581) = 7.43$, $p = 0.006$) confirms that group differences were specific to the no-effort condition. This pattern suggests that effort demands increased motivational engagement in patients, restoring patients' sensitivity to both reward and uncertainty to control levels.

4.4.3 Group differences in fatigue evolution on the passive version of the CQ task

Linear mixed-effects models were conducted to examine whether fatigue levels differed between participant groups and across time in the CQ task with effort. Models included fatigue measured at five time points which corresponded to the start of each block. Results revealed a significant effect of time ($F_{4,85246} = 2548.9$, $p < 0.001$; **Figure 4-5a**) and a significant group × time interaction ($F_{4,85246} = 245.7$, $p = 2.68\times10^{-55}$), indicating that the groups differed in the trajectory of fatigue across the task, although no main effect of group was observed ($F_{1,85246} = 1.05$, $p = 0.306$). Comparisons of subject-specific slopes confirmed no difference in overall rate of fatigue increase between groups (rank-sum $p = 0.980$; t-test $p = 0.569$).

Linear mixed-effects models were also conducted to examine whether fatigue levels differed between participants who did both the effort and no-effort conditions of the CQ task passive version. For the effort condition, fatigue increased over time (time: $F_{4,34300} = 329.19$,

$p = 1.66\times10^{-278}$; **Figure 4-5b**) and showed a significant group × time interaction ($F_{4,34300} = 127.24$, $p = 4.93\times10^{-108}$), with no baseline group difference ($F_{1,34300} = 0.45$, $p = 0.503$). For the no-effort condition, fatigue increased over time (time: $F_{4,33492} = 189.97$, $p = 2.55\times10^{-161}$; **Figure 4-5c**), with a significant group × time interaction ($F_{4,33492} = 265.54$, $p = 4.49\times10^{-225}$) but no baseline group difference ($F_{1,33492} = 2.43$, $p = 0.119$).

Within-group comparisons across experiments indicated that controls exhibited significant differences in fatigue trajectories between the no-effort and effort tasks (time × experiment: $F_{1,38746} = 112.05$, $p = 3.77\times10^{-26}$) without a baseline difference (condition: $F_{1,38746} = 0.25$, $p = 0.615$), whereas SVD patients showed a higher baseline fatigue in the no-effort condition (experiment: $F_{1,29058} = 141.28$, $p = 1.67\times10^{-32}$) with a smaller but significant change in trajectory (Time × experiment: $F_{1,29058} = 4.48$, $p = 0.034$). These findings suggest that both groups' fatigue increased over time, but the effort manipulation primarily altered the trajectory for controls and baseline levels for SVD patients.

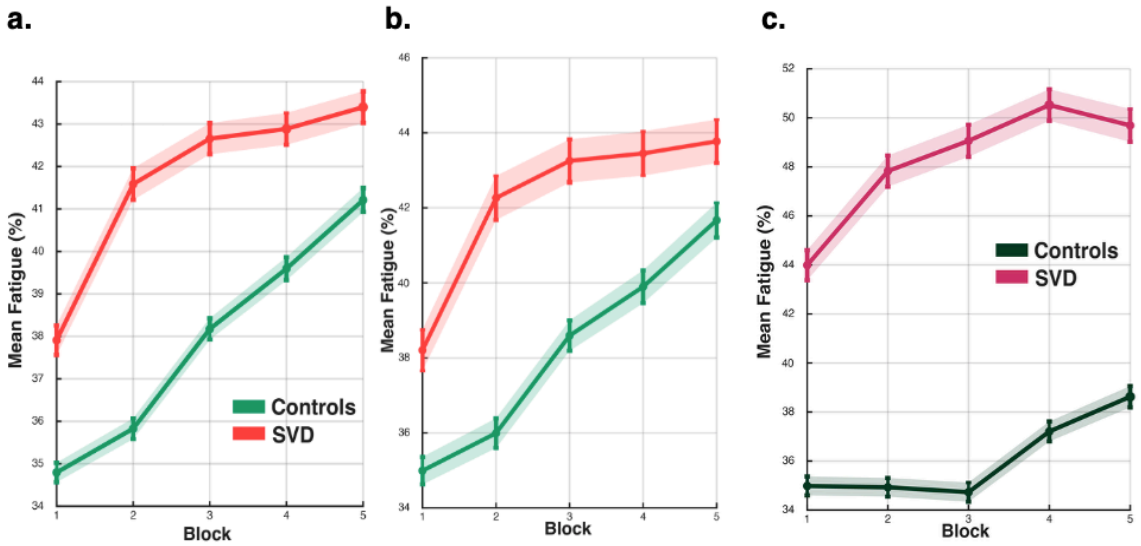

Figure 4-5. Fatigue ratings by participants on the CQ task passive version with and without effort. **(a)** SVD patients reported higher initial fatigue that increased and plateaued, while controls showed fatigue that gradually increased across blocks. **(b)** Among the subset of participants who completed both conditions of the passive version, the pattern described in panel (a) was evident only in the condition involving effort. **(c)** In the absence of effort, SVD patients showed increasing fatigue across blocks except the last, while controls reported increases only in the final two blocks.

4.4.4 Increased offer acceptance on passive tasks predict lower MD in WM tracts

TBSS analysis, with α= 0.05 and correcting for multiple comparisons with TFCE, using the DTI model on the whole cohort (across both groups) demonstrated that lower MD values were associated with increased offer acceptance in the CQ task with effort. These associations were evident in the anterior thalamic radiation, superior longitudinal fasciculus, corticospinal tract, forceps minor and cingulum (**Figure 4-6**).

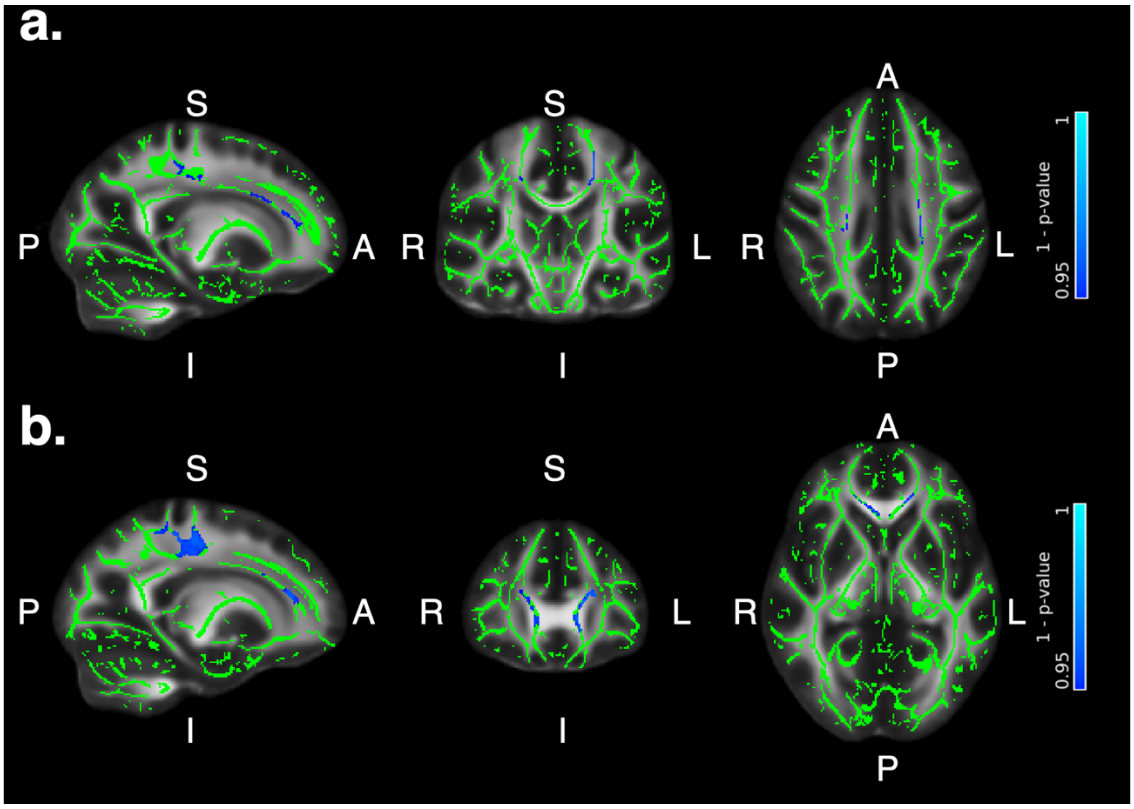

Figure 4-6. TBSS analysis of CQ active version using the DTI model (a) Increased offer acceptance was associated with reduced MD in the anterior thalamic radiation and superior longitudinal fasciculus as well as **(b)** in the corticospinal tract, forceps minor and cingulum

4.4.5 Increased offer acceptance on passive tasks predict higher NDI in WM tracts

TBSS analysis, with α= 0.05 and correcting for multiple comparisons with TFCE, using the NODDI model on the whole cohort demonstrated that lower NDI values were also associated with increased offer acceptance (**Figure 4-7**). These changes were most prominent in the corticospinal tract and superior longitudinal fasciculus.

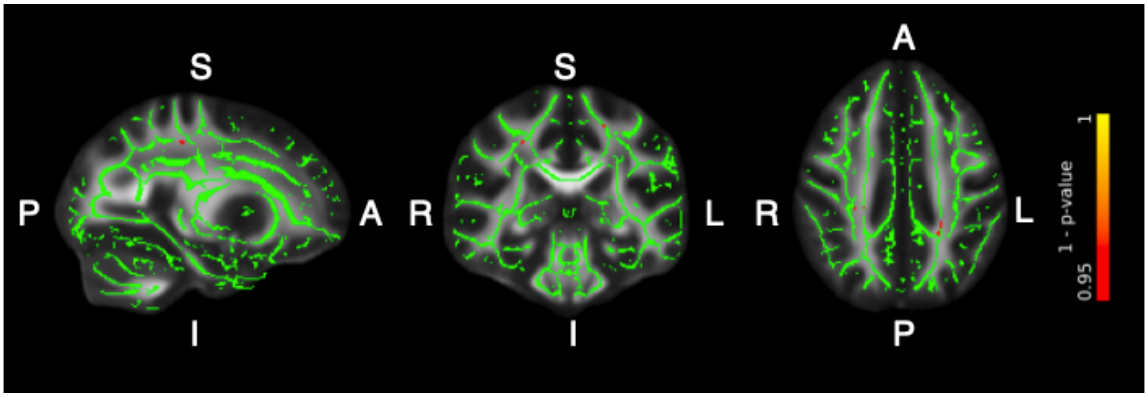

Figure 4-7. TBSS analysis of CQ active version using NODDI. (a) Increased offer acceptance was associated with increased NDI in the corticospinal tract and superior longitudinal fasciculus.

The above TBSS analyses revealed that while there exist associations between WM microstructure and behaviour in both the standard passive CQ task (Ch 3.) and the effortful conditions, the patterns differed subtly. In the standard condition, DTI-based FA highlighted associations between uncertainty ratings and offer acceptance in tracts including the left external capsule, left uncinate fasciculus, anterior corona radiata, right anterior thalamic radiation, genu of the corpus callosum, and left frontal aslant tract. In the effortful condition, both DTI-based MD and NODDI-based NDI revealed associations with offer acceptance in the anterior thalamic radiation, superior longitudinal fasciculus, corticospinal tract, forceps minor, and cingulum. These results indicate that while WM microstructure relates to behaviour in both tasks, the specific tracts implicated differed by task, and these associations were revealed by different diffusion models. Another important distinction is that while increased offer acceptance correlated negatively with WM integrity in the standard passive CQ task (Ch 3.), this behaviour correlated positively with microstructural integrity in the effortful condition.

Additional TBSS analyses using the DTI and NODDI models for other CQ passive version with effort behavioural and clinical metrics did not reveal any further significant effects in FA, ISOVF, and ODI. Analyses examining the relationship between participants' behaviour and WMH burden, as quantified by BIANCA, revealed no significant effects across the performance measures on the CQ effort passive version (e.g., overall uncertainty ratings,

uncertainty rating slopes, and offer acceptance based on uncertainty, reward, and effort). Finally, no significant relationships were observed between behavioural metrics from the CQ effort passive version and clinical measures of cognition, apathy, depression, and impulsivity.

4.4.6 Connectome associated with behaviour in EBDM under uncertainty

Significant TBSS clusters were mapped onto the JHU white-matter atlas to identify implicated tracts and quantify the proportion of supra-threshold voxels within each. Voxel endpoints were assigned to the nearest cortical regions in the Harvard–Oxford atlas, generating a tract-to-cortex mapping. These mappings were then combined to construct a connectome in which edges represent the percentage of affected voxels within each tract. This was done for the significant results from both the DTI (**Figure 4-8**) and NODDI (**Figure 4-9**) models described above.

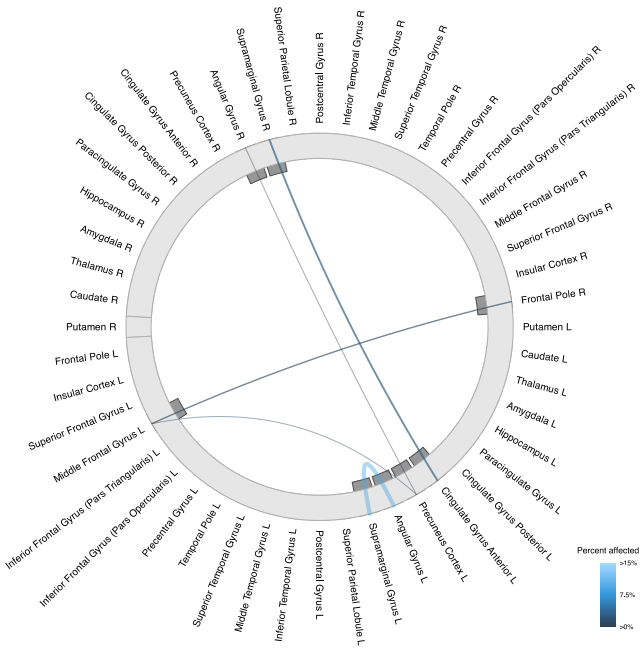

Figure 4-8. Connectome associated with increased offer acceptance based on DTI MD.
Denser connection was observed in WM connections within the left angular gyrus and between the left supramarginal gyrus and left angular gyrus; left anterior cingulate gyrus and right supramarginal gyrus; right frontal pole and left middle frontal gyrus; left precuneus cortex and left angular gyrus; left precuneus cortex and left middle frontal gyrus; and left precuneus cortex and right angular gyrus.

In the DTI model involving reduced MD, increased WM connections positively correlated with offer acceptance (**Figures 4-8**) were confined to the frontal and parietal lobes. In the

NODDI model involving increased NDI, improved WM connectivity associated with increased offer acceptance (**Figures 4-9**) was left lateralized and confined to the frontal and temporal lobes. WM tracts projecting to the left middle frontal gyrus and left precuneus cortex were implicated in both models.

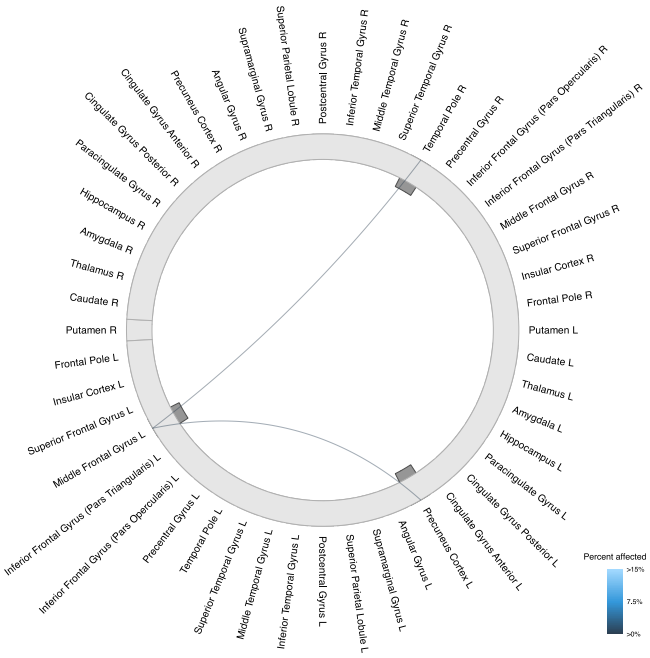

Figure 4-9. Connectome associated with increased offer acceptance based on NODDI NDI.
Higher neurite/axonal density was observed in WM connections within the right temporal pole and left middle frontal gyrus; and between the right temporal pole and left middle frontal gyrus; and left precuneus cortex and left middle frontal gyrus

4.5 Discussion

This chapter set out to examine whether the introduction of physical effort alters SVD patients' sensitivity to reward and uncertainty in decision-making, and to assess how such changes relate to underlying WM microstructure. Building on the findings from Ch 3, where patients showed reduced reward sensitivity and increased risk-taking compared to healthy controls, the current study introduced a physical effort component to the passive version of the CQ task to explore whether engaging EBDM systems would modify this behavioural profile. EBDM has been proposed as a fundamental mechanism for allocating cognitive and physical resources toward goal-directed behaviour (Gómez Escobar & Mitchell, 2025; Kurniawan et al., 2011). It relies

on the capacity to integrate reward value, task demands, and internal states such as fatigue to guide adaptive action (Arulpragasam et al., 2018; Chong et al., 2017a). Given that SVD can lead to disruptions in fronto-striatal and cingulo-opercular networks crucial for these computations(Le Heron, Manohar, et al., 2018; Saleh et al., 2021b), understanding how physical effort modulates motivational decision-making in this population provides important insight into the neural and cognitive underpinnings of apathy and reduced goal-directed behaviour.

The present findings demonstrate that both patients and controls appropriately tracked uncertainty, reward, and effort demands, yet the degree to which these factors influenced their decisions differed. In terms of uncertainty, both groups' subjective ratings scaled positively with objective uncertainty, suggesting that they recognised and responded to changes in outcome probability. However, SVD patients showed a reduced sensitivity to increasing uncertainty, reflected in flatter rating slopes (**Figure 4-2a**). This attenuation might potentially be attributable to consistent with metacognitive inefficiency, potentially linked to impaired communication between brain monitoring systems and those implicated in uncertainty tracking (Fleming et al., 2012). Importantly, there was no significant overall group difference in mean uncertainty ratings, suggesting that patients did not fundamentally misperceive uncertainty but were less responsive to its graded changes. This finding is consistent with emerging evidence of disrupted cost weighting in SVD (Le Heron, Manohar, et al., 2018).

Decision patterns further revealed how reward, uncertainty, and effort jointly shaped choice behaviour. Across both groups, participants were slightly less likely to accept offers as uncertainty increased (**Figure 4-2b**), although this effect did not reach significance due to variability. As expected, acceptance increased with higher rewards (**Figure 4-2c**), but controls showed a steeper rise in acceptance than patients, particularly at higher reward levels. This

replicates the reward hyposensitivity previously observed in SVD (Ch 3) and supports the view that reward valuation processes are blunted in SVD (Hollocks et al., 2015).

Both groups showed reduced acceptance as required effort increased (**Figure 4-2d**), consistent with effort discounting (Nishiyama, 2016). However, SVD patients exhibited a shallower decline across effort levels, suggesting diminished differentiation between low and high effort costs. Interestingly, patients were also more effort-averse at low effort levels, accepting fewer easy offers than controls. This paradoxical pattern implies that reduced engagement cannot be explained purely by physical aversion but may instead reflect a lowered baseline motivation or altered calibration of action costs which is a feature often associated with apathy (Le Heron, Plant, et al., 2018; Saleh et al., 2021b).

The comparison between task conditions highlights the critical role of effort in modulating engagement. Controls were already sensitive to reward and uncertainty in the no-effort condition, as shown in Ch 3, but when effort was introduced, they increased their overall acceptance rates (**Figures 4-4c & 4-4d**), suggesting that the physical demand may have enhanced task salience or reward anticipation (Clay et al., 2022; Pan et al., 2023; Zentall, 2010).

For patients, the addition of effort had an even more striking effect. Although SVD participants had previously shown blunted sensitivity to reward and uncertainty (Ch 3), under effortful conditions their responsiveness increased to levels statistically indistinguishable from controls (**Figures 4-4a & 4-4b**). This finding suggests that effort might potentially have amplified motivation. Similar "effort-activation" effects have been described in healthy individuals and in disorders with motivational deficits, where the physical act of engaging with effortful tasks can enhance arousal and re-engage reward valuation processes (Bogdanov et al., 2022; Clay et al., 2022; Harmon-Jones et al., 2020; Hernandez Lallement et al., 2014; Renz et al., 2022). Within this framework, effort can be understood not only as a cost but also as a

source of motivational salience and its inclusion in the task may have increased perceived control or outcome relevance, thereby compensating for patients' reduced intrinsic drive.

Decision time data further support the interpretation that effort increases deliberative engagement (**Figure 4-3**). Although there were no significant group differences in reaction time within each condition, both groups took longer to decide when effort was introduced, consistent with increased cognitive load and a more deliberate evaluation of cost–benefit trade-offs. This aligns with theoretical accounts positing that effort-based choices engage the ACC to integrate reward and effort information and optimise behavioural allocation (Barakat et al., 2025; P. L. Croxson et al., 2009). The fact that SVD patients showed similar response latencies to controls suggests that basic decision dynamics remain preserved, even when motivational sensitivity differs.

The fatigue data provide further nuance to these behavioural findings. In the effort condition, both groups reported increasing fatigue over time, with no significant overall group difference (**Figures 4-5a & 4-5b**). However, patients began the task at a slightly higher fatigue level, plateauing early, whereas controls started lower and showed a gradual increase. The pattern may suggest that patients experience reduced physiological and cognitive recovery or earlier onset fatigue, which is broadly consistent with existing evidence of fatigue in SVD (Jolly et al., 2024). In the no-effort context (**Figure 4-5c**), patients again began more fatigued—this time significantly so—which likely reflects residual tiredness from having completed the active version of the CQ task immediately beforehand. Again, their fatigue trajectory increased before plateauing, suggesting limited dynamic range or sensitivity in fatigue reporting. Controls, by contrast, showed stable fatigue during the first three blocks and a modest increase only near the end, which may indicate mild boredom due to task repetitiveness rather than exertional fatigue. These findings highlight that while SVD patients do not necessarily tire

more rapidly during task performance, they begin from a higher baseline of subjective fatigue, potentially reflecting diminished baseline arousal or sustained effort readiness.

The neuroimaging analyses offer convergent support for a link between motivational engagement and WM integrity. Across participants in the CQ effort passive version, higher offer acceptance was associated with lower MD from the DTI-based TBSS analysis (**Figure 4-6**) and higher NDI from NODDI-based TBSS (**Figure 4-7**). These complementary findings indicate that individuals with more intact WM microstructure were more likely to engage with effortful offers, consistent with more efficient neural signalling across motivation-related circuits. The implicated tracts, such as the anterior thalamic radiation, superior longitudinal fasciculus, corticospinal tract, forceps minor, and cingulum, form part of the broader fronto-striatal and cingulo-opercular networks involved in reward valuation, cognitive control, and effortful action (Chong et al., 2017a; Le Heron, Plant, et al., 2018). Lower MD and higher NDI are indicative of preserved axonal coherence and myelination (Mascalchi et al., 2019; H. Zhang et al., 2012), suggesting that microstructural integrity within these tracts supports effective cost–benefit integration. These findings resonate with the view that apathy and reduced motivation in SVD are not the result of isolated regional dysfunction, but of network-level disconnection affecting communication between the ACC, basal ganglia, and prefrontal cortex (Benoit & Robert, 2011; Hollocks et al., 2015). Interestingly, no comparable associations emerged for WMH burden.

The connectomics analyses further support a network-level account of motivated decision-making. For DTI-derived MD, increased offer acceptance was associated with denser structural connectivity across frontal–parietal links, including connections involving the left angular and supramarginal gyri, the left anterior cingulate gyrus, the right frontal pole, and several pathways linking the left precuneus to frontal and parietal regions (**Figure 4-8**). These effects were mediated primarily by callosal fibres and the corona radiata. For NODDI-derived

NDI, higher neurite or axonal density was linked to stronger, largely left-lateralised fronto-temporal connections, particularly those involving the temporal pole, middle frontal gyrus, and precuneus (**Figure 4-9**). Notably, both models converged on white-matter pathways projecting to the left middle frontal gyrus and left precuneus, suggesting that these regions may act as key nodes within the broader networks supporting motivated behaviour. This interpretation is consistent with previous work showing that the precuneus has strong structural connections to prefrontal areas via the cingulum (Tanglay et al., 2022), that fronto-parietal and default-mode networks rely on these pathways for coordinated signalling (Cunningham et al., 2016; M. P. van den Heuvel et al., 2009), and that apathy in SVD relates to disruption within frontal and parietal circuits rather than isolated regional pathology (Hollocks et al., 2015; Moretti & Signori, 2016; Tay et al., 2019). Overall, the pattern of reduced MD and increased NDI associated with greater offer acceptance points to more efficient connectivity within distributed valuation and control networks.

An interesting point of comparison with the passive version results from Ch 3 is that, in the non-effortful condition of the CQ task, increased offer acceptance was instead associated with reduced white-matter integrity and was linked to poorer uncertainty estimation and less efficient sampling (in the active version of the CQ task). Notably, several of the same connections—such as pathways involving the left angular and supramarginal gyri, the left anterior cingulate gyrus and right supramarginal gyrus, and links between the right frontal pole and left middle frontal gyrus—were implicated across both experiments but showed opposite relationships with behaviour. This pattern suggests that offer acceptance does not reflect a single underlying cognitive process across tasks. Rather, these fronto-parietal pathways may support different aspects of decision-making depending on the computational demands, promoting adaptive engagement when effort costs are present, but reflecting suboptimal belief updating when choices are made without effort constraints. This pattern aligns with prior work

showing that fronto-parietal and cingulo-opercular networks are flexible and can relate to behaviour in different ways depending on task demands (Y. Li et al., 2021; Wood & Nee, 2023). These pathways might support both effort-based valuation and uncertainty monitoring, and their engagement could reflect different underlying computations across contexts. In SVD and apathy, for example, greater white-matter integrity in these circuits has been linked to improved goal-directed behaviour, whereas reduced integrity is associated with poorer belief updating and diminished exploratory sampling. The observation that overlapping connections predicted opposite behavioural patterns across the two CQ tasks fits well with this literature, suggesting that acceptance behaviour recruits partially shared but functionally flexible networks whose contribution depends on whether decisions require integrating effort costs or evaluating uncertainty.

Together, these results provide new insight into how effort modulates motivated decision-making in SVD. Although both patients and controls appropriately evaluated uncertainty, reward, and effort, patients exhibited reduced sensitivity to these parameters overall, consistent with diminished motivational responsiveness. Yet, the addition of physical effort enhanced their sensitivity, restoring behaviour to control levels. This suggests that effort can act as an external cue that re-engages otherwise underactive motivational circuits or perhaps focuses attention on the decision to a greater degree. The absence of major group differences in decision time and fatigue trajectories indicates that these behavioural changes are unlikely to reflect general cognitive slowing or physical exhaustion. The structural imaging and connectomics findings further strengthen this interpretation, linking greater engagement to better-preserved WM microstructure within tracts in the brain's EBDM network critical for reward–effort integration. However, there were no significant behavioural correlations with apathy scores which might reflect the context-dependent nature of motivational deficits in

behavioural tasks that capture more transient, state-like aspects of motivation, whereas clinical apathy scales measure trait-like or global reductions in goal-directed behaviour.

This study has several limitations. First, participants in the SVD group were primarily in the early stages of the disease and largely non-demented, which limits the generalisability of the findings to the wider SVD population. Individuals with more advanced disease or greater cognitive impairment may show more pronounced deficits in effort-based decision-making, potentially offering a clearer view of how vascular pathology contributes to motivational dysfunction. Second, because patients were recruited from a Cognitive Disorders clinic rather than through community-based screening, the sample may not fully represent the spectrum of SVD severity or typical clinical presentations, introducing a potential selection bias. A third limitation is the use of standard atlases to define white-matter tracts and cortical regions. Consequently, the proposed connectome represents a probabilistic approximation of underlying anatomy, and inter-individual variability in WM architecture may have led to minor inaccuracies in tract or node assignment.

4.6 Conclusion

On the effort-based version of the CQ task, SVD patients showed appropriate sensitivity to reward, effort, and uncertainty. The previous chapter showed that patients were significantly less sensitive than controls to reward and uncertainty, yet the introduction of a physical effort altered this profile. When effort was required, patients' behaviour shifted toward that of controls, though performance differences remained significant, suggesting that effort acted as a catalyst for engagement rather than an additional cost. The imaging results further support this interpretation, showing that greater offer acceptance was linked to lower MD and higher NDI in WM pathways associated with fronto-striatal control and motivational processing. Further imaging analyses to generate a connectome accounting for increased offer acceptance

revealed that these structural effects were reflected in enhanced network-level connectivity, particularly along fronto-parietal and fronto-temporal pathways projecting to hubs such as the left middle frontal gyrus and left precuneus. Together, these findings indicate that effort can transiently normalise motivational behaviour in SVD, possibly by enhancing the salience of decision cues or re-engaging partially preserved neural systems. This work extends current understanding of apathy in cerebrovascular disease, highlighting it not as a fixed loss of motivation but as a context-sensitive deficit that may respond to targeted activation of effort-based mechanisms.

5| Impact of MFL lesioning on DM under uncertainty

5.1 Abstract

Decision-making impairments are frequently reported following focal damage to the medial frontal lobe (MFL). This chapter applied the active and passive versions of the CQ task, previously used in patients with SVD (Chapter 3), to a cohort consisting of individuals with focal MFL lesions, lesion controls (LC) with damage outside the frontal lobes, and age-matched HC. This design enabled investigation of the contribution of the medial frontal cortex to decisions involving the evaluation of sampling cost, reward, and uncertainty.

On the active version of the CQ task, patients with MFL lesions earned less reward, collected fewer samples, demonstrated greater tolerance for uncertainty before committing to a decision, and showed reduced placement accuracy compared to HC, with performance broadly comparable to the LC group. On the passive version of the task, MFL patients exhibited riskier choices, accepting offers in a manner that was less strongly modulated by reward value and more tolerant of uncertainty compared to HC. Reduced sensitivity to uncertainty was also observed in LC relative to HC, though LC did not show the reward-related impairments seen in MFL patients. LC, like the MFL group, tolerated more uncertainty across both task variants, suggesting that decision-making under uncertainty engages medial frontal regions as well as additional neural substrates outside the frontal lobes.

Brain regions associated with these behavioural effects were investigated using lesion mapping in patient groups. This analysis implicated medial frontal regions as key contributors to reward sensitivity and uncertainty processing, while also highlighting the involvement of a broader network of frontal and non-frontal areas in shaping task engagement and sampling behaviour. Overall, the findings provide converging evidence that the medial frontal lobe plays

a critical role in regulating reward-guided behaviour and uncertainty processing, while also demonstrating that these functions depend on distributed neural systems.

5.2 Introduction

Focal damage to the medial frontal lobe (MFL) has long been associated with impairments in decision-making, particularly in contexts involving reward evaluation, uncertainty, and adaptive behaviour (Anderson et al., 1999; Bechara, 1994; Bechara et al., 2000; Clark et al., 2003a, 2008; Clark & Manes, 2004; Manes et al., 2002). While the MFL is widely implicated in the regulation of goal-directed actions, its specific contribution to decision-making under uncertainty remains contested in the literature (Huettel et al., 2005b; Krug et al., 2014; Stern et al., 2014). Several lines of evidence suggest that the MFL, including the anterior cingulate cortex (ACC), pre-supplementary motor area (pre-SMA), and ventromedial prefrontal cortex (vmPFC), plays a central role in monitoring action-outcome contingencies, encoding subjective value, and guiding behaviour in the face of competing demands (Kennerley & Walton, 2011b; O'Doherty, 2011; Passingham et al., 2010; Rushworth, 2008; Volz et al., 2006; Wilson et al., 2010). However, the precise functions of these regions, and the extent to which they support distinct or overlapping components of decision-making, remain matters of ongoing debate. Further complicating the picture is the observation that similar impairments can be produced by damage to non-frontal regions, raising questions about the extent to which these functions are uniquely dependent on medial frontal structures (Huettel et al., 2005b).

Studies using fMRI have been instrumental in shaping our current understanding of MFL function in human decision-making (Boorman et al., 2009; Kolling et al., 2012). A growing body of research highlights how distinct subregions within the MFL contribute to core computations such as value estimation, cost representation, uncertainty monitoring, and information sampling (Arulpragasam et al., 2018; Hogan et al., 2019; Kaanders et al., 2021;

Krug et al., 2014). For example, Arulpragasam et al. (2018) found that the vmPFC encoded expected subjective value in an effort-based decision-making task, while the dorsal ACC and anterior insula tracked deviations from those expectations, indicating their roles in value prediction and prediction error processing, respectively. Regarding cost representation, Hogan et al. (2019) demonstrated that the vmPFC encoded subjective effort cost even in the absence of extrinsic reward, suggesting that this region tracks internal cost signals independent of outcome, whereas ACC activity was more closely related to choice difficulty. Krug et al. (2014) demonstrated that the medial frontal cortex is actively engaged during decision-making under uncertainty, reflecting its key role in monitoring and resolving uncertainty in choice situations.

The MFL also contributes to Information sampling and evidence accumulation In dynamic decision contexts. In a study by Kaanders et al. (2021), activity in the dorsomedial PFC predicted participants' choices to sample additional information before making economic decisions and showed greater activation when participants faced more difficult decisions. This highlights the MFL's role not only in computing value or tracking uncertainty but also in regulating exploratory behaviour in situations where decision outcomes are ambiguous or incomplete.

Together, these findings point to a functional dissociation within the MFL, where ventral regions such as the vmPFC support valuation and reward integration, while more dorsal areas, including the ACC and dorsomedial PFC, monitor uncertainty, compute prediction errors, and guide strategic information gathering during decision-making under uncertainty.

While fMRI has been invaluable in mapping the functional architecture of the MFL, it also presents important methodological limitations that constrain interpretation (Logothetis, 2008). A primary limitation is that fMRI data are correlational. While activation patterns can show links between brain regions and cognitive functions, they do not demonstrate causality. Additionally, susceptibility artifacts and signal dropout are common in ventral brain regions.

These effects can reduce fMRI sensitivity and obscure activity, which may bias findings in areas near air-tissue boundaries such as parts of the medial frontal cortex (Ojemann et al., 1997). Furthermore, the MFL is anatomically complex and functionally heterogeneous (Euston et al., 2012), with closely adjacent subregions such as the vmPFC and dorsal ACC often co-activating during decision-making tasks, making it difficult to disentangle their specific contributions using standard fMRI spatial resolution. These limitations are compounded in tasks involving dynamic or uncertain environments, where cognitive processes like belief updating, prediction error computation, and outcome valuation unfold rapidly and may overlap temporally.

Lesion studies offer a critical complementary approach to fMRI, helping to address its limitations by providing causal evidence about the necessity of specific MFL regions in decision-making processes (Bechara, 1994; Clark et al., 2008; Manes et al., 2002). For example, Bechara et al. (1994) demonstrated that patients with damage to the ventromedial prefrontal cortex (vmPFC) consistently made disadvantageous choices on the Iowa Gambling Task, implicating this region in integrating long-term consequences into current decision-making. Similarly, Clark et al. (2008) used the Cambridge Gamble Task to show that individuals with ventromedial and orbitofrontal lesions exhibited impaired risk adjustment. Despite understanding the odds, these patients placed higher bets and showed reduced sensitivity to probability information, suggesting a breakdown in the valuation and uncertainty-monitoring processes attributed to the vmPFC in neuroimaging research. Manes et al. (2002) further found that patients with vmPFC damage displayed increased impulsivity and made inconsistent decisions, even in clearly disadvantageous situations.

Collectively, these lesion studies show that damage to medial frontal areas, particularly the vmPFC and adjacent orbitofrontal cortex, disrupts core components of value-based decision-making such as risk evaluation, reward sensitivity, and behavioural consistency. By

offering causal insight, lesion research helps validate and refine the functional interpretations derived from fMRI studies and addresses ambiguities that neuroimaging alone cannot fully resolve.

In this chapter, the effect of focal lesions to the MFL on behaviour is investigated in a decision-making task specifically designed to manipulate uncertainty, reward, and sampling cost. The CQ task, previously employed to examine impaired information-seeking in patients with SVD (Chapter 3), is used to assess the behaviour of individuals with focal MFL lesions. This cohort is compared to both patients with damage outside the frontal lobes (lesion controls, LC) and age-matched healthy controls (HC). The inclusion of LC allows for the dissociation of MFL-specific effects from general consequences of brain injury, while the use of both active and passive task variants permits a detailed analysis of volitional and externally driven decision-making under uncertainty.

Finally, behavioural findings are interpreted alongside lesion mapping and structural MRI data to identify the brain regions associated with task performance. This multimodal approach enables the examination of structure-function relationships and provides insight into the extent to which behavioural impairments can be attributed to focal MFL damage versus broader disruptions in distributed neural systems. In doing so, the chapter aims to clarify the functional role of the MFL in uncertainty-guided behaviour, reward evaluation, and adaptive sampling, and to place these findings in the context of existing models of decision-making.

5.3 Methods

5.3.1 Participants, demographics, and consent

Eleven MFL participants aged 53–73 years (6 males, 5 females), all of whom had medial frontal lesions primarily resulting from anterior communicating artery aneurysm rupture, and eight LC participants aged 53–71 years (3 males, 5 females) with brain lesions sparing the medial frontal

lobe due to intracerebral haemorrhage or focal infarcts, were recruited through the Cognitive Disorders Clinic at the John Radcliffe Hospital in Oxford. Their performance in this study was compared to that of thirty-five age-matched healthy controls (HC) who were also part of the cohort in the previous chapter. Demographics are presented in **Table 5-1** and **Table 5-2** carries more information on the lesion characteristics for the patients.

Characteristic	HC N = 35[1]	LC N = 8[1]	MFL N = 11[1]	LC vs HC	LC vs LC	MFL vs HC	MFL vs LC
Age (years)	64 (58, 68)	61 (53, 71)	70 (53, 73)	0.6		0.3	0.2
Unknown	0	1	0				
Gender							
Male	14 (40%)	3 (38%)	6 (55%)				
Female	21 (60%)	5 (63%)	5 (45%)				
YOE	21.0 (18.0, 22.0)	18.5 (16.5, 20.5)	18.0 (17.0, 23.0)	0.053		0.028	>0.9
ACE Total	99.0 (97.0, 99.0)	95.0 (90.0, 96.5)	90.0 (83.0, 98.0)	0.002		<0.001	0.2
AMI Total	1.08 (0.83, 1.56)	1.56 (1.14, 2.08)	1.31 (0.83, 2.06)	0.061		0.3	0.4
Unknown	1	0	1				
BDI Total	5.0 (1.0, 8.0)	8.0 (6.0, 11.5)	9.5 (5.0, 11.0)	0.11		0.007	0.4
Unknown	1	0	1				
BIS Total	63 (53, 77)	81 (77, 85)	77 (76, 82)	<0.001		<0.001	0.8
Unknown	0	0	1				
HADS Depression	2.0 (1.0, 7.0)	8.5 (8.0, 9.5)	8.0 (8.0, 9.0)	<0.001		<0.001	0.6
Unknown	2	0	1				
HADS Anxiety	5.0 (3.0, 12.0)	11.0 (11.0, 13.0)	12.0 (9.0, 13.0)	0.003		0.003	0.8
Unknown	2	0	1				

[1] Median (Q1, Q3); n (%)

Table 5-1: Demographic and questionnaire measures. HC = Healthy Controls, MFL = Patients with Medial Frontal Lobe Lesions, LC = Lesion Controls, YOE = Years of Education, ACE-III = Addenbrooke's Cognitive Examination III, AMI = Apathy Motivation Index, BDI-II=Beck Depression Inventory II, BIS-II = Barrat Impulsiveness Scale II, HADS =Hospital Anxiety and Depression Scale.

Lesion Group	Patient Code	Lesion Volume (voxels)	Lesion Volume (mL)	Lesion Description (location, aetiology, etc.)	Harvard-Oxford atlas defined regions
MFL	302	5240	5.240	Left mPFC	FP L; PCG L; SFG L; JLC L
MFL	306	37888	37.888	Bilateral mPFC	FP; MFG; IFG; SCG L
MFL	310	20048	20.048	Left medial OFC/frontopolar	FP L; MFG L; PCG L; aCG L; SCG L
MFL	314	32920	32.920	Left medial frontal/polar	FP L; MFG L; PCG L; aCG L; SCG L; SFG L
MFL	315	3144	3.144	Right mPFC (tiny ventral stiatal damage)	SCG R
MFL	320	6184	6.184	Left mPFC (small gyrus rectus infarct)	MFG L; PCG L; aCG L; SCG L
MFL	321	144	0.144	Left mPFC, olfactory groove meningioma (not SAH but tiny tumour)	FP L; MFG L
MFL	324	1872	1.872	Left mPFC	PCG L; aCG L
MFL	325	2648	2.648	Left mPFC (gyrus rectus and scattered wm)	FP L; MFG L; IFG L; SCG L; SFG L
MFL	328	9920	9.920	Right mPFC (gyrus rectus and sgACC)	FP R; MFG R; IFG R; PCG R; aCG R; SCG R
MFL	418	5128	5.128	Left temporal, bi-parietal and subgenual	aCG; SCG L; IFG L
LC	401	16696	16.696	Right lateral PFC and temporal lobe	FP R; IFG R; STG R; MTG R
LC	402	8456	8.456	Left parietal lobe (PREC AVM)	PREC L
LC	404	47848	47.848	Right parietal lobe	SFG R; JLC R; pCG R; PreCG R; IPL R; PREC R
LC	408	968	0.968	Left internal capsule / ventral striatal haemorrhage	THA L;CAU L
LC	410	64728	64.728	Left parietal and anterior insula	Insula L; STG L; SMG L; AG L
LC	412	43056	43.056	Left occipitotemporal	LINGL; PHG L
LC	413	14040	14.040	Left head of caudate infarct	Insula L; IFG L
LC	416	664	0.664	Right insula	Insula R; IFG R

All individual patient data from the study.

Table 5-2: Patient Lesion Characteristics. MFL = Patients with Medial Frontal Lobe Lesions, LC = Lesion Controls, Frontal Pole = FP, Paracingulate gyrus = PCG, Superior frontal gyrus = SFG, Juxtapositional lobule cortex = JLC, Middle frontal gyrus = MFG, Inferior frontal gyrus = IFG, Subcallosal gyrus = SCG, Cingulate gyrus anterior= aCG, Superior temporal gyrus = STG, Middle temporal gyrus = MTG, Precuneus = PREC, Cingulate gyrus posterior = pCG, Precentral gyrus = PreCG, Inferior parietal lobule = IPL, Thalamus = THA, Caudate = CAU, Supramarginal gyrus = SMG, Angular gyrus = AG, Lingual gyrus = LING, Parahippocampal gyrus =PHG

The three groups did not differ significantly in terms of age or sex ratio. However, HC had more years of full-time education compared to MFL patients. Cognitive function screening using ACE-III revealed significantly higher scores in HC, although both lesion groups also had scores that were within normal limits for the general population (Hsieh et al., 2013; Mathuranath et al., 2000). There were significantly more people with depression in the lesion cohorts, as measured with Hospital Anxiety and Depression Scale (HADS-dep) (Zigmond & Snaith, 1983). However, this difference in depression as measured using the Beck Depression Inventory-II (BDI-II) was only detected in MFL patients (Beck et al., 1961). Additionally, lesion patients scored higher on the Barratt's Impulsivity Scale (BIS) than control participants (Patton et al., 1995). Participant scores on the Apathy Motivation Index (AMI) did not differ significantly (Ang et al., 2016). Finally, both the Digit Span was administered to both lesion cohorts to test their working memory and both groups scored within the expected range for their age population (Blackburn & Benton, 1957; Choi et al., 2014)

Permission for this study was obtained from the local ethics committee. All participants provided written consent in accordance with the Declaration of Helsinki and the study was approved by the University of Oxford ethics committee.

5.3.2 Neuroimaging and analysis of lesion maps

Patients underwent T1-weighted MRI (2 mm isotropic or 2 × 2 × 5 mm), FLAIR, or CT scanning. Lesions were manually traced using FSL and registered to the MNI152 template via SPM8 or FLIRT, then smoothed with a 1 mm Gaussian kernel. Lesion masks were overlaid onto the Harvard - Oxford Cortical Structural Atlas (RRID:SCR_001476) http://fsl.fmrib.ox.ac.uk/fsl/fslwiki/Atlases, enabling examination of the brain regions affected by lesions.

5.3.3 Experimental setup

"CQ" paradigm

CQ is a decision-making behavioural paradigm comprised of two separate variations:

1. Active information-sampling task and
2. Passive choice task

The tasks were not counterbalanced: all participants performed the active information-sampling task before the passive choice task.

Stimuli

The above tasks were presented on a 17-inch touchscreen PC using MATLAB version 2018a (MathWorks; https://uk.mathworks.com) and Psychtoolbox version 3. Participants performed the tasks in a quiet testing room sitting within reaching distance of the screen (~50 cm). An experimenter was present in the room at all times during the behavioural testing which took about 60 mins on average to complete (Petitet et al., 2021). It is important to note that both the task duration and the number of trials were reduced compared to the administration described in Chapter 3. This adjustment was made because MFL patients appeared to fatigue more quickly and showed greater signs of restlessness compared to SVD patients.

Active information-sampling task

The objective in this condition was to earn as many credits as possible. To accomplish this, participants had to localize a hidden purple circle as precisely as they could using cues (samples) they generated themselves **(Figure 5-1)**. A circular grey mask (search space) was shown on the visual display and individuals were told that a purple circle (radius = 130 pixels; area = 5.80% of the search space) was hidden within this search space. Participants were instructed to tap anywhere within the search space to gather information about where the purple

circle could be hidden. A small dot (radius = 4 pixels) appeared wherever they touched the grey space. If the dot was purple, it signified that this location was within the area of the hidden purple circle. However, if the dot was white instead, this meant the participant had touched outside the area of the hidden purple circle. These dots remained on the screen for the duration of the information-sampling phase and until the end of the trial to reduce memory load for participants.

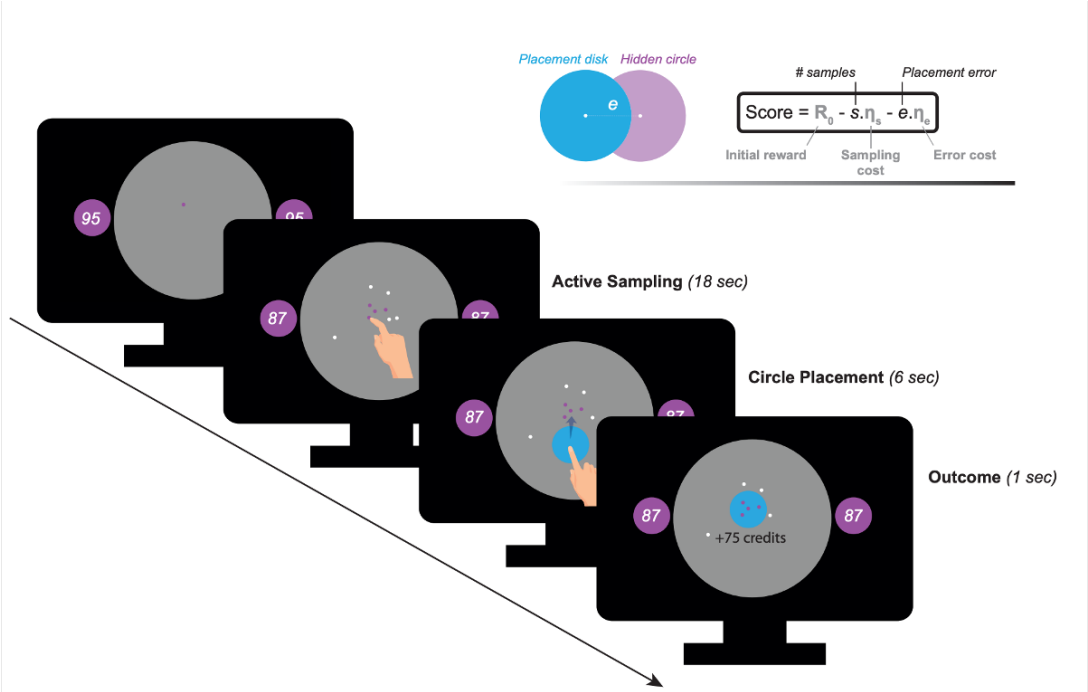

Figure 5-1. Active version of the CQ task. Participants searched for a hidden purple circle by sampling touchscreen locations that produced purple (inside) or white (outside) dots. Two reference circles displayed the initial credit reserve (R_0 = 95 or 130 credits). During an 18 secs sampling period, each touch reduced credits according to the sampling cost (η_s = –1 or –5 credits/sample). Afterward, participants positioned a blue circle to indicate the hidden circle's location, and the resulting score was shown as feedback. *Source: Attaallah et al., eLife (2022), https://elifesciences.org/articles/75834.*

Only one purple circle was hidden within the grey search space during a given trial. Participants were given one purple dot at the start of each trial as an initial hint to the circle's likely location to reduce the search time. The location of this first purple dot was drawn randomly from inside the hidden circle and was always at least 260 pixels away (the diameter of the hidden circle) from the edge of the search space, to ensure it always carried the same amount of information (expected error at the start of the search = 86.7 pixels). For each trial, a

purple circle was shown on both sides of the grey search space to remind participants of the size of the hidden circle they were searching for.

The maximum number of credits a participant could win (reward/stake) per trial was displayed within these perpetual purple circles on either side of the grey search space. The number of credits decreased each time the screen was touched to obtain a sample (sample cost), regardless of whether the dot generated was purple or white. The active information-sampling task was divided into four separate blocks of 8 trials each. Two of these blocks had initial rewards/stakes of 130 credits and the remaining two had initial rewards/stakes of 95 credits. The sampling cost or number of credits decreased by either 1 or 5 credits resulting in 4 different conditions i.e. four separate blocks. These blocks were counterbalanced within participant groups.

For each trial, participants had a maximum of 18 seconds to gather as many samples as they desired. They could stop information gathering at any point before the time ended, however, no extra credits were gained by finishing early. After the 18 seconds, a blue disk—the same size as the hidden purple circle (radius = 130 pixels) — appeared in the middle of the screen. An additional 6 seconds was then provided so this blue circle could be dragged to where participants thought the purple circle was hidden based on the configuration of white and purple dots they had generated. Their final score was then displayed onscreen.

This score was calculated using the formula for reward

$$(R_f) = R_0 - (s \times \eta_s) - (e \times \eta_e) \qquad \textit{Equation 1}$$

where R_f is the final reward, R_0 is initial reward/stake, s is the sampling cost, η_s is the number of samples, e is the penalty per pixel and η_e is the distance (in pixels) of the blue disks centre from that of the hidden purple circle. Essentially, participants won all the remaining credits post sampling ($R_0 - (s \times \eta_s)$) after a penalty reflecting how far they placed the blue disk from the actual hidden circle ($e \times \eta_e$) was deducted. This meant there were two ways to lose

credits: (1) by sampling more information and (2) by greater mis-localization of the true location of the hidden circle. To maximize reward, they had to sample efficiently, using the least number of samples that contained sufficient information to best localize the hidden purple circle. Participants were told that overall credit earnings would later be converted to British pounds, and 400 credits was the equivalent of £1.

Passive choice task

This version of CQ (**Figure 5-2**) did not involve any active sampling, so participants had no agency over the choice or number of samples. Instead, they were shown a 'snapshot' of someone's search and asked to make judgments on how much confidence they had in where the purple circle was located and whether they would accept or reject the offer to place the blue circle on the basis of the information they had and the credits on offer. The experiment involved manipulation of the expected error (uncertainty) in localization and the number of credits on offer (initial reward/stake) in each trial to assess how sensitive individuals were to each variable.

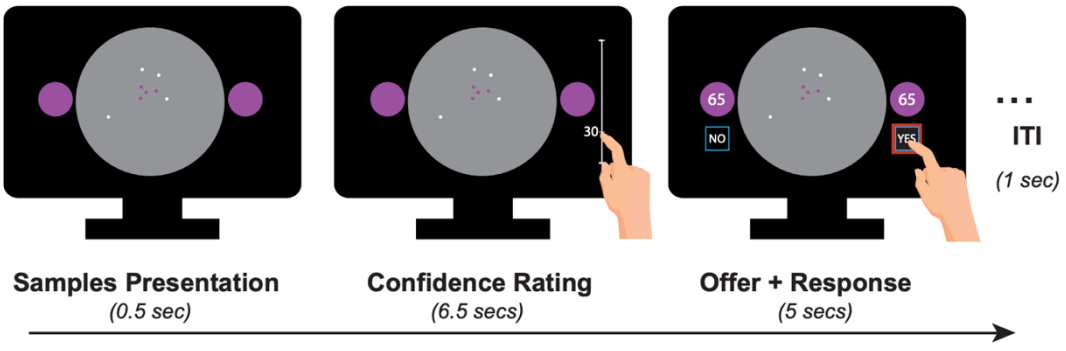

Figure 5-2. Passive version of the CQ task. Participants viewed completed searches and provided confidence ratings (later z-scored and sign-flipped to yield subjective uncertainty estimates) reflecting their perceived ability to locate the hidden circle. Ratings were made by tapping along a vertical scale ranging from 0 (bottom) to 100 (top). After submitting their ratings, participants received a reward offer (R_0 = 40, 65, 90, or 115 credits) and indicated their willingness to place the blue circle by tapping "yes" to accept or "no" to reject the trial.
Source: Attaallah et al., eLife (2022), https://elifesciences.org/articles/75834.

Uncertainty, EE (expected error), was calculated as the mean difference between all potential solutions given the current search using a recursive exponential decay model:

$$EE_s = (1-\alpha)(EE_{s-1} - EE_\infty) + EE_\infty \quad \textit{Equation 2}$$

where EE_s is the expected error after the s^{th} sample, α is the information extraction rate that quantifies the sampling efficiency, EE_{s-1} is the expected error after the previous ($s-1^{th}$) sample and EE_∞ is asymptotic expected error i.e. the lowest error achievable after infinite samples.

The passive choice task was divided into two phases: an uncertainty rating phase and an offer acceptance phase. No feedback was provided in either phase since there were no "correct answers", only subjective responses.

Uncertainty Rating

At the start of each trial participants were shown a 'snapshot' of a completed search with dots on the screen in various configurations. Each trial had eight sample dots in total, half of which were positive samples (purple) and the other half which were negative samples (white). The uncertainty, EE, was manipulated by varying the spatial configuration of the displayed samples. The expected error ranged from 10–70 pixels. This meant the further the positive samples were from each other, the lower the expected error would be. Each participant saw the same exact trials that were in total 40, but the order in which they saw them was randomized. They were asked to make a rating of how confident they were about the location of the hidden purple circle based on the completed search. This rating was done a scale from 1-100 displayed on the side of the screen corresponding to the handedness of the participant. Each completed search appeared onscreen alone for 0.5 seconds after which the rating scale appeared alongside for an additional 6.5 seconds. During this time participants were expected to make their rating. If they

failed to do so in time the task would move on to the subsequent trial. However, the missed trial would later reappear so all participants would complete all 50 trials.

Offer Acceptance

Once a participant made a rating of the completed search, the trial would progress to the next phase of the task: offer acceptance or rejection. The rating scale would disappear at this point and on each side of the completed search, two purple circles containing the number of credits on offer were presented instead. There were four credit options (40, 65, 90 or 115). Below the search space on either side was displayed a 'YES' and a 'NO' option which participants could select to accept or reject an offer respectively for the chance to place the blue disk where the hidden purple circle was located. The 'YES' and 'NO' options switched sides randomly during the task to avoid any bias to choose the same option. Note participants only accepted or rejected reward offers but did not actually place the blue disk. To incentivize the context, they were told they would later receive ten of the trials from those they accepted to then place the blue circle and collect more credits.

Protocol

Cognitive examination and questionnaires

All study participants were received cognitive examination using the Addenbrooke's Cognitive Examination (ACE) which took about 15 mins to complete. Version A of the ACE was administered to the healthy elderly controls while versions B and C were administered to both groups of lesion patients since they were more likely to have already been exposed to version A in a prior study or clinical visits. They were also made to complete the Digit Span Test which assesses an individual's attention and verbal working memory (Blackburn & Benton, 1957; Choi et al., 2014).

In addition to the above cognitive tests, participants completed established self-report questionnaire measures of apathy (Apathy and Memory Index, AMI), impulsivity (Barratt Impulsiveness Scale, BIS), depression (Beck Depression Inventory, BDI) and anxiety (Hospital and Anxiety Depression Scale, HADS) (Ang, 2017; Beck et al., 1961b; Patton et al., 1995; Zigmond & Snaith, 1983). Two of the questionnaires, AMI and BIS, were completed prior to start of CQ while the other two, BDI and HADS, in between the active information-sampling task and the passive choice task of CQ.

Fatigue ratings during the task

Throughout CQ, participants rated their level of subjective fatigue on a scale from 0 to 100 at the start of each experimental block in both the active and passive sampling conditions. Their prompt to report this rating came in the form of a vertical visual analogue scale that appeared in the middle of the screen underneath the text, 'How tired do you feel?' The top of the scale was labelled 'Extremely' and the bottom was labelled 'Not at all' to indicate the highest and lowest extremes of fatigue.

Experimental design

The active-information sampling variant of CQ was preceded by an exposure session during which participants were introduced to the task, given instructions, and allowed to practice sampling and placing the blue disc. First, they had three practice trials that required them to touch the screen and gather cues to the location of the hidden purple circle. They could acquire as many dots as they desired and when they were content with their search, they would hit the spacebar key to make the blue disc appear. Then they would drag this disc to where they thought the hidden purple circle was located. They received feedback in the form of a faded purple circle showing them the actual location of the hidden circle.

The next part of the exposure session had five blocks of 10 exposure trials (50 trials in total). This time participants were shown completed searches with eight samples (four positive dots and four negative dots) in different configurations to vary the level of uncertainty and the blue disk in the middle of the screen. Each trial also had an associated reward offer and these were either 40, 65, 90 or 115 credits. This part of the exposure session introduced individuals to the credit and scoring function of the task. Participants were required to move the blue disk to where they thought the hidden purple circle was located and then they received feedback in the form of the faded purple circle showing them the actual location of the hidden circle and the number of credits they won. Note that it was possible to receive negative credit scores.

After completing the exposure session, participants engaged in the active information-sampling task followed by the passive choice task.

5.4 Results

5.4.1 Lesion profile for MFL patients and LC

Lesion volumes for MFL and LC groups are provided in **Table 5-2**. LC participants had a mean lesion volume of 24.56 mL (SD = 24.08; 24,557 voxels), while MFL participants had a mean volume of 11.38 mL (SD = 13.07; 11,376 voxels). Relative variability was similar across groups (coefficient of variation: LC = 0.98, MFL = 1.15). A Mann–Whitney U test indicated no significant difference in lesion volume between groups (U = 58, p = 0.272; **Figure 5-3**), suggesting that the MFL and LC groups were comparable in overall lesion size.

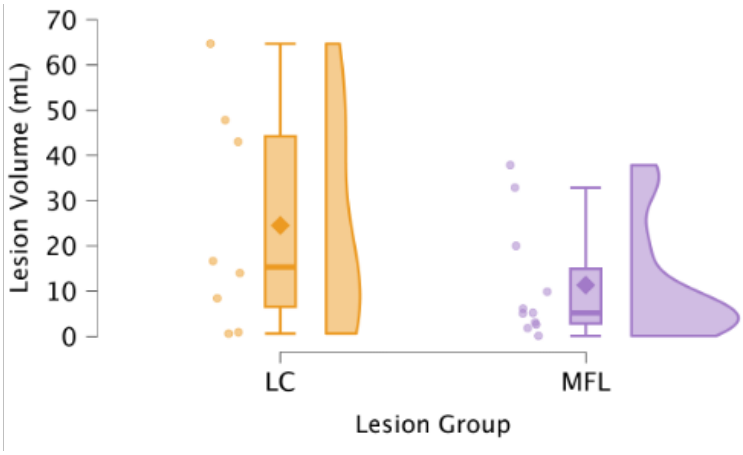

Figure 5-3. Lesion overlap by patient group MFL patients had damage to the medial frontal cortex. LC had damage in lateral parts of the brain or outside of the frontal cortex.

Though the lesion groups were comparable in size, each patient cohort differed by location of focal damage in the brain (**Figures 5-4 & 5-5**). MFL patients had damage mainly to the medial areas of the prefrontal cortex whereas LC had damage mainly in the lateral prefrontal, parietal, temporal and subcortical cortices. Individual lesion maps for each patient are shown in **Figures 5-6 & 5-7**. The specific brain regions with which the lesions overlap are shown in detail in **Table 5-2.**

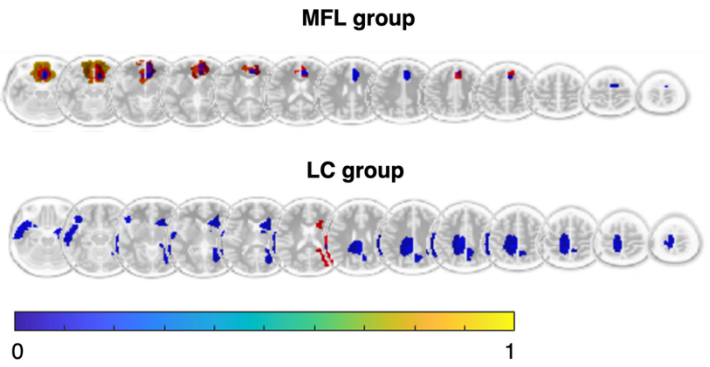

Figure 5-4. Axial view of lesion overlap by patient group MFL patients had damage to the medial frontal cortex. LC had damage in lateral parts of the brain or outside of the frontal cortex. Cool colours signify less overlap, and warm colours signify great overlap in each group.

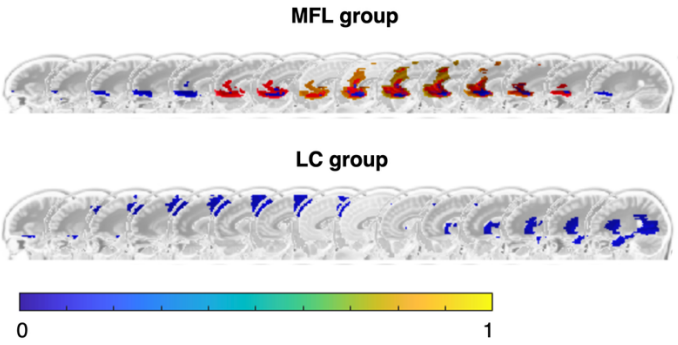

Figure 5-5. Sagittal view of lesion overlap by patient group MFL patients had damage to the medial frontal cortex. LC had damage in lateral parts of the brain or outside of the frontal cortex. Cool colours signify less overlap, and warm colours signify great overlap in each group.

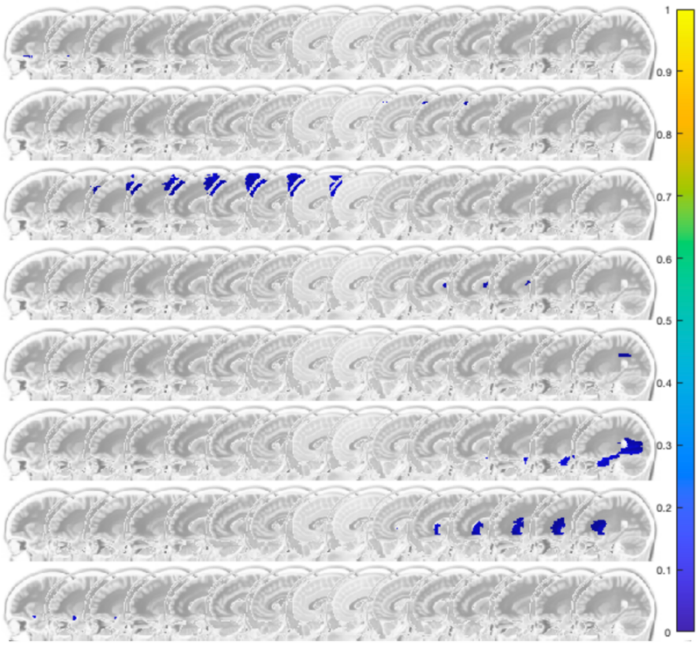

Figure 5-6. Sagittal view of LC brains showing lesion location. The extent of tissue damage varied in the LC group with some participants having lesions in the lateral frontal cortex and others having lesions in the temporal and parietal cortices. Lesions are shown in blue.

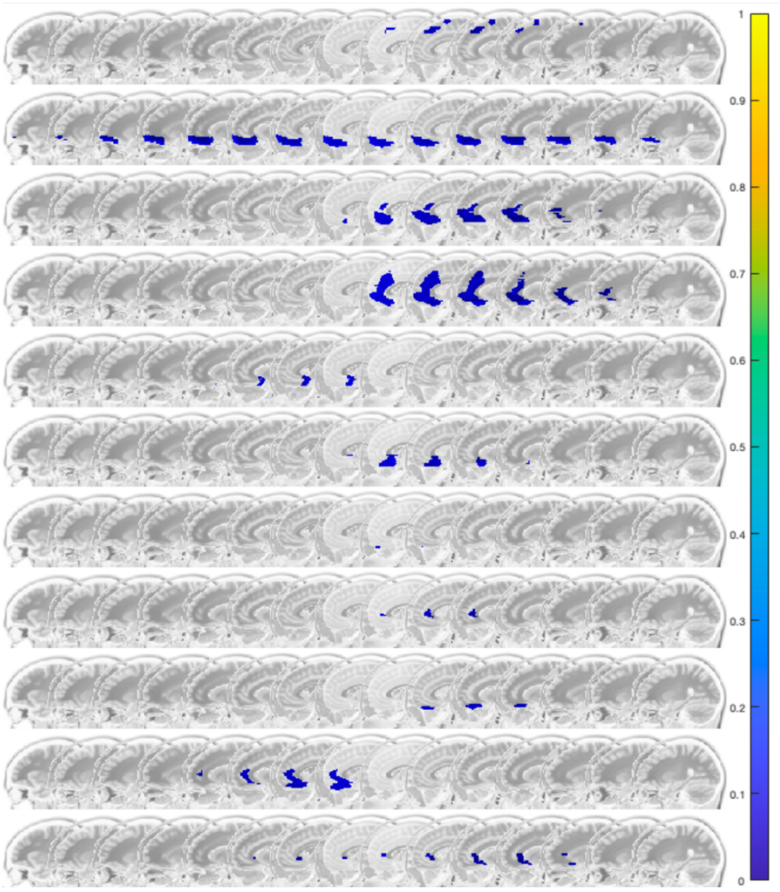

Figure 5-7. Sagittal view of MFL patients' brain showing lesion location. The extent of lesion damage varied in the MFL group but consistently included areas in the medial frontal lobes. Lesions are shown in blue.

5.4.2 Lesion participants earned fewer credits and spent less time on sampling than HC

The effects of group, initial reward, and sampling cost on total credit earnings were examined using a linear mixed-effects model. The omnibus model revealed significant main effects of initial reward and sampling cost on final earnings. Participants earned more when the initial reward was high ($\beta = 36.01$, SE = 1.29, $t_{2922} = 27.94$, $p < 0.0001$; **Figure 5–8a**) and earned fewer credits when sampling cost was high ($\beta = -37.28$, SE = 1.73, $t_{2922} = -21.54$, $p < 0.0001$). There was also a significant main effect of group, indicating overall differences in reward earnings between groups. Relative to healthy controls, both lesion groups earned fewer total

credits (group 2: $\beta = -10.96$, SE = 3.59, $t_{2922} = -3.05$, $p = 0.002$; group 3: $\beta = -11.12$, SE = 4.05, $t_{2922} = -2.74$, $p = 0.006$). A direct contrast between the two lesion groups revealed no significant difference in overall earnings ($\beta = 0.16$, SE = 4.85, $t_{2922} = 0.03$, $p = 0.97$). No interactions between group and initial reward or between group and sampling cost reached significance (all $p > 0.22$), nor was there a significant Initial Reward × Sampling Cost interaction ($p = 0.18$), indicating that group differences in earnings were consistent across reward and cost conditions.

Exploratory post hoc comparisons examining group differences within each cost and reward condition showed that healthy controls earned significantly more credits than lesion participants under low-cost conditions, both when initial reward was low ($t = -3.05$, $p = 0.002$) and high ($t = -2.85$, $p = 0.004$). No significant group differences were observed under high-cost conditions (all $p > 0.09$). Effects observed under low-cost conditions remained significant after Bonferroni correction. Together, these results indicate that all participants were strongly sensitive to both initial reward and sampling cost. However, both lesion groups showed a modest but reliable reduction in overall reward earnings relative to healthy controls, with no evidence for differential impairment between lesion groups, consistent with reduced overall reward maximization efficiency rather than altered sensitivity to reward magnitude or sampling cost.

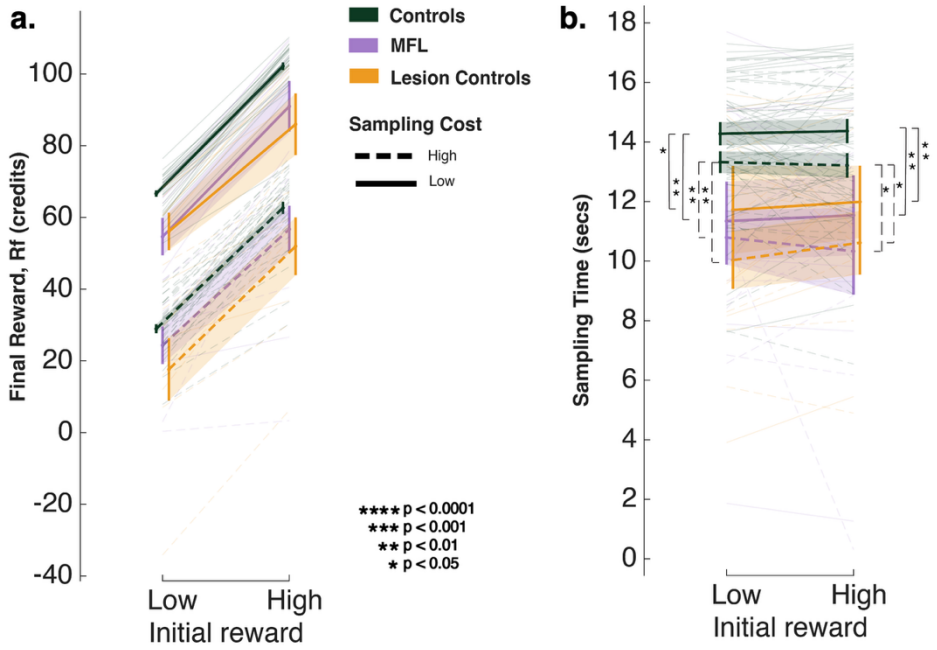

Figure 5-8. Reward earnings and time spent on sampling for participants. (a) Both lesion groups won significantly less reward (credits) than the HC when sampling cost was low. This difference remained true for only the LC at high sampling cost. **(b)** Both lesion groups generally spent significantly less time than HC gathering samples before placing the blue circle.

A separate linear mixed-effects model examined the effects of group, initial reward, and sampling cost on total time spent sampling. The model revealed a significant main effect of sampling cost, with participants sampling for less time overall when sampling cost was high ($\beta = -1.09$, SE = 0.30, $t_{2922} = -3.58$, $p < 0.001$; **Figure 5–8b**), indicating cost-sensitive adjustments in information gathering. In contrast, there was no main effect of initial reward on sampling time ($\beta = -0.003$, SE = 0.27, $t_{2922} = -0.01$, $p = 0.99$), indicating that reward magnitude did not influence sampling duration. The model also revealed a significant main effect of group, indicating overall differences in sampling time between groups. Relative to healthy controls, both lesion groups sampled for significantly shorter durations overall (group 2: $\beta = -2.98$, SE = 0.86, $t_{2922} = -3.46$, $p < 0.001$; group 3: $\beta = -2.93$, SE = 0.97, $t_{2922} = -3.01$, $p = 0.003$). A direct contrast between the two lesion groups revealed no significant difference in overall sampling time ($\beta = -0.05$, SE = 1.16, $t_{2922} = -0.04$, $p = 0.97$). No Group × Sampling Cost or Group × Initial Reward interactions reached significance (all $p > 0.34$),

indicating that the effects of cost and reward on sampling time were similar across groups. Bonferroni-corrected post hoc comparisons across task conditions confirmed that both lesion groups sampled for significantly less time than healthy controls under all combinations of sampling cost and reward (all $p\_corr \leq 0.012$). Together, these results indicate that lesion participants spent less time sampling overall, despite adjusting their sampling behaviour appropriately in response to sampling cost. This pattern suggests intact task understanding but reduced overall engagement in information gathering relative to healthy controls.

5.4.3 MFL patients sampled less, were less sensitive to sampling cost and tolerated more uncertainty

A linear mixed-effects model examined the effects of group, initial reward, and sampling cost on the number of samples taken prior to decision-making. The model revealed a significant main effect of sampling cost, with participants taking fewer samples when sampling cost was high ($\beta = -3.14$, SE = 0.60, $t_{2922} = -5.19$, $p < 0.0001$; **Figure 5–9a**), indicating robust cost-sensitive adjustments in information gathering. There was no main effect of initial reward ($\beta = 0.11$, SE = 0.41, $t_{2922} = 0.28$, $p = 0.78$). The model also revealed a significant effect of group driven by the MFL group. Relative to healthy controls, MFL participants took fewer samples overall ($\beta = -2.45$, SE = 1.19, $t_{2922} = -2.05$, $p = 0.040$), whereas LC participants did not differ significantly from controls ($\beta = -0.95$, SE = 1.35, $t_{2922} = -0.71$, $p = 0.48$). A direct contrast between the two lesion groups was not significant ($\beta = -1.50$, SE = 1.61, $t_{2922} = -0.93$, $p = 0.35$). Importantly, a significant Sampling Cost × Group interaction was observed for the MFL group ($\beta = 1.84$, SE = 0.83, $t_{2922} = 2.22$, $p = 0.026$), indicating reduced cost sensitivity relative to healthy controls, such that MFL participants decreased their sampling less under high-cost conditions. No other interaction terms reached significance (all $p > 0.26$). Exploratory post hoc comparisons were consistent with this pattern, showing group differences under low-

cost conditions, although these effects did not survive Bonferroni correction (all p_corr ≥ 0.16). Together, these findings indicate that while all participants adjusted sampling behaviour in response to cost, MFL participants sampled less overall and showed modestly reduced cost sensitivity, reflecting subtle group-specific differences in information-gathering strategy.

A separate linear mixed-effects model examined deviation from Bayes-optimal sampling. The model revealed a significant main effect of sampling cost ($\beta = 3.87$, SE = 0.55, $t_{2922} = 7.02$, $p < 0.0001$; **Figure 5–9b**), indicating strong cost-dependent deviations from the Bayesian ideal observer (***Equation 1***). Relative to the optimal policy, participants under-sampled in low-cost conditions (mean deviation = −1.71 ± 0.13) and over-sampled in high-cost conditions (mean deviation = 2.57 ± 0.09), demonstrating a systematic directional bias in sampling behaviour. In contrast, there was no main effect of initial reward ($\beta = 0.02$, SE = 0.42, $t_{2922} = 0.05$, $p = 0.96$) and no main effect of group (group 2: $\beta = -1.38$, SE = 1.28, $t_{2922} = -1.08$, $p = 0.28$; group 3: $\beta = -1.97$, SE = 1.45, $t_{2922} = -1.35$, $p = 0.18$). A direct contrast between the two lesion groups revealed no significant difference in deviation from Bayes-optimal sampling ($\beta = 0.58$, SE = 1.73, $t_{2922} = 0.34$, $p = 0.74$). No interaction terms reached significance (all $p > 0.16$), indicating that the effect of sampling cost on deviation from optimal sampling was comparable across groups. Bonferroni-corrected post hoc comparisons supported this conclusion, revealing no reliable group differences in deviation from Bayes-optimal sampling in either cost condition (all p_corr = 1). Together, these results indicate that deviations from optimal sampling were strongly cost-sensitive but not group-dependent, with a consistent pattern of under-sampling when sampling was inexpensive and over-sampling when sampling was costly.

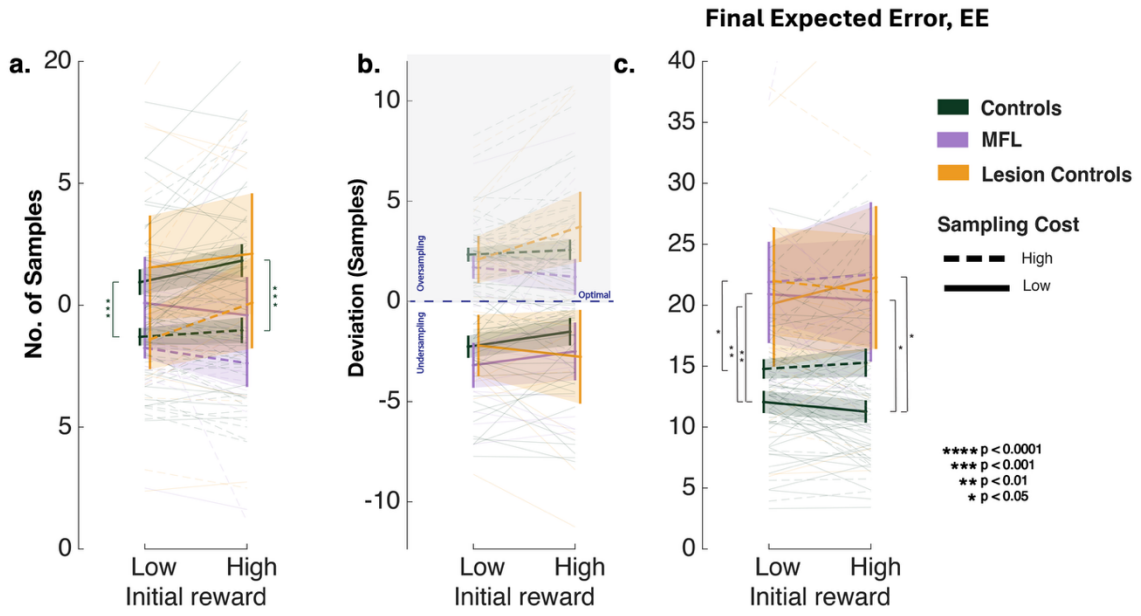

Figure 5-9. Sampling behaviour of participants. (a) HC and LC increased the number of samples they collected significantly more than MFL patients when sampling cost decreased. **(b)** All participant groups oversampled in the high sampling cost condition and undersampled in the low sampling cost condition when compared to the Bayes-optimal sampler. **(c)** HC reduced uncertainty (the expected error) significantly more than both lesion groups before placing the blue circle.

A linear mixed-effects model examined the effects of group and sampling cost on uncertainty reduction. The model revealed a significant main effect of sampling cost, with participants tolerating greater residual uncertainty after sampling when sampling cost was high ($\beta = 3.18$, $SE = 0.80$, $t_{2922} = 3.96$, $p < 0.001$; **Figure 5–9c**), indicating increased uncertainty tolerance when information was more expensive to obtain. There was also a significant main effect of group, indicating overall differences in uncertainty tolerance between groups. Relative to healthy controls, both lesion groups exhibited significantly greater uncertainty tolerance (group 2/MFL: $\beta = 8.43$, $SE = 2.78$, $t_{2922} = 3.04$, $p = 0.002$; group 3/LC: $\beta = 10.96$, $SE = 3.14$, $t_{2922} = 3.49$, $p < 0.001$). A direct contrast between the two lesion groups was not significant ($\beta = -2.53$, $SE = 3.74$, $t_{2922} = -0.68$, $p = 0.50$). A significant Sampling Cost × Group interaction was observed for the LC group ($\beta = -3.49$, $SE = 1.52$, $t_{2922} = -2.30$, $p = 0.022$), indicating that cost-related increases in uncertainty tolerance were attenuated in LC participants relative to healthy controls. No corresponding interaction was

observed for the MFL group ($p = 0.42$), and no other interaction terms reached significance. Bonferroni-corrected post hoc comparisons were consistent with this pattern, confirming reliable group differences under low-cost conditions (all $p_{corr} \leq 0.046$), with weaker effects under high-cost conditions. Together, these findings indicate that higher sampling costs led participants to tolerate greater residual uncertainty after sampling, and that both lesion groups showed elevated uncertainty tolerance overall. This pattern is consistent with a reduced drive to minimize uncertainty through information gathering, with modest modulation of cost sensitivity in the LC group.

5.4.4 MFL patients had lower accuracy and precision compared to HC

A linear mixed-effects model examined factors contributing to localization accuracy, indexed by placement distance from the hidden circle. As expected, localization error increased with greater final expected uncertainty (EE; ***Equation 2***) following sampling, indicating that residual uncertainty at before making a final decision was a primary determinant of accuracy (**Figure 5–10a**). Although lesion groups exhibited greater placement error on average during the active task, these differences coincided with systematic group differences in tolerated uncertainty at decision termination. On average, MFL patients (EE = 21.12 ± 15.96 pixels) and LC participants (EE = 20.64 ± 16.51 pixels) terminated sampling at substantially higher levels of uncertainty than healthy controls (EE = 13.30 ± 7.79 pixels), resulting in greater localization error. No reliable differences were observed between the two lesion groups. To determine whether reduced localization accuracy reflected a general spatial precision deficit rather than task-specific decision processes, a separate analysis examined performance during the training phase (**Figure 5–10b**). Accuracy during training was broadly comparable across groups, with no consistent evidence for lesion-related impairments across uncertainty levels. This suggests that reduced localization accuracy observed during the active task primarily reflects differences

in uncertainty tolerance and sampling termination criteria, rather than impaired spatial precision. Together, these findings indicate that apparent group differences in localization accuracy during active sampling are largely explained by elevated tolerance for residual uncertainty at decision termination in lesion participants, rather than by deficits in perceptual or motor accuracy.

A linear mixed-effects model examined the effects of group, initial reward, and sampling cost on response precision, defined as placement error relative to the optimal location based on each participant's own sampling history. The omnibus test revealed a significant main effect of sampling cost (**Figures 5–11a and 5–11b**), with responses becoming less precise when sampling was costly ($\beta = 2.38$, $SE = 0.54$, $t_{2920} = 4.45$, $p < 0.001$). No significant main effect of initial reward was observed ($p = 0.19$), and no higher-order interactions reached significance.

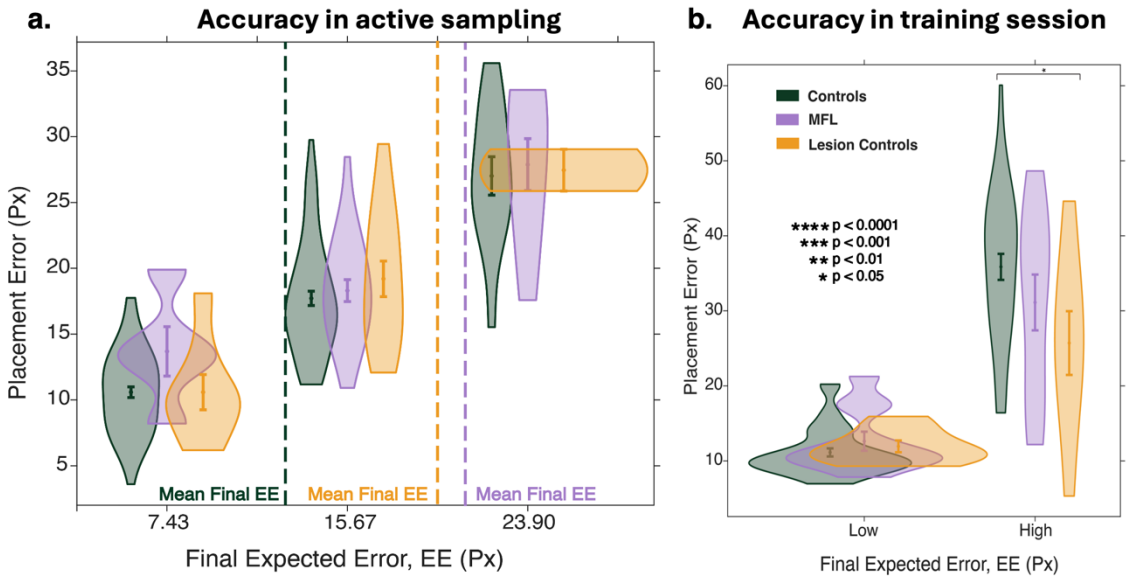

Figure 5-10. Accuracy as a function of expected error. (a) MFL patients placed the blue circle significantly farther from the hidden circle than HC in the active version at lower levels of uncertainty while LC placed the blue circle significantly farther from the hidden circle than HC in the active version at moderate levels of uncertainty. **(b)** In the training session, LC were significantly more accurate at placing the blue circle at high levels of uncertainty than HC and MFL patients.

The omnibus test also revealed a main effect of group, indicating overall differences in response precision. Follow-up comparisons showed that MFL patients were significantly less precise than healthy controls ($\beta = 4.69$, $SE = 1.63$, $t_{2920} = 2.87$, $p = 0.004$), while LC participants

showed a similar but weaker, non-significant trend toward reduced precision (β = 3.06, SE = 1.84, t_{2920} = 1.67, p = 0.096). No reliable differences were observed between the two lesion groups. A significant Sampling Cost × Group interaction for MFL patients (β = −2.06, SE = 0.89, t_{2920} = −2.32, p = 0.020) indicated that group differences were most pronounced under low-cost conditions. Bonferroni-corrected post hoc contrasts confirmed that MFL patients were significantly less precise than healthy controls when sampling cost was low (p_corr = 0.017–0.024), whereas no reliable group differences were observed under high-cost conditions (all p_corr > 0.39). Together, these results indicate that MFL patients exhibit reduced response precision overall, particularly when sampling is inexpensive, whereas healthy controls show greater cost-related degradation in the translation of sampled information into final responses. This pattern suggests differential effects of sampling cost on how sampled information is incorporated into decisions across groups.

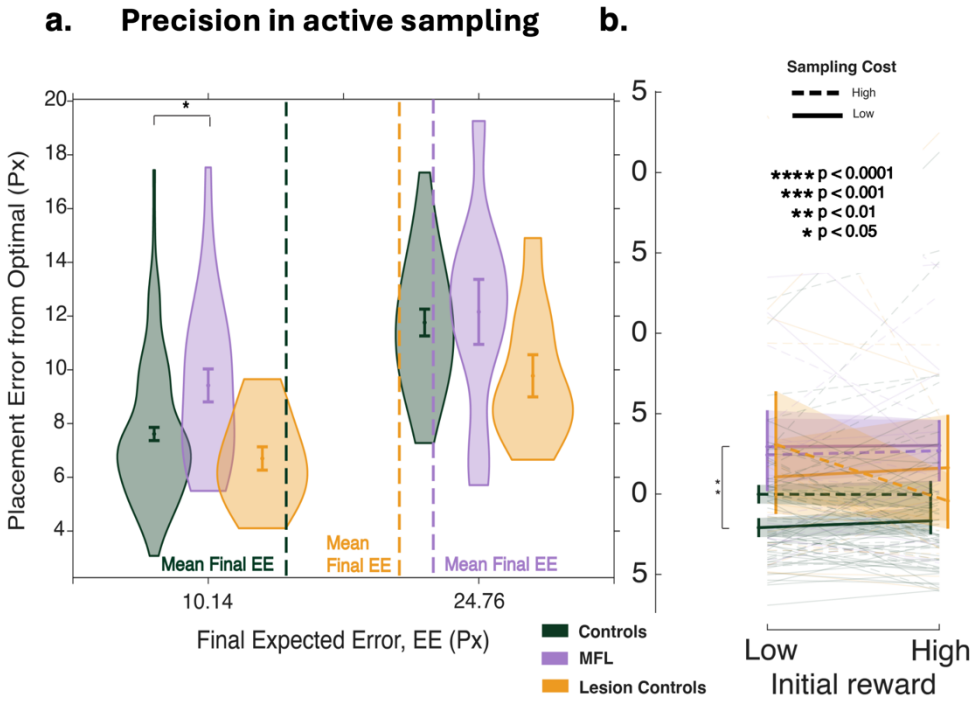

Figure 5-11. Participants' precision of placement (a) MFL patients placed the blue circle at a significantly greater distance from the optimal location defined by their own completed search than both healthy and LC. **(b)** MFL patients were significantly less precise than controls in all four conditions. LC became more precise when both initial reward and sampling cost were high.

5.4.5 Temporal aspects of sampling and placement behaviour

A linear mixed-effects model examined pre-sampling deliberation time, defined as the latency to initiate sampling. The omnibus test revealed a significant main effect of sampling cost, with participants taking longer to begin sampling when sampling was more expensive ($\beta = 0.47$, $SE = 0.10$, $t_{2922} = 4.77$, $p < 0.001$; **Figure 5–12a**), indicating increased initial deliberation under higher informational costs. There were no significant main effects of group (all $p > 0.35$) or initial reward ($p = 0.35$). Significant Sampling Cost × Group interactions were observed for both MFL patients ($\beta = -0.52$, $SE = 0.17$, $t_{2922} = -3.12$, $p = 0.0018$) and LC participants ($\beta = -0.46$, $SE = 0.19$, $t_{2922} = -2.46$, $p = 0.014$), indicating that lesion groups showed attenuated cost-related increases in pre-sampling deliberation relative to healthy controls. Bonferroni-corrected post hoc contrasts confirmed that these group differences were most pronounced under high sampling cost with low initial reward ($p_{corr} = 0.019$), with a weaker, non-significant trend under high-cost, high-reward conditions ($p_{corr} = 0.15$). No differences were observed between the two lesion groups ($p = 0.96$). Together, these results indicate that although higher sampling costs increased deliberation time overall, lesion participants engaged in less preparatory deliberation when information was costly, reflecting reduced adjustment of decision latency in response to rising informational costs.

A separate linear mixed-effects model examined inter-sampling interval (ISI), defined as the time between successive information samples. The omnibus test revealed a significant main effect of sampling cost, with participants waiting longer between samples when sampling was more expensive ($\beta = 0.27$, $SE = 0.04$, $t_{2922} = 7.47$, $p < 0.0001$; **Figure 5–12b**). No significant main effects of initial reward ($p = 0.40$) or group (all $p > 0.30$) were observed. Significant Sampling Cost × Group interactions were observed for both MFL patients ($\beta = -0.18$, $SE = 0.07$, $t_{2922} = -2.51$, $p = 0.012$) and LC participants ($\beta = -0.19$, $SE = 0.08$, $t_{2922} = -2.44$, $p = 0.015$), indicating that both lesion groups exhibited attenuated cost-related increases

in ISI relative to healthy controls. However, Bonferroni-corrected post hoc contrasts did not reveal reliable group differences within individual task conditions (all p_corr > 0.45). No differences were observed between the two lesion groups (p = 0.49). Together, these findings indicate that while participants modulated the temporal spacing of samples in response to cost, lesion groups showed reduced sensitivity to sampling cost, consistent with less adaptive pacing of information gathering.

Finally, a linear mixed-effects model examined placement duration (**Figure 5–12c**). The omnibus test revealed no significant main effects of sampling cost ($\beta = -0.07$, SE = 0.09, $t_{2922} = -0.79$, p = 0.43) or initial reward ($\beta = 0.19$, SE = 0.10, $t_{2922} = 1.92$, p = 0.054). A modest main effect of group was observed, driven by shorter placement durations in MFL patients relative to healthy controls ($\beta = -0.59$, SE = 0.28, $t_{2922} = -2.14$, p = 0.032), whereas LC participants did not differ from controls (p = 0.90), and the two lesion groups did not differ from one another (p = 0.14). No interaction terms reached significance (all p > 0.30). Bonferroni-corrected post hoc contrasts revealed that group differences were present in some high-reward conditions (low-cost/high-reward: p_corr = 0.018; high-cost/high-reward: p_corr = 0.049), but not consistently across task conditions. Together, these findings indicate that placement duration was largely insensitive to sampling cost and reward, with only modest and condition-specific group differences, suggesting that group effects on task performance are unlikely to be driven by systematic differences in the timing of response execution.

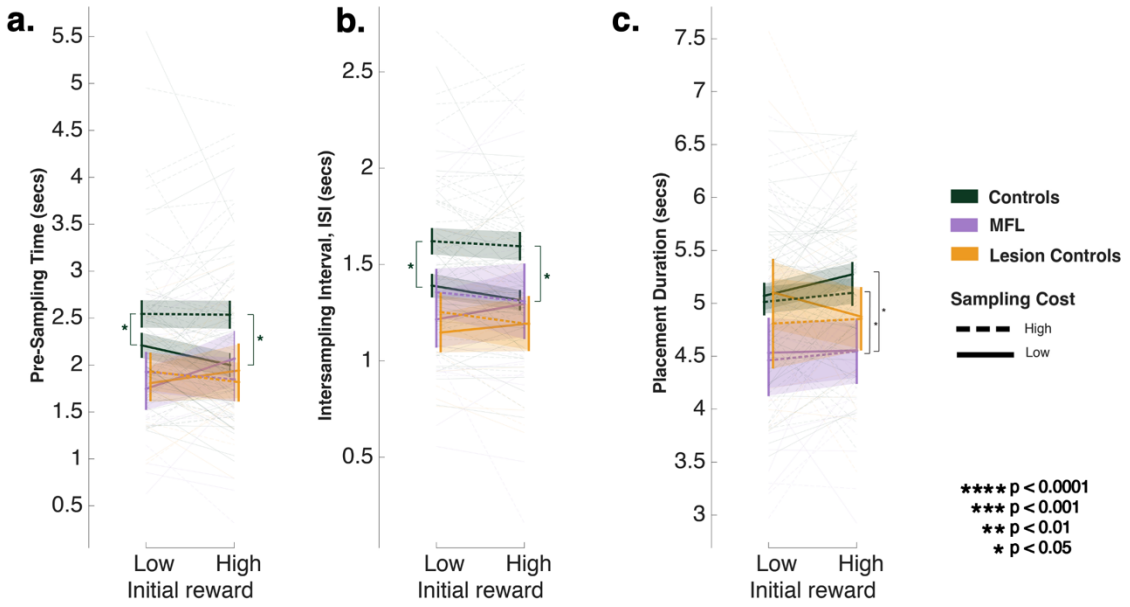

Figure 5-12. Timing-related measures of sampling and response in participants (a) HC began sampling significantly slower when sampling cost was high. **(b)** HC consistently took significantly longer to sample at higher sampling cost. **(c)** MFL patients were quicker at placing the blue circle than both healthy and LC, but not significantly.

5.4.6 Information extraction rate of participants

As reported in the previous section, inter-sampling interval (ISI) did not differ significantly between groups. However, the relationship between ISI and sampling efficiency revealed group-specific patterns. A mixed-effects regression model showed a significant positive association between ISI and sampling efficiency in healthy controls ($\beta = 0.053$, SE = 0.011, $t = 4.99$, $p < 0.0001$; **Figure 5–13a**), indicating that participants extracted more information per sample when sampling more slowly. LC participants exhibited a similar positive relationship ($\beta = 0.045$), which did not differ significantly from healthy controls (ISI × group interaction $p = 0.76$) and reached trend-level significance when tested directly ($p = 0.059$).

In contrast, MFL patients showed no reliable relationship between ISI and sampling efficiency ($\beta = 0.003$, $p = 0.89$). A significant ISI × group interaction ($\beta = -0.051$, $p = 0.026$) indicated that the efficiency benefit of slower sampling observed in healthy controls was significantly attenuated in MFL patients. Direct comparison of ISI slopes between the two lesion groups did not reach significance ($p = 0.17$).A linear mixed-effects model examining

sampling efficiency revealed no robust main effects of initial reward, sampling cost, or group, and no interactions involving sampling cost. A modest Initial Reward × Group interaction was observed for MFL participants; however, Bonferroni-corrected post hoc contrasts did not reveal reliable group differences within any task condition. Together, these results indicate that sampling efficiency was broadly stable across task conditions, but that MFL patients failed to benefit from slower sampling, suggesting a disruption in the effective use of additional deliberation time rather than a generalized inefficiency.

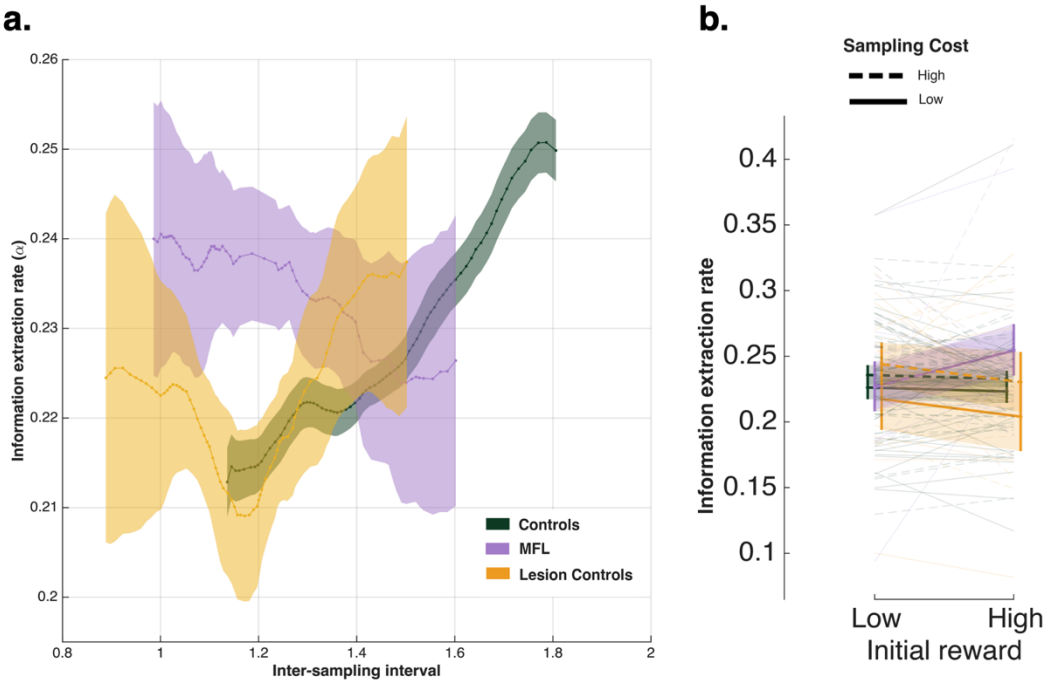

Figure 5-13. Relationship between information extraction and inter-sampling interval (a) MFL patients and LC gathered samples significantly faster than HC but while LC became more efficient as they slowed down, MFL patients became less efficient took longer to place samples. **(b)** MFL patients reached greater levels of efficiency than both healthy and LC.

5.4.7 Participants' cognition predicts their performance on the CQ task active version

Correlations were performed between the behavioural measures from the active version of the CQ task, participant clinical scores (ACE-II, AMI, BDI-II, BIS-II and HADS) and patient lesion volumes. Across participants, ACE scores were significantly associated with both task final reward earnings and final uncertainty before they committed themselves to a decision.

Participants with higher ACE scores earned significantly greater rewards on the task ($R^2 = 0.47$, $p < 0.001$, FDR-adjusted $p < 0.001$; **Figure 5-14a**). ACE scores were also associated with reduced final uncertainty, such that patients with higher cognitive scores tolerated less uncertainty before placing the blue disk ($R^2 = 0.41$, $p < 0.001$, FDR-adjusted $p < 0.001$; **Figure 5-14b**). Additionally, HCs who had higher HADS-anxiety scores tolerated less uncertainty before making a final decision about where the hidden circle was located ($R^2 = 0.35$, $p < 0.001$, FDR-adjusted $p < 0.001$; **Figure 5-15**). No other significant relationships were observed

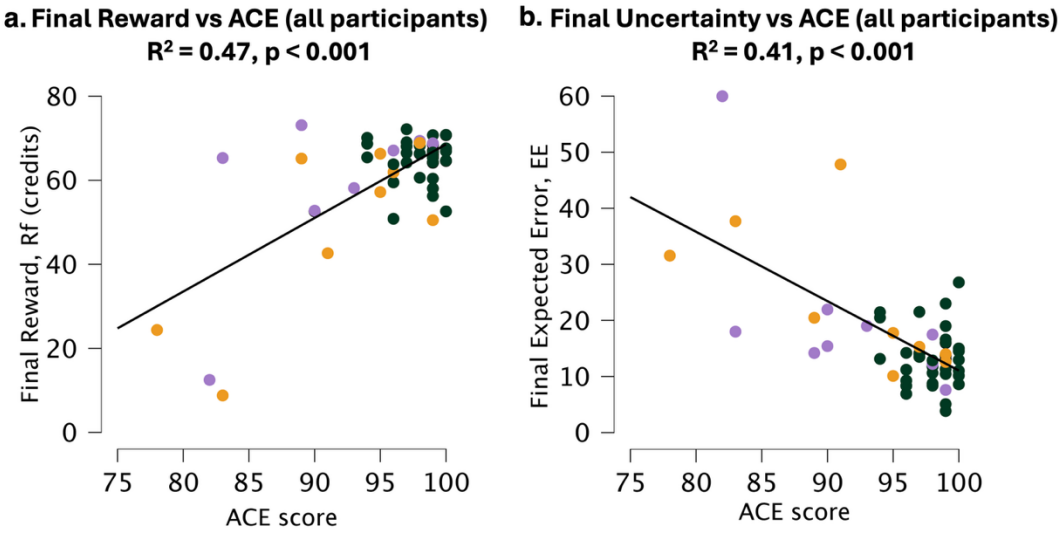

Figure 5-14. Participants' ACE scores predicts their performance on the active version (a) Participants with higher cognition (ACE) scores earned more reward than those with lower cognition scores. **(b)** Participants with higher cognition (ACE) scores tolerated less uncertainty before placing the blue circle, i.e. committing to a final decision.

between behavioural and clinical measures, nor between behavioural measures and lesion volume. These findings indicate that across participants, cognitive ability, as assessed by the ACE, but not self-reported mood, or impulsivity, is selectively linked to maximizing reward and to uncertainty tolerance while anxiety symptoms in HCs is also linked to uncertainty tolerance.

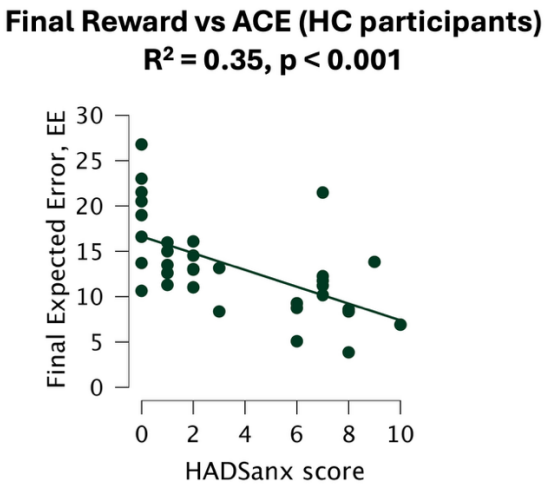

Figure 5-15. Healthy controls' HADS-anxiety scores predict their performance on the CQ active version HC with higher anxiety scores (HADS-anx) tolerated less uncertainty before placing the blue circle i.e. committing to a final decision.

Similar correlations were conducted for the behavioural measures from the passive version of the CQ task and the participants' clinical variables and lesion data. In this case, no significant associations survived correction for multiple comparisons (all FDR-adjusted ps > 0.05;).

5.4.8 MFL patients were less sensitive to uncertainty and reward than HC

A linear mixed-effects model examined participants' ability to rate uncertainty on the passive task. Omnibus tests revealed significant main effects of group and objective uncertainty (EDbin), as well as a significant Group × Uncertainty interaction, indicating that the relationship between objective and subjective uncertainty differed across groups (**Figure 5–16a**). Follow-up slope comparisons showed that healthy controls exhibited a steeper relationship between objective and subjective uncertainty (β = 0.80) than both MFL patients (β = 0.46; HC vs MFL: p = 0.003) and LC participants (β = 0.46; HC vs LC: p = 0.008). The two lesion groups did not differ from one another in slope (p = 0.99), indicating a comparable reduction in sensitivity to changes in uncertainty. Intercept comparisons revealed that LC participants provided significantly lower absolute uncertainty ratings than both healthy controls

($p < 0.0001$) and MFL patients ($p < 0.0001$), while the difference between healthy controls and MFL patients did not reach significance ($p = 0.065$). Together, these findings indicate that although all groups tracked uncertainty in the expected direction, both lesion groups showed reduced sensitivity to objective uncertainty, and LC participants additionally exhibited a pronounced downward shift in overall uncertainty ratings.

Separate mixed-effects models examined offer acceptance as a function of uncertainty and reward. In the uncertainty model, acceptance decreased as uncertainty increased across all groups; however, the magnitude of this effect differed by group (**Figure 5–16b**). Healthy controls exhibited the steepest negative slope ($\beta = -0.012$), indicating the strongest uncertainty aversion, whereas both MFL ($\beta = -0.006$) and LC participants ($\beta = -0.007$) showed significantly attenuated uncertainty sensitivity relative to controls (both $p < 0.001$). The two lesion groups did not differ from one another ($p = 0.45$), indicating a comparable reduction in uncertainty aversion. In the reward model, higher reward increased the likelihood of accepting an offer overall (**Figure 5–16c**); however, this effect was markedly weaker for MFL patients ($\beta = 0.00038$) than for both healthy controls ($\beta = 0.00267$; $p = 0.00066$) and LC participants ($\beta = 0.00325$; $p = 0.00185$), who did not differ from each other ($p = 0.44$). Together, these results indicate that while both lesion groups exhibited reduced sensitivity to uncertainty during choice, reduced reward sensitivity was selective to MFL patients, suggesting partially dissociable alterations in valuation processes across patient groups.

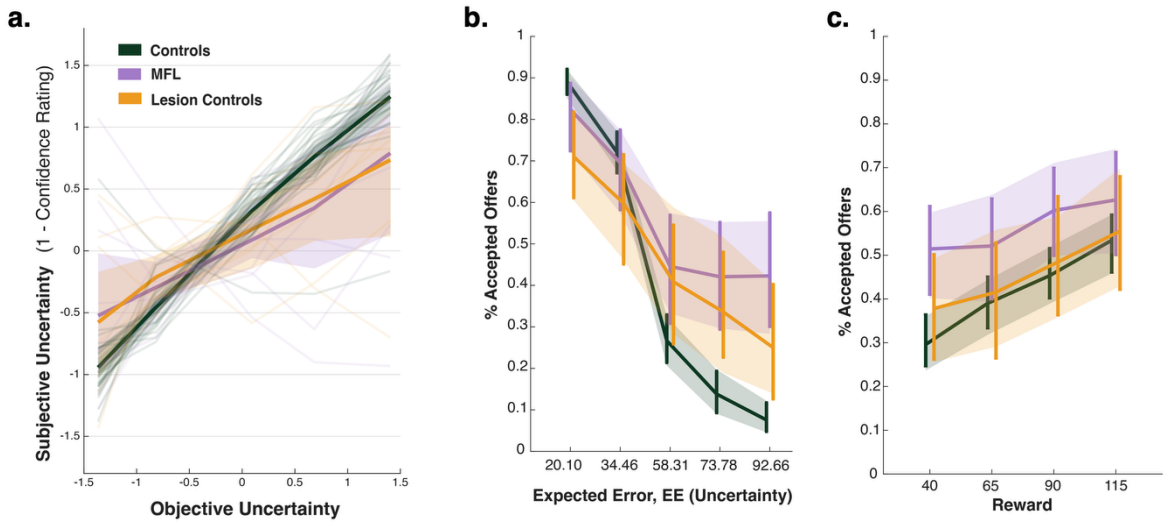

Figure 5-16. Lesion groups had reduced sensitivity to uncertainty and reward than HC (a) MFL patients and LC demonstrated impaired ability to perceive uncertainty compared to HC in the passive version. **(b)** MFL patients and LC accepted significantly more offers at higher levels of uncertainty (expected error) than HC. **(c)** MFL patients and LC did not alter their offer acceptance in the same way as HC, who accepted significantly more offers as reward increased.

5.5 Discussion

This chapter's findings extend current understanding of the MFL's contribution to uncertainty-guided behaviour, reward evaluation, and adaptive sampling. Lesion analysis revealed that though both patient groups had focal damage in distinct brain regions (**Figure 5-4**), they were comparable in regard to the extent of this damage (**Figure 5-3**). Results from the CQ task demonstrate that lesions to the MFL impair both active and passive forms of decision-making, particularly in contexts that require balancing information gain against cost and uncertainty. MFL patients sampled less frequently (**Figure 5-9a**), earned fewer credits (**Figure 5-8a**), and displayed reduced sensitivity to sampling cost (**Figure 5-8b**), indicating an alteration in the cost–benefit computations that normally support efficient information gathering in healthy people. This pattern suggests that the MFL might normally play a critical role in evaluating the expected value of sampling and adjusting behaviour accordingly. Disruption to this part of the brain could lead to maladaptive decision-making in uncertain environments as will be discussed further.

In the active sampling version, both lesion groups showed impairments relative to HC, but the nature of these impairments differed. While LC also tolerated greater uncertainty (**Figure 5-9c**), MFL patients were more strongly characterised by insensitivity to cost and a diminished ability to adjust sampling behaviour based on task demands. The attenuated increase in presampling time (**Figure 5-12a**) and intersampling intervals (**Figure 5-12b**) observed in the MFL group when sampling became more expensive suggests a failure to integrate internal estimates of cognitive effort or opportunity cost into decision-making. Rather than strategically modulating their behaviour, these patients appeared to show reduced strategic modulation of deliberation in response to rising information costs. Lesion volume did not appear to predict patients' behaviour but across all participants, higher cognition predicted larger winnings (**Figure 5-14a**)and reduced uncertainty tolerance (**Figure 5-14b**) before making a final decision while anxiety scores in HCs also predicted uncertainty tolerance (**Figure 5-15**).

MFL participants did not show the efficiency gains associated with slower sampling observed in healthy controls (**Figure 5-13a**), indicating a disruption in the adaptive relationship between sampling pace and information extraction. This dissociation between altered sampling behaviour and reduced sensitivity to cost and uncertainty is consistent with lesion evidence showing that medial frontal damage, particularly to the vmPFC, impairs the integration of cost, effort, and reward signals during decision-making (Bechara et al., 2000; Clark et al., 2008; S. G. Manohar & Husain, 2016). These findings align with the broader functional role of medial frontal regions, including the dorsal ACC and pre-SMA, in monitoring action–outcome relationships, regulating exploratory versus exploitative behaviour, and guiding adaptive information sampling. (Kaanders et al., 2021; Kennerley & Walton, 2011b; Kolling et al., 2012).

The observation that LC also tolerated higher uncertainty suggests that tolerance of uncertainty is not uniquely dependent on MFL integrity but may also reflect the contribution of broader – potentially fronto-parietal – networks involved in belief updating and probabilistic reasoning (Huettel et al., 2005; Volz et al., 2003). Huettel et al. (2005) posited that the dorsal prefrontal and posterior parietal brain regions are essential for resolving uncertainty that arises over short time scales as information is accumulated toward a decision. Moreover, several of the LC had damage to the right hemisphere of the brain which has previously been implicated in the processing of spatial information and stimulus on visual tasks (Bartolomeo, 2006; Corbetta & Shulman, 2002). As such, their inability to reduce uncertainty on a task that relies on dot placement and target localization may be related to spatial impairment, although we did not formally test this here.

In the passive choice version, MFL patients demonstrated reduced sensitivity to both reward offer (**Figure 5-16c**) and uncertainty (**Figure 5-16b**), whereas LC participants showed reduced sensitivity to uncertainty but preserved reward sensitivity. This pattern suggests a partial dissociation between reward valuation and uncertainty monitoring, with uncertainty sensitivity disrupted across lesion groups and reward valuation selectively impaired following MFL damage. The reduced responsiveness to reward outcomes in the MFL group mirrors findings from ventromedial prefrontal and orbitofrontal lesion studies showing attenuated value-based modulation of choice behaviour (Bechara et al., 1994; Clark et al., 2008). Together, these results imply that MFL integrity is essential not only for evaluating uncertain outcomes but also for using reward information to guide future behaviour.

This study has several limitations. First, the patient sample sizes were relatively small, though this is consistent with previous lesion research, as recruitment is constrained by the need for focal damage to a specific brain region and the difficulty of engaging suitable patients. Second, I identified brain regions by overlaying patient lesion masks onto the Harvard–Oxford

cortical atlas rather than using data from locally recruited HC. This approach assumes that the atlas accurately represents the anatomical boundaries of the participants' brains, despite individual variability. Additionally, the atlas provides a relatively coarse parcellation, which limits the ability to examine lesions at a fine-grained, subregional level. Nevertheless, the Harvard–Oxford atlas is a well-validated, population-based reference that allows consistent and reproducible mapping of lesions for structural and connectivity analyses.

5.6 Conclusion

On a relatively new test of decision-making, MFL patients exhibited reduced information sampling, insensitivity to sampling cost, and diminished sensitivity to reward and uncertainty. These deficits cannot be explained solely by the general effects of brain injury, LC showed a more selective pattern of impairment, characterised primarily by increased tolerance for uncertainty and reduced sensitivity to uncertainty during choice, while reward sensitivity remained intact. Together, these findings highlight the medial frontal cortex as a key region for integrating cost, reward, and uncertainty into a unified control signal that supports adaptive, goal-directed behaviour. By combining lesion evidence with the dynamic decision framework of the CQ task, the present study provides causal validation for models derived from functional neuroimaging and advances understanding of the specific computations mediated by the MFL during human decision-making.

6| General Discussion

In this thesis, I have attempted to investigate how humans reduce uncertainty in decision-making and how this capacity is disrupted by brain pathology. Specifically, I tested the hypothesis that WM pathology in SVD and MFL lesions lead to significant effects on decision-making under uncertainty. The findings from Chapters 2 and 3 confirm that widespread WM network disruption is associated with deficits in this domain, with common behavioural features including reduced sensitivity to cost, reward, and uncertainty across both versions of the CQ task. Chapter 4 shows that the introduction of physical effort in the passive CQ task can restore sensitivity to reward and uncertainty, suggesting that motivational engagement may be influenced by task demands. Finally, building on existing research, I extended the CQ paradigm to patients with MFL lesions and found similar patterns of impairment to those found in SVD. In the following pages, I present a summary of each chapter's main findings **(Table 6-1)**, followed by a discussion of their clinical and scientific implications, and propose directions for future research.

6.1 Summary of Experimental findings

6.1.1 Neuroimaging biomarkers of SVD

In Chapter 2, neuroimaging data from healthy controls and SVD patients was analysed to determine whether structural and diffusion parameters differed between the two cohorts. I hypothesized that the patient cohort would present with significantly greater WM damage than controls, providing a representative sample for the study of behavioural effects related to SVD pathology. This pattern was observed, as the SVD group showed a higher average total WMH burden than the control group, who exhibited the expected age-related degree of WMH volume (**Figure 2-3**). These results were further examined in relation to demographic

and clinical measures, including age, years of education, cognition, apathy, anxiety, depression, and impulsivity. In the control group, age, cognition, apathy, and depression were significant predictors of WMH volume, although this was not the case for the SVD group (**Figure 2-5**).

Further analyses of WM microstructure corroborated the finding that the SVD cohort exhibited significantly greater damage. TBSS analysis was conducted using two diffusion-modelling approaches, i.e. DTI and NODDI. The results indicated a widespread reduction in WM integrity across all DTI and NODDI metrics (**Figures 2-6 & 2-7**). Specifically, patients generally showed lower FA and NDI, higher MD and ISOVF, and variable ODI. Cognition and years of education were positively associated with greater WM microstructural integrity (**Figures 2-13 & 2-14 & 2-15 & 2-16**), whereas age, apathy, depression, and impulsivity were positively associated with reduced WM microstructural integrity (**Figures 2-17 & 2-18 & 2-19 & 2-20 & 2-21 & 2-22 & 2-23 & 2-24 & 2-25 & 2-26 & 2-27**).

Taken together, the findings in this chapter support the view that SVD is associated with widespread structural damage to the brain through disruption of WM connections. The impact of SVD on WM integrity appears to extend beyond the characteristic abnormalities detectable on conventional MRI, suggesting that degeneration in affected tracts may begin long before it becomes visible on neuroimaging, as also suggested by other researchers (Barker et al., 2013; Duering et al., 2018; Hu et al., 2022; Mayer et al., 2022; McAleese et al., 2017; Silbert et al., 2021; Tuladhar et al., 2015).

6.1.2 Insights into normative decision-making under uncertainty

Our healthy controls exhibited robust and adaptive decision-making, consistently adjusting their behaviour in response to cost, reward, and uncertainty across all versions of the CQ task. They sampled more when uncertainty was higher, moderated their choices according to

potential rewards, and showed sensitivity to sampling costs, indicating a sophisticated integration of multiple decision parameters. This pattern closely aligns with previous findings in healthy populations performing classic decision-making paradigms, such as the Dart Task (Juni et al., 2016), the Cambridge Gambling Task (Clark et al., 2003, 2008), the Iowa Gambling Task (Bechara et al., 2000), and other probabilistic reward tasks (Rogers, Everitt, et al., 1999; Weller et al., 2007), where healthy controls consistently demonstrated sensitivity to cost, uncertainty, reward contingencies, and future outcomes. These comparisons suggest that the CQ task effectively captures normative decision-making processes and that our control cohort behaves in a manner consistent with established baselines in the literature. In short, the HC group reliably shows strategic, uncertainty-sensitive behaviour, providing a strong benchmark against which to interpret deviations in patient groups.

In our EBDM condition of CQ, the control group displayed effort discounting, accepting fewer offers as physical effort increased, consistent with previous research showing that effort generally functions as a cost in decision-making (Chong et al., 2017a; Kool et al., 2010; Kurniawan et al., 2013; Prévost et al., 2010; Westbrook et al., 2013). Interestingly, when examining offer acceptance as a function of reward and uncertainty, healthy controls accepted more offers at comparable levels of reward and uncertainty under the effort condition. This suggests that effort did not uniformly devalue options but interacted with value computation in a more complex way, effectively shifting the decision curve upward. Such a pattern aligns with the broader "effort paradox" literature, which posits that while effort can act as a cost, it can also enhance subjective valuation under certain contexts, for example by increasing perceived task meaningfulness or motivational engagement (Inzlicht et al., 2018; M. Zhang & Zheng, 2022). These findings indicate that healthy participants are not only sensitive to cost, reward, and uncertainty but also capable of flexible, context-dependent

valuation, highlighting the dynamic nature of decision-making processes even under additional task demands.

6.1.3 Impact of SVD on decision-making under uncertainty

Previously, SVD has primarily been associated with executive and psychomotor dysfunction (Jochems et al., 2025; S. Wang et al., 2022). In Chapter 3, I investigated how a disorder like SVD might affect human-decision making under uncertainty using the relatively novel CQ task. This paradigm has been developed to examine how people sample information prior to making a decision (Petitet et al., 2021). The results from the active version of the task demonstrated that patients spent less time sampling (**Figure 3-3b**), were less sensitive to sampling cost (**Figure 3-4a**), tolerated more uncertainty before they committed themselves to a decision (**Figure 3-4c**) and overall had reduced placement accuracy and precision when localizing the hidden circle (**Figures 3-5a & 3-6**) when compared to age-matched HC. Within the SVD group, higher cognitive scores predicted larger earnings and improved precision. Across all participants, it was shown that WMH burden was negatively correlated with reward earnings but positively correlated with uncertainty tolerance and precision (**Figure 3-11**). At the microstructural level, reduced WM integrity was linked to lower reward earnings (**Figure 3-12a**), fewer samples obtained prior to making a decision (**Figure 3-13a**), reduced sampling efficiency (**Figure 3-13b**) and precision (**Figure 3-12b**).

On the passive version of the CQ task, SVD participants exhibited reduced sensitivity to uncertainty (**Figures 3-10a & 3-10b**) and reward (**Figure 3-10c**). They demonstrated riskier behaviour by accepting more offers at higher levels of uncertainty, though this was not shown to correlate with impulsivity as measured by the BIS-II. However, WM microstructural damage did positively correlate with increased offer acceptance (**Figure 3-14b**) in addition to a reduction in capacity to perceive uncertainty (**Figure 3-14a**).

Taken together, Chapters 2 and 3 build a strong case that functional impairments in decision-making under uncertainty may arise from WM structural damage. Behaviourally, this can manifest as a tendency toward riskier choices, potentially driven by reduced sensitivity to cost, reward, and uncertainty. Furthermore, these poorer behavioural outcomes emerge in both active sampling contexts and passive decision-making tasks. Finally, greater WM macrostructural and microstructural damage predicted worse performance across these domains, suggesting that SVD may produce cognitive deficits that extend beyond impairments in executive functioning and processing speed.

6.1.4 Impact of SVD on EBDM under uncertainty

Chapter 4 extends the findings of the previous chapter by investigating how adding in a decision variable involving physical effort modulates decision-making on the passive version of the CQ task. Both groups were sensitive to the physical effort demands and responded to it appropriately. Effort was shown to increase offer acceptance in control participants (**Figures 4-4c & 4-4d**) and increase sensitivity to reward (**Figure 4-4a**) and uncertainty (**Figure 4-4b**) in SVD patients, whose behaviour became more closely aligned with that of controls on this version of the passive CQ task. Unlike the previous chapter, where increased offer acceptance was shown to positively correlate with reduced integrity in WM tracts, this behaviour was linked to increased integrity.

Taken together, these chapters provide evidence for partial disruption of decision-making under uncertainty arising from WM disruption. The findings from this chapter indicate that previously observed impairments in decision-making under uncertainty can be partially ameliorated by altering task demands, for example by introducing a variable such as physical effort. This suggests that while performance can improve under certain conditions,

the extent to which function can be fully restored appears promising but requires further investigation.

6.1.5 Impact of MFL on decision-making under uncertainty

It has been well established in the literature that patients with lesions in the MFL demonstrate impairments on traditional decision-making paradigms (Bechara, 1994; Bechara et al., 2000; Clark et al., 2003a; Clark & Manes, 2004; Manes et al., 2002). In Chapter 5, I employed the CQ task in this patient cohort alongside LC (lesion control patients with damage in brain regions outside the MFL) and HC. The results from the active version of the task demonstrated that MFL patients spent less time sampling (**Figure 5-8b**), collected fewer samples (**Figure 5-9a**), showed reduced modulation of sampling behaviour by cost (**Figure 5-9a**), tolerated more uncertainty (**Figure 5-9c**) and overall had reduced placement accuracy and precision when localizing the hidden circle (**Figures 5-10 & 5-11**) when compared to age-matched HC. LC patients had a similar behaviour profile except the number of samples they collected did not differ significantly from HC and their sensitivity to sampling cost was less disrupted than in MFL patients (**Figure 5-9a**). Crucially, while both LC and HC participants were shown to improve their sampling efficiency when they sampled slower, MFL patients failed to show the efficiency gains associated with slower sampling that were observed in controls, indicating a disrupted relationship between sampling pace and information extraction (**Figure 5-13a**).

On the passive version of the task, both MFL and LC patients demonstrated reduced sensitivity to uncertainty compared to HC (**Figures 5-16a & 5-16b**) with no reliable difference between the two lesion groups. Both lesion groups also exhibited riskier behaviour by accepting more offers at higher levels of uncertainty. However, a reduced sensitivity to reward was only observed in the MFL group (**Figure 5-16c**).

Taken together, this chapter reinforces the idea that lesions to the MFL lead to impairments in decision-making. Specifically, MFL patients showed reduced evidence accumulation on the active sampling task and riskier behaviour on the passive version of the task. Although both MFL and LC groups appeared impaired on each version of the CQ task, MFL dysfunction seemed characterised by an additional insensitivity to reward and a more pronounced disruption in cost-related modulation of behaviour. This pattern highlights the selective contribution of the MFL to integrating reward and cost signals during decision-making, beyond the broader uncertainty-related impairments shared with LC patients.

6.2 Brain pathology and decision-making under uncertainty

The findings presented in this thesis lend some support to the view that damage to the WM tracts may be sufficient to produce decision-making impairments which typically have been associated with focal cortical lesions. Lesions to the vmPFC, a core region within the MFL, have been consistently linked to broadly suboptimal decision-making across numerous studies. Early work by Bechara and colleagues (Bechara, 1994; Bechara et al., 2000) demonstrated that patients with bilateral vmPFC damage favoured immediate gains over long-term outcomes. Subsequent research confirmed that lesions to the MFL and other prefrontal regions impair adaptive decision-making (Clark et al., 2003b, 2008; Clark & Manes, 2004; Fellows & Farah, 2005; Levens et al., 2014; Manes et al., 2002; Pujara et al., 2015; Studer et al., 2015; Weller et al., 2007), while damage outside the vmPFC does not reliably produce comparable deficits (Rogers, Everitt, et al., 1999). Collectively, these findings indicate that the MFL is critical for integrating affective and cognitive information to guide adaptive choices.

However, these behavioural deficits may arise not only from cortical damage but also from disruption of the WM connections that support distributed prefrontal networks. Studies

in CADASIL, a genetic form of SVD, demonstrate that WM lesions in frontal tracts, including the anterior thalamic radiation and the forceps minor, predict impairments in processing speed and executive function even when controlling for GM atrophy (Duering et al., 2011). Similarly, in healthyageing, increased frontal WM hyperintensities correlate with poorer performance on set-shifting and response inhibition tasks (Boutzoukas et al., 2021). Lesion studies following traumatic brain injury in children further indicate that discrete frontal WM damage can produce deficits in executive function and everyday decision-making, even in the absence of major cortical lesions (Lipszyc et al., 2014). These data support a "disconnection" hypothesis, i.e. lesions to WM tracts, such as those in the MFL, can impair decision-making by disrupting communication between prefrontal and subcortical nodes, even when the cortical regions themselves are intact.

Our results extend this framework by demonstrating how both MFL lesions and WM specific damage manifest in decision-making under uncertainty. In our CQ task, MFL patients showed reduced evidence accumulation during active sampling, collected fewer samples, showed reduced modulation of sampling behaviour by cost, tolerated more uncertainty, and exhibited poorer placement accuracy and precision. LC patients displayed some overlap in uncertainty detection impairments and showed relatively preserved—but attenuated—sensitivity to sampling cost, with weaker efficiency gains compared to healthy controls. SVD patients, whose pathology primarily affects WM, exhibited broad impairments across the active and passive versions of the CQ task, including reduced sampling time, impaired sensitivity to both uncertainty and reward, and riskier choices. Moreover, task performance in the SVD group correlated strongly with WM macro- and microstructural integrity. These findings indicate that while MFL lesions disrupt valuation processes and contribute to uncertainty-guided impairments in decision-making, WM damage can similarly

produce pervasive network-level deficits that compromise multiple components of adaptive choice behaviour.

Together, these findings highlight the complementary roles of cortical regions and WM connectivity in supporting adaptive decision-making. Lesions to the MFL compromise valuation processes and contribute to impairments in uncertainty-guided decision-making, impairing the ability to integrate affective and cognitive information during choice. Disruption of WM pathways, as observed in SVD, can likewise lead to broader network-level deficits, affecting multiple aspects of decision-making, including sampling time, valuation, and uncertainty detection. This convergence supports a network-based view in which impairments may arise not only from focal cortical damage but also from disconnection across distributed prefrontal, parietal and subcortical circuits. Functionally, these results underscore the importance of structural integrity across the MFL and its connections, demonstrating that both node-specific lesions and network disruption can compromise adaptive decision-making under uncertainty. The findings presented in this thesis suggest that some deficits traditionally attributed to cortical lesions may in part reflect impaired connectivity, emphasizing the critical role of WM pathways in supporting the computational processes underlying effective choice behaviour.

6.3 Contextual Restoration of Impaired Decision Processes

When physical effort was added as an additional variable in the passive version of the CQ task, patients in our SVD cohort showed a partial restoration of adaptive decision behaviour. Specifically, they became more sensitive to both reward and uncertainty resulting in their responses being closely aligned with those of healthy controls, in contrast to their baseline performance where WM pathology predicted poorer performance. This suggests that white-matter disruption associated with SVD does not invariably produce a fixed, irreversible

deficit. Rather, under altered task demands or motivational contexts, residual functional capacity can be unmasked, producing more adaptive decision patterns.

Neuroimaging studies in healthy people highlight that cognitive flexibility (the ability to adjust behaviour across different contexts) depends on the alignment between functional activity and the underlying WM network architecture, underscoring the importance of structural connectivity even when cortical nodes are intact (Medaglia et al., 2016). In the case of vascular pathology, there is growing recognition that functional networks may reorganize, or that alternative pathways may partially compensate for disrupted WM connectivity (Schulz et al., 2021). This observation aligns with emerging evidence that the human brain retains a degree of flexibility or resilience after structural changes (DeJong et al., 2023; Tang et al., 2025).

By contrast, lesion studies focusing on MFL/vmPFC damage have rarely demonstrated robust, context-driven "restoration" of decision-making across a broad range of paradigms. The study by Manohar et al. (2021) is perhaps one of the clearest demonstration of context-dependent improvement in MFL lesion patients. This lesion study of medial prefrontal cortex damage included a rare patient with bilateral vmPFC lesions who showed reduced decision biases and often made more "rational" betting decisions compared to controls. The authors themselves note that this does not amount to a wholesale recovery of normal decision-making. Instead, this kind of performance might effectively be the 'impairment' (alteration from normal behaviour) that arose in this patient from bilateral MFL damage. Moreover, other work with vmPFC lesions continues to report persistent deficits in value integration, evaluation, reward/effort discounting, and social or moral decision-making (Lockwood et al., 2024). In short, while structural damage to cortical nodes may sometimes yield paradoxically "cleaner" or less biased behaviour under constrained or simplified task

conditions, there is little systematic evidence that shifting task parameters reliably restores adaptive decision-making to control levels.

Taken together, the SVD patients' behavioural results on the EBDM condition of the CQ task suggest that damage to WM networks may leave a latent capacity for adaptive decision-making that can be revealed under appropriate contextual or motivational conditions. In contrast, damage to cortical valuation hubs such as the MFL appears less amenable to such restoration, at least based on the current lesion literature. This distinction underscores the importance of considering network-level integrity and plasticity, not just focal node damage, when evaluating the neural basis of decision-making deficits.

6.4 Apathy, depression and impulsivity in decision-making under uncertainty

Throughout this thesis, I have sought to characterise how disruptions in WM tracts relate to decision-making behaviour (**Figures 3-12 & 3-13 & 3-14 & 3-15 & 3-16 & 3-17 & 3-18 & 3-19 & 3-20 & 4-6 & 4-7 & 4-8 & 4-9**) and clinical measures of apathy (**Figures 2-20 & 2-21**), depression (**Figures 2-22 & 2-23 & 2-24 & 2-25**), and impulsivity (**Figures 2-26 & 2-27**). The connectomics analyses reveal that task behaviour and clinical symptoms may be associated with partially overlapping patterns of disconnection, particularly involving fronto-parietal pathways and fronto-subcortical projections to structures such as the thalamus, amygdala, and hippocampus. These findings suggest that impaired behaviour, along with motivational and affective symptoms in SVD, may reflect network-level dysfunction rather than isolated damage to any single structure. However, the present data did not demonstrate a direct association between these clinical measures and behavioural performance on the CQ task. This may reflect limitations inherent to the sample, including restricted symptom severity and modest sample size, which may have reduced the statistical power to detect more subtle brain–behaviour relationships.

Nevertheless, the structural disconnections identified here closely align with large-scale networks known to support value-based and uncertainty-driven decision-making. Converging lines of evidence indicate that adaptive behaviour depends on coordinated interactions among distributed neural systems rather than isolated cortical regions. For example, cooperation between the default mode network (DMN) and the frontoparietal control network (FPCN) supports goal-directed cognition, prospective planning, and the flexible use of internally generated information during decision-making (Spreng et al., 2010). Reward-based cognitive control engages a partially overlapping circuitry: interactions between the FPCN (particularly the inferior frontal junction), dopaminergic midbrain systems, and the ACC enable adjustments to behaviour as expected value shifts (Hippmann et al., 2021). Parallel work on uncertainty shows that individuals with heightened intolerance of uncertainty exhibit increased functional connectivity between the right anterior insula and both the dorsal ACC (dACC) and dorsolateral PFC (dlPFC), regions which have been implicated in salience detection and the mobilization of control (Radoman & Gorka, 2023). A recent large-scale meta-analysis further identifies the anterior insula, inferior parietal lobule, and ACC as core hubs consistently engaged across uncertainty-processing tasks, reinforcing the existence of a distributed "uncertainty-regulation" network (Timashkov et al., 2025).

Integrating these strands of evidence with the present structural findings motivates a neurocognitive model in which we might speculate that apathy, depression, impulsivity, and uncertainty-driven decision-making draw upon partially overlapping components of a broader goal-directed control network. Disruption to medial prefrontal and fronto-parietal pathways may undermine the translation of motivational states into behavioural initiation (apathy), while altered connectivity between valuation circuits (e.g., vmPFC, amygdala, ventral striatum) and cognitive control systems may contribute to affective symptoms such as anhedonia and diminished reward responsiveness (depression). At the same time, it is

possible that compromised communication between the anterior insula, ACC, and lateral PFC—regions central to evidence accumulation and cost/uncertainty estimation—could increase impulsivity by weakening the integration of interoceptive signals, value updates, and control allocation. Although the present study did not show direct behavioural–clinical correlations, the overlap in structural disconnections across symptoms and decision-making provides mechanistic scaffolding for understanding how diverse cognitive and affective disruptions may arise from a common architecture of WM disconnection in SVD.

Taken together, these findings provide a theoretically grounded framework for understanding how different clinical symptoms in SVD may emerge from overlapping network-level disruptions, even if the behavioural consequences are not directly observable in the current dataset. They also highlight a key limitation of this thesis: the absence of strong associations between clinical scales and CQ performance which likely reflects both the narrow symptom range and the modest sample size. Future studies with larger, clinically diverse cohorts and multimodal imaging approaches will be essential to validate and refine this model, and to more precisely determine how motivational, affective, and cognitive disruptions arise from the underlying architecture of WM disconnection.

6.5 Decision-making under uncertainty: where next?

A natural next step in advancing the findings of this thesis is to adopt a multimodal imaging approach capable of linking structural disconnection to the real-time neural dynamics that support decision-making under uncertainty. While the present work relied on behavioural modelling and structural connectivity analyses, combining these approaches with high-field neuroimaging, such as 7T fMRI, would provide an opportunity to observe how WM pathology alters the moment-to-moment engagement of decision-related networks and better highlight the contributions of subcortical brain regions (Colizoli et al., 2021; Kalhan et al.,

2022). The passive choice version of the CQ task is particularly well suited for this environment as it requires minimal movement, has clearly separable decision epochs, and generates trial-level estimates of uncertainty and value that can be mapped onto neural activation patterns. Implementing this version of the task in a 7T scanner would allow precise characterisation of the neural correlates of uncertainty sensitivity, reward responsiveness, and offer acceptance behaviour in both healthy individuals and patients with WM pathology.

In contrast, incorporating the active sampling and effort-modulated versions of the CQ task poses practical challenges for neuroimaging. Both paradigms require continuous movements (sampling trajectories, button presses or tapping a screen, grip-force exertion), which introduce motion artefacts that compromise BOLD signal quality, even with advanced correction methods. Although some laboratories have successfully implemented effort-based tasks in MRI environments using MRI-compatible grip-force devices, these typically involve discrete, brief exertion periods rather than the continuous exploratory behaviour seen in the active CQ task (Müller et al., 2021). For this reason, future neuroimaging work might first profitably focus on the passive choice paradigm, using insights gained from neural activation patterns to inform the later development of scanner-compatible versions of the more dynamic task variants. An alternative approach would be to use MEG, which tolerates movement more readily and provides superior temporal resolution for tracking evidence accumulation processes, though at the expense of spatial precision (Dale et al., 2000; Gosseries et al., 2008). Combining MEG with structural connectivity could offer a valuable intermediate step toward characterising the temporal unfolding of decision signals in SVD and MFL lesions.

Before extending this work into MEG or multimodal neuroimaging, an important immediate step is to exploit the full potential of the structural datasets already acquired. The connectomics analyses in this thesis relied on atlas-level TBSS projections to identify likely regions of WM disruption, but this approach does not reconstruct individual streamlines or

quantify connectivity at the subject level. More advanced structural connectomics using the same 3 T diffusion data (such as whole-brain tractography, fixel-based analysis, or network-level graph modelling) would allow a far more anatomically precise characterisation of how SVD alters the structural connectome.

Such methods have been successfully implemented in large cohort studies, for example the UK Biobank 3 T MRI pipeline uses individualised tractography to generate subject-specific structural connectomes from diffusion-weighted imaging (Mansour L. et al., 2023), and fixel-based approaches applied to 3 T dMRI provide fibre-specific metrics of WM degeneration that are more sensitive to disease-related change than TBSS (Raffelt et al., 2017). Similarly, individual-level streamline reconstructions have been used to map disconnection syndromes in stroke and neurodegeneration (Thiebaut de Schotten et al., 2020), demonstrating the utility of tractography-based connectomics for linking WM pathology to behaviour. Applying these techniques to this dataset would allow a much richer understanding of which specific tracts (and which connections in the broader network) drive the uncertainty- and valuation-related impairments observed in SVD and MFL lesions.

Several important questions regarding structural pathology and decision-making under uncertainty remain beyond the scope of this thesis. One concerns the trajectory of decision-making decline: how do uncertainty sensitivity, valuation, or cost processing evolve as WMH burden progresses over time? Longitudinal studies could determine whether early shifts in uncertainty tolerance or sampling behaviour serve as behavioural markers of microstructural decline. Another question is whether physical effort is uniquely capable of restoring aspects of impaired function, as suggested by the improved behaviour seen in SVD participants during the effort-modulated condition. It remains unclear whether this improvement reflects the motivational salience of effort, increased arousal, altered control engagement, or other context-dependent mechanisms. Moreover, it is unknown whether a

similar restoration could be observed in individuals with MFL lesions, or whether cortical damage imposes constraints on flexibility that WM pathology does not. Extending the effort manipulation to the active sampling version of the CQ task may also be illuminating: could introducing effort costs into the sampling process encourage patients to adopt more efficient evidence accumulation strategies and thereby improve performance?

Together, these avenues highlight a broader conceptual direction for future research: understanding not only how structural pathology impairs decision-making under uncertainty, but also when and under what conditions these impairments can be mitigated or reversed. A multimodal, longitudinal, and context-sensitive research programme will be essential for disentangling the interplay between network damage, task demands, and residual cognitive capacity, ultimately providing a more comprehensive account of adaptive and maladaptive decision-making in neurological populations.

6.6 Treatment insights: what else can we do?

Although SVD is a progressive WM disorder, increasing evidence shows that the adult brain retains substantial capacity for structural and functional plasticity even in the presence of longstanding WM damage. For example, rehabilitation studies in multiple sclerosis (MS), another disorder characterised by widespread WM microstructural disruption, demonstrate that targeted motor and cognitive training can lead not only to behavioural improvement but also to measurable changes in WM microstructure and functional connectivity (Prosperini et al., 2015). These findings suggest that structured cognitive rehabilitation may promote compensatory reorganisation in networks affected by WM injury, potentially enhancing goal-directed control, uncertainty monitoring, or motivational drive in SVD. Given the present thesis's evidence that impairments in SVD arise partly from the inefficient engagement of

fronto-parietal and salience-control circuits, rehabilitative paradigms that encourage repeated activation of these circuits may offer a promising non-pharmacological therapeutic avenue.

Complementary evidence comes from behavioural interventions aimed at older adults without neurological disease, such as the recently developed evening autobiographical recall intervention (Blackman et al., 2025). This study demonstrated that simple, low-burden, behaviourally focused interventions can enhance memory performance in older individuals by modulating cognitive control processes and strengthening the retrieval of internally generated information. Although the mechanisms underlying its efficacy may differ from those relevant to uncertainty-driven decision-making, the broader implication is highly relevant to SVD: everyday behavioural routines can engage and potentially strengthen cognitive networks that remain functionally intact despite structural compromise. Translating similar approaches to SVD, for example, routines that scaffold evaluation, reduce uncertainty tolerance, or promote deliberate evidence gathering could support more adaptive decision-making in daily life.

Together, these studies point toward a wider therapeutic possibility: interventions that repeatedly activate goal-directed, fronto-parietal, and salience networks may cultivate compensatory pathways even when WM integrity is compromised. In SVD, this could take the form of:

- Cognitive control training targeting cost sensitivity, uncertainty discrimination, and evidence accumulation
- Motivational or “effort-based” interventions that harness the functional restoration observed when task context changes (as shown in your Chapter 4)
- Structured behavioural routines that enhance top-down control (analogous to autobiographical recall), helping patients regulate impulsive or risk-biased behaviour

- Multimodal rehabilitation combining cognitive exercises with light motor engagement, mirroring effective MS protocols

These approaches are especially promising because the present thesis shows that SVD patients exhibit a partial loss of function and context-dependent restoration under effort conditions. This suggests that the relevant decision-making networks retain enough flexibility to benefit from interventions that enhance engagement, strengthen synaptic efficacy through repetition, or encourage recruitment of alternative pathways. In this way, the plasticity observed in MS and the behavioural malleability observed in healthyageing provide a conceptual and empirical basis for developing network-targeted therapies for decision-making impairments in SVD.

6.7 Concluding remarks

Taken together, the work presented in this thesis demonstrates that decision-making under uncertainty is not governed by any single region or computational mechanism but rather emerges from the coordinated interaction of large-scale brain networks whose effectiveness depends on the integrity of their WM connections. Although disruption to these networks in SVD and focal MFL lesions leads to measurable changes in uncertainty sensitivity, valuation, and evidence accumulation, the findings also reveal a degree of residual flexibility, i.e. behaviour that can be shifted, partially restored, or scaffolded by contextual demands such as the introduction of effort. This combination of vulnerability and resilience underscores a central message: decision-making is a dynamic, distributed, and modifiable process, one that remains open to therapeutic, computational, and technological innovation.

Promisingly, recent developments in clinical neuroscience suggest that the gap between mechanistic understanding and clinical translation is narrowing. The emergence of Brain Health Clinics, for example, represents a major shift toward preventative, personalised,

and data-driven neurology. These clinics integrate structural imaging, cognitive profiling, and biomarker assessment to identify individuals at risk of neurodegenerative or cerebrovascular pathology at much earlier stages (Butters et al., 2025). Such infrastructures could provide an ideal platform for implementing fine-grained decision-making assessments (such as the CQ task) and tracking how uncertainty sensitivity or valuation processes change with disease progression. Parallel advances in remote, longitudinal monitoring, as demonstrated by the feasibility of at-home sleep and cognition tracking in individuals with mild cognitive impairment and dementia (Gabb et al., 2025), further open avenues for capturing decision-making behaviour in ecologically valid, real-world contexts. Together, these innovations will make it increasingly feasible to monitor cognitive network integrity as it evolves and to detect early deviations in decision-making trajectories that may signal developing WM pathology.

At the same time, theoretical and computational progress is rapidly transforming how decision-making is conceptualised. Work identifying a cognitive map of value in the vmPFC (Veselic et al., 2023) suggests that humans navigate abstract value spaces using representational geometry analogous to spatial navigation. Complementary findings from dynamic decision paradigms reveal that humans continuously update behaviour using moment-by-moment changes in evidence and reward, even in non-stationary environments (Ruesseler et al., 2023). New electrophysiological and neuroimaging evidence further delineates the neural correlates of continuous feedback processing, implicating distributed networks whose activity unfolds over time rather than discretely (Hassall et al., 2023). Beyond human studies, deep meta-learning agents are beginning to reveal algorithmic principles of goal-directed navigation and flexible value learning that parallel human strategies under uncertainty (Lan et al., 2025), offering a powerful bridge between biological and artificial decision systems.

Together, these emerging strands of clinical infrastructure, remote cognitive phenotyping, high-resolution imaging, computational modelling, and artificial agents point to a future in which uncertainty-driven decision-making can be quantified with unprecedented precision. The next decade is likely to see the development of fully integrative frameworks in which structural connectivity, functional dynamics, behavioural modelling, and personalised clinical profiles are combined to characterise decision-making in both health and disease. For disorders such as SVD, this could enable early identification of network vulnerability, targeted interventions that harness preserved flexibility, and tailored rehabilitation protocols informed by real-time monitoring of cognitive state. In this sense, there is genuine reason for optimism. Although uncertainty is inherent to both the decisions we study and the disorders we seek to understand, our scientific trajectory is moving toward increasing clarity. The convergence of theoretical, technological, and clinical advances suggests that we are approaching a future in which the mechanisms of human decision-making—and the means to restore them—are more comprehensively understood than ever before.

References

Aarsland, D., Andersen, K., Larsen, J. P., Perry, R., Wentzel-Larsen, T., Lolk, A., & Kragh-Sørensen, P. (2004). The Rate of Cognitive Decline in Parkinson Disease. *Archives of Neurology*, *61*(12), 1906–1911. https://doi.org/10.1001/archneur.61.12.1906

Adam, R., Leff, A., Sinha, N., Turner, C., Bays, P., Draganski, B., & Husain, M. (2013). Dopamine reverses reward insensitivity in apathy following globus pallidus lesions. *Cortex; a Journal Devoted to the Study of the Nervous System and Behavior*, *49*(5), 1292–1303. https://doi.org/10.1016/j.cortex.2012.04.013

Alfaro-Almagro, F., Jenkinson, M., Bangerter, N. K., Andersson, J. L. R., Griffanti, L., Douaud, G., Sotiropoulos, S. N., Jbabdi, S., Hernandez-Fernandez, M., Vallee, E., Vidaurre, D., Webster, M., McCarthy, P., Rorden, C., Daducci, A., Alexander, D. C., Zhang, H., Dragonu, I., Matthews, P. M., … Smith, S. M. (2018). Image processing and Quality Control for the first 10,000 brain imaging datasets from UK Biobank. *NeuroImage*, *166*, 400–424. https://doi.org/10.1016/j.neuroimage.2017.10.034

Alves, G. S., Alves, C. E. de O., Lanna, M. E., Moreira, D. M., Engelhardt, E., & Laks, J. (2008). Subcortical ischemic vascular disease and cognition: A systematic review. *Dementia & Neuropsychologia*, *2*(2), 82–90. https://doi.org/10.1590/S1980-57642009DN20200002

Anderson, S. W., Bechara, A., Damasio, H., Tranel, D., & Damasio, A. R. (1999). Impairment of social and moral behavior related to early damage in human

prefrontal cortex. *Nature Neuroscience*, *2*(11), Article 11. https://doi.org/10.1038/14833

Andersson, J. L. R., Skare, S., & Ashburner, J. (2003). How to correct susceptibility distortions in spin-echo echo-planar images: Application to diffusion tensor imaging. *NeuroImage*, *20*(2), 870–888. https://doi.org/10.1016/S1053-8119(03)00336-7

Andersson, J. L. R., & Sotiropoulos, S. N. (2016). An integrated approach to correction for off-resonance effects and subject movement in diffusion MR imaging. *Neuroimage*, *125*, 1063–1078. https://doi.org/10.1016/j.neuroimage.2015.10.019

Ang, Y.-S. (2017, January 11). *Distinct Subtypes of Apathy Revealed by the Apathy Motivation Index | PLOS ONE*. https://journals.plos.org/plosone/article?id=10.1371/journal.pone.0169938

Ang, Y.-S., Gelda, S., & Pizzagalli, D. (2022). Cognitive effort-based decision-making in major depressive disorder. *Psychological Medicine*, *53*, 1–8. https://doi.org/10.1017/S0033291722000964

Ang, Y.-S., Lockwood, P., Apps, M. A. J., Muhammed, K., & Husain, M. (2016). (PDF) Distinct Subtypes of Apathy Revealed by the Apathy Motivation Index. *ResearchGate*. https://doi.org/10.1371/journal.pone.0169938

Arenaza-Urquijo, E. M., Bosch, B., Sala-Llonch, R., Solé-Padullés, C., Junqué, C., Fernández-Espejo, D., Bargalló, N., Rami, L., Molinuevo, J. L., & Bartrés-Faz, D. (2011). Specific Anatomic Associations Between White Matter Integrity and Cognitive Reserve in Normal and Cognitively Impaired Elders. *The American*

Journal of Geriatric Psychiatry, *19*(1), 33–42. https://doi.org/10.1097/JGP.0b013e3181e448e1

Arulpragasam, A. R., Cooper, J. A., Nuutinen, M. R., & Treadway, M. T. (2018). Corticoinsular circuits encode subjective value expectation and violation for effortful goal-directed behavior. *Proceedings of the National Academy of Sciences*, *115*(22), E5233–E5242. https://doi.org/10.1073/pnas.1800444115

Attaallah, B., Petitet, P., & Husain, M. (2025). Active information sampling in health and disease. *Neuroscience & Biobehavioral Reviews*, *175*, 106197. https://doi.org/10.1016/j.neubiorev.2025.106197

Attaallah, B., Petitet, P., Slavkova, E., Turner, V., Saleh, Y., Manohar, S. G., & Husain, M. (2021). *Hypersensitivity to uncertainty is key feature of subjective cognitive impairment* (p. 2021.12.23.473986). bioRxiv. https://doi.org/10.1101/2021.12.23.473986

Attaallah, B., Petitet, P., Zambellas, R., Toniolo, S., Maio, M., Ganse-Dumrath, A., Irani, S., Manohar, S., & Husain, M. (2024a). The role of the human hippocampus in decision-making under uncertainty. *Nature Human Behaviour*, *8*. https://doi.org/10.1038/s41562-024-01855-2

Attaallah, B., Petitet, P., Zambellas, R., Toniolo, S., Maio, M. R., Ganse-Dumrath, A., Irani, S. R., Manohar, S. G., & Husain, M. (2024b). The role of the human hippocampus in decision-making under uncertainty. *Nature Human Behaviour*, *8*(7), 1366–1382. https://doi.org/10.1038/s41562-024-01855-2

Auer, P., Cesa-Bianchi, N., & Fischer, P. (2002). Finite-time Analysis of the Multiarmed Bandit Problem. *Machine Learning*, *47*(2), 235–256. https://doi.org/10.1023/A:1013689704352

Averbeck, B. B. (2015a). Theory of Choice in Bandit, Information Sampling and Foraging Tasks. *PLOS Computational Biology*, *11*(3), e1004164. https://doi.org/10.1371/journal.pcbi.1004164

Averbeck, B. B. (2015b). *Theory of Choice in Bandit, Information Sampling and Foraging Tasks*. https://doi.org/10.1371/journal.pcbi.1004164

Aykan, S. A., Lai, J. H., Sugimoto, K., Aykan, O., Fung, W. Y., Ho, D., Joutel, A., Sakadzic, S., Chung, D. Y., & Ayata, C. (2025). Impaired Resting-State Functional Connectivity in Cerebral Autosomal-Dominant Arteriopathy, Subcortical Infarcts, and Leukoencephalopathy Mutant Mice. *Stroke*, *56*(4), 987–995. https://doi.org/10.1161/STROKEAHA.124.049772

Baddeley, A. (1992). Working Memory. *Science*, *255*(5044), 556–559. https://doi.org/10.1126/science.1736359

Bailey, A. J., Romeu, R. J., & Finn, P. R. (2021). The problems with delay discounting: A critical review of current practices and clinical applications. *Psychological Medicine*, *51*(11), 1799–1806. https://doi.org/10.1017/S0033291721002282

Baird, A. (2006). *Social and emotional functions in three patients with medial frontal lobe damage including the anterior cingulate cortex*. https://doi.org/10.1080/13546800444000245

Barakat, A., Brochard, J., Pessiglione, M., Godin, J.-P., Cuenoud, B., Xin, L., Clairis, N., & Sandi, C. (2025). *Neurometabolic predictors of mental effort in the frontal cortex* (p. 2024.01.23.576854). bioRxiv. https://doi.org/10.1101/2024.01.23.576854

Barch, D. M., Treadway, M., & Schoen, N. (2014). Effort, Anhedonia, and Function in Schizophrenia: Reduced Effort Allocation Predicts Amotivation and Functional

Impairment. *Journal of Abnormal Psychology*, *123*(2), 387–397. https://doi.org/10.1037/a0036299

Barker, R., Wellington, D., Esiri, M. M., & Love, S. (2013). Assessing white matter ischemic damage in dementia patients by measurement of myelin proteins. *Journal of Cerebral Blood Flow and Metabolism: Official Journal of the International Society of Cerebral Blood Flow and Metabolism*, *33*(7), 1050–1057. https://doi.org/10.1038/jcbfm.2013.46

Barron, G., & Erev, I. (2003). Small feedback-based decisions and their limited correspondence to description-based decisions. *Journal of Behavioral Decision Making*, *16*(3), 215–233. https://doi.org/10.1002/bdm.443

Bartolomeo, P. (2006). A Parietofrontal Network for Spatial Awareness in the Right Hemisphere of the Human Brain. *Archives of Neurology*, *63*(9), 1238–1241. https://doi.org/10.1001/archneur.63.9.1238

Baumann, C., Singmann, H., Gershman, S. J., & von Helversen, B. (2020). A linear threshold model for optimal stopping behavior. *Proceedings of the National Academy of Sciences*, *117*(23), 12750–12755. https://doi.org/10.1073/pnas.2002312117

Bechara, A. (1994). *Insensitivity to future consequences following damage to human prefrontal cortex*.

Bechara, A. (2004). The role of emotion in decision-making: Evidence from neurological patients with orbitofrontal damage. *Brain and Cognition*, *55*(1), 30–40. https://doi.org/10.1016/j.bandc.2003.04.001

Bechara, A., Damasio, A. R., Damasio, H., & Anderson, S. W. (1994). Insensitivity to future consequences following damage to human prefrontal cortex. *Cognition*, *50*(1–3), 7–15. https://doi.org/10.1016/0010-0277(94)90018-3

Bechara, A., Tranel, D., & Damasio, H. (2000). Characterization of the decision-making deficit of patients with ventromedial prefrontal cortex lesions. *Brain*, *123*(11), 2189–2202. https://doi.org/10.1093/brain/123.11.2189

Bechara, A., & Van Der Linden, M. (2005). Decision-making and impulse control after frontal lobe injuries. *Current Opinion in Neurology*, *18*(6), 734–739. https://doi.org/10.1097/01.wco.0000194141.56429.3c

Beck, A. T., WARD, C. H., MENDELSON, M., MOCK, J., & ERBAUGH, J. (1961a). An Inventory for Measuring Depression. *Archives of General Psychiatry*, *4*(6), 561–571. https://doi.org/10.1001/archpsyc.1961.01710120031004

Beck, A. T., WARD, C. H., MENDELSON, M., MOCK, J., & ERBAUGH, J. (1961b). An Inventory for Measuring Depression. *Archives of General Psychiatry*, *4*(6), 561–571. https://doi.org/10.1001/archpsyc.1961.01710120031004

Beishon, L. C., Batterham, A. P., Quinn, T. J., Nelson, C. P., Panerai, R. B., Robinson, T., & Haunton, V. J. (2019). Addenbrooke's Cognitive Examination III (ACE-III) and mini-ACE for the detection of dementia and mild cognitive impairment. *The Cochrane Database of Systematic Reviews*, *12*(12), CD013282. https://doi.org/10.1002/14651858.CD013282.pub2

Benoit, M., & Robert, P. H. (2011). Imaging correlates of apathy and depression in Parkinson's disease. *Journal of the Neurological Sciences*, *310*(1–2), 58–60. https://doi.org/10.1016/j.jns.2011.07.006

Berger, A. (2002). Magnetic resonance imaging. *BMJ : British Medical Journal*, *324*(7328), 35. https://doi.org/10.1136/bmj.324.7328.35

Berry, D. A., Chen, R. W., Zame, A., Heath, D. C., & Shepp, L. A. (1997a). Bandit Problems With Infinitely Many Arms. *The Annals of Statistics*, *25*(5), 2103–2116.

Berry, D. A., Chen, R. W., Zame, A., Heath, D. C., & Shepp, L. A. (1997b). Bandit Problems With Infinitely Many Arms. *The Annals of Statistics*, *25*(5), 2103–2116.

Berwian, I. M., Wenzel, J. G., Collins, A. G. E., Seifritz, E., Stephan, K. E., Walter, H., & Huys, Q. J. M. (2020). Computational Mechanisms of Effort and Reward Decisions in Patients With Depression and Their Association With Relapse After Antidepressant Discontinuation. *JAMA Psychiatry*, *77*(5), 513–522. https://doi.org/10.1001/jamapsychiatry.2019.4971

Binmore, K. (2012). Von Neumann, Morgenstern, and the Creation of Game Theory: From Chess to Social Science, 1900-1960. *History of Political Economy*, *44*(3), 546–550. https://doi.org/10.1215/00182702-1717302

Blackburn, H. L., & Benton, A. L. (1957). Revised administration and scoring of the Digit Span Test. *Journal of Consulting Psychology*, *21*(2), 139–143. https://doi.org/10.1037/h0047235

Blackman, J., Gabb, V., Woodstoke, D., Morrison, H., Taylor, M., Turner, N., Li, H., Biswas, B., Heslegrave, A., Whone, A., Mickes, L., & Coulthard, E. (2025). A new behavioural intervention to enhance memory in older people-evening autobiographical recall. *Neuropsychologia*, *216*, 109191. https://doi.org/10.1016/j.neuropsychologia.2025.109191

Blair, G. W., Hernandez, M. V., Thrippleton, M. J., Doubal, F. N., & Wardlaw, J. M. (2017). Advanced Neuroimaging of Cerebral Small Vessel Disease. *Current Treatment*

Options in Cardiovascular Medicine, *19*(7), 56. https://doi.org/10.1007/s11936-017-0555-1

Blanco, N. J., & Sloutsky, V. M. (2024). Exploration, exploitation, and development: Developmental shifts in decision-making. *Child Development*, *95*(4), 1287–1298. https://doi.org/10.1111/cdev.14070

Bland, A. R., Roiser, J. P., Mehta, M. A., Schei, T., Boland, H., Campbell-Meiklejohn, D. K., Emsley, R. A., Munafo, M. R., Penton-Voak, I. S., Seara-Cardoso, A., Viding, E., Voon, V., Sahakian, B. J., Robbins, T. W., & Elliott, R. (2016). EMOTICOM: A Neuropsychological Test Battery to Evaluate Emotion, Motivation, Impulsivity, and Social Cognition. *Frontiers in Behavioral Neuroscience*, *10*, 25. https://doi.org/10.3389/fnbeh.2016.00025

Bogdanov, M., Renault, H., LoParco, S., Weinberg, A., & Otto, A. R. (2022). Cognitive effort exertion enhances electrophysiological responses to rewarding outcomes. *Cerebral Cortex*, *32*(19), 4255–4270. https://doi.org/10.1093/cercor/bhab480

Bonilha, L., Gleichgerrcht, E., Fridriksson, J., Rorden, C., Breedlove, J. L., Nesland, T., Paulus, W., Helms, G., & Focke, N. K. (2015). Reproducibility of the Structural Brain Connectome Derived from Diffusion Tensor Imaging. *PloS One*, *10*(8), e0135247. https://doi.org/10.1371/journal.pone.0135247

Bonnelle, V., Veromann, K.-R., Burnett Heyes, S., Lo Sterzo, E., Manohar, S., & Husain, M. (2015). Characterization of reward and effort mechanisms in apathy. *Journal of Physiology-Paris*, *109*(1), 16–26. https://doi.org/10.1016/j.jphysparis.2014.04.002

Boorman, E. D., Behrens, T. E. J., Woolrich, M. W., & Rushworth, M. F. S. (2009). How Green Is the Grass on the Other Side? Frontopolar Cortex and the Evidence in

Favor of Alternative Courses of Action. *Neuron*, *62*(5), 733–743. https://doi.org/10.1016/j.neuron.2009.05.014

Bore, M. C., Liu, X., Gan, X., Wang, L., Xu, T., Ferraro, S., Li, L., Zhou, B., Zhang, J., Vatansever, D., Biswal, B., Klugah-Brown, B., & Becker, B. (2023). *Distinct neurofunctional alterations during motivational and hedonic processing of natural and monetary rewards in depression – a neuroimaging meta-analysis* (p. 2022.12.07.22283197). medRxiv. https://doi.org/10.1101/2022.12.07.22283197

Borrelli, P., Cavaliere, C., Salvatore, M., Jovicich, J., & Aiello, M. (2022). Structural Brain Network Reproducibility: Influence of Different Diffusion Acquisition and Tractography Reconstruction Schemes on Graph Metrics. *Brain Connectivity*, *12*(8), 754–767. https://doi.org/10.1089/brain.2021.0123

Bouneffouf, D., Rish, I., & Cecchi, G. A. (2017). *Bandit Models of Human Behavior: Reward Processing in Mental Disorders* (No. arXiv:1706.02897). arXiv. https://doi.org/10.48550/arXiv.1706.02897

Boutzoukas, E. M., O'Shea, A., Albizu, A., Evangelista, N. D., Hausman, H. K., Kraft, J. N., Van Etten, E. J., Bharadwaj, P. K., Smith, S. G., Song, H., Porges, E. C., Hishaw, A., DeKosky, S. T., Wu, S. S., Marsiske, M., Alexander, G. E., Cohen, R., & Woods, A. J. (2021). Frontal White Matter Hyperintensities and Executive Functioning Performance in Older Adults. *Frontiers in Aging Neuroscience*, *13*. https://doi.org/10.3389/fnagi.2021.672535

Bozzali, M., Dowling, C., Serra, L., Spanò, B., Torso, M., Marra, C., Castelli, D., Dowell, N. G., Koch, G., Caltagirone, C., & Cercignani, M. (2015). The impact of cognitive reserve on brain functional connectivity in Alzheimer's disease. *Journal of Alzheimer's Disease: JAD*, *44*(1), 243–250. https://doi.org/10.3233/JAD-141824

Brand, M., Labudda, K., & Markowitsch, H. J. (2006). Neuropsychological correlates of decision-making in ambiguous and risky situations. *Neural Networks*, *19*(8), 1266–1276. https://doi.org/10.1016/j.neunet.2006.03.001

Brandhofe, A., Stratmann, C., Schüre, J.-R., Pilatus, U., Hattingen, E., Deichmann, R., Nöth, U., Wagner, M., Gracien, R.-M., & Seiler, A. (2021). T2 relaxation time of the normal-appearing white matter is related to the cognitive status in cerebral small vessel disease. *Journal of Cerebral Blood Flow and Metabolism: Official Journal of the International Society of Cerebral Blood Flow and Metabolism*, *41*(7), 1767–1777. https://doi.org/10.1177/0271678X20972511

Braverman, M., Mao, J., Schneider, J., & Weinberg, S. M. (2019). Multi-armed Bandit Problems with Strategic Arms. *Proceedings of the Thirty-Second Conference on Learning Theory*, 383–416. https://proceedings.mlr.press/v99/braverman19b.html

Brickman, A. M., Siedlecki, K. L., Muraskin, J., Manly, J. J., Luchsinger, J. A., Yeung, L.-K., Brown, T. R., DeCarli, C., & Stern, Y. (2011). White matter hyperintensities and cognition: Testing the reserve hypothes. *Neurobiology of Aging*, *32*(9), 1588–1598. https://doi.org/10.1016/j.neurobiolaging.2009.10.013

Broche-Pérez, Y., Herrera Jiménez, L. F., & Omar-Martínez, E. (2016). Neural substrates of decision-making. *Neurología (English Edition)*, *31*(5), 319–325. https://doi.org/10.1016/j.nrleng.2015.03.009

Brülhart, M., & Usunier, J.-C. (2004). *Verified Trust: Reciprocity, Altruism and Noise in Trust Games* (SSRN Scholarly Paper No. 664561). https://papers.ssrn.com/abstract=664561

Bubeck, S., Munos, R., Stoltz, G., & Szepesvari, C. (2011). *X-Armed Bandits* (No. arXiv:1001.4475). arXiv. https://doi.org/10.48550/arXiv.1001.4475

Budisavljevic, S., Ameis, S., Berlot, R., Howells, H., & Urbanski, M. (2025). Chapter 30—Linking behavior with white matter networks. In F. Dell'Acqua, M. Descoteaux, & A. Leemans (Eds), *Handbook of Diffusion MR Tractography* (pp. 613–629). Academic Press. https://doi.org/10.1016/B978-0-12-818894-1.00027-6

Bull, P. N., Tippett, L. J., & Addis, D. R. (2015). Decision making in healthy participants on the Iowa Gambling Task: New insights from an operant approach. *Frontiers in Psychology*, *6*, 391. https://doi.org/10.3389/fpsyg.2015.00391

Burgess, P. W. (2010). Assessment of executive function. In J. Marshall, J. Gurd, & U. Kischka (Eds), *The Handbook of Clinical Neuropsychology* (p. 0). Oxford University Press. https://doi.org/10.1093/acprof:oso/9780199234110.003.018

Burks, S. V., Carpenter, J. P., & Verhoogen, E. (2003). Playing both roles in the trust game. *Journal of Economic Behavior & Organization*, *51*(2), 195–216. https://doi.org/10.1016/S0167-2681(02)00093-8

Butters, A. F., Blackman, J., Farouk, H., Meky, S., A Newson, M., Lemke, T., Rosewell, N., Selwood, J. A., Turner, N. L., Coulthard, E. J., & Archer, H. A. (2025). Brain health clinics—An evolving clinical pathway? *The Journal of Prevention of Alzheimer's Disease*, *12*(3), 100051. https://doi.org/10.1016/j.tjpad.2024.100051

Cai, J., Sun, J., Chen, H., Chen, Y., Zhou, Y., Lou, M., & Yu, R. (2022). Different mechanisms in periventricular and deep white matter hyperintensities in old subjects. *Frontiers in Aging Neuroscience*, *14*, 940538. https://doi.org/10.3389/fnagi.2022.940538

Cardoso, C. de O., Branco, L. D., Cotrena, C., Kristensen, C. H., Schneider Bakos, D. D. G., & Fonseca, R. P. (2014). The impact of frontal and cerebellar lesions on decision making: Evidence from the Iowa Gambling Task. *Frontiers in Neuroscience*, *8*, 61. https://doi.org/10.3389/fnins.2014.00061

Cauffman, E. (2010). *Age differences in affective decision making as indexed by performance on the Iowa Gambling Task*.

Cauffman, E., Shulman, E. P., Steinberg, L., Claus, E., Banich, M. T., Graham, S., & Woolard, J. (2010). Age differences in affective decision making as indexed by performance on the Iowa Gambling Task. *Developmental Psychology*, *46*(1), 193–207. https://doi.org/10.1037/a0016128

Cesa-Bianchi, N., & Lugosi, G. (2012). Combinatorial bandits. *Journal of Computer and System Sciences*, *78*(5), 1404–1422. https://doi.org/10.1016/j.jcss.2012.01.001

Chand, G. B., & Dhamala, M. (2016). Interactions Among the Brain Default-Mode, Salience, and Central-Executive Networks During Perceptual Decision-Making of Moving Dots. *Brain Connectivity*, *6*(3), 249–254. https://doi.org/10.1089/brain.2015.0379

Chen, X., Voets, S., Jenkinson, N., & Galea, J. M. (2020). Dopamine-Dependent Loss Aversion during Effort-Based Decision-Making. *Journal of Neuroscience*, *40*(3), 661–670. https://doi.org/10.1523/JNEUROSCI.1760-19.2019

Choi, H. J., Lee, D. Y., Seo, E. H., Jo, M. K., Sohn, B. K., Choe, Y. M., Byun, M. S., Kim, J. W., Kim, S. G., Yoon, J. C., Jhoo, J. H., Kim, K. W., & Woo, J. I. (2014). A Normative Study of the Digit Span in an Educationally Diverse Elderly Population. *Psychiatry Investigation*, *11*(1), 39–43. https://doi.org/10.4306/pi.2014.11.1.39

Chong, T. T.-J., Apps, M., Giehl, K., Sillence, A., Grima, L. L., & Husain, M. (2017a). Neurocomputational mechanisms underlying subjective valuation of effort costs. *PLoS Biology*, *15*(2), e1002598. https://doi.org/10.1371/journal.pbio.1002598

Chong, T. T.-J., Apps, M., Giehl, K., Sillence, A., Grima, L. L., & Husain, M. (2017b). Neurocomputational mechanisms underlying subjective valuation of effort costs. *PLOS Biology*, *15*(2), e1002598. https://doi.org/10.1371/journal.pbio.1002598

Chong, T. T.-J., Bonnelle, V., Manohar, S., Veromann, K.-R., Muhammed, K., Tofaris, G. K., Hu, M., & Husain, M. (2015). Dopamine enhances willingness to exert effort for reward in Parkinson's disease. *Cortex; a Journal Devoted to the Study of the Nervous System and Behavior*, *69*, 40–46. https://doi.org/10.1016/j.cortex.2015.04.003

Clark, L., Bechara, A., Damasio, H., Aitken, M. R. F., Sahakian, B. J., & Robbins, T. W. (2008). Differential effects of insular and ventromedial prefrontal cortex lesions on risky decision-making. *Brain*, *131*(5), 1311–1322. https://doi.org/10.1093/brain/awn066

Clark, L., & Manes, F. (2004). Social and Emotional Decision-making Following Frontal Lobe Injury. *Neurocase*, *10*(5), 398–403. https://doi.org/10.1080/13554790490882799

Clark, L., Manes, F., Antoun, N., Sahakian, B. J., & Robbins, T. W. (2003a). The contributions of lesion laterality and lesion volume to decision-making impairment following frontal lobe damage. *Neuropsychologia*, *41*(11), 1474–1483. https://doi.org/10.1016/S0028-3932(03)00081-2

Clark, L., Manes, F., Antoun, N., Sahakian, B. J., & Robbins, T. W. (2003b). The contributions of lesion laterality and lesion volume to decision-making impairment following frontal lobe damage. *Neuropsychologia*, *41*(11), 1474–1483. https://doi.org/10.1016/S0028-3932(03)00081-2

Clark, L., Robbins, T. W., Ersche, K. D., & Sahakian, B. J. (2006). Reflection Impulsivity in Current and Former Substance Users. *Biological Psychiatry*, *60*(5), 515–522. https://doi.org/10.1016/j.biopsych.2005.11.007

Clark, L., Roiser, J., Robbins, T., & Sahakian, B. (2009). Disrupted 'reflection' impulsivity in cannabis users but not current or former ecstasy users. *Journal of Psychopharmacology (Oxford, England)*, *23*(1), 14–22. https://doi.org/10.1177/0269881108089587

Clay, G., Mlynski, C., Korb, F. M., Goschke, T., & Job, V. (2022). Rewarding cognitive effort increases the intrinsic value of mental labor. *Proceedings of the National Academy of Sciences*, *119*(5), e2111785119. https://doi.org/10.1073/pnas.2111785119

Colizoli, O., de Gee, J. W., van der Zwaag, W., & Donner, T. H. (2021). Functional magnetic resonance imaging responses during perceptual decision-making at 3 and 7 T in human cortex, striatum, and brainstem. *Human Brain Mapping*, *43*(4), 1265–1279. https://doi.org/10.1002/hbm.25719

Colón-Semenza, C., Fulford, D., & Ellis, T. (2021). Effort-Based Decision-Making for Exercise in People with Parkinson's Disease. *Journal of Parkinson's Disease*, *11*(2), 725–735. https://doi.org/10.3233/JPD-202353

Conner, A. K., Briggs, R. G., Sali, G., Rahimi, M., Baker, C. M., Burks, J. D., Glenn, C. A., Battiste, J. D., & Sughrue, M. E. (2018). A Connectomic Atlas of the Human

Cerebrum—Chapter 13: Tractographic Description of the Inferior Fronto-Occipital Fasciculus. *Operative Neurosurgery*, *15*(Suppl 1), S436–S443. https://doi.org/10.1093/ons/opy267

Constantino, S., & Daw, N. D. (2015). Learning the opportunity cost of time in a patch-foraging task. *Cognitive, Affective & Behavioral Neuroscience*, *15*(4), 837–853. https://doi.org/10.3758/s13415-015-0350-y

Constantino, S. M., & Daw, N. D. (2015). Learning the opportunity cost of time in a patch-foraging task. *Cognitive, Affective, & Behavioral Neuroscience*, *15*(4), 837–853. https://doi.org/10.3758/s13415-015-0350-y

Corbetta, M., & Shulman, G. L. (2002). Control of goal-directed and stimulus-driven attention in the brain. *Nature Reviews Neuroscience*, *3*(3), 201–215. https://doi.org/10.1038/nrn755

Critchley, H. D., Mathias, C. J., & Dolan, R. J. (2001). Neural Activity in the Human Brain Relating to Uncertainty and Arousal during Anticipation. *Neuron*, *29*(2), 537–545. https://doi.org/10.1016/S0896-6273(01)00225-2

Croall, I. D., Lohner, V., Moynihan, B., Khan, U., Hassan, A., O'Brien, J. T., Morris, R. G., Tozer, D. J., Cambridge, V. C., Harkness, K., Werring, D. J., Blamire, A. M., Ford, G. A., Barrick, T. R., & Markus, H. S. (2017). Using DTI to assess white matter microstructure in cerebral small vessel disease (SVD) in multicentre studies. *Clinical Science (London, England : 1979)*, *131*(12), 1361–1373. https://doi.org/10.1042/CS20170146

Crockett, R. A., Hsu, C. L., Dao, E., Tam, R., Eng, J. J., Handy, T. C., & Liu-Ambrose, T. (2021). Painting by lesions: White matter hyperintensities disrupt functional

networks and global cognition. *NeuroImage*, *236*, 118089. https://doi.org/10.1016/j.neuroimage.2021.118089

Croxson, P. L., Walton, M. E., O'Reilly, J. X., Behrens, T. E. J., & Rushworth, M. F. S. (2009). Effort-Based Cost–Benefit Valuation and the Human Brain. *The Journal of Neuroscience*, *29*(14), 4531–4541. https://doi.org/10.1523/JNEUROSCI.4515-08.2009

Croxson, P., Walton, M., O'Reilly, J., Behrens, T., & Rushworth, M. (2009). Effort-Based Cost-Benefit Valuation and the Human Brain. *The Journal of Neuroscience : The Official Journal of the Society for Neuroscience*, *29*, 4531–4541. https://doi.org/10.1523/JNEUROSCI.4515-08.2009

Culbreth, A., Moran, E., & Barch, D. (2018). Effort-Based Decision-Making in Schizophrenia. *Current Opinion in Behavioral Sciences*, *22*, 1–6. https://doi.org/10.1016/j.cobeha.2017.12.003

Cunningham, S. I., Tomasi, D., & Volkow, N. D. (2016). Structural and functional connectivity of the precuneus and thalamus to the default mode network. *Human Brain Mapping*, *38*(2), 938–956. https://doi.org/10.1002/hbm.23429

Daducci, A., Canales-Rodríguez, E. J., Zhang, H., Dyrby, T. B., Alexander, D. C., & Thiran, J.-P. (2015). Accelerated Microstructure Imaging via Convex Optimization (AMICO) from diffusion MRI data. *NeuroImage*, *105*, 32–44. https://doi.org/10.1016/j.neuroimage.2014.10.026

Dale, A. M., Liu, A. K., Fischl, B. R., Buckner, R. L., Belliveau, J. W., Lewine, J. D., & Halgren, E. (2000). Dynamic statistical parametric mapping: Combining fMRI and MEG for high-resolution imaging of cortical activity. *Neuron*, *26*(1), 55–67. https://doi.org/10.1016/s0896-6273(00)81138-1

Daniele Bernoulli (1700–1782). (1738). *Specimen Theoriae Novae de Mensura Sortis*. http://archive.org/details/SpecimenTheoriaeNovaeDeMensuraSortis

de Schotten, M. T., Dell'Acqua, F., Forkel, S. J., Simmons, A., Vergani, F., Murphy, D. G. M., & Catani, M. (2011). A lateralized brain network for visuospatial attention. *Nature Neuroscience*, *14*(10), 1245–1246. https://doi.org/10.1038/nn.2905

DeJong, N. R., Jansen, J. F. A., van Boxtel, M. P. J., Schram, M. T., Stehouwer, C. D. A., Dagnelie, P. C., van der Kallen, C. J. H., Kroon, A. A., Wesselius, A., Koster, A., Backes, W. H., & Köhler, S. (2023). Cognitive resilience depends on white matter connectivity: The Maastricht Study. *Alzheimer's & Dementia: The Journal of the Alzheimer's Association*, *19*(4), 1164–1174. https://doi.org/10.1002/alz.12758

Delano-Wood, L., Bondi, M. W., Sacco, J., Abeles, N., Jak, A. J., Libon, D. J., & Bozoki, A. (2009). Heterogeneity in mild cognitive impairment: Differences in neuropsychological profile and associated white matter lesion pathology. *Journal of the International Neuropsychological Society: JINS*, *15*(6), 906–914. https://doi.org/10.1017/S1355617709990257

Deshmukh, A. A., Sharma, S., Cutler, J. W., Moldwin, M., & Scott, C. (2020). *Simple Regret Minimization for Contextual Bandits* (No. arXiv:1810.07371). arXiv. https://doi.org/10.48550/arXiv.1810.07371

DeVito, E. E., Blackwell, A. D., Clark, L., Kent, L., Dezsery, A. M., Turner, D. C., Aitken, M. R. F., & Sahakian, B. J. (2009). Methylphenidate improves response inhibition but not reflection–impulsivity in children with attention deficit hyperactivity disorder (ADHD). *Psychopharmacology*, *202*(1–3), 531–539. https://doi.org/10.1007/s00213-008-1337-y

Dobrynina, L. A., Kremneva, E. I., Shamtieva, K. V., Geints, A. A., Filatov, A. S., Gadzhieva, Z. S., Gnedovskaya, E. V., Krotenkova, M. V., & Maximov, I. I. (2024). Cognitive Impairment in Cerebral Small Vessel Disease Is Associated with Corpus Callosum Microstructure Changes Based on Diffusion MRI. *Diagnostics*, *14*(16), Article 16. https://doi.org/10.3390/diagnostics14161838

Docx, L., de la Asuncion ,Javier, Sabbe ,Bernard, Hoste ,Lode, Baeten ,Robin, Warnaerts ,Nattapon, & and Morrens, M. (2015). Effort discounting and its association with negative symptoms in schizophrenia. *Cognitive Neuropsychiatry*, *20*(2), 172–185. https://doi.org/10.1080/13546805.2014.993463

Duering, M., Biessels, G. J., Brodtmann, A., Chen, C., Cordonnier, C., de Leeuw, F.-E., Debette, S., Frayne, R., Jouvent, E., Rost, N. S., ter Telgte, A., Al-Shahi Salman, R., Backes, W. H., Bae, H.-J., Brown, R., Chabriat, H., De Luca, A., deCarli, C., Dewenter, A., … Wardlaw, J. M. (2023). Neuroimaging standards for research into small vessel disease—Advances since 2013. *The Lancet Neurology*, *22*(7), 602–618. https://doi.org/10.1016/S1474-4422(23)00131-X

Duering, M., Finsterwalder, S., Baykara, E., Tuladhar, A. M., Gesierich, B., Konieczny, M. J., Malik, R., Franzmeier, N., Ewers, M., Jouvent, E., Biessels, G. J., Schmidt, R., de Leeuw, F.-E., Pasternak, O., & Dichgans, M. (2018). Free water determines diffusion alterations and clinical status in cerebral small vessel disease. *Alzheimer's & Dementia*, *14*(6), 764–774. https://doi.org/10.1016/j.jalz.2017.12.007

Duering, M., Righart, R., Csanadi, E., Jouvent, E., Hervé, D., Chabriat, H., & Dichgans, M. (2012). Incident subcortical infarcts induce focal thinning in connected cortical

regions. *Neurology*, *79*(20), 2025–2028. https://doi.org/10.1212/wnl.0b013e3182749f39

Duering, M., Zieren, N., Hervé, D., Jouvent, E., Reyes, S., Peters, N., Pachai, C., Opherk, C., Chabriat, H., & Dichgans, M. (2011). Strategic role of frontal white matter tracts in vascular cognitive impairment: A voxel-based lesion-symptom mapping study in CADASIL. *Brain*, *134*(8), 2366–2375. https://doi.org/10.1093/brain/awr169

Elamin, M., Holloway, G., Bak, T. H., & Pal, S. (2016). The Utility of the Addenbrooke's Cognitive Examination Version Three in Early-Onset Dementia. *Dementia and Geriatric Cognitive Disorders*, *41*(1–2), 9–15. https://doi.org/10.1159/000439248

Elosegi, P., Rahnev, D., & Soto, D. (2024). Think twice: Re-assessing confidence improves visual metacognition. *Attention, Perception, & Psychophysics*, *86*(2), 373–380. https://doi.org/10.3758/s13414-023-02823-0

Erfanian Abdoust, M., Knecht, S., Husain, M., Le Heron, C., Jocham, G., & Studer, B. (2024). Effort-based decision making and motivational deficits in stroke patients. *Brain and Cognition*, *175*, 106123. https://doi.org/10.1016/j.bandc.2023.106123

Ernst, M., & Paulus, M. P. (2005). Neurobiology of Decision Making: A Selective Review from a Neurocognitive and Clinical Perspective. *Biological Psychiatry*, *58*(8), 597–604. https://doi.org/10.1016/j.biopsych.2005.06.004

Euston, D. R., Gruber, A. J., & McNaughton, B. L. (2012). The Role of Medial Prefrontal Cortex in Memory and Decision Making. *Neuron*, *76*(6), 1057–1070. https://doi.org/10.1016/j.neuron.2012.12.002

Fazekas, F., Chawluk, J. B., Alavi, A., Hurtig, H. I., & Zimmerman, R. A. (1987). *MR signal abnormalities at 1.5 T in Alzheimer's dementia and normal aging*. https://doi.org/10.2214/ajr.149.2.351

Fellows, L. K., & Farah, M. J. (2005). Different Underlying Impairments in Decision-making Following Ventromedial and Dorsolateral Frontal Lobe Damage in Humans. *Cerebral Cortex*, *15*(1), 58–63. https://doi.org/10.1093/cercor/bhh108

Fellows, L. K., & Farah, M. J. (2007). The Role of Ventromedial Prefrontal Cortex in Decision Making: Judgment under Uncertainty or Judgment Per Se? *Cerebral Cortex*, *17*(11), 2669–2674. https://doi.org/10.1093/cercor/bhl176

Feng, M., Song, Z., Zhou, Z., Wu, Z., Ma, M., Liu, Y., Wang, Y., & Dai, H. (2024). Cognitive impairment mediates the white matter injury load and gait disorders in subcortical ischemic vascular disease. *Brain Imaging and Behavior*, *18*(6), 1418–1427. https://doi.org/10.1007/s11682-024-00941-3

Feng, Y., Chandio, B. Q., Villalon-Reina, J. E., Thomopoulos, S. I., Nir, T. M., Benavidez, S., Laltoo, E., Chattopadhyay, T., Joshi, H., Venkatasubramanian, G., John, J. P., Jahanshad, N., Reid, R. I., Jack, C. R., Weiner, M. W., Thompson, P. M., & Initiative, for the A. D. N. (2025). Microstructural mapping of neural pathways in Alzheimer's disease using macrostructure-informed normative tractometry. *Alzheimer's & Dementia*, *21*(1), e14371. https://doi.org/10.1002/alz.14371

Fervaha, G., Graff-Guerrero, A., Zakzanis, K. K., Foussias, G., Agid, O., & Remington, G. (2013). Incentive motivation deficits in schizophrenia reflect effort computation impairments during cost-benefit decision-making. *Journal of Psychiatric Research*, *47*(11), 1590–1596. https://doi.org/10.1016/j.jpsychires.2013.08.003

Fleming, S. M., Huijgen, J., & Dolan, R. J. (2012). Prefrontal Contributions to Metacognition in Perceptual Decision Making. *The Journal of Neuroscience*, *32*(18), 6117–6125. https://doi.org/10.1523/JNEUROSCI.6489-11.2012

Forstmann, B. U., Ratcliff, R., & Wagenmakers, E.-J. (2016). Sequential Sampling Models in Cognitive Neuroscience: Advantages, Applications, and Extensions. *Annual Review of Psychology*, *67*, 641–666. https://doi.org/10.1146/annurev-psych-122414-033645

Fu, W., Huang, Z., Li, J., Dong, Q., Li, Y., Li, G., Xu, Y., Xue, B., Li, Z., Chen, C., Sun, S., Zhang, Y., Hou, Z., & Xie, J. (2022). Reduced sensitivity to delayed time and delayed reward of the post-operative insular glioma patients in delay discounting. *NeuroImage: Clinical*, *33*, 102895. https://doi.org/10.1016/j.nicl.2021.102895

Fülöp, J. (2005). Introduction to Decision Making Methods. *ResearchGate*. https://www.researchgate.net/publication/240754177_Introduction_to_Decision_Making_Methods

Furl, N., & Averbeck, B. B. (2011). Parietal Cortex and Insula Relate to Evidence Seeking Relevant to Reward-Related Decisions. *Journal of Neuroscience*, *31*(48), 17572–17582. https://doi.org/10.1523/JNEUROSCI.4236-11.2011

Gabb, V. G., Blackman, J., Morrison, H., Li, H., Kendrick, A., Turner, N., Greenwood, R., Biswas, B., Heslegrave, A., & Coulthard, E. (2025). Longitudinal Remote Sleep and Cognitive Research in Older Adults With Mild Cognitive Impairment and Dementia: Prospective Feasibility Cohort Study. *JMIR Aging*, *8*, e72824. https://doi.org/10.2196/72824

Gajwani, M., Oldham, S., Pang, J. C., Arnatkevičiūtė, A., Tiego, J., Bellgrove, M. A., & Fornito, A. (2023). Can hubs of the human connectome be identified consistently with diffusion MRI? *Network Neuroscience*, *7*(4), 1326–1350. https://doi.org/10.1162/netn_a_00324

Gangopadhyay, P., Chawla, M., Monte, O. D., & Chang, S. W. C. (2021). Prefrontal-Amygdala Circuits in Social Decision-Making. *Nature Neuroscience*, *24*(1), 5–18. https://doi.org/10.1038/s41593-020-00738-9

Gendolla, G. H. E., Tops, M., & Koole, S. L. (2014). *Handbook of Biobehavioral Approaches to Self-Regulation*. Springer New York. http://ebookcentral.proquest.com/lib/oxford/detail.action?docID=1965064

Gigerenzer, G., & Goldstein, D. G. (1996). Reasoning the fast and frugal way: Models of bounded rationality. *Psychological Review*, *103*(4), 650–669. https://doi.org/10.1037/0033-295X.103.4.650

Gigerenzer, G., Martignon, L., Hoffrage, U., Rieskamp, J., Czerlinski, J., & Goldstein, D. G. (2008). Chapter 108 One-Reason Decision Making. In C. R. Plott & V. L. Smith (Eds), *Handbook of Experimental Economics Results* (Vol. 1, pp. 1004–1017). Elsevier. https://doi.org/10.1016/S1574-0722(07)00108-4

Gillespie, S. M., Lee, J., Williams, R., & Jones, A. (2022). Psychopathy and response inhibition: A meta-analysis of go/no-go and stop signal task performance. *Neuroscience and Biobehavioral Reviews*, *142*, 104868. https://doi.org/10.1016/j.neubiorev.2022.104868

Gold, J. M., Kool, W., Botvinick, M. M., Hubzin, L., August, S., & Waltz, J. A. (2015). Cognitive effort avoidance and detection in people with schizophrenia.

Cognitive, Affective & Behavioral Neuroscience, *15*(1), 145–154. https://doi.org/10.3758/s13415-014-0308-5

Gold, J. M., Strauss, G. P., Waltz, J. A., Robinson, B. M., Brown, J. K., & Frank, M. J. (2013). Negative Symptoms of Schizophrenia Are Associated with Abnormal Effort-Cost Computations. *Biological Psychiatry*, *74*(2), 130–136. https://doi.org/10.1016/j.biopsych.2012.12.022

Goldenberg, D., Telzer, E. H., Lieberman, M. D., Fuligni, A. J., & Galván, A. (2017). Greater response variability in adolescents is associated with increased white matter development. *Social Cognitive and Affective Neuroscience*, *12*(3), 436–444. https://doi.org/10.1093/scan/nsw132

Goldstein, A., Covington, B. P., Mahabadi, N., & Mesfin, F. B. (2025). Neuroanatomy, Corpus Callosum. In *StatPearls*. StatPearls Publishing. http://www.ncbi.nlm.nih.gov/books/NBK448209/

Goldwaser, E. L., Du, X., Adhikari, B. M., Kvarta, M., Chiappelli, J., Hare, S., Marshall, W., Savransky, A., Carino, K., Bruce, H., Acheson, A., Kochunov, P., & Elliot Hong, L. (2022). The Role of White Matter Microstructure in Impulsive Behavior. *The Journal of Neuropsychiatry and Clinical Neurosciences*, *34*(3), 254–260. https://doi.org/10.1176/appi.neuropsych.21070167

Gómez Escobar, G., & Mitchell, S. (2025). A systematic review of effort discounting research in humans: Current knowledge, recommendations, and future directions. *Judgment and Decision Making*, *20*, 1–33. https://doi.org/10.1017/jdm.2025.10009

Gootjes, L., Teipel, S. J., Zebuhr, Y., Schwarz, R., Leinsinger, G., Scheltens, P., Möller, H.-J., & Hampel, H. (2004). Regional Distribution of White Matter

Hyperintensities in Vascular Dementia, Alzheimer's Disease and Healthy Aging. *Dementia and Geriatric Cognitive Disorders*, *18*(2), 180–188. https://doi.org/10.1159/000079199

Gosseries, O., Demertzi, A., Noirhomme, Q., Tshibanda, J., Boly, M., Op de Beeck, M., Hustinx, R., Maquet, P., Salmon, E., Moonen, G., Luxen, A., Laureys, S., & De Tiège, X. (2008). [Functional neuroimaging (fMRI, PET and MEG): What do we measure?]. *Revue Medicale De Liege*, *63*(5–6), 231–237.

Gouw, A. A., Van der Flier, W. M., van Straaten, E. C. W., Barkhof, F., Ferro, J. M., Baezner, H., Pantoni, L., Inzitari, D., Erkinjuntti, T., Wahlund, L. O., Waldemar, G., Schmidt, R., Fazekas, F., Scheltens, P., & LADIS Study Group. (2006). Simple versus complex assessment of white matter hyperintensities in relation to physical performance and cognition: The LADIS study. *Journal of Neurology*, *253*(9), 1189–1196. https://doi.org/10.1007/s00415-006-0193-5

Green, L., & Myerson, J. (2004). A Discounting Framework for Choice With Delayed and Probabilistic Rewards. *Psychological Bulletin*, *130*(5), 769–792. https://doi.org/10.1037/0033-2909.130.5.769

Green, M. F., Horan, W. P., Barch, D. M., & Gold, J. M. (2015). Effort-Based Decision Making: A Novel Approach for Assessing Motivation in Schizophrenia. *Schizophrenia Bulletin*, *41*(5), 1035–1044. https://doi.org/10.1093/schbul/sbv071

Griffanti, L., Zamboni, G., Khan, A., Li, L., Bonifacio, G., Sundaresan, V., Schulz, U. G., Kuker, W., Battaglini, M., Rothwell, P. M., & Jenkinson, M. (2016a). BIANCA (Brain Intensity AbNormality Classification Algorithm): A new tool for automated

segmentation of white matter hyperintensities. *NeuroImage*, *141*, 191–205. https://doi.org/10.1016/j.neuroimage.2016.07.018

Griffanti, L., Zamboni, G., Khan, A., Li, L., Bonifacio, G., Sundaresan, V., Schulz, U. G., Kuker, W., Battaglini, M., Rothwell, P. M., & Jenkinson, M. (2016b). BIANCA (Brain Intensity AbNormality Classification Algorithm): A new tool for automated segmentation of white matter hyperintensities. *NeuroImage*, *141*, 191–205. https://doi.org/10.1016/j.neuroimage.2016.07.018

Gu, Z., Gu, L., Eils, R., Schlesner, M., & Brors, B. (2014). Circlize implements and enhances circular visualization in R. *Bioinformatics*, *30*(19), 2811–2812. https://doi.org/10.1093/bioinformatics/btu393

Guo, Y., Wu, H., Li, Z., Zhao, L., & Feng, T. (2022). Episodic future thinking predicts differences in delay discounting: The mediating role of hippocampal structure. *Frontiers in Psychology*, *13*. https://doi.org/10.3389/fpsyg.2022.992245

Gupta, A. K., Smith, K. G., & Shalley, C. E. (2006). The interplay between exploration and exploitation. *Academy of Management Journal*, *49*(4), 693–706. https://doi.org/10.5465/AMJ.2006.22083026

Hamilton, O. K. L., Backhouse, E. V., Janssen, E., Jochems, A. C. C., Maher, C., Ritakari, T. E., Stevenson, A. J., Xia, L., Deary, I. J., & Wardlaw, J. M. (2021). Cognitive impairment in sporadic cerebral small vessel disease: A systematic review and meta-analysis. *Alzheimer's & Dementia: The Journal of the Alzheimer's Association*, *17*(4), 665–685. https://doi.org/10.1002/alz.12221

Harhen, N. C., & Bornstein, A. M. (2023). Overharvesting in human patch foraging reflects rational structure learning and adaptive planning. *Proceedings of the*

National Academy of Sciences of the United States of America, *120*(13), e2216524120. https://doi.org/10.1073/pnas.2216524120

Harmon-Jones, E., Willoughby, C., Paul, K., & Harmon-Jones, C. (2020). The effect of perceived effort and perceived control on reward valuation: Using the reward positivity to test a dissonance theory prediction. *Biological Psychology*, *154*, 107910. https://doi.org/10.1016/j.biopsycho.2020.107910

Hartmann, M. N., Hager, O. M., Reimann, A. V., Chumbley, J. R., Kirschner, M., Seifritz, E., Tobler, P. N., & Kaiser, S. (2015). Apathy But Not Diminished Expression in Schizophrenia Is Associated With Discounting of Monetary Rewards by Physical Effort. *Schizophrenia Bulletin*, *41*(2), 503–512. https://doi.org/10.1093/schbul/sbu102

Hassall, C. D., Yan, Y., & Hunt, L. T. (2023). The neural correlates of continuous feedback processing. *Psychophysiology*, *60*(12), e14399. https://doi.org/10.1111/psyp.14399

Heath, C. J., O'Callaghan, C., Mason, S. L., Phillips, B. U., Saksida, L. M., Robbins, T. W., Barker, R. A., Bussey, T. J., & Sahakian, B. J. (2019). A Touchscreen Motivation Assessment Evaluated in Huntington's Disease Patients and R6/1 Model Mice. *Frontiers in Neurology*, *10*, 858. https://doi.org/10.3389/fneur.2019.00858

Heilbronner, S. R., & Haber, S. N. (2014). Frontal Cortical and Subcortical Projections Provide a Basis for Segmenting the Cingulum Bundle: Implications for Neuroimaging and Psychiatric Disorders. *The Journal of Neuroscience*, *34*(30), 10041–10054. https://doi.org/10.1523/JNEUROSCI.5459-13.2014

Heilbronner, S. R., & Hayden, B. Y. (2016). Dorsal Anterior Cingulate Cortex: A Bottom-Up View. *Annual Review of Neuroscience*, *39*, 149–170. https://doi.org/10.1146/annurev-neuro-070815-013952

Herbet, G., Zemmoura, I., & Duffau, H. (2018). Functional Anatomy of the Inferior Longitudinal Fasciculus: From Historical Reports to Current Hypotheses. *Frontiers in Neuroanatomy*, *12*, 77. https://doi.org/10.3389/fnana.2018.00077

Hernandez Lallement, J., Kuss, K., Trautner, P., Weber, B., Falk, A., & Fliessbach, K. (2014). Effort increases sensitivity to reward and loss magnitude in the human brain. *Social Cognitive and Affective Neuroscience*, *9*(3), 342–349. https://doi.org/10.1093/scan/nss147

Hertwig, R., Barron, G., Weber, E. U., & Erev, I. (2004). Decisions from Experience and the Effect of Rare Events in Risky Choice. *Psychological Science*, *15*(8), 534–539.

Hippmann, B., Tzvi, E., Göttlich, M., Weiblen, R., Münte, T. F., & Jessen, S. (2021). Effective connectivity underlying reward-based executive control. *Human Brain Mapping*, *42*(14), 4555–4567. https://doi.org/10.1002/hbm.25564

Hogan, P., Galaro, J., & Chib, V. (2019). Roles of Ventromedial Prefrontal Cortex and Anterior Cingulate in Subjective Valuation of Prospective Effort. *Cerebral Cortex (New York, N.Y. : 1991)*, *29*, 4277–4290. https://doi.org/10.1093/cercor/bhy310

Hollocks, M. J., Lawrence, A. J., Brookes, R. L., Barrick, T. R., Morris, R. G., Husain, M., & Markus, H. S. (2015). Differential relationships between apathy and depression with white matter microstructural changes and functional outcomes. *Brain*, *138*(12), 3803–3815. https://doi.org/10.1093/brain/awv304

Hong, H., Yu, X., Zhang, R., Jiaerken, Y., Wang, S., Luo, X., Lou, M., Huang, P., & Zhang, M. (2021). Cortical degeneration detected by neurite orientation dispersion and

density imaging in chronic lacunar infarcts. *Quantitative Imaging in Medicine and Surgery*, *11*(5), 2114–2124. https://doi.org/10.21037/qims-20-880

Hsieh, S., Schubert, S., Hoon, C., Mioshi, E., & Hodges, J. R. (2013). Validation of the Addenbrooke's Cognitive Examination III in Frontotemporal Dementia and Alzheimer's Disease. *Dementia and Geriatric Cognitive Disorders*, *36*(3–4), 242–250. https://doi.org/10.1159/000351671

Hu, A.-M., Ma, Y.-L., Li, Y.-X., Han, Z.-Z., Yan, N., & Zhang, Y.-M. (2022). Association between Changes in White Matter Microstructure and Cognitive Impairment in White Matter Lesions. *Brain Sciences*, *12*(4), 482. https://doi.org/10.3390/brainsci12040482

Huang, L., Chen, X., Sun, W., Chen, H., Ye, Q., Yang, D., Li, M., Luo, C., Ma, J., Shao, P., Xu, H., Zhang, B., Zhu, X., & Xu, Y. (2020). Early Segmental White Matter Fascicle Microstructural Damage Predicts the Corresponding Cognitive Domain Impairment in Cerebral Small Vessel Disease Patients by Automated Fiber Quantification. *Frontiers in Aging Neuroscience*, *12*, 598242. https://doi.org/10.3389/fnagi.2020.598242

Huettel, S. A., Song, A. W., & McCarthy, G. (2005a). Decisions under Uncertainty: Probabilistic Context Influences Activation of Prefrontal and Parietal Cortices. *Journal of Neuroscience*, *25*(13), 3304–3311. https://doi.org/10.1523/JNEUROSCI.5070-04.2005

Huettel, S. A., Song, A. W., & McCarthy, G. (2005b). Decisions under Uncertainty: Probabilistic Context Influences Activation of Prefrontal and Parietal Cortices. *The Journal of Neuroscience*, *25*(13), 3304–3311. https://doi.org/10.1523/JNEUROSCI.5070-04.2005

Huijts, M., Duits, A., Van Oostenbrugge, R., Kroon, A., De Leeuw, P., & Staals, J. (2013). Accumulation of MRI Markers of Cerebral Small Vessel Disease is Associated with Decreased Cognitive Function. A Study in First-Ever Lacunar Stroke and Hypertensive Patients. *Frontiers in Aging Neuroscience*, *5*. https://www.frontiersin.org/articles/10.3389/fnagi.2013.00072

Hutchinson, J. M. C., Wilke, A., & Todd, P. M. (2008). Patch leaving in humans: Can a generalist adapt its rules to dispersal of items across patches? *Animal Behaviour*, *75*(4), 1331–1349. https://doi.org/10.1016/j.anbehav.2007.09.006

Ide, T., Yakushiji, Y., Suzuyama, K., Nishihara, M., Eriguchi, M., Ogata, A., Matsumoto, A., Hara, M., & Hara, H. (2024). Associations for progression of cerebral small vessel disease burden in healthy adults: The Kashima scan study. *Hypertension Research*, *47*(2), 302–310. https://doi.org/10.1038/s41440-023-01419-3

Inzlicht, M., Shenhav, A., & Olivola, C. Y. (2018). The Effort Paradox: Effort Is Both Costly and Valued. *Trends in Cognitive Sciences*, *22*(4), 337–349. https://doi.org/10.1016/j.tics.2018.01.007

Ithapu, V., Singh, V., Lindner, C., Austin, B. P., Hinrichs, C., Carlsson, C. M., Bendlin, B. B., & Johnson, S. C. (2014). Extracting and summarizing white matter hyperintensities using supervised segmentation methods in Alzheimer's disease risk and aging studies. *Human Brain Mapping*, *35*(8), 4219–4235. https://doi.org/10.1002/hbm.22472

Jackson, S. A., Kleitman, S., Howie, P., & Stankov, L. (2016). Cognitive Abilities, Monitoring Confidence, and Control Thresholds Explain Individual Differences in Heuristics and Biases. *Frontiers in Psychology*, *7*, 1559. https://doi.org/10.3389/fpsyg.2016.01559

Jacobus, J., Thayer, R. E., Trim, R. S., Bava, S., Frank, L. R., & Tapert, S. F. (2013). White matter integrity, substance use, and risk taking in adolescence. *Psychology of Addictive Behaviors*, *27*(2), 431–442. https://doi.org/10.1037/a0028235

Janelle, F., Iorio-Morin, C., D'amour, S., & Fortin, D. (2022). Superior Longitudinal Fasciculus: A Review of the Anatomical Descriptions With Functional Correlates. *Frontiers in Neurology*, *13*, 794618. https://doi.org/10.3389/fneur.2022.794618

Jin, Y., Huang, C., Daianu, M., Zhan, L., Dennis, E. L., Reid, R. I., Jack, C. R., Zhu, H., & Thompson, P. M. (2016). 3D tract-specific local and global analysis of white matter integrity in Alzheimer's disease. *Human Brain Mapping*, *38*(3), 1191–1207. https://doi.org/10.1002/hbm.23448

Jochems, A. C. C., Arteaga, C., Chappell, F., Ritakari, T., Hooley, M., Doubal, F., Muñoz Maniega, S., & Wardlaw, J. M. (2022). Longitudinal Changes of White Matter Hyperintensities in Sporadic Small Vessel Disease. *Neurology*, *99*(22), e2454–e2463. https://doi.org/10.1212/WNL.0000000000201205

Jochems, A. C. C., Muñoz Maniega, S., Clancy, U., Arteaga-Reyes, C., Jaime Garcia, D., Chappell, F. M., Hamilton, O. K. L., Backhouse, E. V., Barclay, G., Jardine, C., McIntyre, D., Hamilton, I., Sakka, E., Valdés Hernández, M. D. C., Wiseman, S., Bastin, M. E., Stringer, M. S., Thrippleton, M., Doubal, F., & Wardlaw, J. M. (2025). Longitudinal Cognitive Changes in Cerebral Small Vessel Disease: The Effect of White Matter Hyperintensity Regression and Progression. *Neurology*, *104*(4), e213323. https://doi.org/10.1212/WNL.0000000000213323

Jokinen, H., Kalska, H., Ylikoski, R., Madureira, S., Verdelho, A., Van Der Flier, W. M., Scheltens, P., Barkhof, F., Visser, M. C., Fazekas, F., Schmidt, R., O'Brien, J.,

Waldemar, G., Wallin, A., Chabriat, H., Pantoni, L., Inzitari, D., & Erkinjuntti, T. (2009). Longitudinal Cognitive Decline in Subcortical Ischemic Vascular Disease – The LADIS Study. *Cerebrovascular Diseases*, *27*(4), 384–391. https://doi.org/10.1159/000207442

Jolly, A. A., Brown, R. B., Tozer, D. J., Hong, Y. T., Fryer, T. D., Aigbirhio, F. I., O'Brien, J. T., & Markus, H. S. (2024). Are central and systemic inflammation associated with fatigue in cerebral small vessel disease? *International Journal of Stroke: Official Journal of the International Stroke Society*, *19*(6), 705–713. https://doi.org/10.1177/17474930241245613

Juni, M. Z., Gureckis, T. M., & Maloney, L. T. (2016). Information sampling behavior with explicit sampling costs. *Decision (Washington, D.C.)*, *3*(3), 147–168. https://doi.org/10.1037/dec0000045

Kaanders, P., Nili, H., O'Reilly, J. X., & Hunt, L. (2021). Medial Frontal Cortex Activity Predicts Information Sampling in Economic Choice. *The Journal of Neuroscience*, *41*(40), 8403–8413. https://doi.org/10.1523/JNEUROSCI.0392-21.2021

Kable, J. W., & Glimcher, P. W. (2007a). Predicting Adolescent Cognitive and Self-Regulatory Competencies From Preschool Delay of Gratification: Identifying Diagnostic Conditions. *Nature Publishing Group*. https://oce-ovid-com.ezproxy-prd.bodleian.ox.ac.uk/article/00063061-199011000-00014/HTML

Kable, J. W., & Glimcher, P. W. (2007b). The neural correlates of subjective value during intertemporal choice. *Nature Neuroscience*, *10*(12), 1625–1633. https://doi.org/10.1038/nn2007

Kagan, J. (1964). *Matching Familiar Figures Test*. Harvard University.

Kahneman, D., & Tversky, A. (1979). Prospect Theory: An Analysis of Decision under Risk. *Econometrica*, *47*(2), 263–291. https://doi.org/10.2307/1914185

Kalhan, S., McFadyen, J., Tsuchiya, N., & Garrido, M. I. (2022). Neural and computational processes of accelerated perceptual awareness and decisions: A 7T fMRI study. *Human Brain Mapping*, *43*(12), 3873–3886. https://doi.org/10.1002/hbm.25889

Keller, A. M., Taylor, H. A., & Brunyé, T. T. (2020). Uncertainty promotes information-seeking actions, but what information? *Cognitive Research: Principles and Implications*, *5*(1), 42. https://doi.org/10.1186/s41235-020-00245-2

Kennerley, S. W., & Walton, M. E. (2011a). Decision making and reward in frontal cortex: Complementary evidence from neurophysiological and neuropsychological studies. *Behavioral Neuroscience*, *125*(3), 297–317. https://doi.org/10.1037/a0023575

Kennerley, S. W., & Walton, M. E. (2011b). Decision making and reward in frontal cortex: Complementary evidence from neurophysiological and neuropsychological studies. *Behavioral Neuroscience*, *125*(3), 297–317. https://doi.org/10.1037/a0023575

Kilpatrick, Z. P., Davidson, J. D., & El Hady, A. (2021). Uncertainty drives deviations in normative foraging decision strategies. *Journal of The Royal Society Interface*, *18*(180), 20210337. https://doi.org/10.1098/rsif.2021.0337

Kim, S., Han, C. E., Kim, B., Winstein, C. J., & Schweighofer, N. (2022). Effort, success, and side of lesion determine arm choice in individuals with chronic stroke. *Journal of Neurophysiology*, *127*(1), 255–266. https://doi.org/10.1152/jn.00532.2020

Klein-Flügge, M. C., Kennerley, S. W., Friston, K., & Bestmann, S. (2016). Neural Signatures of Value Comparison in Human Cingulate Cortex during Decisions Requiring an Effort-Reward Trade-off. *Journal of Neuroscience*, *36*(39), 10002–10015. https://doi.org/10.1523/JNEUROSCI.0292-16.2016

Koechlin, E. (2016). Prefrontal executive function and adaptive behavior in complex environments. *Current Opinion in Neurobiology*, *37*, 1–6. https://doi.org/10.1016/j.conb.2015.11.004

Kolling, N., Behrens, T. E. J., Mars, R. B., & Rushworth, M. F. S. (2012). Neural Mechanisms of Foraging. *Science*, *336*(6077), 95–98. https://doi.org/10.1126/science.1216930

Konieczny, M. J., Dewenter, A., ter Telgte, A., Gesierich, B., Wiegertjes, K., Finsterwalder, S., Kopczak, A., Hübner, M., Malik, R., Tuladhar, A. M., Marques, J. P., Norris, D. G., Koch, A., Dietrich, O., Ewers, M., Schmidt, R., de Leeuw, F.-E., & Duering, M. (2021). Multi-shell Diffusion MRI Models for White Matter Characterization in Cerebral Small Vessel Disease. *Neurology*, *96*(5), e698–e708. https://doi.org/10.1212/WNL.0000000000011213

Kool, W., McGuire, J. T., Rosen, Z. B., & Botvinick, M. M. (2010). Decision Making and the Avoidance of Cognitive Demand. *Journal of Experimental Psychology. General*, *139*(4), 665–682. https://doi.org/10.1037/a0020198

Kristjánsson, T., Thornton, I. M., Chetverikov, A., & Kristjánsson, Á. (2020). Dynamics of visual attention revealed in foraging tasks. *Cognition*, *194*, 104032. https://doi.org/10.1016/j.cognition.2019.104032

Krug, A., Cabanis, M., Pyka, M., Pauly, K., Walter, H., Landsberg, M., Shah, N. J., Winterer, G., Wölwer, W., Musso, F., Müller, B. W., Wiedemann, G., Herrlich, J.,

Schnell, K., Vogeley, K., Schilbach, L., Langohr, K., Rapp, A., Klingberg, S., & Kircher, T. (2014). Investigation of decision-making under uncertainty in healthy subjects: A multi-centric fMRI study. *Behavioural Brain Research*, *261*, 89–96. https://doi.org/10.1016/j.bbr.2013.12.013

Kurniawan, I. T., Guitart-Masip, M., Dayan, P., & Dolan, R. J. (2013). Effort and Valuation in the Brain: The Effects of Anticipation and Execution. *Journal of Neuroscience*, *33*(14), 6160–6169. https://doi.org/10.1523/JNEUROSCI.4777-12.2013

Kurniawan, I. T., Guitart-Masip, M., & Dolan, R. J. (2011). Dopamine and Effort-Based Decision Making. *Frontiers in Neuroscience*, *5*, 81. https://doi.org/10.3389/fnins.2011.00081

Kveton, B., Szepesvari, C., Vaswani, S., Wen, Z., Ghavamzadeh, M., & Lattimore, T. (2019). *Garbage In, Reward Out: Bootstrapping Exploration in Multi-Armed Bandits* (No. arXiv:1811.05154). arXiv. https://doi.org/10.48550/arXiv.1811.05154

Lahna, D., Schwartz, D. L., Woltjer, R., Black, S. E., Roese, N., Dodge, H., Boespflug, E. L., Keith, J., Gao, F., Ramirez, J., & Silbert, L. C. (2022). Venous Collagenosis as Pathogenesis of White Matter Hyperintensity. *Annals of Neurology*, *92*(6), 992–1000. https://doi.org/10.1002/ana.26487

Lamichhane, B., & Dhamala, M. (2015). The Salience Network and Its Functional Architecture in a Perceptual Decision: An Effective Connectivity Study. *Brain Connectivity*, *5*(6), 362–370. https://doi.org/10.1089/brain.2014.0282

Lan, D. C. L., Hunt, L. T., & Summerfield, C. (2025). Goal-directed navigation in humans and deep reinforcement learning agents relies on an adaptive mix of vector-

based and transition-based strategies. *PLOS Biology*, *23*(7), e3003296. https://doi.org/10.1371/journal.pbio.3003296

Lane, S. D., Steinberg, J. L., Ma, L., Hasan, K. M., Kramer, L. A., Zuniga, E. A., Narayana, P. A., & Moeller, F. G. (2010). Diffusion Tensor Imaging and Decision Making in Cocaine Dependence. *PLOS ONE*, *5*(7), e11591. https://doi.org/10.1371/journal.pone.0011591

Laureiro-Martínez, D., Brusoni, S., Canessa, N., & Zollo, M. (2015). Understanding the exploration–exploitation dilemma: An fMRI study of attention control and decision-making performance. *Strategic Management Journal*, *36*(3), 319–338. https://doi.org/10.1002/smj.2221

Lawrence, A. J., Brookes, R. L., Zeestraten, E. A., Barrick, T. R., Morris, R. G., & Markus, H. S. (2015). Pattern and Rate of Cognitive Decline in Cerebral Small Vessel Disease: A Prospective Study. *PLOS ONE*, *10*(8), e0135523. https://doi.org/10.1371/journal.pone.0135523

Lawrence, A. J., Chung, A. W., Morris, R. G., Markus, H. S., & Barrick, T. R. (2014). Structural network efficiency is associated with cognitive impairment in small-vessel disease. *Neurology*, *83*(4), 304–311. https://doi.org/10.1212/WNL.0000000000000612

Lawrence, A. J., Patel, B., Morris, R. G., MacKinnon, A. D., Rich, P. M., Barrick, T. R., & Markus, H. S. (2013). Mechanisms of Cognitive Impairment in Cerebral Small Vessel Disease: Multimodal MRI Results from the St George's Cognition and Neuroimaging in Stroke (SCANS) Study. *PLoS ONE*, *8*(4), e61014. https://doi.org/10.1371/journal.pone.0061014

Le Heron, C., Manohar, S., Plant, O., Muhammed, K., Griffanti, L., Nemeth, A., Douaud, G., Markus, H. S., & Husain, M. (2018). Dysfunctional effort-based decision-making underlies apathy in genetic cerebral small vessel disease. *Brain*, *141*(11), 3193–3210. https://doi.org/10.1093/brain/awy257

Le Heron, C., Plant, O., Manohar, S., Ang, Y.-S., Jackson, M., Lennox, G., Hu, M. T., & Husain, M. (2018). Distinct effects of apathy and dopamine on effort-based decision-making in Parkinson's disease. *Brain*, *141*(5), 1455–1469. https://doi.org/10.1093/brain/awy110

Lefebvre, G., Summerfield, C., & Bogacz, R. (2022). A Normative Account of Confirmation Bias During Reinforcement Learning. *Neural Computation*, *34*(2), 307–337. https://doi.org/10.1162/neco_a_01455

Lenow, J. K., Constantino, S. M., Daw, N. D., & Phelps, E. A. (2017). Chronic and Acute Stress Promote Overexploitation in Serial Decision Making. *Journal of Neuroscience*, *37*(23), 5681–5689. https://doi.org/10.1523/JNEUROSCI.3618-16.2017

Levens, S. M., Larsen, J. T., Bruss, J., Tranel, D., Bechara, A., & Mellers, B. A. (2014). What might have been? The role of the ventromedial prefrontal cortex and lateral orbitofrontal cortex in counterfactual emotions and choice. *Neuropsychologia*, *54*, 77–86. https://doi.org/10.1016/j.neuropsychologia.2013.10.026

Li, B., Hu, X., Shanks, D. R., Su, N., Zhao, W., Meng, L., Lei, W., Luo, L., & Yang, C. (2024). Confidence ratings increase response thresholds in decision making. *Psychonomic Bulletin & Review*, *31*(3), 1093–1102. https://doi.org/10.3758/s13423-023-02380-5

Li, L., Chu, W., Langford, J., & Schapire, R. E. (2010). A Contextual-Bandit Approach to Personalized News Article Recommendation. *Proceedings of the 19th International Conference on World Wide Web*, 661–670. https://doi.org/10.1145/1772690.1772758

Li, M., Schilling, K. G., Xu, L., Choi, S., Gao, Y., Zu, Z., Anderson, A. W., Ding, Z., & Gore, J. C. (2024). White matter engagement in brain networks assessed by integration of functional and structural connectivity. *NeuroImage*, *302*, 120887. https://doi.org/10.1016/j.neuroimage.2024.120887

Li, Q., Yang, Y., Reis, C., Tao, T., Li, W., Li, X., & Zhang, J. H. (2018). Cerebral Small Vessel Disease. *Cell Transplantation*, *27*(12), 1711–1722. https://doi.org/10.1177/0963689718795148

Li, X., Wang, Z., Zhang, H., Zhao, W., Ji, Q., Zhang, X., Jia, X., Bai, G., Pan, Y., Wu, T., Yin, B., Shi, L., Li, Z., Ding, J., Zhang, J., Salat, D. H., & Bai, L. (2024). Tract-Specific White Matter Hyperintensities Disrupt Brain Networks and Associated With Cognitive Impairment in Mild Traumatic Brain Injury. *Human Brain Mapping*, *45*(17), e70050. https://doi.org/10.1002/hbm.70050

Li, Y., Wang, Y., Yu, F., & Chen, A. (2021). Large-scale reconfiguration of connectivity patterns among attentional networks during context-dependent adjustment of cognitive control. *Human Brain Mapping*, *42*(12), 3821–3832. https://doi.org/10.1002/hbm.25467

Lipszyc, J., Levin, H., Hanten, G., Hunter, J., Dennis, M., & Schachar, R. (2014). Frontal white matter damage impairs response inhibition in children following traumatic brain injury. *Archives of Clinical Neuropsychology: The Official Journal of the*

National Academy of Neuropsychologists, *29*(3), 289–299. https://doi.org/10.1093/arclin/acu004

Lisiecka-Ford, D. M., Tozer, D. J., Morris, R. G., Lawrence, A. J., Barrick, T. R., & Markus, H. S. (2018). Involvement of the reward network is associated with apathy in cerebral small vessel disease. *Journal of Affective Disorders*, *232*, 116–121. https://doi.org/10.1016/j.jad.2018.02.006

Liu, C., Tian, T., Qin, Y., Zhang, S., Li, Y., & Zhu, W. (2025). Changes of network controllability and structural-function coupling in cerebral small vessel disease. *Brain Structure & Function*, *230*(7), 125. https://doi.org/10.1007/s00429-025-02990-w

Liu, Y., Xia, Y., Wang, X., Wang, Y., Zhang, D., Nguchu, B. A., He, J., Wang, Y., Yang, L., Wang, Y., Ying, Y., Liang, X., Zhao, Q., Wu, J., Liang, Z., Ding, D., Dong, Q., Qiu, B., Cheng, X., & Gao, J.-H. (2021). White matter hyperintensities induce distal deficits in the connected fibers. *Human Brain Mapping*, *42*(6), 1910–1919. https://doi.org/10.1002/hbm.25338

Lockwood, P. L., Cutler, J., Drew, D., Abdurahman, A., Jeyaretna, D. S., Apps, M. A. J., Husain, M., & Manohar, S. G. (2024). Human ventromedial prefrontal cortex is necessary for prosocial motivation. *Nature Human Behaviour*, *8*(7), 1403–1416. https://doi.org/10.1038/s41562-024-01899-4

Löffler, A. (2015). *Worth the effort? Measuring component processes of effort-based decision making in lesion patients*. McGill University. https://escholarship.mcgill.ca/concern/theses/jd473027p

Logothetis, N. K. (2008). What we can do and what we cannot do with fMRI. *Nature*, *453*(7197), 869–878. https://doi.org/10.1038/nature06976

Lopez-Gamundi, P., Yao, Y.-W., Chong, T. T.-J., Heekeren, H. R., Herrero, E. M., & Pallares, J. M. (2021). *The neural basis of effort valuation: A meta-analysis of functional magnetic resonance imaging studies* (p. 2021.01.08.425909). bioRxiv. https://doi.org/10.1101/2021.01.08.425909

Manes, F., Sahakian, B., Clark, L., Rogers, R., Antoun, N., Aitken, M., & Robbins, T. (2002). Decision-making processes following damage to the prefrontal cortex. *Brain*, *125*(3), 624–639. https://doi.org/10.1093/brain/awf049

Manohar, S. G., & Husain, M. (2016). Human ventromedial prefrontal lesions alter incentivisation by reward. *Cortex*, *76*, 104–120. https://doi.org/10.1016/j.cortex.2016.01.005

Manohar, S., Lockwood, P., Drew, D., Fallon, S. J., Chong, T. T.-J., Jeyaretna, D. S., Baker, I., & Husain, M. (2021). Reduced decision bias and more rational decision making following ventromedial prefrontal cortex damage. *Cortex; a Journal Devoted to the Study of the Nervous System and Behavior*, *138*, 24–37. https://doi.org/10.1016/j.cortex.2021.01.015

Mansour L., S., Di Biase, M. A., Smith, R. E., Zalesky, A., & Seguin, C. (2023). Connectomes for 40,000 UK Biobank participants: A multi-modal, multi-scale brain network resource. *NeuroImage*, *283*, 120407. https://doi.org/10.1016/j.neuroimage.2023.120407

Marcowski, P., Białaszek, W., & Winkielman, P. (2025). Effort can have positive, negative, and nonmonotonic impacts on outcome value in economic choice. *Journal of Experimental Psychology: General*, *154*(6), 1628–1642. https://doi.org/10.1037/xge0001738

Marek, S., & Dosenbach, N. U. F. (2018). The frontoparietal network: Function, electrophysiology, and importance of individual precision mapping. *Dialogues in Clinical Neuroscience*, *20*(2), 133–140. https://doi.org/10.31887/DCNS.2018.20.2/smarek

Marzecová, A., Kaiser, L. F., & Maddah, A. (2021). Neuromodulation of Foraging Decisions: The Role of Dopamine. *Frontiers in Behavioral Neuroscience*, *15*, 660667. https://doi.org/10.3389/fnbeh.2021.660667

Mascalchi, M., Salvadori, E., Toschi, N., Giannelli, M., Orsolini, S., Ciulli, S., Ginestroni, A., Poggesi, A., Giorgio, A., Lorenzini, F., Pasi, M., De Stefano, N., Pantoni, L., Inzitari, D., Diciotti, S., & VMCI-Tuscany study group. (2019). DTI-derived indexes of brain WM correlate with cognitive performance in vascular MCI and small-vessel disease. A TBSS study. *Brain Imaging and Behavior*, *13*(3), 594–602. https://doi.org/10.1007/s11682-018-9873-5

Mata, F., Neves, F., Lage, G., Moraes, P., Mattos, P., Fuentes, D., Corrêa, D., & Malloy-Diniz, L. (2011). Neuropsychological assessment of the decision making process in children and adolescents: An integrative review of the literature. *Revista de Psiquiatria Clínica*, *38*, 106–115. https://doi.org/10.1590/S0101-60832011000300005

Mathuranath, P. S., Nestor, P. J., Berrios, G. E., Rakowicz, W., & Hodges, J. R. (2000). A brief cognitive test battery to differentiate Alzheimer's disease and frontotemporal dementia. *Neurology*, *55*(11), 1613–1620. https://doi.org/10.1212/01.wnl.0000434309.85312.19

Mayer, C., Nägele, F. L., Petersen, M., Frey, B. M., Hanning, U., Pasternak, O., Petersen, E., Gerloff, C., Thomalla, G., & Cheng, B. (2022). Free-water diffusion MRI

detects structural alterations surrounding white matter hyperintensities in the early stage of cerebral small vessel disease. *Journal of Cerebral Blood Flow & Metabolism*, *42*(9), 1707–1718. https://doi.org/10.1177/0271678X221093579

McAleese, K. E., Walker, L., Graham, S., Moya, E. L. J., Johnson, M., Erskine, D., Colloby, S. J., Dey, M., Martin-Ruiz, C., Taylor, J.-P., Thomas, A. J., McKeith, I. G., De Carli, C., & Attems, J. (2017). Parietal white matter lesions in Alzheimer's disease are associated with cortical neurodegenerative pathology, but not with small vessel disease. *Acta Neuropathologica*, *134*(3), 459–473. https://doi.org/10.1007/s00401-017-1738-2

McCarthy, L., Rubinsztein, J., Lowry, E., Flanagan, E., Menon, V., Vearncombe, S., Mioshi, E., & Hornberger, M. (2024). Cut-off scores for mild and moderate dementia on the Addenbrooke's Cognitive Examination-III and the Mini-Addenbrooke's Cognitive Examination compared with the Mini-Mental State Examination. *BJPsych Bulletin*, *48*(1), 12–18. https://doi.org/10.1192/bjb.2023.27

McClure, S. M., Laibson, D., & Cohen, J. (2004). Separate Neural Systems Value Immediate and Delayed Monetary Rewards. *Science (New York, N.Y.)*, *306*, 503–507. https://doi.org/10.1126/science.1100907

Medaglia, J. D., Huang, W., Karuza, E. A., Thompson-Schill, S. L., Ribeiro, A., & Bassett, D. S. (2016). *Functional Alignment with Anatomical Networks is Associated with Cognitive Flexibility* (No. arXiv:1611.08751). arXiv. https://doi.org/10.48550/arXiv.1611.08751

Mitchell, J. M., Fields, H. L., D'Esposito, M., & Boettiger, C. A. (2005). Impulsive Responding in Alcoholics. *Alcoholism: Clinical and Experimental Research*, *29*(12), 2158–2169. https://doi.org/10.1097/01.alc.0000191755.63639.4a

Mobbs, D., Trimmer, P. C., Blumstein, D. T., & Dayan, P. (2018). Foraging for foundations in decision neuroscience: Insights from ethology. *Nature Reviews Neuroscience*, *19*(7), 419–427. https://doi.org/10.1038/s41583-018-0010-7

Mok, J. N. Y., Green, L., Myerson, J., Kwan, D., Kurczek, J., Ciaramelli, E., Craver, C. F., & Rosenbaum, R. S. (2021). Does Ventromedial Prefrontal Cortex Damage Really Increase Impulsiveness? Delay and Probability Discounting in Patients with Focal Lesions. *Journal of Cognitive Neuroscience*, *33*(9), 1909–1927. https://doi.org/10.1162/jocn_a_01721

Monosov, I. E., Haber, S. N., Leuthardt, E. C., & Jezzini, A. (2020). Anterior cingulate cortex and the control of dynamic behavior in primates. *Current Biology : CB*, *30*(23), R1442–R1454. https://doi.org/10.1016/j.cub.2020.10.009

Moretti, R., & Signori, R. (2016). Neural Correlates for Apathy: Frontal-Prefrontal and Parietal Cortical- Subcortical Circuits. *Frontiers in Aging Neuroscience*, *8*. https://doi.org/10.3389/fnagi.2016.00289

Mori, S., Oishi, K., Jiang, H., Jiang, L., Li, X., Akhter, K., Hua, K., Faria, A. V., Mahmood, A., Woods, R., Toga, A., Pike, B., Neto, P. R., Evans, A., Zhang, J., Huang, H., Miller, M. I., Zijl, P. van, & Mazziotta, J. (2008). Stereotaxic White Matter Atlas Based on Diffusion Tensor Imaging in an ICBM Template. *NeuroImage*, *40*(2), 570–582. https://doi.org/10.1016/j.neuroimage.2007.12.035

Morwitz, V. G., & Fitzsimons, G. J. (2004). The Mere-Measurement Effect: Why Does Measuring Intentions Change Actual Behavior? *Journal of Consumer Psychology*, *14*(1–2), 64–74. https://doi.org/10.1207/s15327663jcp1401&2_8

Müller, T., Klein-Flügge, M. C., Manohar, S. G., Husain, M., & Apps, M. A. J. (2021). Neural and computational mechanisms of momentary fatigue and persistence in effort-based choice. *Nature Communications*, *12*(1), 4593. https://doi.org/10.1038/s41467-021-24927-7

Mushtaq, F., Bland, A. R., & Schaefer, A. (2011). Uncertainty and Cognitive Control. *Frontiers in Psychology*, *2*. https://doi.org/10.3389/fpsyg.2011.00249

Navarro, D. J., Newell, B. R., & Schulze, C. (2016). Learning and choosing in an uncertain world: An investigation of the explore–exploit dilemma in static and dynamic environments. *Cognitive Psychology*, *85*, 43–77. https://doi.org/10.1016/j.cogpsych.2016.01.001

Neumann, john V. (1944). *Theory Of Games And Economic Behavior*. http://archive.org/details/in.ernet.dli.2015.215284

Nishiyama, R. (2016). *Physical, emotional, and cognitive effort discounting in gain and loss situations | Request PDF*. ResearchGate. https://www.researchgate.net/publication/294122142_Physical_emotional_and_cognitive_effort_discounting_in_gain_and_loss_situations

Nitkunan, A., Barrick, T. R., Charlton, R. A., Clark, C. A., & Markus, H. S. (2008). Multimodal MRI in Cerebral Small Vessel Disease. *Stroke*, *39*(7), 1999–2005. https://doi.org/10.1161/STROKEAHA.107.507475

Nyquist, P. A., Yanek, L. R., Bilgel, M., Cuzzocreo, J. L., Becker, L. C., Chevalier-Davis, K., Yousem, D., Prince, J., Kral, B. G., Vaidya, D., & Becker, D. M. (2015). Effect of

white matter lesions on manual dexterity in healthy middle-aged persons. *Neurology*, *84*(19), 1920–1926. https://doi.org/10.1212/WNL.0000000000001557

O'Doherty, J. P. (2011). Contributions of the ventromedial prefrontal cortex to goal-directed action selection. *Annals of the New York Academy of Sciences*, *1239*(1), 118–129. https://doi.org/10.1111/j.1749-6632.2011.06290.x

O'Donnell, L. J., & Westin, C.-F. (2011). An introduction to diffusion tensor image analysis. *Neurosurgery Clinics of North America*, *22*(2), 185–viii. https://doi.org/10.1016/j.nec.2010.12.004

Ogut, E. (2025). Graph-theoretical mapping of cortical and subcortical network alterations in preclinical neurodegeneration. *Discover Neuroscience*, *20*. https://doi.org/10.1186/s13064-025-00214-9

Ojemann, J. G., Akbudak, E., Snyder, A. Z., McKinstry, R. C., Raichle, M. E., & Conturo, T. E. (1997). Anatomic Localization and Quantitative Analysis of Gradient Refocused Echo-Planar fMRI Susceptibility Artifacts. *NeuroImage*, *6*(3), 156–167. https://doi.org/10.1006/nimg.1997.0289

Opris, I., & Bruce, C. J. (2005). Neural circuitry of judgment and decision mechanisms. *Brain Research Reviews*, *48*(3), 509–526. https://doi.org/10.1016/j.brainresrev.2004.11.001

Østergaard, L., Engedal, T. S., Moreton, F., Hansen, M. B., Wardlaw, J. M., Dalkara, T., Markus, H. S., & Muir, K. W. (2016). Cerebral small vessel disease: Capillary pathways to stroke and cognitive decline. *Journal of Cerebral Blood Flow & Metabolism*, *36*(2), 302–325. https://doi.org/10.1177/0271678X15606723

O'Sullivan, M., Jones, D. K., Summers, P. E., Morris, R. G., Williams, S. C., & Markus, H. S. (2001). Evidence for cortical 'disconnection' as a mechanism of age-related cognitive decline. *Neurology*, *57*(4), 632–638. https://doi.org/10.1212/wnl.57.4.632

Oswald, L. M., Wand, G. S., Wong, D. F., Brown, C. H., Kuwabara, H., & Brašić, J. R. (2015). Risky Decision-Making and Ventral Striatal Dopamine Responses to Amphetamine: A Positron Emission Tomography [11C] Raclopride Study in Healthy Adults. *NeuroImage*, *113*, 26–36. https://doi.org/10.1016/j.neuroimage.2015.03.022

Palminteri, S., Lefebvre, G., Kilford, E. J., & Blakemore, S.-J. (2017). Confirmation bias in human reinforcement learning: Evidence from counterfactual feedback processing. *PLOS Computational Biology*, *13*(8), e1005684. https://doi.org/10.1371/journal.pcbi.1005684

Pan, W., Lu, J., Wu, L., Juan, K., & Lei, Y. (2023). Expending Effort May Share Neural Responses with Reward and Evokes High Subjective Satisfaction. *Biological Psychology*, *177*, 108480. https://doi.org/10.1016/j.biopsycho.2022.108480

Pantoni, L. (2010). Cerebral small vessel disease: From pathogenesis and clinical characteristics to therapeutic challenges. *The Lancet Neurology*, *9*(7), 689–701. https://doi.org/10.1016/S1474-4422(10)70104-6

Pasi, M., van Uden, I. W. M., Tuladhar, A. M., de Leeuw, F.-E., & Pantoni, L. (2016). White Matter Microstructural Damage on Diffusion Tensor Imaging in Cerebral Small Vessel Disease. *Stroke*, *47*(6), 1679–1684. https://doi.org/10.1161/STROKEAHA.115.012065

Passingham, R. E., Bengtsson, S. L., & Lau, H. C. (2010). Medial frontal cortex: From self-generated action to reflection on one's own performance. *Trends in Cognitive Sciences*, *14*(1), 16–21. https://doi.org/10.1016/j.tics.2009.11.001

Patt, V. M., Hunsberger, R., Jones, D. A., Keane, M. M., & Verfaellie, M. (2021). Temporal discounting when outcomes are experienced in the moment: Validation of a novel paradigm and comparison with a classic hypothetical intertemporal choice task. *PloS One*, *16*(5), e0251480. https://doi.org/10.1371/journal.pone.0251480

Patt, V. M., Hunsberger, R., Jones, D. A., & Verfaellie, M. (2023). The Hippocampus Contributes to Temporal Discounting When Delays and Rewards Are Experienced in the Moment. *The Journal of Neuroscience*, *43*(31), 5710–5722. https://doi.org/10.1523/JNEUROSCI.2250-22.2023

Patton, J. H., Stanford, M. S., & Barratt, E. S. (1995). Factor structure of the barratt impulsiveness scale. *Journal of Clinical Psychology*, *51*(6), 768–774. https://doi.org/10.1002/1097-4679(199511)51:6%253C768::AID-JCLP2270510607%253E3.0.CO;2-1

Penke, L., Maniega, S. M., Murray, C., Gow, A. J., Valdés Hernández, M. C., Clayden, J. D., Starr, J. M., Wardlaw, J. M., Bastin, M. E., & Deary, I. J. (2010). A General Factor of Brain White Matter Integrity Predicts Information Processing Speed in Healthy Older People. *The Journal of Neuroscience*, *30*(22), 7569–7574. https://doi.org/10.1523/JNEUROSCI.1553-10.2010

Petitet, P., Attaallah, B., Manohar, S. G., & Husain, M. (2021). The computational cost of active information sampling before decision-making under uncertainty. *Nature Human Behaviour*, *5*(7), Article 7. https://doi.org/10.1038/s41562-021-01116-6

Pinter, D. (2015, May 16). *Cerebral small vessel disease, cognitive reserve and cognitive dysfunction | SpringerLink*. https://link.springer.com/article/10.1007/s00415-015-7776-6

Pisner, D. A., Shumake, J., Beevers, C. G., & Schnyer, D. M. (2019). The superior longitudinal fasciculus and its functional triple-network mechanisms in brooding. *NeuroImage : Clinical*, *24*, 101935. https://doi.org/10.1016/j.nicl.2019.101935

Prévost, C., Pessiglione, M., Météreau, E., Cléry-Melin, M.-L., & Dreher, J.-C. (2010). Separate Valuation Subsystems for Delay and Effort Decision Costs. *The Journal of Neuroscience*, *30*(42), 14080–14090. https://doi.org/10.1523/JNEUROSCI.2752-10.2010

Promjunyakul, N., Dodge, H. H., Lahna, D., Boespflug, E. L., Kaye, J. A., Rooney, W. D., & Silbert, L. C. (2018). Baseline NAWM structural integrity and CBF predict periventricular WMH expansion over time. *Neurology*, *90*(24), e2119–e2126. https://doi.org/10.1212/WNL.0000000000005684

Prosperini, L., Piattella, M. C., Giannì, C., & Pantano, P. (2015). Functional and Structural Brain Plasticity Enhanced by Motor and Cognitive Rehabilitation in Multiple Sclerosis. *Neural Plasticity*, *2015*, 481574. https://doi.org/10.1155/2015/481574

Pujara, M. S., Wolf, R. C., Baskaya, M. K., & Koenigs, M. (2015). Ventromedial prefrontal cortex damage alters relative risk tolerance for prospective gains and losses. *Neuropsychologia*, *79*, 70–75. https://doi.org/10.1016/j.neuropsychologia.2015.10.026

Pytlik, N., Soll, D., Hesse, K., Moritz, S., Bechdolf, A., Herrlich, J., Kircher, T., Klingberg, S., Landsberg, M. W., Müller, B. W., Wiedemann, G., Wittorf, A., Wölwer, W., Wagner, M., & Mehl, S. (2020). Problems in measuring the JTC-bias in patients with psychotic disorders with the fish task: A secondary analysis of a baseline assessment of a randomized controlled trial. *BMC Psychiatry*, *20*(1), 554. https://doi.org/10.1186/s12888-020-02959-5

Radoman, M., & Gorka, S. M. (2023). Intolerance of uncertainty and functional connectivity of the anterior insula during anticipation of unpredictable reward. *International Journal of Psychophysiology: Official Journal of the International Organization of Psychophysiology*, *183*, 1–8. https://doi.org/10.1016/j.ijpsycho.2022.09.003

Radwan, A. M., Sunaert, S., Schilling, K., Descoteaux, M., Landman, B. A., Vandenbulcke, M., Theys, T., Dupont, P., & Emsell, L. (2022). An atlas of white matter anatomy, its variability, and reproducibility based on constrained spherical deconvolution of diffusion MRI. *NeuroImage*, *254*, 119029. https://doi.org/10.1016/j.neuroimage.2022.119029

Raffelt, D. A., Tournier, J.-D., Smith, R. E., Vaughan, D. N., Jackson, G., Ridgway, G. R., & Connelly, A. (2017). Investigating white matter fibre density and morphology using fixel-based analysis. *NeuroImage*, *144*, 58–73. https://doi.org/10.1016/j.neuroimage.2016.09.029

Rensma, S. P., van Sloten, T. T., Launer, L. J., & Stehouwer, C. D. A. (2018). Cerebral small vessel disease and risk of incident stroke, dementia and depression, and all-cause mortality: A systematic review and meta-analysis. *Neuroscience &*

Biobehavioral Reviews, *90*, 164–173. https://doi.org/10.1016/j.neubiorev.2018.04.003

Renz, K. E., Pillny, M., & Lincoln, T. M. (2022). Increasing motivation in effort-based decision-making tasks: Effects of salience and reward expectancy manipulations. *Cognitive Neuropsychiatry*, *27*(1), 20–34. https://doi.org/10.1080/13546805.2021.2007068

Renz, K. E., Schlier, B., & Lincoln, T. M. (2023). Are effort-based decision-making tasks worth the effort?—A study on the associations between effort-based decision-making tasks and self-report measures. *International Journal of Methods in Psychiatric Research*, *32*(1), e1943. https://doi.org/10.1002/mpr.1943

Roca, M., Parr, A., Thompson, R., Woolgar, A., Torralva, T., Antoun, N., Manes, F., & Duncan, J. (2010). Executive function and fluid intelligence after frontal lobe lesions. *Brain*, *133*(1), 234–247. https://doi.org/10.1093/brain/awp269

Rogers, R. D. (1999). *Dissociable Deficits in the Decision-Making Cognition of Chronic Amphetamine Abusers, Opiate Abusers, Patients with Focal Damage to Prefrontal Cortex, and Tryptophan-Depleted Normal Volunteers: Evidence for Monoaminergic Mechanisms*. https://doi.org/10.1016/S0893-133X(98)00091-8

Rogers, R. D., Everitt, B. J., Baldacchino, A., Blackshaw, A. J., Swainson, R., Wynne, K., Baker, N. B., Hunter, J., Carthy, T., Booker, E., London, M., Deakin, J. F. W., Sahakian, B. J., & Robbins, T. W. (1999). Dissociable Deficits in the Decision-Making Cognition of Chronic Amphetamine Abusers, Opiate Abusers, Patients with Focal Damage to Prefrontal Cortex, and Tryptophan-Depleted Normal Volunteers: Evidence for Monoaminergic Mechanisms.

Neuropsychopharmacology, *20*(4), 322–339. https://doi.org/10.1016/S0893-133X(98)00091-8

Rogers, R. D., Owen, A. M., Middleton, H. C., Williams, E. J., Pickard, J. D., Sahakian, B. J., & Robbins, T. W. (1999). Choosing between Small, Likely Rewards and Large, Unlikely Rewards Activates Inferior and Orbital Prefrontal Cortex. *The Journal of Neuroscience*, *19*(20), 9029–9038. https://doi.org/10.1523/JNEUROSCI.19-20-09029.1999

Rorden, C., & Karnath, H.-O. (2004). Using human brain lesions to infer function: A relic from a past era in the fMRI age? *Nature Reviews Neuroscience*, *5*(10), 812–819. https://doi.org/10.1038/nrn1521

Ruesseler, M., Weber, L. A., Marshall, T. R., O'Reilly, J., & Hunt, L. T. (2023). Quantifying decision-making in dynamic, continuously evolving environments. *eLife*, *12*, e82823. https://doi.org/10.7554/eLife.82823

Rushworth, M. F. S. (2008). Intention, Choice, and the Medial Frontal Cortex. *Annals of the New York Academy of Sciences*, *1124*(1), 181–207. https://doi.org/10.1196/annals.1440.014

Sachdev, P., Wen, W., Chen, X., & Brodaty, H. (2007). Progression of white matter hyperintensities in elderly individuals over 3 years. *Neurology*, *68*(3), 214–222. https://doi.org/10.1212/01.wnl.0000251302.55202.73

Sahakian, B., LaBuzetta, J. N., Sahakian, B., & LaBuzetta, J. N. (2013). *Bad Moves: How decision making goes wrong, and the ethics of smart drugs*. Oxford University Press.

Salamone, J. D., & Correa, M. (2024). The Neurobiology of Activational Aspects of Motivation: Exertion of Effort, Effort-Based Decision Making, and the Role of

Dopamine. *Annual Review of Psychology*, *75*(Volume 75, 2024), 1–32. https://doi.org/10.1146/annurev-psych-020223-012208

Saleh, Y., Le Heron, C., Petitet, P., Veldsman, M., Drew, D., Plant, O., Schulz, U., Sen, A., Rothwell, P. M., Manohar, S., & Husain, M. (2021a). Apathy in small vessel cerebrovascular disease is associated with deficits in effort-based decision making. *Brain*, *144*(4), 1247–1262. https://doi.org/10.1093/brain/awab013

Saleh, Y., Le Heron, C., Petitet, P., Veldsman, M., Drew, D., Plant, O., Schulz, U., Sen, A., Rothwell, P. M., Manohar, S., & Husain, M. (2021b). Apathy in small vessel cerebrovascular disease is associated with deficits in effort-based decision making. *Brain*, *144*(4), 1247–1262. https://doi.org/10.1093/brain/awab013

Sanderson-Cimino, M., Panizzon, M. S., Elman, J. A., Tu, X., Gustavson, D. E., Puckett, O., Cross, K., Notestine, R., Hatton, S. N., Eyler, L. T., McEvoy, L. K., Hagler, D. J., Neale, M. C., Gillespie, N. A., Lyons, M. J., Franz, C. E., Fennema-Notestine, C., & Kremen, W. S. (2021). Periventricular and Deep Abnormal White Matter Differ in Associations With Cognitive Performance at Midlife. *Neuropsychology*, *35*(3), 252–264. https://doi.org/10.1037/neu0000718

Saperia, S., Felsky, D., Silva, S. D., Siddiqui, I., Rector, N., Remington, G., Zakzanis, K. K., & Foussias, G. (2023). Modeling Effort-Based Decision Making: Individual Differences in Schizophrenia and Major Depressive Disorder. *Biological Psychiatry: Cognitive Neuroscience and Neuroimaging*, *8*(10), 1041–1049. https://doi.org/10.1016/j.bpsc.2023.05.009

Scheltens, P., Barkhof, F., Leys, D., Pruvo, J. P., Nauta, J. J. P., Vermersch, P., Steinling, M., & Valk, J. (1993). A semiquantative rating scale for the assessment of signal

hyperintensities on magnetic resonance imaging. *Journal of the Neurological Sciences*, *114*(1), 7–12. https://doi.org/10.1016/0022-510X(93)90041-V

Schimmelpfennig, J., Topczewski, J., Zajkowski, W., & Jankowiak-Siuda, K. (2023). The role of the salience network in cognitive and affective deficits. *Frontiers in Human Neuroscience*, *17*, 1133367. https://doi.org/10.3389/fnhum.2023.1133367

Schmidt, P., Gaser, C., Arsic, M., Buck, D., Förschler, A., Berthele, A., Hoshi, M., Ilg, R., Schmid, V. J., Zimmer, C., Hemmer, B., & Mühlau, M. (2012). An automated tool for detection of FLAIR-hyperintense white-matter lesions in Multiple Sclerosis. *NeuroImage*, *59*(4), 3774–3783. https://doi.org/10.1016/j.neuroimage.2011.11.032

Schulz, M., Malherbe, C., Cheng, B., Thomalla, G., & Schlemm, E. (2021). Functional connectivity changes in cerebral small vessel disease—A systematic review of the resting-state MRI literature. *BMC Medicine*, *19*, 103. https://doi.org/10.1186/s12916-021-01962-1

Scott, S. L. (2010). A modern Bayesian look at the multi-armed bandit. *Applied Stochastic Models in Business and Industry*, *26*(6), 639–658. https://doi.org/10.1002/asmb.874

Seidenbecher, S. E., Sanders, J. I., Philipsborn, A. C. von, & Kvitsiani, D. (2020). Reward foraging task and model-based analysis reveal how fruit flies learn value of available options. *PLOS ONE*, *15*(10), e0239616. https://doi.org/10.1371/journal.pone.0239616

Shim, Y. S., Yang, D.-W., Roe, C. M., Coats, M. A., Benzinger, T. L., Xiong, C., Galvin, J. E., Cairns, N. J., & Morris, J. C. (2015). Pathological correlates of white matter

hyperintensities on magnetic resonance imaging. *Dementia and Geriatric Cognitive Disorders*, *39*(1–2), 92–104. https://doi.org/10.1159/000366411

Shoda, Y., Mischel, W., & Peake, P. K. (1970). Predicting Adolescent Cognitive and Self-Regulatory Competencies From Preschool Delay of Gratification: Identifying Diagnostic Conditions. *Developmental Psychology*. https://oce-ovid-com.ezproxy-prd.bodleian.ox.ac.uk/article/00063061-199011000-00014/HTML

Silbert, L. C., Roese, N. E., Hurworth, J., Lahna, D., Krajbich, V., Schwartz, D. L., & Woltjer, R. L. (2021). Pathological features of the 7T post-mortem MRI white matter hyperintensity penumbra. *Alzheimer's & Dementia*, *17*(S3), e052304. https://doi.org/10.1002/alz.052304

Silvetti, M., Nuñez Castellar, E., Roger, C., & Verguts, T. (2014). Reward expectation and prediction error in human medial frontal cortex: An EEG study. *NeuroImage*, *84*, 376–382. https://doi.org/10.1016/j.neuroimage.2013.08.058

Simon, H. A. (1955). A Behavioral Model of Rational Choice. *The Quarterly Journal of Economics*, *69*(1), 99–118. https://doi.org/10.2307/1884852

Simonelli, V., Nuzzi, D., Lancia, G. L., & Pezzulo, G. (2025). *Human foraging strategies flexibly adapt to resource distribution and time constraints* (No. arXiv:2408.01350). arXiv. https://doi.org/10.48550/arXiv.2408.01350

Slivkins, A. (2024). *Introduction to Multi-Armed Bandits* (No. arXiv:1904.07272). arXiv. https://doi.org/10.48550/arXiv.1904.07272

Smith, S. M., Jenkinson, M., Johansen-Berg, H., Rueckert, D., Nichols, T. E., Mackay, C. E., Watkins, K. E., Ciccarelli, O., Cader, M. Z., Matthews, P. M., & Behrens, T. E. J. (2006). Tract-based spatial statistics: Voxelwise analysis of multi-subject

diffusion data. *NeuroImage*, *31*(4), 1487–1505. https://doi.org/10.1016/j.neuroimage.2006.02.024

Soriano-Raya, J. J., Miralbell, J., López-Cancio, E., Bargalló, N., Arenillas, J. F., Barrios, M., Cáceres, C., Toran, P., Alzamora, M., Dávalos, A., & Mataró, M. (2012). Deep versus periventricular white matter lesions and cognitive function in a community sample of middle-aged participants. *Journal of the International Neuropsychological Society: JINS*, *18*(5), 874–885. https://doi.org/10.1017/S1355617712000677

Sporns, O., Tononi, G., & Kötter, R. (2005). The Human Connectome: A Structural Description of the Human Brain. *PLOS Computational Biology*, *1*(4), e42. https://doi.org/10.1371/journal.pcbi.0010042

Spreng, R. N., Stevens, W. D., Chamberlain, J. P., Gilmore, A. W., & Schacter, D. L. (2010). Default network activity, coupled with the frontoparietal control network, supports goal-directed cognition. *NeuroImage*, *53*(1), 303–317. https://doi.org/10.1016/j.neuroimage.2010.06.016

Steingroever, H. (2013). *Performance of Healthy Participants on the Iowa Gambling Task*. https://oce-ovid-com.ezproxy-prd.bodleian.ox.ac.uk/article/00012030-201303000-00017/PDF

Stern, E. R., Gonzalez, R., Welsh, R. C., & Taylor, S. F. (2010). Updating Beliefs for a Decision: Neural Correlates of Uncertainty and Underconfidence. *Journal of Neuroscience*, *30*(23), 8032–8041. https://doi.org/10.1523/JNEUROSCI.4729-09.2010

Stern, E. R., Gonzalez, R., Welsh, R. C., & Taylor, S. F. (2014). Medial frontal cortex and anterior insula are less sensitive to outcome predictability when monetary

stakes are higher. *Social Cognitive and Affective Neuroscience*, *9*(10), 1625–1631. https://doi.org/10.1093/scan/nst154

Stewart, C. R., Stringer, M. S., Shi, Y., Thrippleton, M. J., & Wardlaw, J. M. (2021). Associations Between White Matter Hyperintensity Burden, Cerebral Blood Flow and Transit Time in Small Vessel Disease: An Updated Meta-Analysis. *Frontiers in Neurology*, *12*, 647848. https://doi.org/10.3389/fneur.2021.647848

Studer, B., Manes, F., Humphreys, G., Robbins, T. W., & Clark, L. (2015). Risk-Sensitive Decision-Making in Patients with Posterior Parietal and Ventromedial Prefrontal Cortex Injury. *Cerebral Cortex (New York, NY)*, *25*(1), 1–9. https://doi.org/10.1093/cercor/bht197

Stuss, D. T. (2011). Functions of the Frontal Lobes: Relation to Executive Functions. *Journal of the International Neuropsychological Society*, *17*(5), 759–765. https://doi.org/10.1017/S1355617711000695

Stuss, D. T., & Alexander, M. P. (2000). Executive functions and the frontal lobes: A conceptual view. *Psychological Research*, *63*(3–4), 289–298. https://doi.org/10.1007/s004269900007

Su, N., Zhai, F.-F., Zhou, L.-X., Ni, J., Yao, M., Li, M.-L., Jin, Z.-Y., Gong, G.-L., Zhang, S.-Y., Cui, L.-Y., Tian, F., & Zhu, Y.-C. (2017). Cerebral Small Vessel Disease Burden Is Associated with Motor Performance of Lower and Upper Extremities in Community-Dwelling Populations. *Frontiers in Aging Neuroscience*, *9*, 313. https://doi.org/10.3389/fnagi.2017.00313

Summerside, E., & Ahmed, A. (2021). Using metabolic energy to quantify the subjective value of physical effort. *Journal of the Royal Society, Interface*, *18*, 20210387. https://doi.org/10.1098/rsif.2021.0387

Sutton, R. S. (1988). Learning to predict by the methods of temporal differences. *Machine Learning*, *3*(1), 9–44. https://doi.org/10.1007/BF00115009

Taghvaei, M., Cook, P., Sadaghiani, S., Shakibajahromi, B., Tackett, W., Dolui, S., De, D., Brown, C., Khandelwal, P., Yushkevich, P., Das, S., Wolk, D. A., & Detre, J. A. (2023). Young versus older subject diffusion magnetic resonance imaging data for virtual white matter lesion tractography. *Human Brain Mapping*, *44*(10), 3943–3953. https://doi.org/10.1002/hbm.26326

Tang, H., Zhao, H., Liu, H., Jiang, J., Kochan, N., Jing, J., Brodaty, H., Wen, W., Sachdev, P. S., & Liu, T. (2025). Structural damage-driven brain compensation among near-centenarians and centenarians without dementia. *NeuroImage*, *308*, 121065. https://doi.org/10.1016/j.neuroimage.2025.121065

Tanglay, O., Young, I. M., Dadario, N. B., Briggs, R. G., Fonseka, R. D., Dhanaraj, V., Hormovas, J., Lin, Y.-H., & Sughrue, M. E. (2022). Anatomy and white-matter connections of the precuneus. *Brain Imaging and Behavior*, *16*(2), 574–586. https://doi.org/10.1007/s11682-021-00529-1

Tay, J., Tuladhar, A. M., Hollocks, M. J., Brookes, R. L., Tozer, D. J., Barrick, T. R., Husain, M., de Leeuw, F.-E., & Markus, H. S. (2019). Apathy is associated with large-scale white matter network disruption in small vessel disease. *Neurology*, *92*(11), e1157–e1167. https://doi.org/10.1212/WNL.0000000000007095

Teng, Z., Dong, Y., Zhang, D., An, J., & Lv, P. (2017). Cerebral small vessel disease and post-stroke cognitive impairment. *International Journal of Neuroscience*, *127*(9), 824–830. https://doi.org/10.1080/00207454.2016.1261291

Thiebaut de Schotten, M., Foulon, C., & Nachev, P. (2020). *Brain disconnections link structural connectivity with function and behaviour*. https://doi.org/10.1101/2020.02.27.967570

Timashkov, A., Anderson, S., & Zinchenko, O. (2025). Neural correlates of uncertainty processing: Meta-analysis of fMRI studies. *Frontiers in Neuroscience*, *19*, 1662272. https://doi.org/10.3389/fnins.2025.1662272

Timpe, J. C., Rowe, K. C., Matsui, J., Magnotta, V. A., & Denburg, N. L. (2011). White matter integrity, as measured by diffusion tensor imaging, distinguishes between impaired and unimpaired older adult decision-makers: A preliminary investigation. *Journal of Cognitive Psychology*, *23*(6), 760–767. https://doi.org/10.1080/20445911.2011.578065

Treadway, M. T., Buckholtz, J. W., Cowan, R. L., Woodward, N. D., Li, R., Ansari, M. S., Baldwin, R. M., Schwartzman, A. N., Kessler, R. M., & Zald, D. H. (2012). Dopaminergic Mechanisms of Individual Differences in Human Effort-Based Decision-Making. *The Journal of Neuroscience*, *32*(18), 6170–6176. https://doi.org/10.1523/JNEUROSCI.6459-11.2012

Treadway, M. T., Buckholtz, J. W., Schwartzman, A. N., Lambert, W. E., & Zald, D. H. (2009). Worth the 'EEfRT'? The Effort Expenditure for Rewards Task as an Objective Measure of Motivation and Anhedonia. *PLoS ONE*, *4*(8), e6598. https://doi.org/10.1371/journal.pone.0006598

Tuladhar, A. M., van Norden, A. G. W., de Laat, K. F., Zwiers, M. P., van Dijk, E. J., Norris, D. G., & de Leeuw, F.-E. (2015). White matter integrity in small vessel disease is related to cognition. *NeuroImage : Clinical*, *7*, 518–524. https://doi.org/10.1016/j.nicl.2015.02.003

Tversky, A., & Edwards, W. (1966). Information Versus Reward in Binary Choices. *Journal of Experimental Psychology*, *71*(5), 680. https://doi.org/10.1037/h0023123

Tversky, A., & Kahneman, D. (1974). Judgment under Uncertainty: Heuristics and Biases. *Science*, *185*(4157), 1124–1131. https://doi.org/10.1126/science.185.4157.1124

Vaidya, A., & Fellows, L. K. (2017). The Neuropsychology of Decision-Making. In *Decision Neuroscience: An Integrative Perspective* (pp. 277–289). https://doi.org/10.1016/B978-0-12-805308-9.00022-1

van As, S., Beckers, D. G. J., Geurts, S. A. E., Kompier, M. A. J., Husain, M., & Veling, H. (2021). The Impact of Cognitive and Physical Effort Exertion on Physical Effort Decisions: A Pilot Experiment. *Frontiers in Psychology*, *12*. https://doi.org/10.3389/fpsyg.2021.645037

van den Heuvel, D. M. J., ten Dam, V. H., de Craen, A. J. M., Admiraal-Behloul, F., Olofsen, H., Bollen, E. L. E. M., Jolles, J., Murray, H. M., Blauw, G. J., Westendorp, R. G. J., & van Buchem, M. A. (2006). Increase in periventricular white matter hyperintensities parallels decline in mental processing speed in a non-demented elderly population. *Journal of Neurology, Neurosurgery, and Psychiatry*, *77*(2), 149–153. https://doi.org/10.1136/jnnp.2005.070193

van den Heuvel, M. P., Mandl, R. C. W., Kahn, R. S., & Hulshoff Pol, H. E. (2009). Functionally linked resting-state networks reflect the underlying structural connectivity architecture of the human brain. *Human Brain Mapping*, *30*(10), 3127–3141. https://doi.org/10.1002/hbm.20737

van der Flier, W. M., van Straaten, E. C. W., Barkhof, F., Verdelho, A., Madureira, S., Pantoni, L., Inzitari, D., Erkinjuntti, T., Crisby, M., Waldemar, G., Schmidt, R., Fazekas, F., & Scheltens, P. (2005). Small vessel disease and general cognitive function in nondisabled elderly: The LADIS study. *Stroke*, *36*(10), 2116–2120. https://doi.org/10.1161/01.STR.0000179092.59909.42

Vega, A. de la, Chang, L. J., Banich, M. T., Wager, T. D., & Yarkoni, T. (2016). Large-Scale Meta-Analysis of Human Medial Frontal Cortex Reveals Tripartite Functional Organization. *Journal of Neuroscience*, *36*(24), 6553–6562. https://doi.org/10.1523/JNEUROSCI.4402-15.2016

Verdelho, A., Madureira, S., Ferro, J. M., Basile, A.-M., Chabriat, H., Erkinjuntti, T., Fazekas, F., Hennerici, M., O'Brien, J., Pantoni, L., Salvadori, E., Scheltens, P., Visser, M. C., Wahlund, L.-O., Waldemar, G., Wallin, A., Inzitari, D., & Study, on behalf of the L. (2007). Differential impact of cerebral white matter changes, diabetes, hypertension and stroke on cognitive performance among non-disabled elderly. The LADIS study. *Journal of Neurology, Neurosurgery & Psychiatry*, *78*(12), 1325–1330. https://doi.org/10.1136/jnnp.2006.110361

Vergoossen, L. W. M., Jansen, J. F. A., van Sloten, T. T., Stehouwer, C. D. A., Schaper, N. C., Wesselius, A., Dagnelie, P. C., Köhler, S., van Boxtel, M. P. J., Kroon, A. A., de Jong, J. J. A., Schram, M. T., & Backes, W. H. (2021). Interplay of White Matter Hyperintensities, Cerebral Networks, and Cognitive Function in an Adult Population: Diffusion-Tensor Imaging in the Maastricht Study. *Radiology*, *298*(2), 384–392. https://doi.org/10.1148/radiol.2021202634

Veselic, S., Muller, T. H., Gutierrez, E., Behrens, T. E. J., Hunt, L. T., Butler, J. L., & Kennerley, S. W. (2023). A cognitive map for value-guided choice in ventromedial

prefrontal cortex. *bioRxiv: The Preprint Server for Biology*, 2023.12.15.571895. https://doi.org/10.1101/2023.12.15.571895

Villar, S. S., Bowden, J., & Wason, J. (2015). Multi-armed Bandit Models for the Optimal Design of Clinical Trials: Benefits and Challenges. *Statistical Science : A Review Journal of the Institute of Mathematical Statistics*, *30*(2), 199–215. https://doi.org/10.1214/14-STS504

Volz, K. G., Schubotz, R. I., & von Cramon, D. Y. (2003). Predicting events of varying probability: Uncertainty investigated by fMRI. *NeuroImage*, *19*(2), 271–280. https://doi.org/10.1016/S1053-8119(03)00122-8

Volz, K. G., Schubotz, R. I., & Von Cramon, D. Y. (2006). Decision-making and the frontal lobes. *Current Opinion in Neurology*, *19*(4), 401–406. https://doi.org/10.1097/01.wco.0000236621.83872.71

Voytek, B., Davis, M., Yago, E., Barceló, F., Vogel, E. K., & Knight, R. T. (2010). Dynamic Neuroplasticity after Human Prefrontal Cortex Damage. *Neuron*, *68*(3), 401–408. https://doi.org/10.1016/j.neuron.2010.09.018

Wahlund, L. O., Barkhof, F., Fazekas, F., Bronge, L., Augustin, M., Sjögren, M., Wallin, A., Ader, H., Leys, D., Pantoni, L., Pasquier, F., Erkinjuntti, T., & Scheltens, P. (2001). A New Rating Scale for Age-Related White Matter Changes Applicable to MRI and CT. *Stroke*, *32*(6), 1318–1322. https://doi.org/10.1161/01.STR.32.6.1318

Wang, D., Luo, Y., Mok, V. C. T., Chu, W. C. W., & Shi, L. (2016). Tractography atlas-based spatial statistics: Statistical analysis of diffusion tensor image along fiber pathways. *NeuroImage*, *125*, 301–310. https://doi.org/10.1016/j.neuroimage.2015.10.032

Wang, S., Shi, Y., & Li, B.-M. (2017). Neural representation of cost–benefit selections in rat anterior cingulate cortex in self-paced decision making. *Neurobiology of Learning and Memory*, *139*, 1–10. https://doi.org/10.1016/j.nlm.2016.12.003

Wang, S., Zhang, F., Huang, P., Hong, H., Jiaerken, Y., Yu, X., Zhang, R., Zeng, Q., Zhang, Y., Kikinis, R., Rathi, Y., Makris, N., Lou, M., Pasternak, O., Zhang, M., & O'Donnell, L. J. (2022). Superficial white matter microstructure affects processing speed in cerebral small vessel disease. *Human Brain Mapping*, *43*(17), 5310–5325. https://doi.org/10.1002/hbm.26004

Wang, Y., Liu, M., Chen, Y., Qiu, Y., Han, X., Xu, Q., Shen, D., & Zhou, Y. (2024). Trade-offs among brain structural network characteristics across the cognitive decline process in cerebral small vessel disease. *Frontiers in Aging Neuroscience*, *16*. https://doi.org/10.3389/fnagi.2024.1465181

Wardlaw, J. M., Smith, C., & Dichgans, M. (2019). Small vessel disease: Mechanisms and clinical implications. *The Lancet Neurology*, *18*(7), 684–696. https://doi.org/10.1016/S1474-4422(19)30079-1

Wardlaw, J. M., Smith, E. E., Biessels, G. J., Cordonnier, C., Fazekas, F., Frayne, R., Lindley, R. I., O'Brien, J. T., Barkhof, F., Benavente, O. R., Black, S. E., Brayne, C., Breteler, M., Chabriat, H., DeCarli, C., De Leeuw, F.-E., Doubal, F., Duering, M., Fox, N. C., … Dichgans, M. (2013). Neuroimaging standards for research into small vessel disease and its contribution to ageing and neurodegeneration. *The Lancet Neurology*, *12*(8), 822–838. https://doi.org/10.1016/S1474-4422(13)70124-8

Watts, T. W., Duncan, G. J., & Quan, H. (2018). Revisiting the Marshmallow Test: A Conceptual Replication Investigating Links Between Early Delay of Gratification

and Later Outcomes. *Psychological Science*, *29*(7), 1159–1177. https://doi.org/10.1177/0956797618761661

Weller, J. A., Levin, I. P., Shiv, B., & Bechara, A. (2007). Neural Correlates of Adaptive Decision Making for Risky Gains and Losses. *Psychological Science*, *18*(11), 958–964. https://doi.org/10.1111/j.1467-9280.2007.02009.x

Wen, W., & Sachdev, P. (2004). The topography of white matter hyperintensities on brain MRI in healthy 60- to 64-year-old individuals. *NeuroImage*, *22*(1), 144–154. https://doi.org/10.1016/j.neuroimage.2003.12.027

Westbrook, A., Kester, D., & Braver, T. S. (2013). What Is the Subjective Cost of Cognitive Effort? Load, Trait, and Aging Effects Revealed by Economic Preference. *PLoS ONE*, *8*(7), e68210. https://doi.org/10.1371/journal.pone.0068210

Wilkosz, P. A., Seltman, H. J., Devlin, B., Weamer, E. A., Lopez, O. L., DeKosky, S. T., & Sweet, R. A. (2010). Trajectories of cognitive decline in Alzheimer's disease. *International Psychogeriatrics*, *22*(2), 281–290. https://doi.org/10.1017/S1041610209991001

Wilson, C. R. E., Gaffan, D., Browning, P. G. F., & Baxter, M. G. (2010). Functional localization within the prefrontal cortex: Missing the forest for the trees? *Trends in Neurosciences*, *33*(12), 533–540. https://doi.org/10.1016/j.tins.2010.08.001

Wittmann, B. C., Daw, N. D., Seymour, B., & Dolan, R. J. (2008). Striatal Activity Underlies Novelty-Based Choice in Humans. *Neuron*, *58*(6), 967–973. https://doi.org/10.1016/j.neuron.2008.04.027

Wolf, D. H., Satterthwaite, T. D., Kantrowitz, J. J., Katchmar, N., Vandekar, L., Elliott, M. A., & Ruparel, K. (2014). Amotivation in Schizophrenia: Integrated Assessment

With Behavioral, Clinical, and Imaging Measures. *Schizophrenia Bulletin*, *40*(6), 1328–1337. https://doi.org/10.1093/schbul/sbu026

Wood, J. L., & Nee, D. E. (2023). Cingulo-Opercular Subnetworks Motivate Frontoparietal Subnetworks during Distinct Cognitive Control Demands. *The Journal of Neuroscience*, *43*(7), 1225–1237. https://doi.org/10.1523/JNEUROSCI.1314-22.2022

Wu, M., & Zheng, Y. (2023). Physical effort paradox during reward evaluation and links to perceived control. *Cerebral Cortex (New York, N.Y. : 1991)*, *33*. https://doi.org/10.1093/cercor/bhad207

Wyatt, L. E., Hewan, P. A., Hogeveen, J., Spreng, R. N., & Turner, G. R. (2024). Exploration versus exploitation decisions in the human brain: A systematic review of functional neuroimaging and neuropsychological studies. *Neuropsychologia*, *192*, 108740. https://doi.org/10.1016/j.neuropsychologia.2023.108740

Xue, G., CHEN, C., LU, Z.-L., & DONG, Q. (2010). Brain Imaging Techniques and Their Applications in Decision-Making Research. *Xin Li Xue Bao. Acta Psychologica Sinica*, *42*(1), 120–137. https://doi.org/10.3724/SP.J.1041.2010.00120

Yang, S., Zhou, Y., Wang, F., He, X., Cui, X., Cai, S., Zhu, X., & Wang, D. (2024). Diffusion tensor imaging in cerebral small vessel disease applications: Opportunities and challenges. *Frontiers in Neuroscience*, *18*. https://doi.org/10.3389/fnins.2024.1473462

Yu, L. Q., Kan, I. P., & Kable, J. W. (2020). Beyond a rod through the skull: A systematic review of lesion studies of the human ventromedial frontal lobe. *Cognitive*

Neuropsychology, *37*(1–2), 97–141. https://doi.org/10.1080/02643294.2019.1690981

Yuan, P., & Raz, N. (2014). Prefrontal cortex and executive functions in healthy adults: A meta-analysis of structural neuroimaging studies. *Neuroscience & Biobehavioral Reviews*, *42*, 180–192. https://doi.org/10.1016/j.neubiorev.2014.02.005

Yue, Y., Broder, J., Kleinberg, R., & Joachims, T. (2012). The K-armed dueling bandits problem. *Journal of Computer and System Sciences*, *78*(5), 1538–1556. https://doi.org/10.1016/j.jcss.2011.12.028

Zanon Zotin, M. C., Sveikata, L., Viswanathan, A., & Yilmaz, P. (2021). Cerebral small vessel disease and vascular cognitive impairment: From diagnosis to management. *Current Opinion in Neurology*, *34*(2), 246–257. https://doi.org/10.1097/WCO.0000000000000913

Zentall, T. R. (2010). Justification of Effort by Humans and Pigeons: Cognitive Dissonance or Contrast? *Current Directions in Psychological Science*, *19*(5), 296–300. https://doi.org/10.1177/0963721410383381

Zhang, H., Schneider, T., Wheeler-Kingshott, C. A., & Alexander, D. C. (2012). NODDI: Practical in vivo neurite orientation dispersion and density imaging of the human brain. *NeuroImage*, *61*(4), 1000–1016. https://doi.org/10.1016/j.neuroimage.2012.03.072

Zhang, M., & Zheng, Y. (2022). Neural dynamics of effort-modulated reward processing. *Psychophysiology*, *59*(10), e14070. https://doi.org/10.1111/psyp.14070

Zhang, S., & Arfanakis, K. (2014). White Matter Segmentation Based on a Skeletonized Atlas: Effects on Diffusion Tensor Imaging Studies of Regions of Interest. *Journal*

of Magnetic Resonance Imaging : JMRI, *40*(5), 1189–1198. https://doi.org/10.1002/jmri.24445

Zigmond, A. S., & Snaith, R. P. (1983). The Hospital Anxiety and Depression Scale. *Acta Psychiatrica Scandinavica*, *67*(6), 361–370. https://doi.org/10.1111/j.1600-0447.1983.tb09716.x